Canadian
Journal of Chemistry

AMINO ACID DISTRIBUTION IN BIOLOGICALLY ACTIVE PEPTIDES[1]

SAUL B. NEEDLEMAN,[2] R. QUENTIN BLACKWELL, AND LEONARD S. FOSDICK

ABSTRACT

A group of biologically active peptides were examined for possible favored chain positions exhibited by some of the 21 constituent amino acids as well as for the unusual occurrence of specific peptide linkages. High levels of significance were revealed for certain amino acid couplets when they were subjected to chi-square analyses.

The work of Scheraga (1), Koshland (2), and others dealing with the spatial orientation and sequential arrangement of amino acids has engendered much speculation as to the nature of the active sites of biologically significant peptides. The extremely detailed study of Sorm *et al.* (3) represents one novel approach to the study of amino acid sequences.

The present work deals with a statistical evaluation of peptide structure in which a group of peptides with totally established amino acid sequences were examined for the occurrence of relative chain position preferences of the individual constituent amino acids and for statistically significant repeating amino acid sequences (4).

A list of all of the dipeptide couplets which appear in the peptides included in this analysis was prepared by recording each succeeding pair of amino acid residues beginning at the N-terminus and proceeding along the chain, one residue at a time.

RESULTS

In the primary peptides, 21 different amino acids occurred a total of 184 times. The combined amino acid percentage composition of the group of peptides is not strikingly different from that of numerous general proteins. Although the study was restricted to biologically active peptides because of the availability of complete sequence analyses, there is no reason to believe that these data would differ significantly from that which will be found when the sequence of many "structural" as well as "biologically active" proteins are known (3). There is no unusual concentration of one or more specific amino acids to be noted in the individual peptides. In general, it would appear that the amino acid content of these peptides being studied does not account for their special biological action. The only point of difference distinguishing these peptides from numerous proteins, so far as amino acid composition is concerned, is the occurrence of certain D-configuration amino acids in bacitracin A and of ornithine only in some antibiotics.

A principal concern of the present study is the relative position in the peptide chain occupied by the individual amino acids. Examination of the amino acid distribution in the peptides investigated for this study reveals an interesting tendency towards adventi-

tious positional concentrations. By plotting each amino acid in terms of its numerical position within the peptide chain as well as according to its fractional distance from the amino end, it was possible to draw certain conclusions. Figure 1 depicts the relative or

Fraction of Total Distance From Amino End
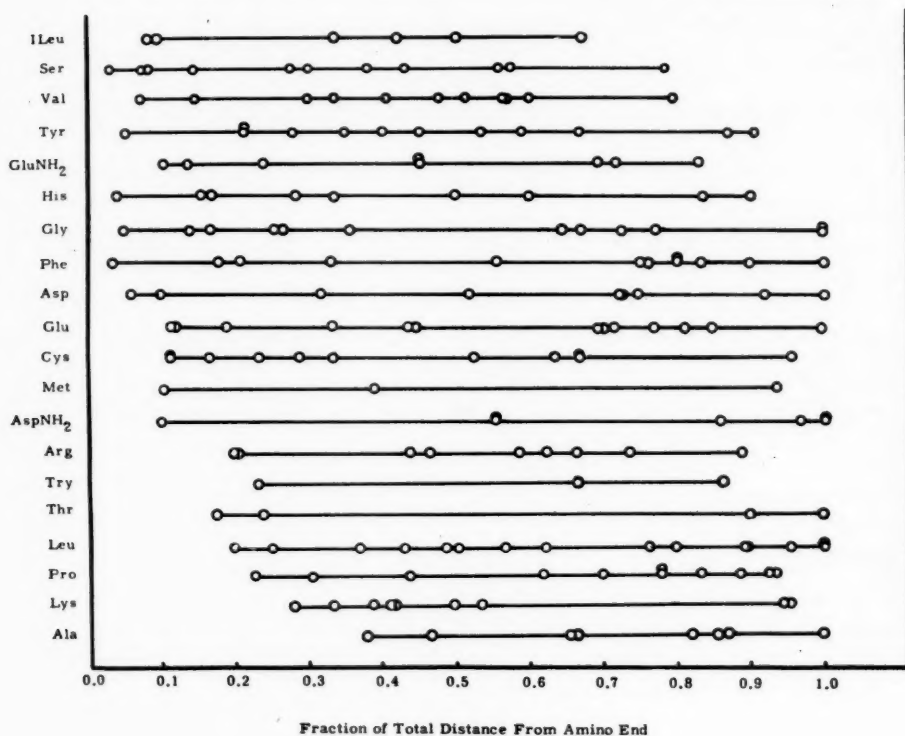
FIG. 1.

fractional distance of the individual amino acid moiety along the peptide chain. Our data show that certain acids, including glycine, glutamic acid, phenylalanine, and aspartic acid, are widely distributed from N- to C-terminal moieties. A few amino acids appear mainly in the interior: glutamine, methionine, tryptophan, and lysine. Cysteine predominates near the ends of the peptide chains. Others are found to tend toward one end of the molecule. For example, isoleucine, serine, valine, and histidine are associated more with the N-terminus while alanine, leucine, threonine, and proline are closer to the C-terminus. The remainder of the amino acids present do not fit well into any of the above groupings.

Some of the relationships may be seen best in terms of actual numerical positions within the peptide. For example, isoleucine does not appear in any of the peptides beyond the 8th moiety from the N-terminus, histidine not beyond the 10th, serine not beyond the 16th, although all of them occur in longer peptides and thus, presumably, have the opportunity to occupy more distant positions. In the same way alanine is not found more than 14 positions from the C-terminus and leucine not more than 17. With two exceptions, all of the lysine moieties were clumped near the second quadrant of the peptide chains.

Of the total of 11 prolines present in the peptides, 4 were located in the third position from the C-terminus and 3 more were in the fourth position. Proline also was found to exhibit a periodicity of 12 in the corticotropins and the β–MSH hormones. It appears, at least, at the 12, 24, and 36 positions from the N-terminus of the three corticotropins (A, α, β); in the β–MSH molecules it appears at the 4 and 16 positions.

For the analysis of terminal amino acids a number of proteins and peptides were added to the peptides used in the remainder of the study. Sixteen of the 21 amino acids found to be present are found as N-terminal groups and 11 are found one or more times as the C-terminal groups. A total of 17 different amino acids are found at one or the other end; only methionine, tryptophan, ornithine, and glutamine were absent from terminal positions.

Another object of the present study was to compare the significance of occurrence of a number of dipeptide couplets making up the structure of a select group of peptides and proteins. It was desirable to determine whether a dipeptide sequence occurred more frequently or less frequently than could be predicted purely by chance based on the quantity of each of the amino acids making up the pool. The concept of chi-squares which considers the theoretical as well as the actual occurrence of each dipeptide moiety was used to compare the significance of uniquely occurring entities.

The dipeptide structures arise by removal from the metabolic pool of those amino acids necessary to synthesize the total host peptide. The metabolic pool may be different in different tissues. For the purpose of the present study, the metabolic pool arbitrarily was taken to consist of all the amino acids present in the peptides examined, in concentrations determined by the numbers present in each of these peptides. Although the resulting pool is derived from heterogeneous peptides, valid conclusions can be made from the corresponding chi-square values. That the pool bears no necessary relationship to its derivative peptides can be seen in the work of Ramachandran and Winnick (5), whose analysis of the very short peptides of the pituitary metabolic pool showed no sequential correlation to the peptide hormones derived from the pituitary.

For significance at the 10% level and for one degree of freedom, the chi-square for a dipeptide moiety should exceed a value of 2.706 (6). Table I lists all of the dipeptide couplets which were found to have significant chi-square values. Only four of the 122 couplets which occurred only once had a chi-square exceeding the requisite statistical limit; the occurrence ratio also indicated a much greater than expected existence. Two of these couplets make up one tripeptide fraction, $-AspNH_2-Met-Met-$, found in the protein, ribonuclease. Another dipeptide, $-Orn-Ileu-$, appears in bacitracin and closely resembles the related $-Orn-Leu-$ occurring in other peptide antibiotics. The fourth couplet, $-Try-D-Phe-$, is in the tyrothricin B sequence but is in part of the peptide which differs from tyrothricin A.

For dipeptide couplets occurring more than once there was an expected increase in statistical significance. Thus, for couplets appearing twice, more than one-fifth (10 of 49) had significant chi-squares. In a few cases, the dipeptide occurred twice within the same protein molecule. Such moieties generally contained amino acids rich in functional groups rather than simple aliphatic types.

Since a total of 294 dipeptides form all the compounds included in this communication and since these are made up of 202 different types, it is evident that almost all dipeptide couplets as well as their parent peptides are unique structures.

It is evident that the mere occurrence of a particular combination of amino acid residues, even those having significant chi-square values, does not confirm a strict functional

TABLE I

Dipeptide couplets having significant chi-square values

Dipeptide couplet	Occurrence* ratio	x^2†	Dipeptide couplet	Occurrence* ratio	x^2†
Gly–Ileu	4.218	4.981	Tyr–Ileu	5.510	7.471
Ser	2.654	3.094	Ser	3.486	5.325
Ala–Glu	2.973	5.202	Lys–Asp	3.006	4.164
GluNH₂	3.090	2.804			
			Arg–Try	14.848	26.899
Leu–Phe	2.530	2.753	Arg	5.330	6.906
Val–Orn	12.642	31.740	Orn–Leu	12.005	30.250
Glu	2.686	4.228	Ileu	11.000	9.201
Ser–Met	6.217	8.820	Pro–Val	4.582	16.791
His	3.380	3.370	Lys	2.917	5.049
Arg	3.090	2.804			
Thr–Ser	3.988	6.750	Try–Phe	4.674	2.972
Cys–Cys	8.072	43.191	Asp–Asp	4.421	7.915
			Glu	3.529	7.289
Met–Met	11.731	9.200	AspNH₂–Met	5.331	3.453
Glu	4.718	5.949	GluNH₂	5.785	7.779
AspNH₂	5.333	3.451			
			Glu–Ala	2.974	5.280
His–Leu	5.835	2.747	Asp	2.650	3.095
Phe–His	3.380	3.370	GluNH₂–Cys	3.270	3.167
Arg	3.090	2.804			

*The expected "chance" frequency, C, may be calculated for the dipeptide couplet $X–Y$ from (X/T) $\times (Y/T-1)$, where X is the number of residues of the first amino acid comprising the couplet and Y is the number of units of the second amino acid. T represents the total of all amino acid units in the system.

The "actual" frequency, A, is found from the number of occurrences of $X–Y$ divided by the total number of dipeptide couplets.

The occurrence ratio is A/C.

†The chi-square value is calculated from the formula, $X^2 = (A-C)^2/C$, where A is the "actual" occurrence of a particular dipeptide unit and C is the "chance" occurrence of that couplet.

requirement for that combination of amino acids. Nevertheless, although couplets involved in other than activity functions may have chi-squares of significance, the technique may nevertheless be helpful for purposes of sequence characterization.

The existence of a number of significant chi-square values for certain couplets led to the reconstruction of the "characteristic" segments of some physiologically active peptide sequences. These sequences vary in length from five residues in the corticotropins to dipeptide couplets. In glucagon, in a span of nine residues, there are six hydroxyl-containing moieties. At least part of this unit is markedly characteristic through the –Thr–Ser– and –Tyr–Ser– couplets (Table I). Only one-third of the insulin A molecule, the portion at the N-terminus, showed non-random linkage frequencies by our test, while in the B chain, there was a continuous sequence of 12 residues, at the C-terminus, for which the chi-squares were not significant.

An interesting example which supports the possible usefulness of statistical evaluation of the dipeptide units can be noted from the specific biological activity of a synthetic peptide made up of the N-terminal portion of oxytocin and the C-terminus of vasopressin (7). This artificial hormone has a degree of activity of both natural peptides and contains only the statistically characteristic couplets of each.

Of the 441 unique dipeptidic arrangements which are possible for 21 different amino acids, 202 appeared in those compounds examined. Even under the best arrangements, it was not possible to find all 441 moieties since only a total of 294 dipeptide sequences comprised the pool. Assuming that naturally occurring proteins arise from metabolic pools similar to those yielding the peptides of this study, it would be reasonable to expect that certain of the missing couplets will yet appear as the sequence of additional proteins are unravelled. However, as has already been suggested in the work of Sorm (3), 897 couplets were examined and found to contain only 247 unique moieties. That is, by introducing an additional 603-couplet arrangement only 45 new and different dipeptide sequences were gained. One may further conclude that a natural barrier appears to exist for the occurrence of certain amino acid sequences in peptides. One might agree with Fox (8), who suggests that formation of peptides takes place by self-selection of the amino acid sequences, perhaps by a process akin to Darwinian selection which directs the synthesis of more adapted protein molecules from those of less value to the organism.

REFERENCES

1. H. A. SCHERAGA, C. Y. CHA, J. HERMANS, JR., and C. L. SCHILDKRAUT. Abstr. 136th Meeting, Am. Chem. Soc., Atlantic City, N.J. (1959).
2. D. E. KOSHLAND, JR. and M. J. ERWIN. J. Am. Chem. Soc. 79, 2657 (1957).
3. F. SORM, B. KEIL, V. HOLEYSOVSKI, V. KANESSLOVA, V. KOSTKA, P. MASIAR, B. MELOUN, O. MIKES, V. TOMASEK, and J. VANECEK. Collection Czechoslov. Chem. Commun. 22, 1310 (1957).
4. S. B. NEEDLEMAN, R. Q. BLACKWELL, and L. S. FOSDICK. Abstr. 132nd Meeting, Am. Chem. Soc., New York, N.Y. (1957).
5. L. K. RAMACHANDRAN and T. WINNICK. Biochem. Biophys. Acta, 23, 533 (1957).
6. G. W. SNEDECOR. Statistical methods applied to experiments in agriculture and biology. 5th ed. Iowa State College Press, Ames, Iowa. 1956. p. 28.
7. P. G. KATSOYANNIS. J. Am. Chem. Soc. 79, 209 (1957).
8. S. W. FOX. Am. Scientist, 44, 347 (1956).

SURFACE EFFECTS IN BUTANE OXIDATION[1]

M. Cherneskey and J. Bardwell

ABSTRACT

The oxidation of butane is considerably affected by the nature of the vessel surface. With a silica vessel, vigorous combustion accompanied by multiple cool flames occurs between 280° C and 320° C. These reactions are strongly inhibited when the vessel walls are coated with metal oxides or metal halides. Higher pressures are required for ignition at all temperatures. Of the compounds studied, lead monoxide is the most effective inhibitor. The results suggest that in the antiknock action of lead tetraethyl the true inhibitor is lead monoxide.

INTRODUCTION

There is considerable evidence that the oxidation of hydrocarbons is subject to surface effects. Kinetic experiments have revealed a dependence of rate on vessel diameter (1, 2) and on the previous treatment of the vessel walls (3, 4, 5). Although systematic investigations of surface effects have been made with hydrogen (6, 7, 8) and methane (4, 9) there is a lack of information about the role of the surface in the oxidation of the higher hydrocarbons, where mechanisms not found with methane come into play (10, 11). A better understanding of the part played by the surface in these reactions is desirable for several reasons: it would clarify some of the puzzling anomalies in the reaction kinetics (12, 13); it might suggest improvements in petrochemical processes; finally, it might help reveal the mechanism of "knock" and antiknock action in engines.

Although knock and its suppression have been subjected to much investigation (14, 15, 16) there is still considerable disagreement about the nature of the process. The work of King and co-workers (17, 18, 19) and of Walsh and co-workers (20, 21, 22) may be cited as illustrating both the lack of agreement on mechanism and the possible importance of heterogeneous processes.

King (17, 18) ascribes the action of antiknock agents such as iron carbonyl or lead tetraethyl to deposition of metals or metal oxides which are believed to promote the formation of steam and oxides of carbon; these gases may then dilute the combustible mixture and reduce its inflammability. Walsh and co-workers (20, 21, 22) ascribe the antiknock action of lead tetraethyl to the formation of a colloidal smoke of lead monoxide, which is assumed to inhibit the knocking reaction by virtue of a surface destruction of free radical chains. Each group of investigators claims supporting evidence from combustion experiments. The positive-catalyst theory favored by King is said to be supported by the results of flow experiments with fuels such as pentane and hydrogen (18, 19). The negative-catalyst theory favored by Walsh finds support from static experiments with fuels such as methane and ethers (21, 22).

The question of antiknock action has continued to be a contentious one (16, 23, 24). It appeared desirable to establish empirically the effects of various inorganic compounds on the combustion behavior of a typical hydrocarbon. For this investigation the fuel chosen was n-butane, which oxidizes at convenient rates between 250° C and 500° C. This compound's oxidation is accompanied by cool flames, two-stage ignition, and other phenomena associated with the low-temperature combustion of paraffin hydrocarbons and related substances (11, 25).

EXPERIMENTAL

Apparatus

The apparatus used was a conventional one, consisting of a reaction vessel heated in a well-lagged furnace and connected to a manometer, a pumping system, and storage vessels for the reactants. The n-butane and oxygen were admitted separately to the vessel and the progress of reaction was followed by pressure measurements and by observation through a window. The reaction vessel was of clear silica, and was cylindrical in shape, 6 cm in diameter and 9 cm long. It was fitted with a capillary inlet tube and a ground joint.

Procedure for Modifying the Surface

Deposition of Soluble Salts

Sufficient salt solution (20% by weight) was transferred to the clean vessel, to leave, on drying, a salt coating of 2.5 mg per sq. cm. The vessel was heated to about 80° C by immersion in a water bath, and then connected to an aspirator for evaporation of solvent. During solvent evaporation, the vessel was continuously rotated in such a way as to bring the solution in contact with all parts of the inner surface.

Deposition of Insoluble Powders

The powder was screened and the portion that passed a 200-mesh screen was used. The fine powder was suspended in a small volume of water and transferred to the vessel. The water was evaporated as described above. Deposits amounting to 0.9 mg per sq. cm were used in most experiments; observations with other amounts are described below. It was found that the technique described yielded deposits that were reasonably uniform and that remained in place after numerous combustion experiments.

Cleaning the Vessel

On completion of combustion experiments with a given surface coating, the vessel was detached, washed with water and then with dilute nitric acid or other suitable solvent. For removal of possible contamination by organic matter, the vessel was left in contact for 1 hour with a freshly prepared mixture of concentrated nitric acid and concentrated sulphuric acid held at about 100° C. The vessel was then thoroughly rinsed with hot distilled water and dried. The vessel so treated will henceforth be referred to as "acid-cleaned".

When combustion experiments were done with the acid-cleaned vessel the rates found at first were similar to those with the new untreated vessel. These rates differed slightly, however, from those obtained subsequently with the same vessel. It is therefore necessary to distinguish two types of "clean" surface, the freshly acid-cleaned vessel and the "aged" vessel. The aged vessel showed slightly higher rates and improved reproducibility. Similar "aging" effects have been reported by other investigators (2, 4, 12) but their cause remains obscure.

Comparison of Results with Different Surfaces

It has been shown that with hydrocarbons such as propane and n-butane the pressure changes that accompany oxidation run roughly parallel with the consumption of reactants and the appearance of products (25, 26, 27). With n-butane the pressure–time curves show the usual shape: at first there is an induction period, ranging in duration from seconds to hours; at the beginning of the induction period the rate of pressure change is often immeasurably small, but it usually increases in an approximately exponential way, culminating in a period of more rapid reaction. During the latter period there may occur

pressure surges, which accompany luminescence in the vessel and indicate the occurrence of cool flames or ignition. Of the various criteria of reaction rate that may be used to evaluate the influence of the surface, the following will be employed in this paper:

(a) the length of the induction period which, for this purpose, will be defined as the time elapsing between the admission of the reactants to the vessel and the attainment of maximum reaction rate (or the passing of a cool flame);

(b) the magnitude of the maximum rate of pressure change for a given reaction mixture and vessel temperature;

(c) the pressure–temperature limits for the onset of ignition;

(d) the range of occurrence of cool flames.

RESULTS

Effect of Surface on Induction Period and on Maximum Rate

Table I illustrates the large differences in reaction rate encountered with different surface materials, under otherwise identical experimental conditions.

TABLE I

Induction period and maximum rate of pressure change in the oxidation of n-butane under different surface conditions

Surface treatment	Induction period, minutes	Maximum rate, mm/min
Clean silica (aged)	0.3	Ignition
KI coated	2	7
PbO coated	27	0.24

NOTE: Initial pressure of n-butane, 150 mm; initial pressure of oxygen, 150 mm; temperature of vessel, 292° C.

On the basis of these results, which are typical of many, the aged silica surface may be designated as "active", the KI-treated surface as "moderately inhibiting", and the PbO-treated surface as "strongly inhibiting".

Effect of Surface on Ignition Limits

The pressure–temperature limits for ignition of equimolar mixtures of n-butane and oxygen under different conditions of surface are shown in Fig. 1. The adverse effect of a
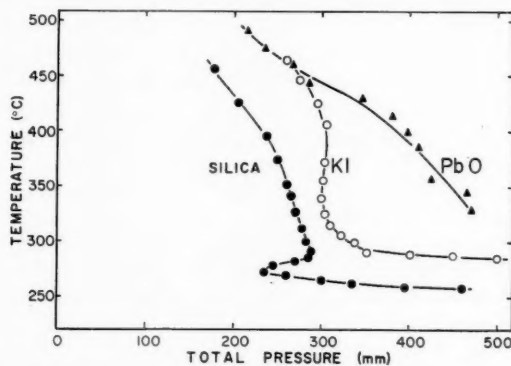
FIG. 1. Ignition limits for equimolar n-butane – oxygen mixtures with a silica vessel, untreated, and coated with KI and with PbO.

coating of KI or PbO on reaction rate is here revealed by an increase in the pressure required for ignition. Again it is clear that PbO is the more effective inhibitor, at least in the low-temperature region.

The results in Table I and Fig. 1 illustrate the difficulty of arriving at a satisfactory quantitative criterion of inhibition with a branching-chain reaction. The ratio of induction periods in Table I indicates that at 292° C reaction proceeds about 90 times faster in the aged vessel than in the PbO-coated vessel. On the other hand, the minimum pressures for ignition, in the low-temperature region, differ by a factor of a little less than two. This apparent discrepancy is believed to be related to the fact that reaction rate is strongly dependent on reactant pressure (1, 28, 29).

In subsequent sections of this paper, changes in ignition limits and cool flame limits will be used for assessing the magnitude of surface effects. It should be remembered that these limits are in general much less sensitive measures of inhibition than others that might have been employed, such as induction period or maximum rate. General use of the latter is made difficult or impossible by the marked changes in the nature of the reaction resulting from surface changes.

Ignition Diagram with an Active Surface

With *n*-butane, as with most hydrocarbons, intense reaction is frequently found even though the pressure is insufficient for ignition. Figure 2 shows, in a pressure–temperature
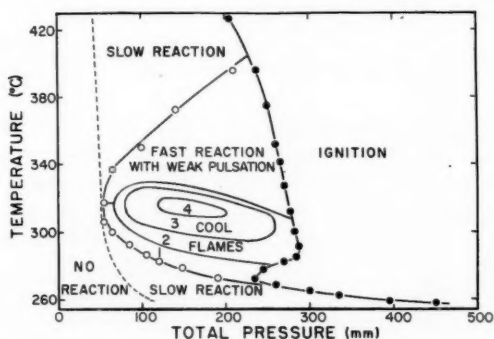
FIG. 2. Range of occurrence of combustion phenomena with equimolar *n*-butane – oxygen mixtures in a silica vessel, 6 cm in diameter. The numbers shown indicate the numbers of cool flames observed.

diagram, the range of occurrence of the various phenomena encountered when equimolar *n*-butane – oxygen mixtures were admitted to an aged silica vessel in the temperature range 250° C to 430° C. The phenomena include:

(*a*) No reaction: here the induction period is of infinite duration (28, 29).

(*b*) Slow reaction: the oxidation is accompanied by little if any luminescence, and the pressure increases without any surges or pulsations. This type of reaction occurs both at low temperatures and at high temperatures; for example, with a total pressure of 80 mm the maximum rate has a value of 10 mm/min at 287° C, at 380° C, and at 452° C (29).

(*c*) Single cool flame: the self-acceleration of the reaction is interrupted by a moderate pressure surge during which a bluish flame is seen in the vessel.

(*d*) Multiple cool flames: here a definite periodicity is present, the flames being separated by intervals of up to 100 seconds. The pressure–time record for this type of reaction is

illustrated in Fig. 3 (curve for 284° C). The passing of each flame brings about a marked deceleration of the reaction.

(*e*) Fast reaction with weak pulsation: As the vessel temperature is increased beyond about 320° C the periodic nature of the reaction becomes much less pronounced. The initial acceleration of the reaction is rapid, but the pressure surge is relatively weak and it is not followed by a substantial deceleration; instead reaction continues at a rapid rate. Figure 3 (curve for 360° C) illustrates the pressure–time record for this type of reaction and shows the contrast with the multiple cool flames that occur at lower temperatures.
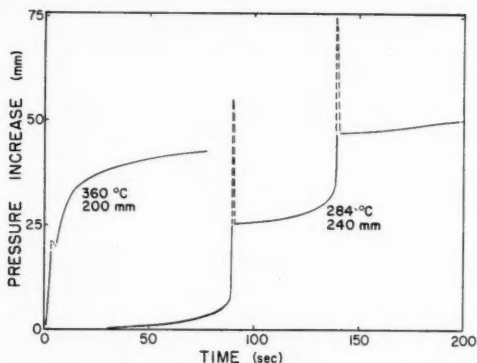
FIG. 3. Typical pressure–time record for double cool flame and for fast reaction with weak pulsation.

(*f*) Ignition: a bright blue or yellow flame traverses the reaction vessel and is associated with a large pressure increase. Below about 400° C, the ignition is a two-stage process, a cool flame preceding the hot flame. Many investigators have commented on the similarity of such ignition and the phenomenon of knock in engines (10, 11, 16).

The main features of the diagram in Fig. 2 are similar to those found by other investigators (using glass or silica vessels) with propane (26, 30), *n*-pentane (5), and butanone (31). As with these compounds the ignition limit is L-shaped with a peninsula at about 275° C.

As mentioned earlier, experiments with the acid-cleaned vessel gave somewhat slower reaction than those with the aged vessel. Examples are shown in Table II where some of the pressure–temperature limits are given. The differences, although appreciable, are evidently much smaller than those found between limits for the clean and the treated surfaces.

Ignition Diagram with a Moderately Inhibiting Surface

Typical results with a moderately inhibiting surface are shown in Fig. 4 which gives the ignition diagram for a NiO-coated surface. Comparison with Fig. 2 shows the following evidence of inhibition:

(*a*) A much larger region of no reaction.

(*b*) Elimination of multiple cool flames. The pressure–temperature conditions that usually give rise to these with the active surface, i.e., moderate pressures and temperatures in the range 280° C to 320° C now lead to either slow reaction or no reaction at all.

(*c*) Significantly higher ignition limits.

The ignition diagram in the low-temperature region was also determined with the surface coated in turn with the following metal oxides: Cu_2O, Fe_2O_3, Pb_3O_4, and PbO. The results are summarized in Table II. It is seen that Cu_2O, Fe_2O_3, and Pb_3O_4 give limits very similar to those for NiO. Furthermore, the ignition diagrams showed the same general features as found in Fig. 4, namely an L-shaped ignition boundary and a large area where the pressure–time record was similar to that in Fig. 3 (360° curve). In no case was the pressure–time record similar to the 284° C curve in Fig. 3, i.e., clearly marked multiple cool flames were not observed. The exceptionally strong inhibition found with PbO will be discussed below.

Table II also summarizes the results for the vessel coated with the following metal halides: $MnCl_2$, $NiCl_2$, $CuCl_2$, $PbCl_2$, KCl, and KI. With the exception of KCl, which appears to be a rather ineffective inhibitor, these metal halides also give limits that differ little from those for a NiO coating. The ignition diagrams again were found to resemble

TABLE II

Pressure–temperature limits for various surface treatments

Surface treatment	Minimum ignition temperature at 400 mm pressure, °C	Minimum temperature for pulsating reaction at 300 mm pressure, °C	Minimum pressure for pulsating reaction at 335° C	Minimum pressure for ignition at 335° C
Aged silica	259	265	65	267
Acid-cleaned silica	262	268	75	270
NiO	301	306	150	320
Cu_2O	296	302	140	315
Fe_2O_3	293	300	140	315
Pb_3O_4	303	308	125	295
$MnCl_2$	296	300	135	305
$NiCl_2$	295	302	130	300
$CuCl_2$	295	303	150	310
$PbCl_2$	305	312	130	295
KI	288	293	150	300
KCl	282	287	120	279
PbO	395	344	195	465

that in Fig. 4; the ignition boundary was L-shaped, no multiple cool flames were found, but fast reaction with weak pulsation took place above about 310° C.

Ignition Diagram with a Strongly Inhibiting Surface

The exceptionally potent inhibition brought about by a PbO coating will now be presented in greater detail. Figure 5 shows the ignition behavior between 250° C and 435° C. The diagram is evidently much altered from that with the active surface (Fig. 2). Particularly noteworthy is the persistence of slow reaction in regions of pressure and temperature, e.g., 400 mm and 350° C, that lead to vigorous explosion with all the other surface treatments used.

Effect of Differences in Amount of Deposit

Some experiments were done to find out to what extent the inhibiting effect of PbO depends on the amount of it, present on the surface. Coatings amounting to 0.1, 0.9, and 2.2 mg per sq. cm were used.

The limit chosen for the comparison was the position of the upper boundary of the slow reaction zone, at 300 mm pressure, i.e., the temperature marking the transition from
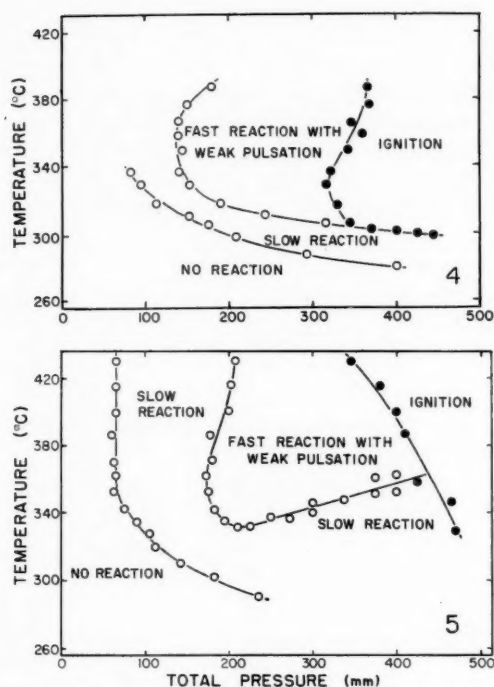
FIG. 4.   Range of occurrence of combustion phenomena with equimolar *n*-butane – oxygen mixtures in a silica vessel coated with NiO.

FIG. 5.   Range of occurrence of combustion phenomena with equimolar *n*-butane – oxygen mixtures in a silica vessel coated with PbO.

TABLE III

Effect of amount of PbO used on the degree
of inhibition

Amount of PbO deposited, mg per sq. cm	Upper limit of slow reaction zone at 300 mm pressure, °C
0	268
0.1	321
0.9	344
2.2	343

non-pulsating reaction to reaction with pulsation. Table III shows that, by this criterion, the extent of inhibition increases sharply with the first addition of PbO (0.1 mg per sq. cm). When the coating is increased from 0.1 to 0.9 mg per sq. cm, there is some further inhibition, but increase beyond 0.9 mg per sq. cm is without effect.

Inert Gas Effects

The response of a free radical reaction to inert gas additions can provide a clue to the role of the surface. Attention will be confined to experimental conditions where the reaction proceeds without appreciable self-heating, since otherwise complications arise

because of heat capacity effects (25). The effects of inert gas additions on the slow development of the reaction in the induction period will therefore be considered.

With the aged silica vessel the rate of development of the reaction was found to be unaffected by inert gas additions. Measurements in the slow combustion region (270° C, 160 mm pressure) and in the cool flame region (284° C, 240 mm) showed that nitrogen additions of 200 mm had no effect on the length of the induction period. Additions of argon and of water vapor were also found to be without effect.

A different result was obtained when an acid-cleaned vessel was used. Inert gas additions at 300° C now had a moderate accelerating effect. For example, with a total reactant pressure of 160 mm, addition of 200 mm of nitrogen shortened the induction period from 130 seconds to 60 seconds. It is of interest that with the aged vessel under the same experimental conditions (300° C, 160 mm pressure, no inert gas) the induction period was only 24 seconds. On the basis of these results it might be anticipated that the differences in induction period between the acid-cleaned vessel and the aged vessel would disappear if experiments were done in the presence of sufficient inert gas.

Still greater effects were found with a PbO-coated vessel. Measurements were made in the slow combustion zone (312° C, 150 mm pressure). Addition of only 108 mm of nitrogen shortened the induction period from 20 minutes to only 2 minutes and increased the maximum rate from 0.34 mm/min to 1.0 mm/min.

DISCUSSION

There seems little reason to doubt that the large effects of the different surface materials on the rate have their origin in different efficiencies of these substances in destroying intermediates, probably free radicals. The chain-breaking efficiency of the aged silica vessel appears to be relatively low. This conclusion is supported by the observations that with this surface, lively reaction develops over a wide range of experimental conditions (Figs. 2 and 3), and its rate of development is not accelerated by inert gas additions. The latter observation shows that, under typical experimental conditions, there is no serious depletion of radicals by diffusion to the walls. Such depletion does apparently become significant, however, when the pressure is sufficiently reduced, as there is complete suppression of the reaction at pressures below about 50 mm (Fig. 2).

The acid-cleaned surface is evidently somewhat more efficient in breaking chains than is the aged surface; this is indicated by the longer induction period, the acceleration by inert gas, and the slightly higher pressure–temperature limits for cool flames and ignition (Table II).

Of the 11 inorganic compounds used as surface coatings, all but KCl and PbO lead to approximately the same degree of inhibition. For example, Table II shows that at 400 mm pressure the ignition temperatures show a range of 136° when all the surfaces are considered; these nine compounds, however, show a range of only 17°. It is interesting that KCl, which has frequently been used to provide an inhibiting surface in oxidation experiments (2, 3, 8), appears, from this investigation, to be the least effective of all the compounds tested.

It seems difficult to avoid the conclusion that PbO is an exceptionally efficient chain-breaking agent. Evidence of unusually strong inhibition by this substance has been presented in Tables I and II and in Fig. 5. Corroboration may be found in a comparison of the data in Tables II and III. It is seen that even a light coating of PbO (0.1 mg/sq. cm) leads to greater inhibition than the normal coating (0.9 mg/sq. cm) of the other metal oxides or even the heavy coating (2.5 mg/sq. cm) of the metal halides. The latter

comparison makes it unlikely that the observed difference between the results with PbO and with the other compounds is due to some unsuspected experimental factor such as differences in particle size distribution of the powders.

A complete discussion of surface effects would include identification of the radicals that suffer destruction at the walls. From indirect evidence Walsh and co-workers have suggested that the radical HO_2 plays such a role in the oxidation of methane at about 500° C (20, 22). In the oxidation of higher paraffins at low temperatures, many other radicals have been postulated as participating in the reaction mechanism (10, 27, 32). It is unlikely that some of the more complex of these radicals, e.g., C_4H_9OO, participate appreciably in wall reactions since there is evidence that they undergo rapid pyrolysis or isomerization reactions in the gas phase (27, 33). An additional possibility in the low-temperature range is the occurrence of heterogeneous side-reactions of intermediate molecules such as peroxides or aldehydes, whose normal reactions are believed responsible for chain-branching (12, 28).

Relation to Other Investigations

Although there appears to be no previous investigation of surface effects in the oxidation of n-butane, some information is available for propane and ethers. Day and Pease (30) determined cool flame limits and ignition limits for propane using three different surface treatments—cleaning with hot HNO_3, etching with HF, and rinsing with a KCl solution which was then drained out of the vessel. They found only small differences in the various limits and concluded that "the nature of the surface has no great effect on the cool flame and ignition characteristics of the reaction". In view of the results given above for n-butane and the general similarity of combustion behavior of propane and n-butane (25, 26), this generalization appears to be premature. A repetition of the work of Day and Pease, with thicker deposits and other compounds, would be desirable.

Chamberlain and Walsh (21) measured the ignition limits of diethyl ether using a silica vessel, with and without a coating of PbO. The PbO coating was found to raise the ignition pressure by 11% at 400° C and by 14% at 210° C. These results may be compared with those given above for n-butane, namely an increase of about 65% at 400° C and a slightly larger effect at lower temperatures, e.g., 75% at 330° C (Fig. 1). The lack of quantitative agreement is not surprising since ethers and hydrocarbons show other differences in their oxidation behavior (10, 33). There may also be a difference in amount of deposit used.

Relation to the Mechanism of Antiknock Action

The results given in this paper suggest that PbO may well be the true inhibitor when lead tetraethyl acts as an antiknock agent. It is worth while to compare the inhibition of the oxidation of n-butane by PbO with the known behavior of lead tetraethyl. As shown above in Tables I and II and in Figs. 1 and 5, the inhibition by PbO is pervasive; this substance greatly lengthens the induction period, it suppresses the phenomenon of multiple cool flames, and it raises ignition pressures by about 70%. Lead tetraethyl, on the other hand, has been found to have little effect on the induction period both with n-heptane (10, 16, 35) and with diethyl ether (34); its inhibiting effect apparently comes into play only at later stages of the reaction. The extent of inhibition by lead tetraethyl may be estimated from its effect on ignition pressures. Townend and Mandlekar found that this additive, when used in amounts similar to those required for satisfactory antiknock action (0.1%), brought about an increase in ignition pressure of about 5% with

n-butane and n-pentane (11, 36). It is interesting that, with some fuels, lead tetraethyl fails to give any antiknock effect and may even act as a proknock agent (10).

The complicated behavior of lead tetraethyl becomes more understandable if the true inhibitor is in fact PbO. The observation that the early stages of the reaction proceed at about the same rate whether lead tetraethyl is present or not (10, 16, 34) is explained if there is a delay in the formation of PbO; such a delay is to be expected if both chemical transformation of lead tetraethyl into PbO vapor and physical condensation of PbO vapor to solid particles are required. Furthermore, the chemical transformation is likely to release ethyl radicals into the combustion mixture and so cause some promoting action. An explanation is then available for the observation that lead tetraethyl has a net promoting effect under certain experimental conditions, for example, at very high temperatures (17) or with fuels that are believed to oxidize via very short chains (10, 20).

It has been suggested by Norrish and co-workers that in the inhibition of combustion reactions by lead compounds the processes are probably homogeneous and depend on vapor molecules, possibly including PbO vapor at very high temperatures (23, 24). The results reported in this paper, however, leave little doubt that heterogeneous processes are predominant in the temperature range considered here. The large influence of added inert gas on reaction rate points to surface breaking of chains. Furthermore, if vapor molecules were responsible for the inhibition, one would expect that the effect would be roughly proportional to the vapor pressure of PbO and so would increase markedly with increase of vessel temperature and would be independent of the amount of solid PbO on the surface. Figure 1 and Table III show that these expectations are not fulfilled.

While heterogeneous chain breaking at the vessel surface appears to be the predominant process responsible for the inhibition described in this paper, somewhat different mechanisms may be important under the higher pressure conditions found in engines when lead compounds exert an antiknock effect. The suggestion of Chamberlain and Walsh (21) that lead tetraethyl reacts with oxygen to form a colloidal smoke of PbO particles appears to be a plausible one. This mechanism makes possible heterogeneous chain breaking without, however, necessitating a long diffusion path.

<div align="center">REFERENCES</div>

1. B. AIVAZOV and M. B. NEUMANN. Z. physik. Chem. (Leipzig), B, 33, 349 (1936).
2. M. PRETTRE. Symposium on Combustion. 3rd Symposium, 1949. p. 397.
3. R. N. PEASE. Chem. Revs. 21, 279 (1937).
4. D. E. HOARE and A. D. WALSH. Symposium on Combustion. 5th Symposium, 1955. p. 467.
5. M. LUCQUIN and P. LAFFITTE. Compt. rend. 242, 2944 (1956).
6. D. R. WARREN. Proc. Roy. Soc. (London), A, 211, 86 (1952).
7. D. R. WARREN. Proc. Roy. Soc. (London), A, 211, 96 (1952).
8. A. H. WILLBOURN and C. N. HINSHELWOOD. Proc. Roy. Soc. (London), A, 185, 376 (1946).
9. D. E. HOARE and A. D. WALSH. Proc. Roy. Soc. (London), A, 215, 454 (1952).
10. B. LEWIS and G. VON ELBE. Combustion, flames and explosions of gases. Academic Press Inc., New York. 1951. pp. 128–199.
11. D. T. A. TOWNEND and M. R. MANDLEKAR. Proc. Roy. Soc. (London), A, 141, 484 (1933).
12. M. F. MULCAHY and M. J. RIDGE. Trans. Faraday Soc. 49, 1297 (1953).
13. Z. G. SZABO. Symposium on Combustion. 7th Symposium, 1959. p. 118.
14. W. P. HAWTHORNE and E. J. Y. SCOTT. Advances in Chem. Ser. No. 20. 1958. p. 187.
15. J. D. B. OGILVIE, S. G. DAVIS, A. L. THOMPSON, W. T. GRUMMITT, and C. A. WINKLER. Can. J. Research, F, 26, 246 (1948).
16. A. J. PAHNKE. Advances in Chem. Ser. No. 20. 1958. p. 202.
17. R. O. KING. Can. J. Research, F, 25, 326 (1947).
18. R. O. KING. Can. J. Research, F, 26, 228 (1948).
19. R. O. KING, W. A. WALLACE, and B. MAHAPATRA. Can. J. Research, F, 26, 264 (1948).
20. G. H. N. CHAMBERLAIN, D. E. HOARE, and A. D. WALSH. Discussions Faraday Soc. No. 14, 89 (1953).
21. G. H. N. CHAMBERLAIN and A. D. WALSH. Proc. Roy. Soc. (London), A, 215, 175 (1952).

22. D. E. CHEANEY, D. A. DAVIES, A. DAVIS, D. E. HOARE, J. PROSTHEROE, and A. D. WALSH. Symposium on Combustion. 7th Symposium, 1959. p. 183.
23. K. H. L. ERHARD and R. G. W. NORRISH. Proc. Roy. Soc. (London), A, 234, 178 (1956).
24. R. G. W. NORRISH. Symposium on Combustion. 7th Symposium, 1959. p. 203.
25. J. BARDWELL. Symposium on Combustion. 5th Symposium, 1955. p. 529.
26. D. M. NEWITT and L. S. THORNES. J. Chem. Soc. 1656 (1937).
27. N. N. SEMENOV. Some problems of chemical kinetics and reactivity. Vol. I. Pergamon Press, New York. 1958. pp. 85–117.
28. F. E. MALHERBE and A. D. WALSH. Trans. Faraday Soc. 46, 824 (1950).
29. NAN-CHIANG WU SHU and J. BARDWELL. Can. J. Chem. 33, 1415 (1955).
30. R. A. DAY and R. N. PEASE. J. Am. Chem. Soc. 62, 2234 (1940).
31. J. BARDWELL and C. N. HINSHELWOOD. Proc. Roy. Soc. (London), A, 205, 375 (1951).
32. R. G. W. NORRISH. Discussions Faraday Soc. No. 10, 269 (1951).
33. C. E. BOORD. Advances in Chem. Ser. No. 20. 1958. p. 5.
34. L. OUELLET, E. LEGER, and C. OUELLET. J. Chem. Phys. 17, 746 (1949).
35. A. J. PAHNKE, P. M. COHEN, and B. M. STURGIS. Ind. Eng. Chem. 46, 1024 (1954).
36. D. T. A. TOWNEND and M. R. MANDLEKAR. Proc. Roy. Soc. (London), A, 143, 168 (1934).

REMOVAL OF OXYGEN FROM METHANE AND THE USE OF NUCLEAR SPIN RELAXATION TO MEASURE OXYGEN CONCENTRATION[1]

H. S. Sandhu, J. Lees, and M. Bloom

ABSTRACT

Nuclear spin relaxation measurements are used to measure quantitatively the amount of oxygen present in methane. An upper limit of $2.5 \times 10^{-4}\%$ is placed on the amount of oxygen present in methane after treatment with a getter made of misch metal.

The proton spin relaxation time, T_1, in liquid and solid CH_4 has been found by us to be very sensitive to small amounts of oxygen in the sample, because of the fact that the O_2 molecule is paramagnetic. The effect of paramagnetic impurities on nuclear spin relaxation in diamagnetic liquids has long been known (1), and precautions must usually be taken to eliminate such impurities if one is interested in studying T_1 of the pure liquid (2). In our first measurements of T_1 in liquid CH_4 (3), T_1 was found to depend on the sample, the longest T_1 obtained being about 0.6 second while some "chemically pure" samples gave us T_1 values as low as 10^{-2} seconds. All samples used were obtained commercially, the purest samples being supplied by Phillips Petroleum Co.

Since the vapor pressure readings for such samples also disagreed with those published for pure CH_4 (4), it was considered necessary to find a reliable method of purifying our samples. Different techniques were used to remove oxygen. It may be noted that we plan to study T_1 in deuterated samples of methane, so that it is of importance that the purification method does not require very large quantities of the sample.

An attempt was first made to use the fact that the normal boiling point of oxygen (90° K) is lower than that of methane (112° K). The liquid was maintained at a temperature (106° K) such that most of the oxygen might boil off. The vapors were then pumped off. This process was repeated a number of times. Each time we pumped off the vapors and measured T_1 in the liquid, we obtained a longer relaxation time. Although T_1 values as long as 10 seconds were obtained, this technique for purification was finally dropped because T_1 values so obtained were not reproducible and the method was very wasteful of methane.

The second technique employed was to circulate methane over heated copper. This method was not satisfactory because the gas decomposed during the process.

The technique found to be most suitable for our purposes involved the use of a getter, misch metal, which consists of rare earths derived from monazite and alloyed with iron. This metal was selected because it was found by Ehrke and Slack (5) in their study of the gettering power of various metals like aluminum, magnesium, barium, and misch metal that misch metal is the most effective for removal of oxygen. As described in the following paragraph, our procedure is a slightly simplified version of that described by Ehrke and Slack (5).

A $\frac{1}{2}$-liter flask drawn into a long tube on one side is used as shown in Fig. 1. The end of the tube fits into an NMR probe to make T_1 measurements. A tungsten coil of five or six turns of 0.01-in. diameter, with two or three small pieces of misch metal in the coil, is sealed into the flask. The flask is then connected to a diffusion pump through a trap and evacuated to a pressure of the order of 10^{-6} cm. The flask is baked by flaming
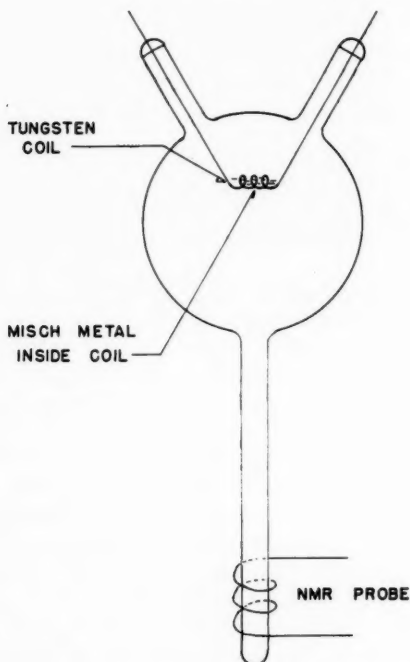
FIG. 1. Schematic drawing of the sample container.

several times during pumping to get rid of oxygen adsorbed on the walls. The tungsten coil is also degassed during pumping. When the flask has been thoroughly baked and pumped, it is filled with argon to a pressure of 1 to 2 mm. The getter is then flashed by passing current through the tungsten coil using a Variac to control the current, until a characteristic diffused layer of the deposit is produced. The presence of argon is necessary to produce a diffused deposit the gettering power of which is much higher than the bright shiny type (5). The argon is then pumped off, leaving an uncontaminated getter layer of high activity. Methane at 1-atmosphere pressure is introduced into the flask which is then sealed off from the system.

When this procedure was followed, T_1 was always found to increase to 14 seconds at 108° K, this value being reproduced whether the measurements were done on different samples or the same sample at different times during a period of several days. One of the samples studied had had approximately 0.5% oxygen purposely added as an impurity. The addition of nitrogen to the samples did not affect T_1.

In order to make quantitative measurements on the contribution of oxygen to T_1, a sample of CH_4 was prepared with approximately 1% oxygen. Mass spectrometer measurements performed at the Department of Chemistry, University of Washington, showed that the sample contained about 1.08% oxygen. T_1 was measured as a function of temperature and will be reported for this sample and other similarly prepared samples in a future publication. For purposes of using T_1 as a method of analyzing the oxygen concentration quantitatively, we give here only values of T_1 in CH_4 liquid under its

own vapor pressure at 108° K. The measurements were made using pulse techniques (3) and were accurate to about 5%.

For 1.08% O_2, we obtained $T_1 = 34 \times 10^{-3}$ sec. It is expected that $1/T_1^0 \propto f$ where T_1^0 is the contribution to T_1 due to the oxygen, and f is the percentage of oxygen molecules. This was borne out by studying a sample containing 2.54% oxygen, as measured by the mass spectrometer, which gave $T_1 = 15 \times 10^{-3}$ sec at 108° K.

Because of the oxygen background in the mass spectrometer, it was impossible to analyze the oxygen concentration with it in a region where T_1 measurements indicated that f was less than about 0.1%. Therefore, our T_1 measurements represent a more sensitive means of detecting oxygen than a mass spectrometer unless special steps are taken to cut down the oxygen background in the mass spectrometer.

If T_1^n represents the natural relaxation time of pure CH_4, we can write

$$\frac{1}{T_1} = \frac{1}{T_1^n} + \frac{1}{T_1^0}.$$

Our measurements indicate that $T_1^n = 14$ seconds at 108° K, since our measurements were reproducible from day to day and we would have been able to detect a change of less than 10% in T_1. If T_1^0 were about 14 seconds at 108° K, this would correspond to $f = 2.5 \times 10^{-3}$%. On the basis of the reproducibility of T_1 with time and in different samples, we are probably justified in saying that our purification procedure resulted in $f \lesssim 2.5 \times 10^{-4}$ %.

It would seem that the technique described here would be well suited to removal of oxygen from other hydrocarbons and this is being planned in connection with future measurements of T_1 of higher hydrocarbons in this laboratory.

REFERENCES

1. N. BLOEMBERGEN, E. M. PURCELL, and R. V. POUND. Phys. Rev. **73**, 679 (1948).
2. J. H. SIMPSON and H. Y. CARR. Phys. Rev. **111**, 1201 (1958).
3. H. S. SANDHU and M. BLOOM. Bull. Am. Phys. Soc. **3**, 324 (1958).
4. G. T. ARMSTRONG, F. G. BRICKWEDDE, and R. B. SCOTT. J. Research Natl. Bur. Standards, **55**, 39 (1955).
5. L. F. EHRKE and C. M. SLACK. J. Appl. Phys. **11**, 129 (1940).

THE ACTION OF PYRIDINE ON THE DINITRATE ESTERS OF 1,4;3,6-DIANHYDROHEXITOLS[1]

M. Jackson and L. D. Hayward

ABSTRACT

In contrast to the rapid and selective replacement of a secondary O-nitro group by hydrogen in the hexitol hexanitrates at 25–50° C, the dinitrate esters of the 1,4;3,6-dianhydrides of D-mannitol, D-glucitol, and L-iditol (*cis*-isohexides) reacted slowly in anhydrous pyridine at 87–115° C. The chief products were a polymer, nitrogen oxides, and pyridinium nitrate; the yield of mononitrates did not exceed 10% and none of the parent diols were formed.

The relative rates of the first-order decomposition of the nitroxy groups in the isomeric dinitrates were in reverse order to that for S_N2 reaction at carbon in these compounds. Activation energies and frequency factors were determined and water was shown to have a retarding effect.

Thermal decomposition of the dinitrates in solution in nitrobenzene, *m*-xylene, or *sym*-tetrachloroethane was much slower than the pyridine reaction at the same temperature and was independent of the polarity of the solvent and the conformation of the ester.

INTRODUCTION

Dulcitol and D-mannitol hexanitrates have been shown to react selectively with pyridine to yield the corresponding 1,2,4,5,6-pentanitrates (1, 2). The rate of reaction was different for the two hexitol derivatives and the resulting pentanitrates were essentially stable to pyridine under the same conditions. Sorbitol hexanitrate reacted similarly with pyridine but the pentanitrate was not fully characterized (3). The reaction was inconveniently fast for kinetic studies even at 25° C and the multiplicity of nitroxy groups and molecular conformations further complicated the problem of sorting out the reaction mechanism.

The three known isomeric 1,4;3,6-dianhydrohexitols (the *cis*-isohexides) and their derivatives have been shown to behave characteristically in certain types of reactions due to differences in their restricted conformations (4, 5). In an attempt to determine the mechanism of the pyridine – nitrate ester reaction the dinitrates of the isohexides (I–III, Fig. 1) were selected for study since observation of similar steric effects in their reactions with pyridine would aid in diagnosis of the type of mechanism involved. The presence of only two, non-vicinal, secondary, nitroxy groups in these isomers was also expected to simplify analysis of the results.

RESULTS AND DISCUSSION

The three isohexide dinitrates (Fig. 1) were prepared in crystalline form and characterized through their nitrogen contents, infrared spectra, and nearly quantitative conversion to the parent diols. The physical constants and nitrogen contents of the isomers are shown in Table I. The dinitrates dissolved readily in pyridine and the colorless solutions were stable over several weeks at room temperature. No vigorous reaction occurred on heating under reflux; however, slow decomposition, accompanied by a red coloration of the solution and evolution of oxides of nitrogen, began at temperatures above 50° C.

At 115° C 0.424 M solutions of the isohexide dinitrates in anhydrous pyridine decomposed according to an apparent first-order rate law for loss of nitroxy groups (Fig. 2). Since pyridine, as solvent, was present in constant excess, it was likely that the reaction actually involved a second-order process which appeared to be first order because of this
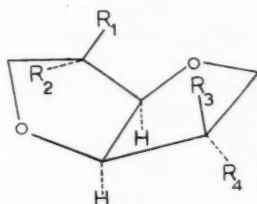
FIG. 1. 2,5-Dinitrates of 1,4;3,6-dianhydrohexitols.

I $R_1 = ONO_2$, $R_2 = H$, $R_3 = ONO_2$, $R_4 = H$: isomannide dinitrate
II $R_1 = ONO_2$, $R_2 = H$, $R_3 = H$, $R_4 = ONO_2$: isosorbide dinitrate
III $R_1 = H$, $R_2 = ONO_2$, $R_3 = H$, $R_4 = ONO_2$: isoidide dinitrate

TABLE I

1,4;3,6-Dianhydrohexitol dinitrates

	Isomannide dinitrate (I)	Isosorbide dinitrate (II)	Isoidide dinitrate (III)	Ref.
Melting point, ° C				
Found	64.5–65.5	50.5–51.5	68–69	
Reported	65.5	70	—	(6)
		71		(7)
		52		(8)
$[\alpha]_D$ Found	+335	+141	+72.9	
Reported	—	+134	—	(8)
Nitrogen content (%)				
Found	11.8[a]	11.9[a]	11.8[a,b]	
Required	11.87	11.87	11.87	

[a]Modified micro-Kjeldahl method.
[b]Determined by Mr. I. G. Csizmadia. Found: C, 30.9; H, 3.95%. Calc. for $C_6H_8N_2O_8$: C, 30.5; H, 3.41%.
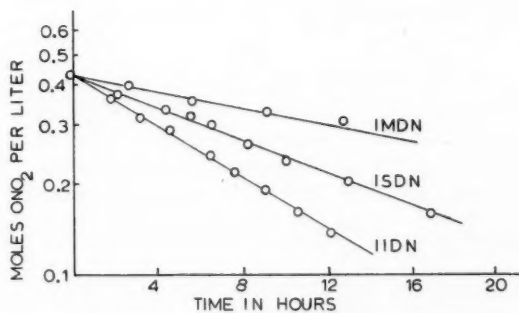
FIG. 2. Rate plots of isohexide dinitrate – pyridine reaction at 115° C. IMDN, isomannide dinitrate; ISDN, isosorbide dinitrate; IIDN, isoidide dinitrate.

limitation (9). The course of the reaction was followed by colorimetric determination of unreacted nitrate ester in aliquots of the reaction mixture. The rates were confirmed by quantitative isolation of the unreacted material followed by complete characterization. The rate of nitroxy group decomposition was also determined at 100° C and 87° C

TABLE II

Rates of decomposition of the isohexide dinitrates in pyridine

Conditions		Rate constants, $sec^{-1} \times 10^{-6}$		
Temperature, °C	Moles water per mole nitroxy group	Isoidide dinitrate	Isosorbide dinitrate	Isomannide dinitrate
87	0	3.20	1.15	0.13
100	0	8.58	2.29	0.74
115	0	25.4	15.2	8.07
115	0.5	18.8	12.7	3.3
115	1.0	13.5	10.0	3.6
115	2.0	10.3	7.9	3.1

(Table II). From these results Arrhenius activation energies of 21, 24, and 41 kcal and log frequency factors of 7.6, 8.9, and 18.3 were found for isoidide, isosorbide, and isomannide dinitrates respectively.

None of the parent diols could be detected in the reaction products by chromatography. Isohexide mononitrates were isolated and characterized but accounted for a maximum of 10% of the decomposed dinitrate in runs with aqueous pyridine; with anhydrous pyridine only traces of mononitrate could be detected. Most of the weight of the reaction products was brown-black, polymeric material. In addition to pyridinium nitrate a small amount of an unidentified, optically active oil was also isolated.

For comparison with the pyridine reaction the rate of thermal decomposition of the dinitrates was determined in four solvents with boiling points above 115° C and dipole moments ranging from 0.37 to 3.98 Debye units. The slow decomposition of isosorbide dinitrate at 100° and 115° C in these solvents is shown in Table III. The other two

TABLE III

Thermal decomposition of isosorbide dinitrate in various solvents

Solvent	μ, Debyes	Decomposition, %			
		100° C		115° C	
		25 hours	50 hours	25 hours	50 hours
Nitrobenzene	3.98	2	5	18	37
m-Xylene	0.37	6	8	23	32
s-Tetrachloroethane	1.36	4	7	25	46
Diethylcarbinol	1.64	29	40	45	53

isomers decomposed at the same rate in sym-tetrachloroethane but were not tested in the other solvents.

The rates of decomposition of the nitroxy groups were very similar in nitrobenzene, m-xylene, and sym-tetrachloroethane with first-order rate constants of 0.41×10^{-6} and 2.7×10^{-6} sec^{-1} at 100° C and 115° C respectively. The more rapid reaction in diethylcarbinol was probably due to incursion of a transnitration reaction:

$$RONO_2 + R'OH \rightleftharpoons ROH + R'ONO_2.$$
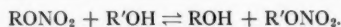
It is well established that the first and rate-determining step in the thermal decomposition of nitrate esters in the gaseous state is the fission of the oxygen–nitrogen bond, generating a free alkoxyl radical (10, 11). A similar mechanism for the first-order thermal

decomposition of the esters in the condensed state seems probable (12). Thermal decomposition of the esters in solution, however, has not been previously investigated.

For the first-order decomposition of the isohexide nitrates in the non-hydroxylic solvents the activation energy of 37 kcal/mole and log frequency factor of 15 calculated from the data of Table III were in good agreement with the values quoted for gaseous and condensed nitrate esters (10, 11, 12). This suggested a free radical mechanism for this case also. Additional evidence of a free radical mechanism was the fact that the rates were independent of the polarity of the solvent (9). Since the rate of the thermal reaction was exceeded by a factor of 5.6 in the pyridine reaction with isosorbide dinitrate at both temperatures it was concluded that thermal decomposition did not play a major part in the pyridine reaction.

It was noted that the decomposition went faster with well-dried pyridine. To test the effect of water on the rate a series of runs was made with increasing amounts of water present. There was appreciable decrease in rate with increase in water content (Table II) but the nature of the products was not altered substantially. The rate law,

$$\text{rate} = \frac{k_1 \text{ [nitrate ester]}}{1 + k_2[\text{H}_2\text{O}]},$$

was followed where k_1 was 2.54×10^{-5} and k_2 1.70 for isoidide dinitrate.

The $S_N 2$ reactions at carbon of isohexide O-derivatives, such as the replacement of sulphonoxy group by iodine, had a characteristic order of rates due to steric hindrance at one face of the molecule (5). The *endo* group (as in isomannide) reacted several times faster than the *exo* group (as in isoidide). The order of the rates of the pyridine – nitrate ester reaction, however, was exactly the reverse and hence ruled out this mechanism.

On the other hand these results were consistent with nucleophilic attack by pyridine at the nitrogen of the nitroxy group resulting in heterolytic cleavage of the low energy O—NO$_2$ bond.

$$\text{C}_5\text{H}_5\text{N}: \quad \overset{\text{O} \quad \text{O}}{\underset{|}{\overset{\diagdown\diagup}{\text{N}}}} \quad \rightarrow \quad [\text{C}_5\text{H}_5\text{N}:\text{NO}_2]^+ \quad \text{RO}^-$$
$$\text{OR}$$
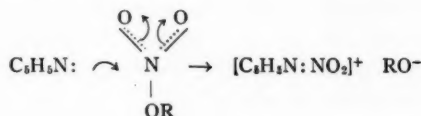
The approach of the bulky pyridine molecule to the *exo*-nitroxy group would be least hindered by the isohexide skeleton in this case. The unstable N-nitrated pyridine intermediate was recently synthesized by Oláh and co-workers by direct nitration of pyridine with nitronium tetrafluoroborate (13). This mechanism also agrees with retention of configuration at asymmetric carbons actually found with the hexitol hexanitrates. The subsequent reaction of the alkoxide ion led to polymer formation in the isohexide case. The failure to detect the parent diols was not due to their decomposition since they could be added to the reaction mixture and recovered quantitatively.

The nitroxy groups in the isohexide isomers were well separated on the carbon chain, and, except in the case of isomannide dinitrate (Fig. 1), were also well separated in space. These isolated groups reacted only slowly with pyridine. In the hexitol hexanitrates the secondary nitroxy groups were contiguous and closely packed; steric compression in the initial state was clearly indicated by the molecular models. The proximity of the α-nitroxy groups must therefore be of considerable importance in the activation of the center groups and in the lifetime of the alkoxide ion.

EXPERIMENTAL

1,4;3,6-Dianhydrohexitols (cis-Isohexides)

Isomannide and isosorbide were prepared from D-mannitol and sorbitol respectively by the method of Wiggins (14). Isoidide was most conveniently prepared, together with isosorbide, through hydrogenation of L-sorbose followed by dehydration.

L-Sorbose (50 g) in water (200 ml) was hydrogenated at 55 p.s.i. and 80° C for 4 hours with Raney nickel catalyst (from 10 ml of the alcoholic sludge). The catalyst and solvent were removed and the residue was dissolved in concentrated hydrochloric acid (300 ml). The solution was saturated with hydrogen chloride and refluxed for 24 hours. Hydrogen chloride was removed by repeated evaporation under reduced pressure alternated with addition of water, and the residual sirup was fractionally distilled under reduced pressure: fraction 1, b.p. 135–140° C at 0.18–0.20 mm, 8 g, crystallized (isosorbide); fraction 2, b.p. 140–143° C at 0.20–0.22 mm, 5 g, sirup (mixture); fraction 3, b.p. 143–155° C at 0.22–0.25 mm, 12 g, crystallized (isoidide). Fraction 3 after recrystallization from ethyl acetate had m.p. 44–46° C and specific rotation in water $[\alpha]_D^{23}$ +21.0° (c, 1.1). Cope and Shen (4) reported m.p. 43–45.5° C, $[\alpha]_D^{25}$ +18.7° (c, 2; water) for isoidide.

1,4;3,6-Dianhydrohexitol Dinitrates (I–III)

The nitrate esters were prepared from the isohexides by the method of Forman et al. (6) in a yield of about 50%; the yield was increased to 85–90% by nitration in acetic anhydride – nitric acid – acetic acid mixture.

Fuming nitric acid (sp. gr. 1.45, 5 ml) was slowly added to acetic acid – acetic anhydride (1:1, 15 ml) maintained at −2 to 5° C. The mixture was added dropwise, with stirring, to the isohexide (2 g) in acetic acid – acetic anhydride (2:1, 15 ml) maintained at 0° C. After standing for 2 hours at 5° C the mixture was poured into ice water (400 ml). Part of the nitrate ester (2.2 g) crystallized out on standing for 18 hours at 20° C and a further amount (0.6 g) was recovered by ether extraction of the mother liquor. The esters were recrystallized from methanol and analyzed for nitrate–nitrogen (Table I). The infrared spectra of the isomers (potassium bromide window) showed covalent nitrate group absorption at 1650, 1265, and 750 cm^{-1} and no hydroxyl or carbonyl peaks.

Hydrogenation of the nitrates in alcohol solution over palladium–charcoal (1) gave the parent diols in 90–98% yield.

Decomposition of Isohexide Dinitrates in Solution

(a) Solvents

Reagent grade pyridine was distilled and the middle fraction of 80% was collected and dried over calcium hydride for 48 hours, decanted, and redistilled immediately before use. Reagent grade nitrobenzene was dried over calcium chloride, distilled, redried over phosphorus pentoxide, and redistilled under reduced pressure. m-Xylene and sym-tetrachloroethane were dried over calcium chloride and distilled. Technical grade diethyl-carbinol was dried over anhydrous sodium sulphate and distilled and the middle fraction was used.

(b) Decomposition in Pyridine

The reactions were conducted in glass bulbs (2.5-cm diameter) with long stems (30 cm) fitted with water jackets and closed by drying tubes containing Drierite. An initial concentration of 0.100 g of isohexide dinitrate in 2 ml pyridine was used (0.424 mole nitroxy group per liter). The bulbs were heated in an oil bath for reactions at 115° C (reflux temperature), in the vapor of boiling water (100° C), or in the vapor of a boiling two-layer mixture of 2-butanol and water (87° C).

Aliquots of the reaction mixture (0.100 or 0.200 ml) were removed at intervals, distilled water (2 ml) was added, and the mixture was extracted three times with 1-ml portions of ether. Tests with added amounts of the dinitrates showed that extraction was then complete. The combined ether extracts were made up to 10 ml and 1-ml samples were taken for colorimetric determination of nitrate ester (15, 16).

The nitrate sample, containing 10–80 μg nitrogen, was added to 15 ml of 70% (v/v) sulphuric acid in a 250-ml flask and 1 ml of a 1% solution of 3,4-dimethylphenol was added. After being mixed, the solution was let stand for 30–60 minutes at 30° C. Water (150 ml) was then added, boiling stones introduced, and the flask fitted with a U-shaped distilling tube leading into a 25-ml volumetric flask containing 2% sodium hydroxide solution (2.5 ml). Distillation was carried out with the volumetric flask cooled in ice water and 20 ml of distillate was collected. The distillate was made up to 25 ml and brought to 24.0±0.5° C before colorimetric estimation at 435 mμ in a Bausch and Lomb Spectronic 20 colorimeter. The nitrate–nitrogen content of the sample was given by O.D.×103 = μg nitrogen.

(c) Thermal Decomposition in Solution

The nitrate ester (50 mg) and solvent (1 ml) were placed in a reaction bulb as used in the pyridine studies and heated in the vapor of boiling diethylcarbinol (114–115° C). After the reaction period the contents of the bulb were transferred with ether to a 7.5 mm ×20 em column of alumina (Alcoa Grade F-20, acid-washed, activated at 400° C for 4 hours). The column was eluated with ether followed by ether – ethyl acetate (9:1). Fractions of the eluate containing nitrate (diphenylamine test) were pooled and evaporated under reduced pressure. The residual sirupy dinitrates crystallized on seeding and were identified by their melting and mixed melting points.

(d) Reaction Products

Isohexide dinitrate (5 g) in pyridine (50 ml) was refluxed under anhydrous conditions until 50–90% decomposed. The mixture was poured into water (500 ml), extracted with ether (600 ml), and the solutions were filtered. The precipitate was a brown-black amorphous solid (product A, 0.5–1.5 g).

The ether solution was evaporated to dryness *in vacuo* to remove traces of pyridine and yielded a pale brown sirup (0.5–2.5 g). Samples of this sirup were chromatographed on paper in hexane–methanol solvent (17). Unreacted isohexide dinitrate and a faint nitrate-containing spot with lower R_f value were detected in the products from each reaction. Quantitative separation was obtained by chromatography on alumina columns developed with ether – ethyl acetate (9:1) followed by acetone–methanol (1:1). The ether – ethyl acetate fractions yielded unreacted isohexide dinitrate which was recrystallized and characterized by mixed melting point determinations.

The acetone–methanol fractions yielded a small amount of sirup which had R_f 0.05 on papergrams developed with hexane–methanol. The nitrate–nitrogen content was 5.6% (required for isohexide mononitrate, 7.3%). Complete nitration of the sirup gave a spot running parallel to isohexide dinitrate on papergrams.

The aqueous solution was evaporated *in vacuo* to a dark red sirup (0.5–1.5 g). Extraction of the sirup with hot ethanol (50 ml) left a brown, amorphous solid (product B, 0.5–1.0 g). A red-brown sirup (0.5–1.5 g) was recovered on evaporation of the ethanol solution. Celite column chromatography with 1-butanol – water as solvent (18) showed that this sirup contained no isohexide since the fractions had zero optical rotation. Isohexide added to the initial reaction mixture in some runs was recovered quantitatively from the Celite column by this technique.

The alcohol extract was subjected to ion-exchange and charcoal chromatography and pyridinium nitrate (0.2–0.8 g) was isolated together with a trace of an acidic, optically active oil.

Products A and B burned slowly in a Bunsen flame and were insoluble in organic solvents and water. Product A partially dissolved in 3 N sodium hydroxide solution and product B was soluble in aqueous pyridine and in 0.1 N sodium hydroxide solution. A brown-black solid was precipitated from the latter solution on acidification or addition of alcohol. Infrared spectra of the solid fractions thus obtained were very similar to each other and no functional groups could be identified. It was concluded that products A and B were polymers differing mainly in molecular weight.

ACKNOWLEDGMENTS

REFERENCES

1. L. D. HAYWARD. J. Am. Chem. Soc. 73, 1974 (1951).
2. G. G. McKEOWN and L. D. HAYWARD. Can. J. Chem. 33, 1392 (1955).
3. T. URBANSKI and S. KWIATKOWSKA. Roczniki Chem. 25, 312 (1951).
4. A. C. COPE and T. Y. SHEN. J. Am. Chem. Soc. 78, 3177 (1956).
5. M. JACKSON and L. D. HAYWARD. Can. J. Chem. 37, 1048 (1959).
6. S. E. FORMANN, C. J. CARR, and J. C. KRANTZ. J. Am. Pharm. Assoc. 30, 132 (1941).
7. L. F. WIGGINS. Advances in Carbohydrate Chem. 5, 206 (1950).
8. L. GOLDBERG. Acta Physiol. Scand. 15, 173 (1948).
9. C. K. INGOLD. Structure and mechanism in organic chemistry. Cornell Univ. Press, Ithaca, N.Y. 1953.
10. J. B. LEVY. J. Am. Chem. Soc. 76, 3254 (1954).
11. P. GRAY and A. WILLIAMS. Chem. Revs. 59, 239 (1959).
12. M. A. COOK. The science of high explosives. Reinhold Publishing Corp., New York. 1958.
13. G. OLÁH, I. KUHN, and A. MLINKÓ. J. Chem. Soc. 4257 (1956).
14. L. F. WIGGINS. J. Chem. Soc. 4 (1945).
15. H. BARNES. Analyst, 75, 388 (1950).
16. A. C. HOLLER and R. V. AUCH. Anal. Chem. 21, 1385 (1949).
17. D. F. MEIGH. Nature, 169, 706 (1952).
18. R. U. LEMIEUX, C. T. BISHOP, and G. E. PELLETIER. Can. J. Chem. 34, 1365 (1956).

THE ELECTRON SPIN RESONANCE SPECTRA OF THE POSITIVE AND NEGATIVE IONS OF DIPHENYLENE[1]

C. A. McDowell and J. R. Rowlands

ABSTRACT

The electron spin resonance spectra of the positive and negative ions of diphenylene have been measured. It has been found that these spectra consist of five lines showing that the observed hyperfine interaction is caused by four equivalent protons. The over-all extent of the positive ion spectrum is 18 gauss compared with that of 12.9 gauss for the negative ion. The hyperfine splittings observed are 4.0 gauss and 2.75 gauss respectively.

INTRODUCTION

The electron spin resonance spectra (e.s.r.) of both positive and negative ions of a number of alternant hydrocarbons have been measured in recent years (1). It has been shown that the qualitative features of the experimental spectra can be interpreted by use of unpaired electron spin densities calculated from the simple Hückel molecular orbital theory. The hyperfine interactions found in the e.s.r. spectra of these aromatic hydrocarbon ions are attributed to interactions between the odd electron spin and the nuclear spins of the protons attached to the carbon atoms. It has been shown that the hyperfine splitting produced by a proton attached to a given carbon atom is linearly proportional to the unpaired electron density on that carbon atom (2), i.e.,

$$[1] \qquad \Delta H = Q\rho_\mu,$$

where ΔH is the hyperfine splitting observed, and ρ_μ is the odd electron spin density on carbon atom μ.

From the properties of even alternant hydrocarbons it is evident that the odd electron spin densities on carbon atom μ, of an electron moving in a molecular orbital ϕ_i, are given by the equation

$$[2] \qquad \rho_\mu = c_{i\mu}^2.$$

It has been shown (3) that the atomic orbital coefficients $c_{i\mu}$ in paired orbitals are equal in magnitude, i.e. if orbitals ϕ_i and ϕ_j are paired in energy, then

$$[3] \qquad c_{i\mu} = \pm c_{j\mu}.$$

We can, therefore, expect that if ΔH^+ is the hyperfine splitting found in the monopositive ion, and ΔH^- that of the mononegative ion of a particular alternant hydrocarbon, and if Q is the same for both species, then

$$[4] \qquad \Delta H^+ = \Delta H^-.$$

It has been found experimentally for alternant hydrocarbons that although both species give the same number of components of hyperfine interaction, the over-all width of the monopositive ion spectra is in general about 4 gauss greater than the corresponding mononegative ions (1). The complexity of the spectra has made the determination of hyperfine splitting constants difficult. Where an analysis of the experimental spectra is possible, we have a choice of (i) assuming that the unpaired spin densities in both positive and negative ions are equal and are predicted accurately by the Hückel theory, and determining suitable values of the proportionality constant Q for the two species, or (ii)

assuming that this proportionality constant Q is the same for the two species, and is in fact constant for all even alternant hydrocarbons, and comparing the experimentally determined spin densities with those predicted from the Hückel molecular orbital theory.

In this paper on the ions of diphenylene the latter procedure has been followed.

EXPERIMENTAL

The mononegative ion of diphenylene was prepared by distilling dry tetrahydrofuran under vacuum into a bulb containing a freshly prepared sodium film. Attached to the bulb via a side arm was a narrow tube which held the diphenylene. The bulb was sealed off from the solvent source by freezing both sides with liquid nitrogen, pumping off any unfrozen tetrahydrofuran, and then sealing off at a constriction just above the neck of the bulb. When the solvent in the bulb was at room temperature the diphenylene was dissolved in it by shaking. The diphenylene then immediately reacted with the sodium to give a solution of the mononegative ion. Measurements of the e.s.r. spectra were then made by tipping the solution into the narrow tube, which was then placed in the cavity of the spectrometer operating in a TE012 mode. All the spectra were recorded on a high-resolution electron spin resonance spectrometer operating at 9000 Mc/sec. The magnetic field of approximately 3300 gauss was supplied by a Varian 6-in. magnet with shimmed pole faces. A modulating frequency of 10 kc/sec was used and the derivation of the spectra recorded on a Leeds & Northrup recorder as phase-sensitive detection was used. The monopositive ion of diphenylene was prepared by dissolving the hydrocarbon in concentrated sulphuric acid. Calibrations of all runs were made, by determining with the e.s.r. spectrum of Fremi's salt under identical sweep conditions.

RESULTS

The spectra of the negative and positive ions of diphenylene are shown in Figs. 1 and 2, together with the integrated absorption curves for each case. Each ion gives a spectrum containing five completely resolved lines with approximate intensity ratios of 1:4:6:4:1. No further hyperfine splitting could be detected for either ion, although the spectra were

13 gauss
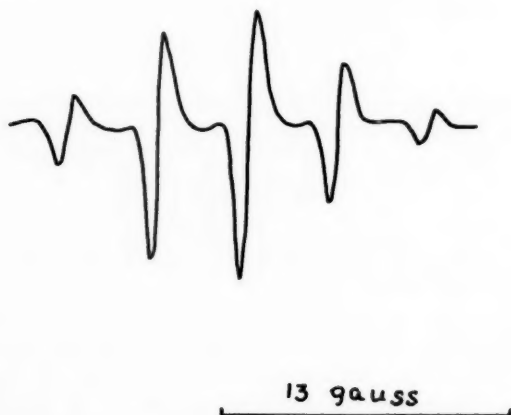
FIG. 1. The electron spin resonance absorption spectrum of the diphenylene positive ion in concentrated sulphuric acid.

13 gauss
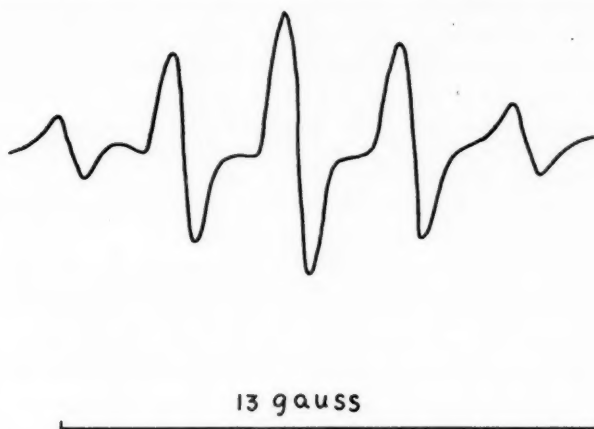
FIG. 2. The electron spin resonance absorption spectrum of the diphenylene negative ion in tetrahydrofuran.
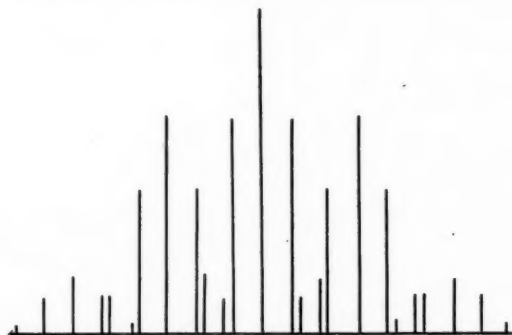
FIG. 3. Theoretical electron spin resonance absorption spectrum of diphenylene positive (or negative) ion on the Hückel molecular orbital approximation.

measured over a range of concentrations. Figure 3 is the theoretical spectrum built up using the calculated Hückel spin densities, assuming that all Coulomb integrals for the carbon atoms are the same and that all resonance integrals for the C—C bonds are also equal. The theoretical spectra of both positive and negative ions are of course identical on this picture.

DISCUSSION

It can be seen from Figs. 1 and 2 that the observed spectra consist of five lines. These lines are well resolved and there is no trace of any other fine structure on the spectra of either the positive or negative ion even when spectra have been taken with extreme care and very high resolution. The theoretical spectrum calculated from the Hückel electron densities indicates that there are 25 lines to be expected (see Fig. 3). Our observed spectra must, therefore, be interpreted on the assumption that there are only four equivalent protons contributing to the hyperfine splitting. These can be taken to be the protons attached to carbon atoms 2, 3, 6, and 7, which of the two sets of carbon atoms with protons

attached are those having the highest electron density on the Hückel theory. Carbon atoms 9, 10, 11, and 12 have no protons attached and for this reason the e.s.r. spectra of the ions of diphenylene extend only over about half the range observed for the ions of other alternant hydrocarbons. Thus the spectrum of the positive ion of diphenylene extends over only 18 gauss compared with about 33 gauss for the anthracene positive ion. The spin densities on carbon atoms 9, 10, 11, and 12 total about 54% of the total spin densities at all the carbon atoms in diphenylene; hence we would expect the e.s.r. spectrum of this substance to extend only over about half the range of spectrum of say the anthracene positive ion. This is in agreement with our observations.

Although the intensity distribution of the experimental spectra of the two ions is the same, there is a marked difference in the magnitude of the hyperfine interaction. The over-all width of the positive ion spectrum is 18 gauss, with a splitting constant of 4.0 gauss. The corresponding figures for the negative ion are 12.9 gauss and 2.75 gauss respectively.

If we take the value of the proportionality constant Q to be the same for the two species, then there is a difference in the odd electron distribution in the two ions. In Table I we have listed the experimental spin densities for the two ions, obtained by using a value of Q derived from the benzene negative ion spectrum, which is the only alternant hydrocarbon

TABLE I

Electron spin densities for the mononegative and monopositive ions of diphenylene
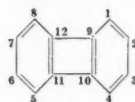
		Expt.	Calc., Hückel theory	Calc., assuming $\alpha_{C_9} = \alpha_C + 1/5\,\beta$
Diphenylene$^+$ ion				
	ρ_1		0.0269	0.0179
	ρ_2	0.1739	0.0873	0.0906
	ρ_9	0.0000	0.1360	0.1414
Diphenylene$^-$ ion				
	ρ_1		0.0269	0.0372
	ρ_2	0.1195	0.0873	0.0853
	ρ_9	0.0000	0.1360	0.1274

for which accurate spin densities are known. Column 2 of Table I lists the spin densities calculated from the Hückel theory, with the assumption of equal Coulomb integrals for the carbon atoms. In column 3 of the table we have included spin densities obtained by assigning the four central carbon atoms with a Coulomb integral equal to the normal carbon Coulomb integral *plus one-fifth* the carbon–carbon resonance integral. It may be seen from the table that this makes the calculated spin densities of the positive ion different from those of the negative ion. Since in diphenylene we are studying a derivative of cyclobutadiene, it is quite plausible that we should treat it as containing two different types of carbon atom. It is quite obvious from the lack of agreement between experiment and theory that the simple Hückel molecular orbitals obtained by the assumption of equal Coulomb and resonance integrals are inadequate. It must, however, be recalled that other workers have previously noted that exact agreement between the electron densities calculated from the simple Hückel molecular orbital theory and the experimental values

is lacking. Further it has also been observed that in other alternant hydrocarbon systems there are significant differences between the positive and negative ion spectra which cannot be explained on the basis of the simple Hückel molecular orbital theory.

ACKNOWLEDGMENTS

REFERENCES

1. T. R. TUTTLE, Jr., R. L. WARD, and S. I. WEISSMAN. J. Chem. Phys. **25,** 189 (1956).
2. S. I. WEISSMAN and E. DE BOER. J. Am. Chem. Soc. **80,** 4549 (1958).
3. S. I. WEISSMAN. J. Chem. Phys. **25,** 890 (1956).
4. H. M. McCONNELL. J. Chem. Phys. **24,** 764 (1956).
5. H. S. JARRETT. J. Chem. Phys. **25,** 1289 (1956).
6. C. A. COULSON and G. S. RUSHBROOKE. Proc. Cambridge Phil. Soc. **36,** 193 (1940).

THE CHEMISTRY OF THE "AMINOCHROMES"

PART III. ON THE STRUCTURES OF "IODOÖXOADRENOCHROME" AND IODOEPINOCHROME[1,2]

R. A. HEACOCK AND B. D. SCOTT

ABSTRACT

A substance prepared by the oxidation of adrenaline with iodic acid and described in the literature as 2-idoöxoadrenochrome appears, after consideration of a number of its physical and chemical properties to be identical with 2-iodoadrenochrome. The iodine atom in iodo-epinochrome, obtained by the oxidation of epinine with potassium iodate, has been shown to be in the 2-position of the heterocyclic ring in the molecule.

During the course of a study of the infrared spectra of the aminochromes and related compounds (1) it was observed that the spectrum of a substance described by Macciotta as 2-iodoöxoadrenochrome (formulated as I) (2) was identical with those obtained from
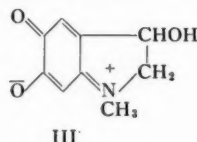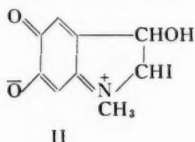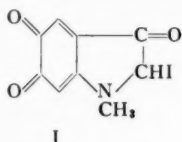
specimens of 2-iodoadrenochrome (usually formulated as II) prepared by the methods described in the literature (3, 4, 5, 6). The general form of the spectrum was more in keeping with a structure of type II than with one of type I. A definite hydrogen-bonded O—H stretching band was observed at 3410 cm^{-1} (microanalysis indicated that the compounds were anhydrous and therefore this peak could not have arisen from water of crystallization in I, and the "carbonyl" region was very similar to that of adrenochrome, usually formulated as III (cf. 7). It occurred to the authors that the possibility that Macciotta's compound was, in fact, merely 2-iodoadrenochrome (II) should be investigated, especially since no other "oxoaminochromes" have been isolated. The preparation, in solution, of "oxoadrenochrome" was reported (8), but this claim has since been disputed (9).

These compounds, which are very dark violet-brown in color, decompose on heating without melting and consequently melting point and mixed melting point determinations gave only inconclusive results. The analytical values obtained for carbon, hydrogen, and nitrogen were in good agreement in both cases with those calculated for II, although it must be admitted that only the hydrogen values are sufficiently different in the two cases to warrant drawing any conclusions. The ultraviolet and visible absorption spectra of I and II were identical and very similar to those of 2-iodoaminochromes in general (cf. 3). If I had the structure assigned to it by Macciotta it would contain a different chromophoric system to the 2-iodoaminochromes and would be expected to exhibit a different absorption spectrum.

Macciotta reported that reduction of I with sodium hydrosulphite gave 3,5,6-

trihydroxy-2-iodoindole (IV: R = H), m.p. 116°, which gave a triacetyl derivative (IV: R = CH₃CO), m.p. 140°. In the hands of the authors the sodium hydrosulphite

IV

V

reduction products of I and II were identical. This was demonstrated by paper chromatography of the crude reaction mixtures and by the physical and chemical pr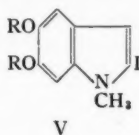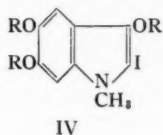operties of the crystalline compounds isolated in each case. The infrared spectra of these products were much more consistent with their being 5,6-dihydroxy- rather than 3,5,6-trihydroxyindoles. In the latter case the product would be an indoxyl which would exist in the keto form in the solid state and consequently its infrared spectrum should show the indoxyl carbonyl peak (7, 10). However there are no peaks in the "carbonyl" region of the spectra of either of these substances. Their ultraviolet absorption spectra resemble that of 5,6-dihydroxy-N-methylindole more closely than that of adrenolutin, the corresponding 3,5,6-trihydroxy derivative. These products are considered by the present authors to be 5,6-dihydroxy-2-iodo-N-methylindole (V: R = H). The diacetyl derivatives of both reduction products were also identical; the m.p.'s of 151.5–152.5° and 152° (derived from I and II respectively) obtained by the authors for these products are very similar to the value quoted by Bergel and Morrison (153–155°) for a substance described as 5,6-diacetoxy-2-iodo-N-methylindole (V: R = CH₃CO) obtained by the direct acetylation of the crude sodium hydrosulphite reduction products of 2-iodoadrenochrome (11).

The reaction mixtures obtained from the reduction of I and II with several reducing agents including sodium hydrosulphite, sodium bisulphite, sodium borohydride, zinc and 2% acetic acid, ascorbic acid, B.A.L. (2,3-dimercapto-1-propanol), and glutathione were studied paper chromatographically (cf. 12). It can easily be seen by inspection of Table I that the chromatographic patterns obtained from I and II with each reducing agent were virtually identical. The main reduction product in all but two cases was 5,6-dihydroxy-2-iodo-N-methylindole (R_f ca. 0.20). (The standard R_f value for this substance was obtained from a specimen of the pure crystalline material isolated from the sodium hydrosulphite reduction products.) It was also noticed that with most of the reagents studied, greater or lesser amounts of 5,6-dihydroxy-N-methylindole ($R_f = 0.44 \pm 0.02$) were produced presumably by the elimination of the iodine atom during the process of reduction; when reduction was effected with zinc and dilute acetic acid, total deiodination occurred and no 5,6-dihydroxy-2-iodo-N-methylindole was detected among the products. The reduction of the aminochromes will be discussed in more detail in a later paper in this series (13); the results of the chromatographic studies are merely presented here to support the author's thesis of the similarity of I and II.

3,5,6-Triacetoxy-2-iodo-N-methylindole (IV: R = CH₃CO) was obtained from the action of acetic anhydride in pyridine on II (4), and an identical triacetyl derivative was prepared from I by the same experimental procedure.

The oxidation of epinine (3,4-dihydroxyphenylethylmethylamine) with potassium iodate in aqueous solution gives iodoepinochrome, a violet-brown crystalline solid (3, 14). There has been some disagreement in the literature as to the position of the iodine atom; Sobotka and Austin suggested the 2-position (3), whilst Bu'Lock and Harley-Mason proposed that the iodine atom was present in the 3-position (14), since the 5,6-diacetoxy-

TABLE I

Paper chromatography of some reduction products of 2-iodoöxoadrenochrome (I)
and 2-iodoadrenochrome (II)

Average R_f values and color reactions† of major spots derived from the reduction products of I and II

Reducing agents and chromogenic reagents	2-Iodoadrenochrome (II)					2-Iodoöxoadrenochrome (I)				
Sodium hydrosulphite	21		45[w]	82[*w]	90[*]	20		44[w]	80[*w]	92[*]
Ehr.	BV		BV	Y[s]	RV[s]	BV		BV	Y[s]	RV[s]
DPNA	VBr		VBr	RBr	RBr	VBr		VBr	RBr	RBr
F and C	BGy		BGy	BGy	BGy	BGy		BGy	BGy	BGy
Gib.	Br		Br	Br	VBr	Br		Br	Br	VBr
Sodium bisulphite			67[w]	84[*w]	90[*]			64[w]	83[*w]	90[*]
Ehr.			V[w]	Y[s]	RV[s]			V	Y[s]	RV[s]
F and C			BGy	BGy	BGy			BGy	BGy	BGy
Gib.			Br	Br	VBr			Br	Br	VBr
Sodium borohydride	22		46[vw]	87[w]		20		46[vw]	83[w]	
Ehr.	BV		BV	RV[s]		BV		BV	RV[s]	
DPNA	VBr		VBr	—		VBr		VBr	—	
Gib.	Br		Br	Br		Br		Br	Br	
Zinc and dilute acetic acid		44		87[w]			46		86[w]	
Ehr.		BV		YBr[s]			BV		YBr[s]	
DPNA		VBr		Br[s]			VBr		Br[s]	
F and C		BGy		BGy			BGy		BGy	
Gib.		Br		Br			Br		Br	
Ascorbic acid	20	31	41[w]	56[w]	86	20	30	42[w]	55[w]	82
Ehr.	BV	GBr	BV	BG	Y[s]	BV	GBr	BV	BG	Y[s]
Fe.	B	B	B	B	B	B	B	B	B	B
Gib.	Br	Br	Br	Br	VBr	Br	Br	Br	Br	VBr
B.A.L.	21		44[w]	72[vw]	83	22		45[w]	75[vw]	83
Ehr.	BV		BV	V	P[s]	BV		BV	V	P[s]
DPNA	VBr		VBr	—	0	VBr		VBr	—	0
F and C	BGy		BGy	B	B	BGy		BGy	B	B
Glutathione	21		44[w]	67	88	20		43[w]	62	89
Ehr.	BV		BV	V	Y[s]	BV		BV	V	Y[s]
Cin.	P		OBr	O	OBr[s]	P		OBr	O	OBr[s]
F and C	BGy		BGy	B	B	BGy		BGy	B	

REAGENTS: Ehr. = Ehrlich's reagent; Cin. = cinnamaldehyde; DPNA = diazotized p-nitroaniline; F and C = Folin and Ciocalteu's reagent; Fe = ferric chloride/potassium ferricyanide; Gib. = Gibb's reagent.

COLORS: BV = blue-violet; RV = red-violet; V = violet; B = blue; VBr = violet-brown; BGy = blue-grey; Br = brown; Y = yellow; BG = blue-green; GBr = green-brown; RBr = red-brown; YBr = yellow-brown; P = pink; O = orange; OBr = orange-brown.

SUPERSCRIPTS: w = only weak color reactions obtained from this spot; vw = only a very weak color reaction obtained from this spot; * = there appear to be two substances produced both by $Na_2S_2O_4$ and by $NaHSO_3$ of high R_f which are not efficiently separated with this solvent system; s = color develops slowly. †Color observed after 24 hours.

iodo-N-methylindole obtained from the action of acetic anhydride and pyridine on iodo-epinochrome had m.p. 146–147°, whereas the 5,6-diacetoxy-iodo-N-methylindole obtained from 2-iodoadrenochrome by Bergel and Morrison (11) had m.p. 153–155°. We have repeated the preparation of these two 5,6-diacetoxy-iodo-N-methylindoles from iodoepino-chrome and iodoadrenochrome and obtained m.p.'s of 148–150° and 152° respectively; a mixed melting point showed no depression. The infrared spectra ("NUJOL" mulls and chloroform solutions), and the ultraviolet absorption spectra of the two 5,6-diacetoxy-iodo-N-methylindoles were identical, indicating that the iodine atom was in the same position in the heterocyclic ring in both cases; Harley-Mason is now also of this opinion (15). Preliminary paper chromatographic examination of the products obtained from the treatment of iodoepinochrome with a number of reducing agents indicated that a complex mixture of products was usually obtained, but that the internal rearrangement product,

i.e. 5,6-dihydroxy-2-iodo-N-methylindole ($R_f = 0.2$), was invariably detected among the products.

In conclusion it may be stated that: (a) the oxidation of adrenaline with iodic acid, carried out under the conditions described by Macciotta, gave, in the hands of the authors, a product that behaved identically to 2-iodoadrenochrome and did not exhibit the properties that would be expected for an oxoaminochrome; (b) the oxidation of epinine with potassium iodate gave an iodoepinochrome with the iodine atom in the 2-position in the nucleus (i.e. VI).
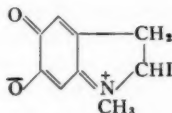
VI

EXPERIMENTAL

Oxidation of Adrenaline with Iodic Acid

Adrenaline (1.0 g) was oxidized with iodic acid according to the procedure of Macciotta (2). A brownish-violet crystalline solid (I) (1.1 g) was obtained (this was described as 2-iodoöxoadrenochrome by Macciotta). Found: C, 35.26; H, 2.62; N, 4.70. $C_9H_8NO_2I$ requires C, 35.43; H, 2.64; N, 4.59% (i.e. 2-iodoadrenochrome). $C_9H_6NO_3I$ requires C, 35.66; H, 1.99; N, 4.62% (i.e. 2-iodoöxoadrenochrome).

Oxidation of Adrenaline with Potassium Iodate

Adrenaline (1.0 g) was oxidized with potassium iodate according to the method of Sobotka and Austin (3) and 2-iodoadrenochrome (II) (1.5 g) was obtained in brownish-violet needles. Found: C, 35.11; H, 2.61; N, 4.76. $C_9H_8NO_3I$ requires C, 35.43; H, 2.64; N, 4.59%.

Reduction of I and II with Sodium Hydrosulphite (cf. Macciotta (2))

(a) A suspension of sodium hydrosulphite (2.0 g) in water (5 ml) was added to a suspension of freshly prepared I (1.0 g) in water (40 ml) and the reaction mixture stirred vigorously. The dark-violet solid dissolved with the formation of a cloudy yellow solution, from which a pale yellow flocculent precipitate separated, m.p. 96–97.5° (with decomposition), which gave pale yellow needles (product A, 0.22 g), m.p. 105–106° (with decomposition), on recrystallization from benzene – light petroleum (b.p. 80–100°).

(b) II (1.0 g) was reduced in the manner described above; the crude product, m.p. 94–95.5° (with decomposition), was recrystallized from benzene – light petroleum (b.p. 80–100°) and pale yellow needles (product B, 0.27 g), m.p. 105° (with decomposition), were obtained. A mixed melting point between the products A and B showed no depression (i.e. 105°, with decomposition). Found: product A: C, 37.66; H, 2.92%; product B: C, 37.63; H, 2.98%. $C_9H_8NO_2I$ requires C, 37.39; H, 2.79%. Macciotta, who considered product A to be 3,5,6-trihydroxy-2-iodo-N-methylindole ($C_9H_8NO_3I$ requires C, 35.43; H, 2.64), recorded a m.p. of 116°. However, consideration of the above analytical results, and those of the acetyl derivatives described below, together with the ultraviolet and infrared spectroscopic data strongly suggest that these substances are, in fact, 5,6-dihydroxy-2-iodo-N-methylindole.

Acetylation of Products A and B

The dihydroxy compound (i.e. product A or B) (0.2 g) was dissolved in acetic

anhydride (5 ml) and dry pyridine (5 ml); after standing overnight at room temperature the reaction mixture was poured into ice water and a white solid was obtained. The diacetyl derivatives were purified by recrystallization from benzene – light petroleum (b.p. 80–100°) and obtained as very pale yellow plates. Melting points: from A, 151–152.5°; from B, 152°; mixed m.p. (A+B), 151.5–152.5°. Found: C, 41.79; H, 3.30; N, 3.84; I, 33.91. $C_{13}H_{12}NO_4I$ requires C, 41.84; H, 3.24; N, 3.75; I, 34.01%. Macciotta obtained a substance, m.p. 140° (found: C, 41.52; H, 3.41; N, 3.30%), from the acetylation of the product he obtained by the reduction of I with sodium hydrosulphite which he erroneously considered to be 3,5,6-triacetoxy-2-iodo-N-methylindole. Bergel and Morrison obtained a substance, m.p. 153–155° (found: I, 33.9%), which they described as 5,6-diacetoxy-2-iodo-N-methylindole, from the acetylation of the crude sodium hydrosulphite reduction products of II (11). The substances obtained by the present authors by the acetylation of products A and B are in all probability both 5,6-diacetoxy-2-iodo-N-methylindole.

Paper Chromatographic Study of the Reduction Products of I *and* II

The method used was essentially the same as that employed by the authors for preliminary studies on the reduction of adrenochrome (12). I (or II) (0.01 g) was suspended in water (1.0 ml) and treated with a slight excess of the reducing agent at room temperature until no dark particles of the starting material remained in suspension, and the product filtered to obtain a clear solution. Spots, consisting of ca. 30 μl of the reaction mixture, were examined on Whatman No. 1 paper (previously washed for 48 hours with 2% acetic acid) using 2% acetic acid as running solvent. After drying, the developed chromatograms were examined for fluorescence in ultraviolet light and sprayed with Ehrlich's reagent, Gibb's reagent, diazotized p-nitroaniline, and Folin and Ciocalteu's reagent.

The results obtained with seven reducing agents, i.e. sodium hydrosulphite, sodium bisulphite, sodium borohydride, zinc and dilute acetic acid, ascorbic acid, B.A.L., and glutathione are given in Table I. It can be seen from the table the same reduction products are obtained from I and II in each case.

The Action of Acetic Anhydride in Pyridine on I *and* II

A solution of I (or II) (0.5 g) in a mixture of acetic anhydride (10 ml) and dry pyridine (10 ml) was allowed to stand overnight at room temperature. The reaction mixture was then poured into ice water and the white solid, which separated, recrystallized from light petroleum (b.p. 100–120°); the triacetyl derivatives were obtained in colorless prisms. Melting points: product from I, 150.5°; product from II, 148–149°; mixed m.p. 148.5–150.5°. (Found: C, 41.75; H, 3.30; N, 3.33; I, 29.42. $C_{15}H_{14}NO_6I$ requires C, 41.78; H, 3.27; N, 3.25; I, 29.44%.) In both cases the substance was 3,5,6-triacetoxy-2-iodo-N-methylindole. This substance had previously been obtained by Bu'Lock and Harley-Mason by the above procedure (m.p. 150°) (4).

The Action of Acetic Anhydride in Pyridine on Iodoepinochrome

Iodoepinochrome (0.4 g), prepared by the method of Sobotka and Austin (3), was dissolved in a mixture of acetic anhydride (10 ml) and dry pyridine (10 ml) and the solution allowed to stand at room temperature for 24 hours. The reaction mixture was then poured into ice water; a white solid separated, which gave 5,6-diacetoxy-2-iodo-N-methylindole as pale yellow prisms on recrystallization from benzene – light petroleum (b.p. 80–100°), m.p. 148–150°, undepressed on admixture with a sample prepared from 2-iodoadrenochrome by the method described above. Bu'Lock and Harley-Mason obtained a substance, m.p. 146–147°, from iodoepinochrome by the above procedure

which they considered to be 5,6-diacetoxy-3-iodo-N-methylindole (14), since its melting point differed from that (153–155°) previously reported by Bergel and Morrison for the corresponding 2-iodo compound (11).

Spectroscopic Studies

(a) Ultraviolet and Visible

The ultraviolet and visible absorption spectra of I and II, their sodium hydrosulphite reduction products (i.e. products A and B), the acetyl derivatives of A and B, the direct acetylation products of I, II, and iodoepinochrome were measured on a Warren Spectracord instrument. The results are given in Table II and it can easily be seen that

TABLE II

Ultraviolet and visible absorption spectra

Substance*	Solvent	Absorption maxima, mμ	Absorption minima, mμ
(1) "2-Iodoöxoadrenochrome" (I)	W	233; 303; 535	268; 385
(2) 2-Iodoadrenochrome (II)	W	233; 304; 535	268; 385
(3) Product A (from I)	M	282; 303; (313)†	256; 297
(4) Product B (from II)	M	282; 303; (313)	256; 296
(5) Diacetyl derivative of A	M	231; (280); 294; (303)	255
(6) Diacetyl derivative of B	M	231; (280); 293; (303)	255
(7) Product from direct acetylation of I	M	233; 302	263
(8) Product from direct acetylation of II	M	233; 301	263
(9) Product from direct acetylation of iodoepinochrome	M	231; (280); 293; (303)	254

NOTE· W = water; M = methanol.

*The above descriptions of the substances are given to indicate how each compound was obtained. In fact, (1) and (2) are both 2-iodoadrenochrome; (3) and (4) are both 5,6-dihydroxy-2-iodo-N-methylindole; (5), (6), and (9) are all 5,6-diacetoxy-2-iodo-N-methylindole; (7) and (8) are both 3,5,6-triacetoxy-2-iodo-N-methylindole.

†Figures in parentheses represent shoulders on the main peak.

the positions of the absorption maxima and minima are identical for corresponding pairs in the two series of compounds from I and II. It can also be seen that the absorption curve of the direct acetylation product of iodoepinochrome is the same as those of the diacetyl derivatives of products A and B.

(b) Infrared

The spectra were recorded on a Perkin–Elmer Infracord spectrophotometer. The spectra of I and II were obtained as "NUJOL" mulls and those of the various 5,6-dihydroxy- and 5,6-diacetoxy-indoles (i.e. compounds 3–9 in Table II) were obtained both as "NUJOL" mulls and in chloroform solution. The spectra of the corresponding pairs of substances in the two series of compounds from I and II were identical and that of the direct acetylation product of iodoepinochrome was the same as those of the diacetyl derivatives of the reduction products of I and II. The curves obtained from these last three substances together with those obtained from I and II are shown in Fig. 1.

Some of the more salient features of the infrared spectra are as follows. The products A and B (i.e. 5,6-dihydroxy-2-iodo-N-methylindole) showed a hydrogen-bonded O—H stretching band at 3240 cm^{-1} (in "NUJOL"). The ester carbonyl peak of the 5,6-diacetyl derivatives of A and B was observed at 1765 cm^{-1} (both in "NUJOL" and in chloroform). In the spectra of the direct acetylation products of I and II (i.e. 3,5,6-triacetoxy-2-iodo-N-methylindole), the main carbonyl absorption occurred at 1770 cm^{-1} in chloroform solution; in "NUJOL" the main peak was observed at 1757 cm^{-1} with a well-defined shoulder at ca. 1786 cm^{-1}.
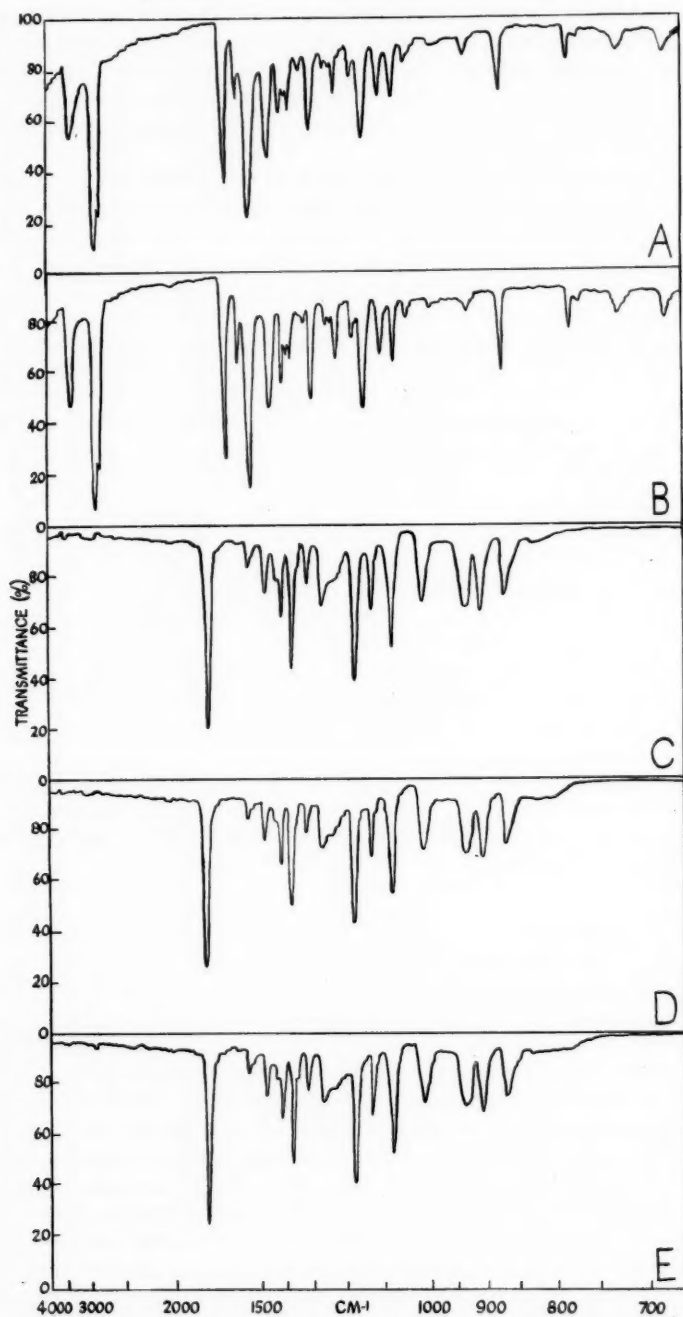
Fig. 1.

ACKNOWLEDGMENTS

REFERENCES

1. R. A. HEACOCK. In preparation.
2. E. MACCIOTTA. Gazz. chim. ital. **81**, 485 (1951).
3. H. SOBOTKA and J. AUSTIN. J. Am. Chem. Soc. **73**, 3077 (1951).
4. J. BU'LOCK and J. HARLEY-MASON. J. Chem. Soc. 712 (1951).
5. P. BOUVET. Ann. pharm. franc. **7**, 721 (1949).
6. D. RICHTER and H. BLASCHKO. J. Chem. Soc. 601 (1937).
7. R. A. HEACOCK and M. E. MAHON. Can. J. Chem. **36**, 1550 (1958).
8. G. N. COHEN. Compt. rend. **220**, 796, 927 (1945).
9. J. HARLEY-MASON. J. Chem. Soc. 1276 (1950).
10. S. J. HOLT, A. E. KELLIE, D. G. O'SULLIVAN, and P. W. J. SADLER. J. Chem. Soc. 1217 (1958).
11. F. BERGEL and A. L. MORRISON. J. Chem. Soc. 48 (1943).
12. R. A. HEACOCK and B. D. LAIDLAW. Chem. & Ind. (London), 1510 (1958).
13. R. A. HEACOCK and B. D. SCOTT. In preparation.
14. J. BU'LOCK and J. HARLEY-MASON. J. Chem. Soc. 2248 (1951).
15. J. HARLEY-MASON. Private communication. 1959.

FIG. 1. Infrared spectra of: A,* "2-iodoöxoadrenochrome" (I); B,* 2-iodoadrenochrome; C, diacetyl derivative of product A; D, diacetyl derivative of product B; E, product from the direct acetylation of iodoepinochrome.

Note: (a) A and B are both 2-iodoadrenochrome (spectra shown are of "NUJOL" mulls). (b) C, D, and E are 5,6-diacetoxy-2-iodo-N-methylindole (spectra shown are of solutions in chloroform).

*The letters A and B here refer o the infrared spectra of I and II and not to products A and B.

THE CHEMISTRY OF THE "AMINOCHROMES"

PART IV. SOME NEW AMINOCHROMES AND THEIR DERIVATIVES[1,2]

R. A. HEACOCK AND B. D. SCOTT

ABSTRACT

N-Ethylnoradrenochrome, N-isopropylnoradrenochrome, adrenochrome methyl ether, adrenochrome ethyl ether, and their 2-iodo derivatives have been prepared in crystalline form. The action of acetic anhydride in pyridine on these aminochromes has been studied; acetylated rearrangement products were obtained in each case. N-Ethylnoradrenochrome monosemicarbazone, N-ethylnoradrenolutin, 5,6-diacetoxy-N-ethyl-2-iodoindole, and 5,6-diacetoxy-2-iodo-N-isopropylindole have been prepared. The ultraviolet and visible absorption spectra of the aminochromes described above and several 5,6-diacetoxy- and 3,5,6-triacetoxy-N-alkylindoles have been measured and the paper chromatographic behavior of the unhalogenated aminochromes studied.

Adrenochrome (I: $R_1 = CH_3$; $R_2 = H$; $R_3 = OH$) (see 1 for list of references) and epinochrome (I: $R_1 = CH_3$; $R_2 = R_3 = H$) (2) are the only unhalogenated aminochromes

that have, so far, been fully characterized in the solid state. Noradrenochrome ($I: R_1 = R_2 = H$; $R_3 = OH$) has been described as "red rings on the side of the flask" (3) and N-isopropylnoradrenochrome (I: $R_1 = i\text{-}C_3H_7$; $R_2 = H$; $R_3 = OH$) is referred to in the patent literature as a purplish-red crystalline solid (4). A preliminary report on the isolation of solid adrenochrome methyl ether (I: $R_1 = CH_3$; $R_2 = H$; $R_3 = OCH_3$) has appeared recently (5). Adrenochrome is usually prepared by the oxidation of adrenaline (II: $R_1 = CH_3$; $R_2 = H$; $R_3 = OH$) in methanol with silver oxide. It has recently been demonstrated that contamination of the product with residual silver (colloidal and/or ionic) derived from the oxidizing agent was minimized by passage of the reaction mixture through a Dowex-1 (Cl⁻) resin bed prior to crystallization (6); in this way a stable crystalline product was obtained. The apparent instability of some of the earlier preparations of adrenochrome may have been due to contamination with silver. This general technique has now been successfully utilized for the preparation of crystalline N-ethylnoradrenochrome (I: $R_1 = C_2H_5$; $R_2 = H$; $R_3 = OH$) from N-ethylnoradrenaline (II: $R_1 = C_2H_5$; $R_2 = H$; $R_3 = OH$) and N-isopropylnoradrenochrome (I: $R_1 = i\text{-}C_3H_7$; $R_2 = H$; $R_3 = OH$) from N-isopropylnoradrenaline (II: $R_1 = i\text{-}C_3H_7$; $R_2 = H$; $R_3 = OH$); these two aminochromes were obtained in somewhat higher yield than the corresponding yield of adrenochrome from adrenaline. N-Ethylnoradrenochrome has also been obtained in crystalline form by the oxidation of N-ethylnoradrenaline in 90% methanol with the calculated quantity of iodic acid (cf. preparation of adrenochrome by Macciotta (7)); the N-isopropyl analogue has been obtained in the solid state by oxidation of a suspension of N-isopropylnoradrenaline hydrochloride in dry acetonitrile with silver

oxide. These compounds are stable dark red-violet crystalline solids, decomposing without melting and exhibiting very similar physical and chemical properties to adrenochrome. The monosemicarbazone of N-ethylnoradrenochrome was obtained by a standard method for the preparation of semicarbazones; N-isopropylnoradrenochrome monosemicarbazone has previously been described (8); both are bright orange crystalline solids.

Although oxidation of the adrenaline ethers (II: $R_1 = CH_3$; $R_2 = H$; $R_3 = OCH_3$ or OC_2H_5) with silver oxide in methanol gave red solutions (from which the monosemi-carbazones of the adrenochrome ethers have been isolated (9)) no solid could be isolated after cooling the solutions to $-20°$ (even after the addition of dry ether). However, oxidation of a suspension of adrenaline methyl ether hydrochloride in dry acetonitrile with silver oxide proceeded readily and crystalline adrenochrome methyl ether $(I: R_1 = CH_3; R_2 = H; R_3 = OCH_3)$ could be obtained as a dark red solid on concentration of the solution (cf. 5). Adrenochrome ethyl ether (I: $R_1 = CH_3$; $R_2 = H$; $R_3 = OC_2H_5$) was prepared similarly.

When the oxidation of catecholamines is carried out with potassium iodate in aqueous solution (under acid conditions and with excess iodate) iodine-substituted aminochromes (e.g. 2-iodoadrenochrome, I: $R_1 = CH_3$; $R_2 = I$; $R_3 = OH$) are obtained (see 1 for references). N-Ethyl-2-iodonoradrenochrome (I: $R_1 = C_2H_5$; $R_2 = I$; $R_3 = OH$) and 2-iodo-N-isopropylnoradrenochrome (I: $R_1 = i$-C_3H_7; $R_2 = I$; $R_3 = OH$) have been obtained in good yield by the oxidation of N-ethylnoradrenaline and N-isopropylnor-adrenaline respectively with potassium iodate, by an adaptation of the procedure described by Sobotka and Austin for the preparation of 2-iodoadrenochrome (2). The isopropyl derivative was obtained previously in lower yield by a slightly different procedure, the oxidation being carried out in more concentrated solution (8). The oxidation of adrenaline methyl and ethyl ethers with potassium iodate by the dilute solution technique (cf. 2) gave deep violet solutions but no precipitation of the iodoaminochrome occurred; however, when the reaction was carried out in more concentrated solution (cf. Bu'Lock and Harley-Mason's general procedure for the preparation of iodoaminochromes (8)) 2-iodoadrenochrome methyl ether (I: $R_1 = CH_3$; $R_2 = I$; $R_3 = OCH_3$) and 2-iodoadreno-chrome ethyl ether (I: $R_1 = CH_3$; $R_2 = I$; $R_3 = OC_2H_5$) were obtained as brownish-purple crystalline solids.

The well-known hydroxyl ion catalyzed rearrangement of aminochromes to 5,6-dihydroxyindoles or 5,6-dihydroxyindoxyls (see 1 for references) has been extended to the preparation of N-ethyl-5,6-dihydroxyindoxyl (i.e. "N-ethylnoradrenolutin" (III)); the

III   IV
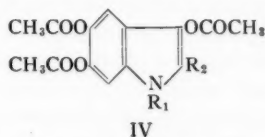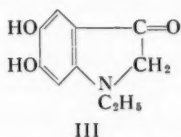
N-isopropyl analogue has previously been described (8). Aqueous solutions of N-ethyl-5,6-dihydroxyindoxyl resemble those of the corresponding N-methyl and N-isopropyl compounds in exhibiting a very strong apple-green fluorescence, and also in being unstable in air, rapidly undergoing a destructive oxidation resulting in the disappearance of the fluorescence followed by the formation of a black melanitic precipitate. The treatment of an aminochrome with acetic anhydride in the presence of pyridine leads to the forma-tion of acetylated rearrangement products (8, 10, 11) (e.g. adrenochrome gives 3,5,6-triacetoxy-N-methylindole (IV: $R_1 = CH_3$; $R_2 = H$)). 3,5,6-Triacetoxy-N-ethylindole

(IV: $R_1 = C_2H_5$; $R_2 = H$), 3,5,6-triacetoxy-N-isopropylindole (IV: $R_1 = i\text{-}C_3H_7$; $R_2 = H$), and 3,5,6-triacetoxy-N-ethyl-2-iodoindole (IV: $R_1 = C_2H_5$; $R_2 = I$) have been obtained in this manner from the corresponding aminochromes. Adrenochrome methyl and ethyl ethers and their 2-iodo derivatives appeared to behave similarly on treatment with acetic anhydride and pyridine. The products obtained analyzing well for 5,6-diacetoxy-3-methoxy-N-methylindole (V: $R_1 = CH_3$; $R_2 = H$; $R_3 = OCH_3$), 5,6-diacetoxy-3-ethoxy-N-methylindole (V: $R_1 = CH_3$; $R_2 = H$; $R_3 = OC_2H_5$), 5,6-diacetoxy-2-iodo-3-methoxy-N-methylindole (V: $R_1 = CH_3$; $R_2 = I$; $R_3 = OCH_3$), and 5,6-diacetoxy-3-ethoxy-2-iodo-N-methylindole (V: $R_1 = CH_3$; $R_2 = I$; $R_3 = OC_2H_5$)

V
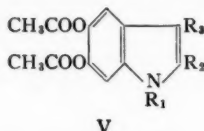
respectively. The infrared spectra ("NUJOL" mulls) of the acetylated rearrangement products from adrenochrome methyl and ethyl ethers and from 2-iodoadrenochrome methyl ether exhibited a double ester "carbonyl" peak (e.g. the product from the methyl ether had two distinct peaks at 1770 and 1752 cm^{-1}). This behavior was in contrast to that observed in the spectra of several other 5,6-diacetoxy-N-alkylindoles available to the authors, which show only a single peak in the carbonyl region (e.g. 5,6-diacetoxy-2-iodo-N-methylindole has a single peak at 1765 cm^{-1}, cf. 12) and the product obtained from 2-iodoadrenochrome ethyl ether also showed only a single peak in this region at 1761 cm^{-1}.

5,6-Diacetoxy-2-iodo-N-methylindole (V: $R_1 = CH_3$; $R_2 = I$; $R_3 = H$) was obtained by Bergel and Morrison by the acetylation of the crude sodium hydrosulphite reduction products of 2-iodoadrenochrome (13); recently the intermediate 5,6-dihydroxy-2-iodo-N-methylindole has been isolated in crystalline form, and gave the same product (i.e. V: $R_1 = CH_3$; $R_2 = I$; $R_3 = H$) on acetylation (12). By an extension of this procedure 5,6-diacetoxy-N-ethyl-2-iodoindole (V: $R_1 = C_2H_5$; $R_2 = I$; $R_3 = H$) and 5,6-diacetoxy-2-iodo-N-isopropylindole (V: $R_1 = i\text{-}C_3H_7$; $R_2 = I$; $R_3 = H$) have been prepared by acetylation of the reduction products (obtained with sodium hydrosulphite or sodium borohydride) of N-ethyl-2-iodonoradrenochrome or 2-iodo-N-isopropylnoradrenochrome respectively.

It was reported in an earlier paper in this series that the paper chromatography of adrenochrome could be carried out satisfactorily on acid-washed paper using water or 2% acetic acid/water as running solvents, but that the employment of other common solvent systems usually resulted in decomposition of the adrenochrome (6). In the course of a chromatographic study of the reduction products of the aminochromes derived from "dopa" (3,4-dihydroxyphenylalanine, II: $R_1 = R_3 = H$; $R_2 = COOH$), dopamine (3,4-dihydroxyphenylethylamine, II: $R_1 = R_2 = R_3 = H$) and noradrenaline (II: $R_1 = R_2 = H$; $R_3 = OH$), Bouchilloux and Kodja reported the R_f's of dopachrome (I: $R_1 = R_3 = H$; $R_2 = COOH$), norepinochrome (I: $R_1 = R_2 = R_3 = H$), and noradrenochrome (I: $R_1 = R_2 = H$; $R_3 = OH$) as 0.92, 0.70, and 0.75 respectively on prewashed Whatman No. 1 paper with water as the running solvent (14). These authors also stated that the quinonoid pigments were unstable in butanol/acetic acid/water mixtures. Recently Bouchilloux has stressed the need to work with well-washed papers when studying the paper chromatography of the aminochromes, since traces of residual bisulphites in the paper combine with the aminochromes with great avidity to form

stable addition compounds (15). These products, which form bright yellow fluorescent spots, have high R_f's in water and 2% acetic acid/water, and low R_f's in butanol/aqueous acetic acid (cf. 16, 17). N-Ethylnoradrenochrome, N-isopropylnoradrenochrome, adrenochrome methyl ether, and adrenochrome ethyl ether behave similarly to adreno-chrome and can be satisfactorily chromatographed on acid-washed paper with 10% acetic acid/water as running solvent; their R_f's were found to be: 0.79, 0.77, 0.81, and 0.82 respectively. The spots, being red in color, are self-indicating; however, the red color of the spots fades when the developed chromatograms are dried (cf. 6). The aminochrome spots give violet colors with Ehrlich's reagent. The aminochrome ethers are readily distinguished from aminochromes without the 3-alkoxy group by spraying the chromato-grams with 10% zinc acetate solution, the "ethers" gave non-fluorescent dark blue spots and not the yellow "lutin" spots exhibiting the vivid apple-green fluorescence given by aminochromes with a 3-OH group. All attempts to chromatograph epinochrome solutions (in 2% acetic acid/water) gave in addition to the epinochrome spot (R_f ca. 0.8) an intense spot due to 5,6-dihydroxy-N-methylindole (the rearrangement product (cf. 11)) at $R_f = 0.44$ (cf. 17) and a spot due to an unknown substance (R_f = ca. 0.25) giving a violet color with Ehrlich's reagent. When the chromatograms were sprayed with 2% zinc acetate solution the red epinochrome spot was converted into a colorless spot, exhibiting a weak blue fluorescence, probably due to the formation of 5,6-dihydroxy-N-methylindole.

The ultraviolet and visible absorption spectra of adrenochrome and a few simple aminochromes have been reported in aqueous and alcoholic solutions (see 1, 18 for references). In general, with the unhalogenated aminochromes maxima occur at ca. 205–215, 300, and 470–500 mμ; with the iodoaminochromes the short wavelength maximum was observed at ca. 230 mμ, and the long wavelength maximum shifted to ca. 520–535 mμ; however, the position of the third peak remained unchanged in the region of 300 mμ (cf. 1, 2, 18). The spectra of the new aminochromes described in this paper have been measured in aqueous or methanolic solution, and in general the absorption maxima and minima occur at the wavelengths expected for this class of compounds. In all cases but one (2-iodoadrenochrome ethyl ether) the visible absorption peak was observed at a somewhat longer wavelength in water than in methanol; the same was true, to a lesser extent, of the peak near to 300 mμ. In the series adrenochrome, N-ethylnoradreno-chrome, N-isopropylnoradrenochrome, there was a progressive small shift of the visible absorption peak towards lower frequencies with the increase in size of the alkyl group (i.e. 486, 490, 495 mμ, in water, respectively). This phenomenon was not observed in the case of their 2-iodo derivatives, the visible absorption peak in aqueous solution was observed at 535 mμ in each case. Adrenochrome methyl and ethyl ethers gave absorption curves similar to adrenochrome whilst that from 2-iodoadrenochrome methyl ether was very similar to that obtained from 2-iodoadrenochrome. 2-Iodoadrenochrome ethyl ether appeared to behave somewhat anomalously, the expected maximum was observed at 300 mμ but the high-frequency peak occurred at ca. 222 mμ and the long wavelength maximum was observed at 508 mμ in methanol and 505 mμ in water. In this case the wavelengths of these absorption maxima are about 10–20 mμ less than those usually observed for the iodoaminochromes. The ultraviolet spectra of several 5,6-diacetoxy- and 3,5,6-triacetoxy-N-alkylindoles have been measured in methanol solution; they all show the general form expected for a compound containing the indole chromophore. 5,6-Diacetoxy-N-methylindole and the N-ethyl and N-isopropyl analogues have maxima at 225 and 287–288 mμ ("shoulders" are present on the latter peak at 280 and 296 mμ). Iodination of these compounds in the 2-position results in a small shift (ca. 6 mμ) in the

position of all the peaks towards longer wavelengths. The 3,5,6-triacetoxy-N-alkylindoles show two main maxima, one in the region 225–229 mμ and the other at 292 mμ. Once again, the introduction of an iodine atom in the 2-position results in a slight shift in position of these maxima (i.e. to 233 and 301 mμ respectively).

EXPERIMENTAL

N-*Ethylnoradrenochrome* (cf. Preparation of Adrenochrome (a) by Heacock, Nerenberg, and Payza (6) and (b) by Macciotta (7))

(a) DL-N-Ethylnoradrenaline (5.0 g) was suspended in absolute methanol (150 ml) and 98% formic acid added dropwise, with stirring, until a clear solution was obtained. Freshly prepared silver oxide (20.0 g) was added portionwise to the well-stirred solution and the agitation continued for a further 3 minutes. The temperature of the reaction mixture was not allowed to exceed 25° during the oxidation. The product was filtered (with suction) through a Dowex-1 (Cl⁻) resin bed (diam. = 6.5 cm; height = 1.8 cm),* and on cooling the deep red filtrate at −20° for 6 hours N-ethylnoradrenochrome separated in very dark red-violet (almost black) prisms (1.83 g) (decomposes without melting at 115°)†. Found: C, 62.24; H, 5.61; N, 7.20. $C_{10}H_{11}NO_3$ requires C, 62.16; H, 5.70; N, 7.31%. Dry ether (100 ml) was added to the filtrate and after cooling overnight at −20° a second crop of crystalline N-ethylnoradrenochrome (0.23 g) was obtained.

(b) DL-N-Ethylnoradrenaline (1.08 g) was suspended in methanol (50 ml) and just enough glacial acetic acid added to clarify the solution. A solution of iodic acid (0.5 g) in water (5 ml) was added and the solution, which rapidly became deep red in color, cooled to −20° for 6 hours; N-ethylnoradrenochrome (0.15 g) was obtained in dark red-violet prisms. A satisfactory second crop of crystalline material could not be obtained by the addition of dry ether and further cooling of the solution; only a black amorphous powder was obtained.

N-*Ethylnoradrenochrome Monosemicarbazone*

DL-N-Ethylnoradrenaline (1.05 g) was suspended in methanol (16.5 ml) and 98% formic acid added dropwise until a clear solution was obtained. Freshly prepared silver oxide (4.2 g) was added to the stirred solution and after the addition was complete, stirring was continued for 3 minutes. The reaction mixture was filtered through a Dowex-1 (Cl⁻) resin bed (diam. = 2.5 cm; height = 1 cm) directly into a solution of semicarbazide hydrochloride (0.5 g) and sodium acetate (1 g) in water (6.5 ml). After standing at 0° for 4 hours bright orange-red needles of N-ethylnoradrenochrome monosemicarbazone (0.48 g) were obtained, m.p. 215° (with decomposition). Found: C, 52.67; H, 5.58; N, 22.32. $C_{11}H_{14}N_4O_3$ requires C, 52.80; H, 5.64; N, 22.40%. The ultraviolet and visible absorption spectra were measured in aqueous solution (λ_{max}: 354 with a shoulder at 435 mμ).

N-*Isopropylnoradrenochrome*

(a): (i) DL-N-Isopropylnoradrenaline (10.0 g) was suspended in absolute methanol (250 ml) and 98% formic acid added dropwise with stirring until a clear solution was obtained. Freshly prepared silver oxide (40.0 g) was added portionwise to the stirred solution and the stirring continued for a further 3 minutes. The reaction temperature was

---

*Unless otherwise stated the resin (200/400 mesh size) used in all the preparations described in this paper was prepared by extensive washing with: (1) 3 N hydrochloric acid, (2) with water until neutral to litmus, and (3) finally with dry methanol.

†The decomposition points of all the aminochromes described in this paper were measured on a Leitz hot-stage instrument.

not allowed to rise above 25° during the oxidation. The product was filtered (with suction) through a Dowex-1 (Cl⁻) resin bed (diam. = 6.5 cm; height = 3.5 cm) and the deep red filtrate allowed to crystallize slowly for 6 hours at −20°; N-isopropylnoradrenochrome was obtained in deep red-violet needles (2.0 g) (decomposes without melting at 123°). Found: C, 63.40; H, 6.36; N, 6.74. $C_{11}H_{13}NO_3$ requires C, 63.74; H, 6.32; N, 6.76%. Dry ether (150 ml) was added to the filtrate and after standing overnight at −20° a second crop (1.4 g) of N-isopropylnoradrenochrome was obtained.

(a): (ii) The above oxidation procedure was repeated except that DL-N-isopropylnor-adrenaline hydrochloride (10 g), which was freely soluble in dry methanol (250 ml), was used in place of the free base and therefore in this instance the addition of formic acid was not required. A slightly better yield of crystalline N-isopropylnoradrenochrome (1st crop, 3.5 g; 2nd crop, 1.32 g) was obtained in this case.

(b) Freshly prepared silver oxide (4.0 g) was added to a well-stirred suspension of N-isopropylnoradrenaline hydrochloride (1.0 g) in dry acetonitrile (25 ml). An exothermic reaction ensued (the temperature rose to ca. 35–40°) and the red suspension was stirred for a further 5 minutes; the reaction mixture was filtered and after standing at −20° overnight the filtrate deposited deep red-violet needles of N-isopropylnoradrenochrome (0.20 g).

Like adrenochrome, when pure, these substances appear to be quite stable when kept in the dry state. They are readily soluble in water and other polar solvents to give deep red solutions, but are virtually insoluble in non-polar solvents. Similarly to adrenochrome, they form bright yellow solutions in concentrated sulphuric acid.

N-Ethyl-2-iodonoradrenochrome (cf. Preparation of 2-Iodoadrenochrome by Sobotka and Austin (2))

N-Ethylnoradrenaline (4.3 g) was suspended in water (3000 ml) and concentrated hydrochloric acid added, dropwise with stirring, until a clear solution was obtained. Potassium iodate (6.9 g) was added and the stirring continued until all the potassium iodate was in solution. After standing at room temperature for 4 hours N-ethyl-2-iodonoradrenochrome (5.9 g) was obtained as deep violet rods (decomposed without melting at 134.5°). Found: C, 37.73; H, 3.23; N, 4.37. $C_{10}H_{10}NO_3I$ requires C, 37.63; H, 3.16; N, 4.39%.

2-Iodo-N-isopropylnoradrenochrome (cf. Preparation of N-ethyl-2-iodonoradrenochrome (Above))

Potassium iodate (3.3 g) was added to a solution of N-isopropylnoradrenaline hydro-chloride (2 g) in water (1600 ml); the solution was stirred until all the iodate was in solution. After standing at room temperature for 4 hours 2-iodo-N-isopropylnoradreno-chrome (1.63 g) was obtained as deep violet-brown needles (completely decomposes without melting at 105.5°). Found: C, 39.68; H, 3.80; I, 38.21. $C_{11}H_{12}NO_3I$ requires C, 39.66; H, 3.63; I, 38.12%. (This substance had previously been obtained, in a lower yield, by Bu'Lock and Harley-Mason as the hemihydrate (8), who carried out the reaction in more concentrated solutions.)

Adrenochrome Methyl Ether

(a) Adrenaline methyl ether hydrochloride (1.0 g, prepared by the method of Hukki and Seppäläinen (9)) was dissolved in dry methanol (30 ml) and freshly prepared silver oxide (4.0 g) added. After standing for 5 minutes the bright red solution was filtered through a Dowex-1 (Cl⁻) resin bed (diam. = 2.5 cm; height = 1 cm). No crystallization

occurred after allowing the solution to stand at $-20°$ overnight and no solid product was obtained after the addition of dry ether (30 ml) and further cooling at $-20°$.

(b) Freshly prepared silver oxide (4.0 g) was added to a well-stirred suspension of adrenaline methyl ether hydrochloride (1 g) in dry acetonitrile (20 ml). The suspension rapidly developed a deep red color and the temperature rose to ca. 35–40°; the stirring was continued for 5 minutes. After filtration, the deep red filtrate was concentrated, *in vacuo* (with a nitrogen "leak"), below 35° to small bulk, dry ether (10 ml) was added and after cooling to $-20°$, adrenochrome methyl ether (0.46 g) was obtained as a deep red microcrystalline solid, m.p. 83° (with decomposition).* Found: C, 61.83; H, 5.61; N, 7.63. $C_{10}H_{11}NO_3$ required C, 62.16; H, 5.70; N, 7.31%.

Adrenochrome Ethyl Ether

Adrenaline ethyl ether hydrochloride (1.0 g, prepared by the method of Hukki and Seppäläinen (9)) was oxidized as described in section (b) above; adrenochrome ethyl ether (0.55 g) was obtained as a deep red microcrystalline powder, m.p. 70–72° (with decomposition).* Found: C, 63.25; H, 6.29. $C_{11}H_{13}NO_3$ requires C, 63.74; H, 6.32%.

The adrenochrome ethers were readily soluble in polar solvents to give deep red solutions; their solubility in non-polar solvents (e.g. chloroform), whilst being low, was considerably higher than that of adrenochrome. In this respect these compounds show a stronger resemblance to rubreserine than to adrenochrome.

2-Iodoadrenochrome Methyl Ether (cf. Preparation of Iodoaminochromes by Bu'Lock and
        Harley-Mason (8))

A solution of adrenaline methyl ether hydrochloride (2.0 g) in water (70 ml) was treated at 0° with a solution of potassium iodate (2.2 g) in water (70 ml). A dark violet tarry precipitate soon began to separate out and was removed by filtration after standing at 0° for 30 minutes and a further quantity of tar was filtered off after 1 hour; at this stage a crystalline precipitate began to form and after standing overnight at 0°, 2-iodoadrenochrome methyl ether (1.05 g) was obtained in violet-brown needles (completely decomposes without melting at 85°). Found: C, 38.07; H, 3.11; N, 4.15; I, 39.60. $C_{10}H_{10}NO_3I$ requires C, 37.63; H, 3.16; N, 4.39; I, 39.78%.

2-Iodoadrenochrome Ethyl Ether (cf. Preparation of Methyl Ether (Above))

A solution of adrenaline ethyl ether hydrochloride (2.0 g) in water (70 ml) was treated at 0° with potassium iodate (2.2 g) in water (70 ml). After filtration of the black tarry precipitates that formed during the first hour, a crystalline precipitate began to separate out and after standing overnight at 0°, 2-iodoadrenochrome ethyl ether (0.71 g) was obtained in violet-brown needles (decomposes without melting at 88°). Found: C, 39.92; H, 3.76. $C_{11}H_{12}NO_3I$ requires C, 39.66; H, 3.63%. These iodoadrenochrome ethers appear to be more soluble in water than 2-iodoadrenochrome and when the oxidation was carried out under more dilute conditions (cf. 2) deep violet solutions were obtained but no precipitation occurred even after standing at 0° for 24 hours.

N-Ethyl-5,6-dihydroxyindoxyl (*i.e. N-Ethylnoradrenolutin*) (cf. Preparation of Adrenolutin
        by Heacock and Mahon (20))

N-Ethylnoradrenaline (5 g) was suspended in water (150 ml) and concentrated hydrochloric acid was added dropwise until a clear solution was obtained. Freshly prepared silver oxide (20.0 g) was added to the well-stirred solution and the stirring continued for

*In contrast to the aminochromes without the 3-alkoxy group which decompose without melting, these substances appeared to actually form a liquid phase before decomposing.

a further 3 minutes. The reaction mixture was then filtered through a Dowex-1 (Cl⁻) resin bed (diam. = 6.5 cm; height = 1.5 cm)* and the filtrate cooled in ice. A stream of nitrogen was passed through the cooled filtrate, and 10% sodium hydroxide solution (50 ml) added. The brownish-green solution, which exhibited a typical "lutin" fluorescence was stirred and acidified by the dropwise addition of glacial acetic acid. N-Ethylnoradrenolutin (1.52 g) separated out as a bright yellow crystalline precipitate which was filtered off, washed with a little water, and rapidly dried *in vacuo* at room temperature. The product was obtained in very small yellow-orange prisms (m.p. indefinite, decomposes without melting at ca. 170°) on recrystallization from water (containing a little sodium hydrosulphite to prevent oxidation). In contrast to adrenolutin this product did not contain water of crystallization. Found: C, 62.01; H, 5.87; N, 7.21. $C_{10}H_{11}NO_3$ requires C, 62.16; H, 5.70; N, 7.31%. Although the crystalline material as prepared above tended to darken in color on keeping, a sample (decomposes without melting at 174–175°) which was purified by vacuum sublimation (190–200°/0.2 mm) and obtained in very small bright yellow rods showed no tendency to lose its bright yellow color. The ultraviolet and visible absorption spectra were measured in methanol solution (λ_{max}: 224, 259, 288 (with a shoulder at 308), 415 mμ; λ_{min}: 239, 274, 335 mμ).

The Action of Acetic Anhydride and Pyridine on the Aminochromes Described Above (cf. Bu'Lock and Harley-Mason (8))

The aminochrome (1.0 g) was dissolved in a mixture of acetic anhydride (15 ml) and dry pyridine (15 ml) and the solution allowed to stand at room temperature for 36 hours, after which time it was poured, with stirring, into ice water, when either an amorphous solid or an oil separated. If solid, the crude product was removed by filtration; if oily, it was extracted with peroxide-free ether (4×100 ml) (the ethereal extract washed with 5% sodium bicarbonate solution (4×100 ml) and with water (100 ml)) and concentration of the dried (Na_2SO_4) extract gave the crude product, usually as a greenish-yellow gum. In some instances it was possible to purify the product directly by recrystallization, but where this was not possible, chromatographic purification on silica gel columns was carried out.

N-Ethylnoradrenochrome gave 3,5,6-triacetoxy-N-ethylindole (0.61 g), m.p. 84.5–85.5°, in pale yellow prisms after chromatographic purification on silica gel using benzene as eluent and recrystallization from benzene – light petroleum (b.p. 80–100°). Found: C, 60.19; H, 5.41; N, 4.41. $C_{16}H_{17}NO_6$ requires C, 60.17; H, 5.37; N, 4.39%.

N-Isopropylnoradrenochrome gave 3,5,6-triacetoxy-N-isopropylindole (0.25 g), m.p. 85.5–87.5°, after chromatographic purification on silica gel using benzene as eluent. The product was initially obtained as a gum and only crystallized with difficulty after seeding with an authentic specimen. This compound had previously been prepared by Bu'Lock and Harley-Mason by the deiodination of 3,5,6-triacetoxy-2-iodo-N-isopropylindole (8), who reported a melting point of 87°. The product obtained by the authors did not depress the melting point of a sample prepared by Bu'Lock and Harley-Mason's method.

N-Ethyl-2-Iodonoradrenochrome gave 3,5,6-triacetoxy-N-ethyl-2-iodoindole (1.2 g) in pale yellow plates, m.p. 142–143.5°, after recrystallization from benzene – light petroleum (b.p. 80–100°). Found: C, 43.09; H, 3.45; I, 28.50. $C_{16}H_{16}NO_6I$ requires C, 43.15; H, 3.62; I, 28.51%.

Adrenochrome methyl ether gave 5,6-diacetoxy-3-methoxy-N-methylindole (0.4 g) in pale yellow prisms, m.p. 140–141°, after chromatographic purification on silica gel using

---

This resin bed was prepared as previously described, except that the final washing with methanol was omitted.

benzene as eluent and three recrystallizations from benzene – light petroleum (b.p. 80–100°). Found: C, 60.62; H, 5.41; N, 5.12; O—COCH$_3$, 31.5%; mol. wt., 311. C$_{14}$H$_{15}$NO$_5$ requires C, 60.64; H, 5.45; N, 5.05; O—COCH$_3$, 31.04%; mol. wt., 277. The peaks in the "carbonyl" region of the infrared spectrum* occur at 1770 and 1752 cm^{-1}.

Adrenochrome ethyl ether gave 5,6-diacetoxy-3-ethoxy-N-methylindole (0.47 g) in pale yellow-green elongated prisms, m.p. 84.5–85.5°, after chromatographic purification on silica gel using benzene as eluent and two recrystallizations from benzene – light petroleum (b.p. 80–100°). Found: C, 61.39; H, 5.86; N, 4.81%; mol. wt., 272. C$_{15}$H$_{17}$NO$_5$ requires C, 61.84; H, 5.88; N, 4.81%; mol. wt., 291. The peaks in the "carbonyl" region of the infrared spectrum occur at 1776 and 1755 cm^{-1}.

2-Iodoadrenochrome methyl ether gave 5,6-diacetoxy-2-iodo-3-methoxy-N-methylindole (0.57 g) in pale yellow plates, m.p. 191–192°, on recrystallization from benzene – light petroleum (b.p. 80–100°). Found: C, 41.88; H, 3.53; N, 3.20; I, 32.00; O—COCH$_3$, 21.66%; mol. wt., 406. C$_{14}$H$_{14}$NO$_5$I requires C, 41.70; H, 3.49; N, 3.47; I, 31.48; O—COCH$_3$, 21.35%; mol. wt., 403. The peaks in the "carbonyl" region of the infrared spectrum occur at 1779 and 1767 cm^{-1}.

2-Iodoadrenochrome ethyl ether gave 5,6-diacetoxy-3-ethoxy-2-iodo-N-methylindole (0.61 g) in pale yellow prisms, m.p. 149.5°, on recrystallization from benzene – light petroleum (b.p. 80–100°). Found: C, 43.45; H, 3.86; N, 3.54; I, 30.29%; mol. wt., 400. C$_{15}$H$_{16}$NO$_5$I requires C, 43.17; H, 3.86; N, 3.36; I, 30.42%; mol. wt., 417. There is apparently only one peak in the "carbonyl" region of the infrared spectrum of this compound occurring at 1761 cm^{-1}.

5,6-Diacetoxy-N-ethyl-2-iodoindole

A suspension of sodium hydrosulphite (2.0 g) in water (5 ml) was added to a stirred suspension of N-ethyl-2-iodonoradrenochrome (1.0 g) in water (40 ml). After being stirred at room temperature for 1 hour the reaction mixture was extracted with peroxide-free ether (6×50 ml). Concentration of the combined dried (Na$_2$SO$_4$) extracts in vacuum (nitrogen "leak"), below 35°, gave a greenish gum which was dissolved in a mixture of acetic anhydride (10 ml) and dry pyridine (10 ml). After standing overnight at room temperature the reaction mixture was poured into ice water; a pale yellow solid separated which afforded 5,6-diacetoxy-N-ethyl-2-iodoindole (0.5 g), m.p. 157.5–158.5°, in pale yellow small plates on recrystallization from benzene – light petroleum (b.p. 80–100°). Found: C, 43.00; H, 3.66; I, 32.30. C$_{14}$H$_{14}$NO$_4$I requires C, 43.43; H, 3.65; I, 32.79%.

5,6-Diacetoxy-2-iodo-N-isopropylindole

(*a*) 2-Iodo-N-isopropylnoradrenochrome (1.0 g) was reduced with sodium hydrosulphite as described above for the N-ethyl analogue and gave 5,6-diacetoxy-2-iodo-N-isopropylindole (0.38 g), m.p. 111–112.5°, in white prisms after chromatographic purification on silica gel using benzene as eluent and recrystallization from light petroleum (b.p. 80–100°). Found: C, 45.04; H, 4.17; I, 31.60. C$_{15}$H$_{16}$NO$_4$I requires C, 44.91; H, 4.02; I, 31.64%.

(*b*) 2-Iodo-N-isopropylnoradrenochrome (1.0 g) was suspended in water (25 ml) and solid sodium borohydride added very slowly to the stirred suspension until a clear yellow solution was obtained. After decomposition of the excess reducing agent by the cautious dropwise addition of 2 N sulphuric acid, the reaction mixture was immediately extracted with peroxide-free ether (4×100 ml). The combined dried (Na$_2$SO$_4$) extracts were

---

*The infrared spectra were recorded as "NUJOL" mulls on a Perkin–Elmer Infracord spectrophotometer using a sodium chloride prism.

concentrated to dryness *in vacuo* (nitrogen "leak"), below 35°, and the residue dissolved in a mixture of acetic anhydride (10 ml) and dry pyridine (10 ml). After standing overnight at room temperature the acetylation mixture was poured into ice water and a yellow oil separated, which was extracted with peroxide-free ether (4×100 ml). After washing the combined ethereal extracts with 5% aqueous sodium bicarbonate (2×50 ml) and water (100 ml), the dried (Na_2SO_4) extract gave, on concentration, a yellowish-green gum which was purified chromatographically on a silica gel column using benzene as

TABLE I

R_f's in 2% acetic acid and color reactions of some aminochromes

| Aminochrome	R_f	Ehrlich*	DMCA*,†	10% zinc acetate	DPNA‡
Adrenochrome	0.78	BV	BG	Y^f	RBr
N-Ethylnoradrenochrome	0.79	BV	BG	Y^f	RBr
N-Isopropylnoradrenochrome	0.77	BV	BG	Y^f	RBr
Adrenochrome methyl ether	0.81	RV	GyG	B	YGy
Adrenochrome ethyl ether	0.82	RV	GyG	B	YGy

*The colors reported for Ehrlich's reagent and DMCA were those observed 12 hours after spraying the papers.
†DMCA = *p*-Dimethylaminocinnamaldehyde (cf. Harley-Mason and Archer (21)).
‡DPNA = diazotized *p*-nitroaniline.
NOTE: BV = blue-violet; RV = red-violet; BG = blue-green; GyG = grey-green; Y^f = yellow exhibiting a yellow-green fluorescence in ultraviolet light; B = blue; RBr = red-brown; YGy = yellow-grey.

TABLE II

Absorption spectra of some aminochromes (in the range 220–650 mμ)
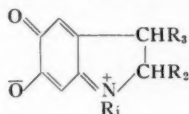
Substance	R_1	R_2	R_3	Solvent	Absorption maxima, mμ		Absorption minima, mμ	
N-Ethylnoradrenochrome	C_2H_5	H	OH	M	301	472	262	380
				W	303	490	261	368
N-Isopropylnoradrenochrome*	i-C_3H_7	H	OH	M	301	482	263	364
				W	305	495	261	366
Epinochrome*	CH_3	H	H	E†	305	470	—	—
				W	308	480	257	364
Adrenochrome methyl ether	CH_3	H	OCH_3	M	297	480	270	372
				W	302	492	262	374
Adrenochrome ethyl ether	CH_3	H	OC_2H_5	M	297	478	272	377
				W	302	488	262	370
2-Iodoadrenochrome‡	CH_3	I	OH	M	233 302	528	268	385
				W	233 304	535	268	385
N-Ethyl-2-iodonoradrenochrome	C_2H_5	I	OH	M	232 303	525	270	400
				W	232 303	535	268	386
2-Iodo-N-isopropylnoradrenochrome	i-C_3H_7	I	OH	M	233 302	528	268	380
				W	232 306	535	268	390
2-Iodoadrenochrome methyl ether	CH_3	I	OCH_3	M	233 300	530	268	390
				W	233 302	535	267	388
2-Iodoadrenochrome ethyl ether	CH_3	I	OC_2H_5	M	222 300	508	265	375
				W	223 302	505	264	372

NOTE: M = methanol; W = water; E = ethanol.

*Beaudet oxidized N-isopropylnoradrenaline and epinine hydrochlorides in aqueous solution with silver oxide and recorded the absorption maxima of the products as 480, 300, and 220 mμ for the former and 470, 310, and 205 mμ for the latter (19).
†Results quoted by Sobotka *et al.* (18).
‡Sobotka *et al.* recorded the absorption maxima of 2-iodoadrenochrome in ethanolic solution as 530, 302, and 234 mμ (18). The maxima in aqueous solution have been reported to occur at 520, 305, and 233 mμ (22) and 525, 301, and 232 mμ (23).

eluent; 5,6-diacetoxy-2-iodo-N-isopropylindole (0.67 g), m.p. 111–113°, was obtained in white prisms after recrystallization of the product from light petroleum (b.p. 80–100°).

Paper Chromatography

Whatman No. 1 paper was washed with (a) 2% acetic acid for 24 hours, and (b) water for 12 hours, and dried prior to use. The descending method of chromatography was employed in all cases and 2% acetic acid/water was used as the running solvent. The solvent was allowed to descend ca. 15 inches; this required about 2.5 to 3 hours running time. The R_f's (under these conditions) of N-ethylnoradrenochrome, N-isopropylnor-adrenochrome, adrenochrome methyl ether, and adrenochrome ethyl ether were determined, ca. 20 μg of the compound being applied to the paper in each case. (The results are given in Table I). All four compounds are colored and therefore are self-indicating and location of the spots with spray reagents is not necessary; however, the colors developed by the aminochrome spots with a number of reagents are given in Table I.

Absorption Spectra

(a) The ultraviolet and visible absorption spectra of a number of aminochromes were measured in freshly prepared aqueous or methanol solutions of the pure crystalline aminochrome at a concentration of 1–2 mg/100 ml, using a Warren Spectracord instrument. The results are given in Table II.

TABLE III

Ultraviolet absorption spectra of some 5,6-diacetoxy- and 3,5,6-triacetoxy-N-alkylindoles (in methanol)
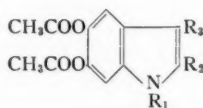
Substance	R_1	R_2	R_3	Absorption maxima, mμ	Absorption minima, mμ
5,6-Diacetoxy-N-methylindole*	CH$_3$	H	H	225; (279);† 287; (296)	252
5,6-Diacetoxy-N-ethylindole*	C$_2$H$_5$	H	H	225; (280); 288; (297)	252
5,6-Diacetoxy-N-isopropylindole*	i-C$_3$H$_7$	H	H	225; (281); 287; (297)	253
5,6-Diacetoxy-2-iodo-N-methylindole‡	CH$_3$	I	H	231; (280); 293; (303)	255
5,6-Diacetoxy-N-ethyl-2-iodoindole	C$_2$H$_5$	I	H	230; (280); 294; (303)	255
5,6-Diacetoxy-2-iodo-N-isopropylindole	i-C$_3$H$_7$	I	H	230; (282); 293; (303)	255
3,5,6-Triacetoxy-N-methylindole§	CH$_3$	H	OCOCH$_3$	225; 292	ca. 260
3,5,6-Triacetoxy-N-ethylindole	C$_2$H$_5$	H	OCOCH$_3$	228; 292	260
3,5,6-Triacetoxy-N-isopropylindole	i-C$_3$H$_7$	H	OCOCH$_3$	229; 292	260
3,5,6-Triacetoxy-2-iodo-N-methylindole‖	CH$_3$	I	OCOCH$_3$	233; 301	263
3,5,6-Triacetoxy-N-ethyl-2-iodoindole	C$_2$H$_5$	I	OCOCH$_3$	233; 301	263
5,6-Diacetoxy-3-methoxy-N-methylindole	CH$_3$	H	OCH$_3$	239; (286); 296	266
5,6-Diacetoxy-3-ethoxy-N-methylindole	CH$_3$	H	OC$_2$H$_5$	239; (285); 296	267
5,6-Diacetoxy-2-iodo-3-methoxy-N-methylindole	CH$_3$	I	OCH$_3$	242; (285); 314	272
5,6-Diacetoxy-3-ethoxy-2-iodo-N-methylindole	CH$_3$	I	OC$_2$H$_5$	242; (285); 313	272

*Prepared by a method to be described shortly (Part V of this series).
†Figures shown in parentheses indicate shoulders on the main peak.
‡Prepared by the method described in Part III of this series.
§Results quoted by Lund (24).
‖Prepared by the method of Bu'Lock and Harley-Mason (8).

(b) The ultraviolet absorption spectra of a number of 5,6-diacetoxy- and 3,5,6-triacetoxy-N-alkylindoles were measured in methanol at a concentration of 1–2 mg/100ml, using the apparatus described above. The results are given in Table III.

ACKNOWLEDGMENTS

REFERENCES

1. R. A. HEACOCK. Chem. Revs. **59**, 181 (1959).
2. H. SOBOTKA and J. AUSTIN. J. Am. Chem. Soc. **73**, 3077 (1951).
3. P. MARQUARDT and E. CARL. Naturwissenschaften, **39**, 210 (1952).
4. H. SOBOTKA. U.S. Patent No. 2,655,510 (October, 1953); Chem. Abstr. **48**, 12809 (1954).
5. R. A. HEACOCK. Chem. & Ind. (London), 752 (1959).
6. R. A. HEACOCK, C. NERENBERG, and A. N. PAYZA. Can. J. Chem. **36**, 853 (1958).
7. E. MACCIOTTA. Gazz. chim. ital. **81**, 485 (1951).
8. J. BU'LOCK and J. HARLEY-MASON. J. Chem. Soc. 712 (1951).
9. J. HUKKI and N. SEPPÄLÄINEN. Acta. Chem. Scand. **12**, 1231 (1958).
10. J. HARLEY-MASON. J. Chem. Soc. 1276 (1950).
11. J. AUSTIN, J. D. CHANLEY, and H. SOBOTKA. J. Am. Chem. Soc. **73**, 2395, 5299 (1951).
12. R.-A. HEACOCK and B. D. SCOTT. This issue.
13. F. BERGEL and A. L. MORRISON. J. Chem. Soc. 48 (1943).
14. S. BOUCHILLOUX and A. KODJA. Compt. rend. **247**, 2484 (1958).
15. S. BOUCHILLOUX. Compt. rend. soc. biol. **153**, 642 (1959).
16. J. VAN ESPEN. Pharm. Acta Helv. **33**, 207 (1958).
17. R. A. HEACOCK and B. D. LAIDLAW. Chem. & Ind. (London), 1510 (1958).
18. H. SOBOTKA, N. BARSEL, and J. D. CHANLEY. Fortschr. Chem. org. Naturstoffe, **14**, 217 (1957).
19. C. BEAUDET. Experientia, **7**, 291 (1951).
20. R. A. HEACOCK and M. E. MAHON. Can. J. Chem. **36**, 1550 (1958).
21. J. HARLEY-MASON and A. A. P. G. ARCHER. Biochem. J. **69**, 60P (1958).
22. F. G. STOCK and L. W. HINSON. J. Pharm. and Pharmacol. **7**, 512 (1955).
23. I. EHRLEN. Farm. Revy, **47**, 321 (1948); Chem. Abstr. **42**, 5075 (1948).
24. A. LUND. Acta Pharmacol. Toxicol. **5**, 121 (1949).

LYCOPODIUM ALKALOIDS

IX. CYCLIZED PRODUCTS FROM α- AND β-CYANOBROMOLYCOPODINE[1]

D. B. MacLean, Won-Ryul Song, and W. A. Harrison[2]

ABSTRACT

A study has been made of the products formed on treatment of α- and β-cyanobromolyco-podine with potassium hydroxide in methanol and potassium acetate in ethanol, respectively. The product derived from the α-isomer is apparently formed in a cyclization reaction taking place alpha to the carbonyl group while that formed from the β-isomer may be an enol ether. The olefin expected from a normal dehydrobromination of α-cyanobromolycopodine has been prepared by an indirect method. Attempts to prepare the analogous olefin in the β-series led to the formation of a saturated cyclic ether. The hydrogenolysis product of β-cyanobromo-lycopodine has been prepared.

The reaction of lycopodine, $C_{16}H_{25}ON$, with cyanogen bromide to yield two isomeric bromocyanamides was first reported by MacLean, Manske, and Marion (1). A number of reactions of the bromocyanamides were reported at the same time. The study of their reactions has since been extended by Barclay and MacLean (2) and by MacLean and Harrison (3), and it is now known that both bromides are primary.

Among the reactions reported in the initial study were those leading to the formation of two isomeric compounds of the formula $C_{17}H_{24}ON_2$ from α-cyanobromolycopodine I, $C_{17}H_{25}ON_2Br$, and β-cyanobromolycopodine II, $C_{17}H_{25}ON_2Br$. Both isomers were formed in an elimination reaction with loss of hydrogen bromide. The α-isomer III was the product of the reaction of I with boiling methanolic potassium hydroxide. It also formed, along with a product of demethylation V, when α-cyanotrimethylaminolycopodine bromide IV was converted to the quaternary base and pyrolyzed. The β-isomer VI was obtained by the action of boiling ethanolic potassium acetate on the β-bromide II. Since neither compound displayed any evidence of unsaturation, it was suggested that III and VI were formed in cyclization reactions. This work is summarized below.

A more detailed study of the two compounds III and VI has now been undertaken and is reported here.

The product III, $C_{17}H_{24}ON_2$, was prepared from α-cyanobromolycopodine according to the method of MacLean, Manske, and Marion (1) and was examined by infrared and ultraviolet spectroscopy. The infrared spectrum of III showed a strong band at 1700 cm⁻¹ in the carbonyl region but there was no absorption characteristic of an olefin linkage. The ultraviolet spectrum did not reveal the presence of a conjugated system in the molecule. The presence of the carbonyl group in III was confirmed chemically for it readily under-went reduction to the alcohol VII, $C_{17}H_{26}ON_2$, on treatment with sodium borohydride. Compound VII was in turn converted to III by oxidation with chromic acid.

Indirect evidence that a cyclization reaction had occurred adjacent to the carbonyl group came from the following observations. Compound III failed to react with benzal-dehyde when it was treated under the same conditions that led to reaction with α-cyanolycopodine VIII (in α-cyanolycopodine the bromine atom of I has been replaced by hydrogen) (1, 2). When III was hydrolyzed to the secondary base and methylated

$C_{16}H_{25}ON$

Lycopodine

BrCN

$\alpha\text{-}C_{17}H_{25}ON_2Br$ I

$\beta\text{-}C_{17}H_{25}ON_2Br$ II

$(CH_3)_2N$

Alcoholic KOH

$C_{20}H_{34}ON_3Br$ IV

KOAc in ethanol

1. Ag OH
2. Pyrolysis

$\alpha\text{-}C_{17}H_{24}ON_2$ III   ◄

$\beta\text{-}C_{17}H_{24}ON_2$ VI

$C_{19}H_{31}ON_3$ V
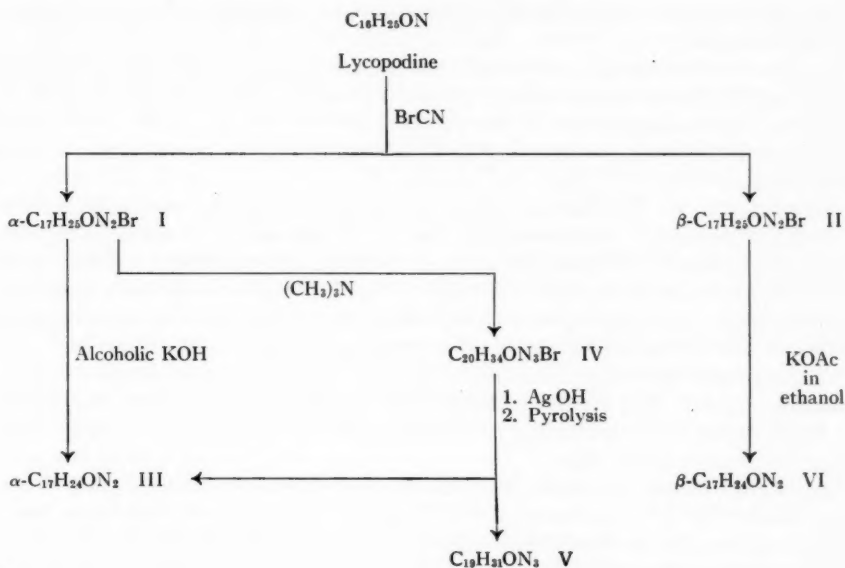
to the tertiary base, the latter failed to react with phenyl lithium. The first observation suggests that the methylene group, which has been shown to be present in VIII (2), is absent or more hindered in III. The failure of III to form a benzylidene derivative cannot be taken as conclusive evidence for the absence of a methylene group for it has been reported that lycopodine, which must contain the methylene group found in α-cyano-lycopodine, does not react with benzaldehyde (4). The second observation indicates that the carbonyl group in III is more hindered than in lycopodine, which reacts readily with phenyl lithium (1). Both observations lend support to a cyclization alpha to the carbonyl function. It has also been shown in the sequence outlined below, in which the olefin expected from a normal dehydrobromination of I has been prepared by an indirect method, that in the absence of the carbonyl group cyclization does not occur. One may conclude therefore that III is formed in a cyclization reaction and that, if cyclization is to occur, the carbonyl function must be present.

In the preparation of the olefin derived from compound I the following procedure was followed. The bromide I was treated with dimethylamine and yielded the dimethylamino compound V. Treatment of V with sodium borohydride yielded the dimethylamino alcohol IX, $C_{19}H_{33}ON_3$, which was in turn converted to its methiodide X. The Hofmann decomposition of X with potassium tertiary butoxide in boiling tertiary butanol proved the most satisfactory of a number of methods investigated. The product of this reaction was separated into a neutral and a basic fraction. The basic fraction was a mixture of V and IX which was separated by chromatography on alumina. The neutral fraction yielded two olefinic products XI, $C_{17}H_{24}ON_2$, and XII, $C_{17}H_{26}ON_2$. The olefin XI had absorption in the carbonyl region at 1700 cm^{-1} and in the olefin region at 1640 cm^{-1}, while the olefin XII showed no carbonyl absorption but had hydroxyl and olefin absorption. Both compounds had cyanamide absorption at 2200 cm^{-1}. The presence of the ketonic products

V and XI in this reaction is probably the result of oxidation catalyzed by potassium tertiary butoxide.

Compound XI was readily converted into XII on treatment with sodium borohydride. Treatment of XI with hydrogen over a platinum catalyst yielded α-cyanolycopodine VIII, indicating that rearrangement of the carbon skeleton had not occurred in the reaction. Ozonolysis of XII yielded formaldehyde, thus establishing the terminal character of the olefin linkage.

Compound VI, $C_{17}H_{24}ON_2$, was prepared originally by MacLean, Manske, and Marion (1) by treatment of β-cyanobromolycopodine II with potassium acetate in boiling ethanol. MacLean and Harrison (3) have found that it is also the main product formed on treatment of II with silver acetate in boiling benzene. In this laboratory it has been found that VI forms readily in a variety of basic media. For instance, it is the sole product formed on treatment of II with boiling methanolic potassium hydroxide. It is also formed when β-cyanobromolycopodine is treated with a solution of dimethylamine in methanol (5) and when a solution of II in ethanol is added to an excess of sodium borohydride in ⟨ ⟩anol (6). In the latter case it is possible to induce the reaction to follow a different course and this is described in detail later.

Like its α-isomer, compound VI has been examined by infrared and ultraviolet spectroscopy. The infrared spectrum of VI has an absorption band at 1675 cm⁻¹ which is less intense than that of the carbonyl absorption of lycopodine or of its α-isomer III and is shifted by about 25 cm⁻¹. There is no absorption in the 1600–1650 cm⁻¹ region which might be expected of a compound with a terminal vinyl linkage. The ultraviolet spectrum is lacking in any absorption characteristic of a conjugated system. Chemically, the compound has proved to be peculiarly inert. It has been recovered unchanged after treatment with sodium borohydride under conditions which readily reduced its α-isomer III. Lithium aluminum hydride in boiling tetrahydrofuran converted VI into the secondary base XIII, $C_{16}H_{25}ON$, an oil which would not crystallize, and which was converted to its N-methyl base XIV, $C_{17}H_{27}ON$, which readily formed a crystalline perchlorate. Both XIII and XIV retained the characteristic absorption at 1675 cm⁻¹ exhibited by VI. The N-methyl base XIV was recovered unchanged after treatment with phenyl lithium or further treatment with sodium borohydride or lithium aluminum hydride. This lack of reactivity toward hydride reducing agents makes it unlikely that there is a carbonyl function in VI, and accordingly, non-ketonic structures were considered.

The most reasonable alternative to a ketonic structure is one in which the oxygen is present in a cyclic enol ether linkage. This is compatible with the infrared spectrum of VI since some cyclic enol ethers have a strong band near 1675 cm⁻¹ (7). The enol ether structure explains the inertness of XIV to hydrides and phenyl lithium, but inertness of this system to the addition of hydrogen as reported previously (1) and confirmed by us is not to be expected. Furthermore, an enol ether might be expected to cleave readily on treatment with acids, but the base XIV proved to be relatively stable under acidic conditions. It is true that treatment over prolonged periods with strong mineral acids yielded unidentified products which showed absorption in the carbonyl region at 1700 cm⁻¹ and in the hydroxyl region. The fact that we were able to isolate the secondary base XIII by acid hydrolysis of VI is ample indication of the stability of the unsaturated function of VI, XIII, and XIV in an acidic medium.

An attempt to form the normal product of dehydrobromination of β-cyanobromo-

lycopodine led instead to the formation of a cyclic saturated ether. A procedure analogous to that used in the preparation of the olefin XI in the α-series was employed. Although Barclay (6) has reported that compound VI is formed when β-cyanobromolycopodine is treated with an excess of sodium borohydride, we have been able to alter the reaction conditions so that the reaction follows a different course. When II was dissolved in ethanol, cooled to 0°, and treated with an ethanolic solution of sodium borohydride, the main reaction product was the hydroxybromide XV, $C_{17}H_{27}ON_2Br$. The hydroxybromide XV was readily converted to the quaternary salt XVI, $C_{20}H_{36}ON_3Br$, on treatment with trimethylamine. When the quaternary salt XVI was decomposed with potassium tertiary butoxide in boiling tertiary butanol, trimethylamine was liberated and a new compound XVII, $C_{17}H_{26}ON_2$, was isolated. This compound showed no hydroxyl or olefin absorption in its infrared spectrum and it can be concluded that an ether linkage formed in the reaction. This is substantiated by the appearance of a strong band in its infrared spectrum in the region characteristic of ethers. This is the third instance in which a cyclization involving the oxygen function has been observed in the β-series. Two of these have been discussed in this paper while the third was the formation of the lactone reported by MacLean and Harrison (3).

The ease with which the compound VI formed in a variety of basic media led us to investigate again the hydrogenolysis of the β-bromide II reported by MacLean, Manske, and Marion (1). We have found that under their conditions at least 90% of the reaction product was compound VI and not the expected hydrogenolysis product as they reported. If, however, the hydrogenolysis was carried out at dry ice temperature, and in the absence of a large excess of alkali, a normal reaction course was followed. The product of this reaction contained none of the cyclized compound VI but, instead, a new compound XVIII, $C_{17}H_{26}ON_2$, which had a normal carbonyl absorption in its infrared spectrum near 1700 cm^{-1}. Compound XVIII, designated β-cyanolycopodine, has also been prepared indirectly in the following manner. The hydroxybromide XV, $C_{17}H_{27}ON_2Br$, was treated with hydrogen over a palladium catalyst and underwent hydrogenolysis in a normal manner to give the compound XIX, $C_{17}H_{28}ON_2$, and that in turn was oxidized by the Oppenauer method to β-cyanolycopodine, identical in all respects with the compound prepared directly from II.

The reactions which have been discussed here can be accommodated by the partial formula A below which was recently proposed by MacLean and Harrison (3).

A
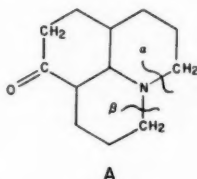
Compound III would form in a displacement reaction by the enolate ion involving C-alkylation to yield either structure B or C while compound VI would form in a displacement reaction by the enolate ion involving O-alkylation to give structure D. Partial structures of other compounds mentioned in the text can be deduced in a logical fashion from structure A.

B   C   D
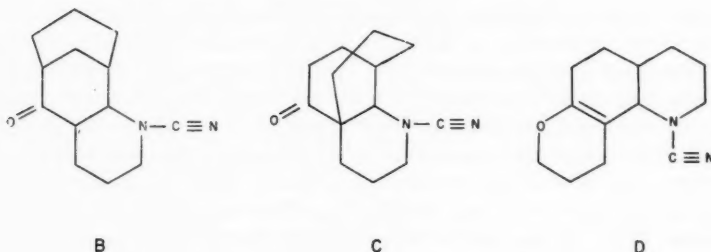
The evidence in support of the cyclization reaction adjacent to the carbonyl group in the α-series is substantial, but we have been unable to differentiate between structures B and C. Support for structure D is meager but it appears to be the only plausible formulation for this peculiarly unreactive compound. The double bond has been assigned the position shown, rather than the alternative position, since this compound shows no $=C—H$ stretching absorption in the region 3000–3120 cm^{-1} in its infrared spectrum.

EXPERIMENTAL

Treatment of α-Cyanobromolycopodine with Potassium Hydroxide in Methanol

The reaction was carried out and the product isolated according to the procedure of MacLean, Manske, and Marion (1). The infrared spectrum* of this product showed strong absorption at 1700 cm^{-1} in the carbonyl region and cyanamide absorption at 2200 cm^{-1}. The ultraviolet spectrum had no peaks characteristic of a conjugated system. This compound, ., would not form a benzylidene derivative under conditions which were successful :th α-cyanolycopodine (2).

Reduction of III, $C_{17}H_{24}ON_2$, with Sodium Borohydride

Compound III (1.7 g) was added to a solution of 3.5 g of sodium borohydride in 80 ml of 95% ethanol and the solution was stirred for 3 hours and then allowed to stand overnight. The excess borohydride was destroyed with formaldehyde and the solution was made nearly neutral by the addition of mineral acid. The solvent was evaporated, water was added to the residue, and the resulting mixture was extracted with chloroform. The chloroform extract was evaporated to yield a residue which was purified by chromatography on alumina using chloroform as eluant. There was recovered 1.5 g of product VII which crystallized from ether and melted at 219°. Calc. for $C_{17}H_{26}ON_2$: C, 74.4; H, 9.55; N, 10.2%. Found: C, 74.5; H, 9.48; N, 10.0%.

The infrared spectrum had strong hydroxyl and cyanamide absorption but no absorption in the carbonyl region. The compound was converted to III upon treatment with chromic acid in pyridine.

Hydrolysis and Methylation of III, $C_{17}H_{24}ON_2$

Compound III (3.3 g) was dissolved in a mixture of 100 ml of 95% ethanol and 15 ml of 12 M hydrochloric acid. The solution was heated under reflux on a steam bath for 30 hours and then evaporated to dryness. The residue was dissolved in water, filtered, made basic with ammonia, and extracted with chloroform. The crude reaction product (2.3 g) was dissolved in acetone and acidified with perchloric acid. A crystalline perchlorate

*Infrared spectra were run in Nujol mull using a sodium chloride prism unless otherwise stated.

separated which, after recrystallization from acetone, melted at 300°. Calc. for $C_{16}H_{25}ON \cdot HClO_4$: C, 55.2; H, 7.53; N, 4.0%. Found: C, 55.3; H, 7.39; N, 4.1%.

The free base was liberated from the perchlorate and crystallized from petroleum ether. It melted at 105–106°. Calc. for $C_{16}H_{25}ON$: C, 77.7; H, 10.12; N, 5.7%. Found: C, 77.4; H, 9.97; N, 5.6%.

The infrared spectrum of the base had a sharp peak at 3330 cm^{-1} in the $=NH$ region and a carbonyl peak at 1695 cm^{-1}.

The secondary base (2.0 g) obtained above was dissolved in a mixture of 40% formaldehyde (2.4 ml) and 90% formic acid (0.8 ml) and refluxed for a period of 33 hours. The mixture was quenched in water, made basic with ammonia, and extracted with ether. From the ether extract a residue was obtained on evaporation which was purified by chromatography on alumina using chloroform as eluant. There was obtained 1.6 g of tertiary base which was converted to its perchlorate in acetone solution. The crystalline perchlorate which separated was recrystallized from acetone and melted at 249–250°. Calc. for $C_{17}H_{27}ON \cdot HClO_4$: C, 56.4; H, 7.80; N, 3.8%. Found: C, 56.6; H, 7.77; N, 3.9%.

The free base, regenerated from the perchlorate, crystallized in the absence of solvent and melted at 87–88°. Calc. for $C_{17}H_{27}ON$: C, 78.2; H, 10.33; N, 5.4%. Found: C, 78.0; H, 10.30; N, 5.4%.

This base was recovered unchanged after treatment with phenyl lithium under the same conditions which gave a successful reaction with lycopodine (1).

α-Cyanodimethylaminolycopodine V

This compound was prepared by the reaction of α-cyanobromolycopodine I with a saturated solution of dimethylamine in methanol. After removal of methanol the residue was dissolved in water, made basic with ammonia, and extracted with chloroform. Evaporation of the chloroform yielded the free base which was dissolved in acetone and treated with perchloric acid. A crystalline perchlorate separated which was recrystallized from boiling acetone. This compound proved to be identical with the compound isolated by MacLean, Manske, and Marion (1) from the pyrolysis of the quaternary base derived from the quaternary bromide IV. The melting point of a mixture of the two samples was not depressed and their infrared spectra were identical. The yield was virtually quantitative.

Reduction of V with Sodium Borohydride

α-Cyanodimethylaminolycopodine (1.90 g) was added to a solution of 0.95 g of sodium borohydride in 200 ml of 95% ethanol and the mixture was stirred for 3 hours. After standing overnight at room temperature the mixture was worked up in the manner previously described to yield 1.80 g of the reduced compound IX, which melted at 190–191° after recrystallization from acetone. Calc. for $C_{19}H_{32}ON_3$: C, 71.5; H, 10.34; N, 13.2%. Found: C, 71.2; H, 9.85; N, 13.0%.

Conversion of the Base IX to its Methiodide X

A solution of 0.43 g of IX in 10 ml of acetone was treated with methyl iodide and set aside in the refrigerator. A fine, crystalline precipitate, which was collected and recrystallized from acetone, separated after a few hours. It melted at 231–232°. Calc. for $C_{20}H_{36}ON_3I \cdot H_2O$: C, 50.1; H, 7.52; N, 9.0%. Found: C, 50.6; H, 7.67; N, 9.0%.

Decomposition of the Quaternary Salt X with Potassium Tertiary Butoxide

Metallic potassium (7.4 g) was added in pieces over a period of 1 hour to 160 ml of dry

tertiary butyl alcohol. The methiodide X (6.7 g) was added to the above solution and the mixture was refluxed for 42 hours. The reaction mixture was taken to dryness under vacuum and the residue mixed with water and extracted with ether. From the ether extract 2.0 g of a basic fraction and 2.2 g of neutral fraction were obtained. The basic fraction proved to be a mixture of V and IX, in which the latter predominated. The neutral fraction was separated into two fractions by chromatography on alumina using chloroform as eluant. The first fraction eluted was recovered from the chloroform and purified by crystallization from ether. It melted at 112–113°. Calc. for $C_{17}H_{24}ON_2$: C, 75.0; H, 8.82; N, 10.3%. Found: C, 74.9; H, 8.84; N, 10.3%.

The infrared spectrum of compound XI had a strong carbonyl absorption at 1700 cm^{-1}, double-bond absorption at 3070, 1640, and 910 cm^{-1}, but no absorption in the hydroxyl region. The ultraviolet absorption spectrum showed no evidence of conjugation.

The more strongly adsorbed fraction was recovered from the chloroform and recrystallized from ether. It melted at 201–202°. Calc. for $C_{17}H_{26}ON_2$: C, 74.4; H, 9.55; N, 10.2%. Found: C, 74.6; H, 9.25; N, 10.5%.

The infrared spectrum of this compound showed olefin absorption at 3070 and 1640 cm^{-1} and hydroxyl absorption at 3400 cm^{-1}. Both compounds had the usual cyanamide absorption at 2200 cm^{-1}.

The keto-olefin XI was converted to the hydroxyolefin XII by reduction with sodium borohydride in 95% ethanol. Hydrogenation of the keto-olefin yielded α-cyanolycopodine (1) identified by a mixed melting point determination and by comparison of its infrared spectrum with an authentic sample.

Ozonolysis of the Hydroxyolefin XII

The hydroxyolefin XII (0.30 g) was dissolved in a solution of 10 ml of anhydrous ethyl acetate and 1 ml of glacial acetic acid and cooled to 20°. A stream of ozone-containing oxygen was passed through the mixture until absorption of ozone no longer occurred. The solution was then transferred to a 50-ml flask, 10 ml of glacial acetic acid and 0.4 g of zinc dust were added, and the mixture was heated under reflux for 5 minutes. The apparatus was then arranged for distillation and the mixture was distilled until the vapor temperature reached 97°. The distillate was collected in an ethanolic solution of 0.28 g of dimedone containing a drop of piperidine and the resulting mixture was allowed to stand for 1 hour. The solvent was then evaporated and the residue was allowed to crystallize from aqueous alcohol. There was obtained 0.13 g of white crystalline solid which melted at 189°, and which did not depress the melting point of an authentic sample of the dimedone derivative of formaldehyde.

Reaction of β-Cyanobromolycopodine II with Potassium Hydroxide in Methanol

A sample of II (0.5 g) was heated at reflux temperature with a mixture of 1 g of potassium hydroxide in 40 ml of methanol for 12 minutes. The solution was made slightly acid and evaporated to dryness under vacuum. The residue was treated with water and extracted with chloroform. Evaporation of the chloroform extract yielded 0.38 g of crystalline product which, when recrystallized from petroleum ether, melted at 98–100°. This compound, VI, proved to be identical with the product which MacLean, Manske, and Marion (1) obtained by treatment of II with ethanolic potassium acetate. The infrared spectrum of a solution of the compound in carbon tetrachloride had a strong absorption band at 1675 cm^{-1}, while the band at 1700 cm^{-1} in the starting compound had completely disappeared. The spectrum of crystalline VI in Nujol mull showed a slight shift of the band to 1680 cm^{-1}. The determination of the spectrum of VI in carbon

tetrachloride solution was repeated with a calcium fluoride prism in the spectrophoto-meter. No bands or inflections were detected in the region 3000–3120 cm^{-1} characteristic of the $=$C—H stretching absorption. The ultraviolet absorption spectrum showed no evidence of conjugation.

Acid Hydrolysis of Compound VI

A sample of the cyclized compound VI (0.60 g) was dissolved in a mixture of 6 ml of 1-propanol and 30 ml of 2 M hydrochloric acid. The mixture was heated for 20 hours on the steam bath and then evaporated to dryness under vacuum. The residue was partitioned between ether and dilute hydrochloric acid solution. The acid solution was then made basic with ammonia and extracted with ether to yield 0.33 g of acid-soluble material. This base was adsorbed on alumina and the column was eluted with chloroform. A fraction (0.24 g) was obtained which had strong infrared absorption at 1675 cm^{-1} and no cyanamide absorption. This semicrystalline fraction was converted to the hydrochloride in acetone solution. Recrystallization of the salt from acetone–ether yielded a sample which melted at 256–257°.

Reduction of Compound VI with Lithium Aluminum Hydride

A solution of VI (0.60 g) in anhydrous tetrahydrofuran was added to lithium aluminum hydride (1 g) in tetrahydrofuran (25 ml). The mixture was heated under reflux for 4 hours and then allowed to stand overnight. The excess hydride was destroyed with wet tetrahydrofuran and the tetrahydrofuran solution was filtered from inorganic residue. The precipitated hydroxides were washed well with warm chloroform and the combined filtrates were evaporated to dryness. The residue yielded 0.21 g of basic material which was dissolved in acetone and converted to the hydrochloride. The hydrochloride was identical with that obtained from the hydrolysis of VI in acid solution.

Methylation of the Secondary Base XIII

The secondary base XIII (0.2 g), derived from the hydrochloride above, was treated with a solution of 0.08 ml of 98% formic acid and 0.24 ml of formalin. The mixture was heated on the steam bath for 4 hours and allowed to stand overnight. The resulting solu-tion was treated with dilute hydrochloric acid, filtered, made alkaline with ammonia, and extracted with ether. The dried ether extract yielded an oily residue (0.2 g) which was dissolved in acetone and treated with perchloric acid. The crystalline perchlorate, which separated, melted at 232° after recrystallization from acetone. Calc. for $C_{17}H_{27}ON.HClO_4$: C, 56.4; H, 7.80; N, 3.8%. Found: C, 56.5; H, 7.64; N, 3.7%.

Reduction of β-Cyanobromolycopodine II with Sodium Borohydride

A solution of 0.45 g of sodium borohydride in 95% ethanol was added dropwise over $\frac{1}{2}$ hour to a stirred, ice-cooled solution of 0.50 g of β-cyanobromolycopodine in 95% ethanol. The reaction mixture was stirred for 7 hours at 0°, then made slightly acid with dilute hydrochloric acid and evaporated to dryness under reduced pressure. Water was added to the residue and the mixture extracted with ether. The ether extract was washed with dilute hydrochloric acid and with water, and dried over anhydrous sodium sulphate. Evaporation of the ether solution yielded a crystalline residue whose infrared spectrum exhibited strong hydroxyl and cyanamide absorption and very weak absorption in the carbonyl region. The presence of only a very small peak at 1675 cm^{-1} showed that little cyclization to form compound VI had taken place. Recrystallization of the product from ether gave 0.25 g of a compound, XV, which melted at 139–141° with decomposition. The

compound gave a positive Beilstein test for halogen. Calc. for $C_{17}H_{27}ON_2Br$: C, 57.5; H, 7.66; N, 7.9%. Found: C, 57.5; H, 7.66; N, 8.0%.

Preparation of the Quaternary Salt XVI

An ice-cold methanolic solution of 200 mg of the hydroxybromide XV was treated with an excess of a methanolic solution of trimethylamine. The solution was left overnight in the refrigerator. The solvent and excess amine were removed by evaporation under reduced pressure and the crystalline residue was washed with warm ether and then dissolved in acetone. Concentration of the acetone solution yielded a crop of crystals (135 mg) which melted at 271–272° with decomposition. The infrared spectrum exhibited strong cyanamide absorption at 2200 cm^{-1}, a band of medium strength at 1640 cm^{-1}, and three bands in the hydroxyl region: a strong band at 3315 cm^{-1} and medium bands at 3490 and 3550 cm^{-1}. When the sample was dried under vacuum at 56° for 4 hours a loss of weight of about 8% was observed, which corresponds to a loss of 2 moles of water. On exposure to the atmosphere the sample recovered about half of the weight loss in less than 5 minutes, but further gain in weight took place very much more slowly. The infrared spectrum of the material which had been dried and then exposed to the air showed cyanamide absorption as before, but only two bands in the hydroxyl region: a strong one at 3370 cm^{-1} and a very weak one at 3600 cm^{-1}. The band at 1640 cm^{-1} was no longer present but several very weak peaks were observed in the region 1600–1660 cm^{-1}. The analytical sample, which melted with decomposition at 271–272°, was taken from material which had been dried and then exposed to the atmosphere. Calc. for $C_{20}H_{36}ON_3Br \cdot H_2O$: C, 55.5; H, 8.86; N, 9.7%. Found: C, 55.6; H, 8.62; N, 9.5%.

Decomposition of the Quaternary Salt XVI with Potassium Tertiary Butoxide

A solution of potassium tertiary butoxide was prepared by dissolving 0.35 g of potassium metal in 10 ml of tertiary butanol. To this solution was added 75 mg of the quaternary salt XVI. The reaction mixture was heated under reflux for 3 hours, then the solvent was removed under vacuum. The residue was treated with water and extracted with ether. The ether solution was washed with dilute hydrochloric acid and dried over anhydrous sodium sulphate. Evaporation of the ether yielded a crystalline residue (48 mg) which, after recrystallization from petroleum ether and a second recrystallization from ether, melted at 130–136°. An analytical sample, m.p. 135.5–137.5°, was prepared by sublimation of this material at a pressure of about 0.05 mm of mercury and at 75–110°. Calc. for $C_{17}H_{26}ON_2$: C, 74.4; H, 9.55%. Found: C, 74.1; H, 9.47%.

The infrared spectrum of the product showed strong cyanamide absorption, but no hydroxyl or olefin absorption. A strong band was observed at 1070 cm^{-1}, which is in the region where the ether C—O stretching absorption has been found to occur.

Reduction of the Hydroxybromide XV with Hydrogen in an Alkaline Medium

A pellet (ca. 50 mg) of potassium hydroxide and 30 mg of 2% palladium – calcium carbonate catalyst were added to a hydrogenation bottle containing a methanolic solution of 30 mg of the hydroxybromide. The mixture was shaken under hydrogen at a pressure of 24 lb/sq. in. for 4.5 hours, then filtered and the filtrate evaporated. The residue was treated with water and extracted several times with ether. The ether solution was dried over anhydrous sodium sulphate and filtered. Removal of the solvent by evaporation yielded a crystalline product, which melted at 183–185.5° after recrystallization from ether. The product XIX gave a negative Beilstein halogen test. Calc. for $C_{17}H_{28}ON_2$: C, 73.9; H, 10.21; N, 10.1%. Found: C, 73.9; H, 10.36; N, 9.8%.

Oppenauer Oxidation of β-Cyanodihydrolycopodine XIX

To a solution of 0.20 g of β-cyanodihydrolycopodine in 25 ml of anhydrous benzene were added 2.5 ml of acetone and 0.50 g of aluminum isopropoxide. The mixture was refluxed for 24 hours, then poured into water and the benzene layer separated and dried over anhydrous sodium sulphate. Evaporation of the benzene solution yielded a residue (0.20 g) which partially crystallized on standing. Recrystallization from ether – petroleum ether yielded 54 mg of unreacted XIX. The material recovered from evaporation of the mother liquor was dissolved in benzene and chromatographed on an alumina column using benzene as the eluant. The first fractions yielded 84 mg of crystalline material whose infrared spectrum showed carbonyl and cyanamide absorption at 1705 and 2210 cm^{-1}, respectively, and no hydroxyl absorption. Recrystallization from ether – petroleum ether yielded an analytical sample, m.p. 82.5–84°. Calc. for $C_{17}H_{26}ON_2$: C, 74.4; H, 9.55; N, 10.2%. Found: C, 74.6; H, 9.60; N, 10.5%.

After the band containing the oxidation product, designated β-cyanolycopodine XVIII, had been collected, elution of the column was continued with 99:1 benzene–methanol and a fraction yielding a further 40 mg of starting material was obtained.

Treatment of β-Cyanobromolycopodine II with Hydrogen in Alkaline Medium

β-Cyanobromolycopodine II (0.2 g) was dissolved in 25 ml of methanol containing 1 g of potassium hydroxide and 0.2 g of 2% palladium – calcium carbonate catalyst. The mixture was shaken with hydrogen at 40 lb/sq. in. for 6 hours and then worked up in the manner described in the account of the hydrogenolysis of the hydroxybromide XV. The reaction conditions are those which are given by MacLean, Manske, and Marion (1). The crude crystalline product gave a negative Beilstein test for halogen. The infrared spectrum of the product had a strong absorption band at 1675 cm^{-1} and only weak absorption at 1700 cm^{-1}. After recrystallization from petroleum ether the product melted at 98–100° and proved to be identical with that obtained by treatment of β-cyanobromolycopodine with methanolic potassium hydroxide. No β-cyanolycopodine XVIII was isolated.

The reaction was repeated under the same conditions and this time the crude product was treated with sodium borohydride in order to reduce any β-cyanolycopodine present to β-cyanodihydrolycopodine and thus facilitate chromatographic separation. The hydride reduction mixture was worked up in the usual way and the crude product was adsorbed on alumina and eluted with benzene–methanol. After the cyclized compound had passed through the column a fraction was collected which contained 15 mg of material whose infrared spectrum had absorption in the hydroxyl region and at 1630–1650 cm^{-1}. It could not be ascertained whether or not β-cyanodihydrolycopodine was present in this fraction. Further elution of the column failed to yield any more material.

A methanol solution of 0.25 g of β-cyanobromolycopodine was poured into a hydrogenation bottle containing a solution of 0.05 g of potassium hydroxide in methanol which had been cooled to about −60° by fitting the bottle with a jacket packed with dry ice. Palladium – calcium carbonate catalyst (0.2 g) was added to the solution and the mixture was shaken under hydrogen at 40 lb/sq. in. for 6 hours. During the first 1–2 hours of shaking, a low temperature was maintained by keeping the jacket filled with dry ice, but after this period the mixture was allowed to come to room temperature. The mixture was worked up by the usual procedure. The infrared spectrum of the crude product showed strong cyanamide absorption at 2210 cm^{-1} and a strong band at 1705 cm^{-1} in the carbonyl region. The 1675 cm^{-1} absorption characteristic of the cyclized compound was absent. The material was purified by chromatography on alumina using benzene–methanol as

eluant. The product (0.15 g) melted at 82–84° after recrystallization from ether – petroleum ether and was found to be identical with β-cyanolycopodine XVIII prepared by Oppenauer oxidation of compound XIX.

ACKNOWLEDGMENTS

REFERENCES

1. D. B. MacLean, R. H. F. Manske, and L. Marion. Can. J. Research, B, **28**, 460 (1950).
2. L. R. C. Barclay and D. B. MacLean. Can. J. Chem. **34**, 1519 (1956).
3. D. B. MacLean and W. A. Harrison. Can. J. Chem. **37**, 1757 (1959).
4. B. Douglas, D. G. Lewis, and L. Marion. Can. J. Chem. **31**, 272 (1953).
5. W. R. Song. M.Sc. Thesis, McMaster University, Hamilton, Ont. May, 1958.
6. L. R. C. Barclay. Ph.D. Thesis, McMaster University, Hamilton, Ont. October, 1957.
7. G. D. Meakins. J. Chem. Soc. 4170 (1953).

RADIATION CHEMISTRY OF CYCLOHEXANE

I. ISOTOPIC COMPOSITION OF HYDROGEN EVOLVED FROM MIXTURES OF C$_6$D$_{12}$ AND C$_6$H$_{12}$[1]

P. J. DYNE AND W. M. JENKINSON

ABSTRACT

The yield of D$_2$ formed by a unimolecular process in the γ-ray irradiation of cyclohexane-d_{12} has been deduced from the isotopic composition of hydrogen evolved from C$_6$H$_{12}$–C$_6$D$_{12}$ mixtures. A value of 0.25 molecule/100 ev is found for this "molecular" yield. This yield is only slightly reduced by iodine but is considerably reduced in the presence of biphenyl.

Hydrogen is the principal gaseous product formed in the fast-electron irradiation of cyclohexane, its initial yield being 5.5–5.8 molecules/100 ev. This yield is quite sharply reduced by small additions of solutes. Solutions containing $\sim 5 \times 10^{-3}$ moles/liter iodine, for instance, have $G(\mathrm{H_2}) \sim 4.0$ (1); solutions of cyclohexane with benzene (1, 2), biphenyl, and terphenyls (3, 4) show a similar behavior. From a study of curves of $G(\mathrm{H_2})$ vs. iodine concentration, Burton *et al.* (1) conclude that hydrogen is produced by two mechanisms each with a yield of 2 to 3 molecules/100 ev, one of which is more rapidly suppressed by iodine than the other. Studies of $G(\mathrm{H_2})$ in biphenyl solutions lead to a similar conclusion (3, 4).

The two mechanisms could be (*a*) a bimolecular mechanism involving hydrogen-atom abstraction from the parent molecule and (*b*) a unimolecular mechanism in which molecular hydrogen is split off in one step from an excited parent molecule. These two types of mechanisms are sometimes referred to as "radical and molecular" or "intermolecular and intramolecular".

The existence of two such processes has been demonstrated by Dewhurst (5) in the radiolytic decomposition of *n*-hexane. The high probability of "molecular" processes in organic molecules is shown by Dorfman's work on the gas-phase radiolysis of ethane (6) where it was shown that 66% of the molecular hydrogen is formed by a molecular detachment process not involving free hydrogen atoms.

By examining the variation of the D$_2$ yield in C$_6$D$_{12}$–C$_6$H$_{12}$ mixtures we have determined the value of the 'unimolecular' yield of D$_2$ from C$_6$D$_{12}$. Its value is low, $G(\mathrm{D_2})$ (unimolecular) being 0.25 molecule/100 ev.

## THE METHOD OF SEPARATING UNIMOLECULAR AND BIMOLECULAR YIELDS

In a mixture of C$_6$H$_{12}$, (C$_\mathbf{H}$), and C$_6$D$_{12}$, (C$_\mathbf{D}$), the amount of D$_2$ produced by a unimolecular process will have a first-order dependence on the concentration of C$_\mathbf{D}$ and the amount produced by a bimolecular process will have a second-order dependence on C$_\mathbf{D}$. For a precise development of the relation between the yield of D$_2$ and the relative amounts of C$_\mathbf{H}$ and C$_\mathbf{D}$ we symbolize the reactive intermediates in the bimolecular process as X$_\mathbf{H}$ and X$_\mathbf{D}$ and all other products by P. The symbols X$_\mathbf{H}$ and X$_\mathbf{D}$ are used for the reactive intermediates to stress the generality of the reasoning. The argument is independent of the identity of the intermediates. The unimolecular process is
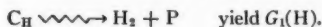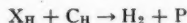
$$\mathrm{C_H} \rightsquigarrow \mathrm{H_2 + P} \qquad \text{yield } G_1(\mathrm{H}).$$

The bimolecular process consists of two steps. The first

$$C_H \leadsto X_H + P$$
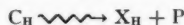
has a yield $G_2(H)$ and is followed by

$$X_H + C_H \rightarrow H_2 + P$$

which has a specific rate constant k_1.

In mixtures of C_6H_{12} and C_6D_{12} the following additional reactions will occur:

$C_D \leadsto D_2 + P$	yield	$G_1(D)$
$C_D \leadsto X_D + P$	yield	$G_2(D)$
$X_D + C_H \rightarrow HD + P$	rate constant	k_2
$X_H + C_D \rightarrow HD + P$	rate constant	k_3
$X_D + C_D \rightarrow D_2 + P$	rate constant	k_4
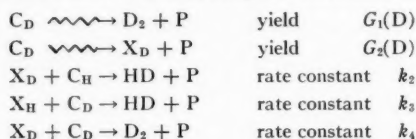
In a mixture containing C_H and C_D gram-molecules of the two components the fraction of ionization energy absorbed by each species is proportional to the mole fractions $C_H/(C_H + C_D)$ and $C_D/(C_H + C_D)$. The number of species X_D formed on the absorption of 100 I ev is $I.G_2(D).C_D/(C_H + C_D)$. The fraction of these species which react to give D_2 is $k_4C_D/(k_2C_H + k_4C_D)$. The number of molecules of D_2 formed by the bimolecular process is therefore

$$\frac{I.G_2(D).k_4C_D{}^2}{(C_D+C_H)\,(k_2C_H+k_4C_D)}$$

which reduces to $I.G_2(D)\,(k_4/k_2)F^2$ where $F = C_D/C_H$ for mixtures in which $C_H \gg C_D$.

Similarly the number of molecules of D_2 formed by the unimolecular process is $IG_1(D).C_D/(C_D + C_H)$ which reduces to $I.G_1(D).F$ for mixtures in which $C_H \gg C_D$.

For these dilute solutions therefore we find that the yield of deuterium $G(D_2)$ based on the amount of energy absorbed in the mixture is given by

[1] $$G(D_2) = G_2(D).(k_4/k_2)F^2 + G_1(D)F$$

or

$$G(D_2)/F = G_2(D).(k_4/k_2)F + G_1(D).$$

A plot of the left side of equation 1 against F should give a straight line with an intercept of $G_1(D)$, the unimolecular yield.

The tacit assumption has been made that products P do not react with the intermediates X to any extent. This will only be generally true at low conversions.

EXPERIMENTAL

Cyclohexane-d_{12} was obtained from Merck and Co. The analysis given by the manufacturers was 94.8 mole % cyclohexane-d_{12}, 5.2 mole % cyclohexane-d_{11}, and 0.4% benzene-d_6 corresponding to an isotopic purity of 99.6%. Dilution of C_6D_{12} with C_6H_{12} was done in two stages. First, an accurate dilution by weighing was made to give a solution containing about 40% C_6D_{12}. Small amounts of this mixture (100–500λ) were added to 2-ml samples of light cyclohexane to give solutions containing up to 7% C_6D_{12}. These 2-ml samples were degassed by freezing, pumping, and thawing five times and were irradiated at room temperature under vacuum for 16 hours in glass vessels in a Co^{60} source at a dose rate of 8.5×10^{21} ev/lt hr. The residual vacuum above the frozen sample

was <0.1 micron before irradiation. Dosimetry is based on the Fricke dosimeter $G(Fe^{3+}) = 15.5$. The gas was pumped off, the amount measured in a conventional gas-analysis line and analyzed on a Consolidated 21-610 mass spectrometer. The mass spectrometer was calibrated against synthetic mixtures of H_2, HD, and D_2.

In blank experiments solutions of D_2 in C_6H_{12} were irradiated. No significant radiation-induced exchange was observed. This is to be expected when it is noted that the parent hydrocarbon, which can react with H atoms, is present in a very much higher concentration than the D_2.

THE YIELDS OF HD AND D_2

Results on mixtures of C_6D_{12} and C_6H_{12} are shown in Table I. They are plotted in the form required by equation 1 in Fig. 1. The experimental points extrapolate to give a value of $G_1(D)$, the unimolecular yield of 0.25 molecule/100 ev.

TABLE I

Isotopic composition of hydrogen from C_6H_{12}–C_6D_{12} mixtures

Mole % C_6D_{12}	$F = C_D/C_H$ $\times 10^2$	G (hydrogen)*	% HD	% D_2	G(HD)	$G(D_2) \times 10^2$	$\dfrac{G(D_2)}{F}$
1.63	1.66	4.85	1.26	0.091$_5$	0.061$_2$	0.44$_4$	0.26$_8$
1.63	1.66	4.57	1.30	0.096$_2$	0.059$_5$	0.43$_9$	0.26$_5$
3.12	3.22	4.91	2.35	0.19$_4$	0.115	0.95$_3$	0.29$_6$
3.12	3.22	4.63	2.42	0.19$_6$	0.112	0.90$_7$	0.28$_1$
5.72	6.06	4.94	4.32	0.38$_0$	0.213	1.8$_8$	0.31$_4$
6.86	7.36	4.96	5.22	0.46$_5$	0.258	2.3$_0$	0.31$_8$

*This is total chemical hydrogen, i.e. ($H_2 +$ HD $+ D_2$).

Results on mixtures of C_6D_{12} and C_6H_{12} with added iodine or biphenyl are given in Table II and Table III and are also plotted in Fig. 1. The value of $G_1(D)$ in the presence of iodine is 0.22, approximately 10% lower than in the absence of iodine. The value of $G_1(D)$ is much more strongly reduced by biphenyl, the intercept being 0.12.

TABLE II

Isotopic composition of hydrogen from C_6H_{12}–C_6D_{12} mixtures saturated with I_2

Mole % C_6D_{12}	G (hydrogen)	% HD	% D_2	G(HD)	$G(D_2) \times 10^2$	$\dfrac{G(D_2)}{F}$
1.63	3.20	1.43	0.12$_2$	0.045	0.39	0.23$_5$
3.12	3.20	2.71	0.25	0.086	0.80	0.24$_8$
5.72	3.16	5.12	0.51$_4$	0.164	1.6$_2$	0.26$_8$
6.86	3.20	6.12	0.64	0.19$_5$	2.0$_4$	0.27$_8$

TABLE III

Isotopic composition of hydrogen from C_6H_{12}–C_6D_{12} mixtures with $10^{-1} M$ biphenyl

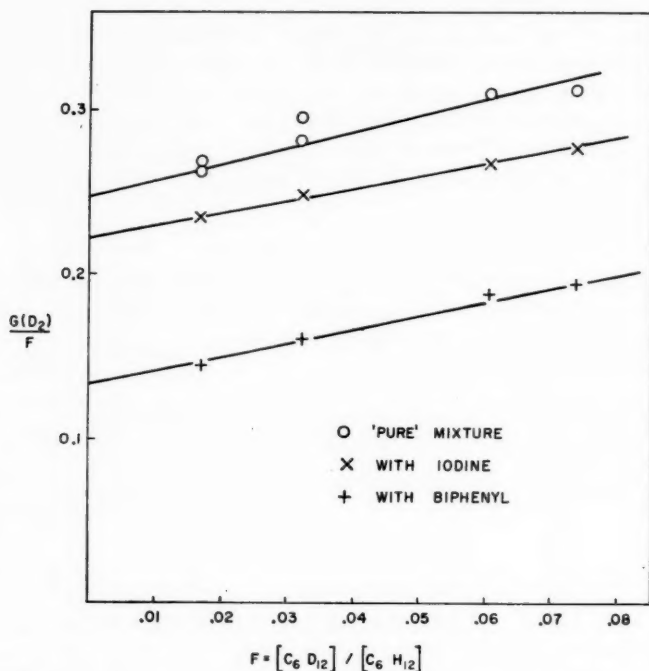| Mole % C_6D_{12}	Biphenyl moles/liter $\times 10^2$	G (hydrogen)	% HD	% D_2	G(HD)	$G(D_2) \times 10^2$	$\dfrac{G(D_2)}{F}$
1.63	9.76	2.51	1.4$_8$	0.09$_7$	0.037$_1$	0.24$_3$	0.14$_6$
3.12	9.32	2.55	2.8$_4$	0.20$_4$	0.072$_4$	0.52	0.16$_1$
5.72	8.54	2.63	5.21	0.43$_4$	0.13$_7$	1.1$_4$	0.18$_8$
6.86	8.20	2.65	6.24	0.53$_9$	0.16$_5$	1.4$_2$	0.19$_4$

FIG. 1. The experimental results plotted in the form required by eq. 1. The intercept when $F = 0$ is the value of the "molecular" yield of D_2 from C_6D_{12} and from C_6D_{12} containing iodine and biphenyl.

DISCUSSION

The value of 0.25 for the unimolecular yield is for D_2 from C_6D_{12}. The corresponding yield for H_2 from C_6H_{12} will, in all probability, be considerably larger. This general prediction is borne out by Gordon and Burton's (7) measurements of $H_2(D_2)$ yields from benzene and benzene-d_6 and by Boyd's measurements of $H_2(D_2)$ and "polymer" yields from deuterated biphenyl and terphenyl (8). A value between 0.5 and 1.0 for $G_1(H)$ is reasonable. This estimate is in agreement with the limiting yield of cyclohexene observed by Dewhurst (9) in the presence of dissolved oxygen. A constant yield of 0.7 molecule $C_6H_{10}/100$ ev was observed which was assigned to the yield of the unimolecular process which would not be reduced by radical scavengers such as oxygen.

The small effect of iodine on the unimolecular yield in our experiments is consistent with our interpretation. The difference in the intercepts, which is of the order of 10%, may not be experimentally significant. While the isotopic measurements have a high degree of internal consistency the principal parameter determining the intercept is the total hydrogen yield. These experiments were not suited to the measurements of hydrogen yield to the highest accuracy and the values of $G(H_2) = 3.2$ are lower than the values we obtained for larger samples of cyclohexane and iodine, viz. 3.5.

The 50% reduction of the unimolecular yield by 10^{-1} M biphenyl is significant. If the mechanism of the "unimolecular" yield is

$$C_6H_{12} \rightsquigarrow C_6H_{12}*$$

$$C_6H_{12}* \rightsquigarrow C_6H_{10} + H_2$$
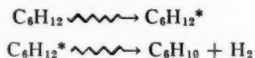
where $C_6H_{12}^*$ represents an excited intermediate state, then the reduction of the yield can only be due to quenching of the $C_6H_{12}^*$ by the biphenyl. This is an example of the energy-transfer process postulated by Manion and Burton (2).

The main conclusion to be drawn from these results is that the yield of "molecular" hydrogen from C_6H_{12} is a small fraction, 10–20%, of the total. If the balance of the hydrogen yield comes from two processes each with yields of between 2 and 3 molecules/ 100 ev as suggested in reference 1 it follows that both these processes are bimolecular.

A similar measurement of $G_1(H)$ using solutions of C_6H_{12} in C_6D_{14} was attempted. The isotopic purity of the C_6D_{12}, now the major constituent of the mixture, was not, however, sufficient to allow the application of the simple interpretation given above.

REFERENCES

1. M. BURTON, J. CHANG, S. LIPSKY, and M. P. REDDY. Radiation Research, 8, 203 (1958).
2. J. P. MANION and M. BURTON. J. Phys. Chem. 56, 560 (1952).
3. P. J. DYNE and J. W. FLETCHER. Unpublished.
4. J. H. BAXENDALE. Private communication.
5. H. A. DEWHURST. J. Phys. Chem. 62, 15 (1958).
6. L. M. DORFMAN. J. Phys. Chem. 62, 29 (1958).
7. S. GORDON and M. BURTON. Discussions Faraday Soc. 12, 88 (1952).
8. A. W. BOYD. Private communication.
9. H. A. DEWHURST. J. Phys. Chem. 63, 813 (1959).

FREE RADICALS BY MASS SPECTROMETRY

XIX. PRIMARY STEPS IN THE MERCURY-PHOTOSENSITIZED DECOMPOSITION OF FORMALDEHYDE[1]

A. G. HARRISON[2] AND F. P. LOSSING

ABSTRACT

In the Hg^3P, photosensitized decomposition of formaldehyde, evidence from deuterium labelling shows that 40% of the primary dissociation proceeds by way of an intramolecular elimination of H_2. The remainder dissociates by formation of H and HCO, or of 2H and CO. A clear distinction between these latter two processes cannot be made under the reaction conditions employed.

INTRODUCTION

Although the direct photolysis of formaldehyde has been rather extensively studied by a number of authors, no investigation of the mercury-photosensitized decomposition appears to have been made. One question of particular interest is whether the relative probability of occurrence of free radical and intramolecular rearrangement processes is dependent on the means of activation. If one uses the symbol HCHO* to designate a formaldehyde molecule which has been excited by a quantum, either by direct absorption or by collision with an excited mercury atom, the two primary dissociation processes of interest are

$$HCHO^* \rightarrow H + HCO, \qquad [1]$$
$$\rightarrow H_2 + CO. \qquad [2]$$

At wavelengths shorter than 2700 Å, a third reaction becomes energetically possible:

$$HCHO^* \rightarrow 2H + CO. \qquad [3]$$

In this wavelength region reaction [1] might become indistinguishable from reaction [3] if the lifetime of the HCO radical were sufficiently shortened by energy carried over from the primary dissociation step.

Information as to the relative importance of these three primary steps in the direct photolysis at various wavelengths is rather ambiguous. Gorin (1) investigated the photolysis at 2537 Å, 3130 Å, and 3650 Å, using iodine as a radical trap. He concluded that at 2537 Å and 3130 Å reaction [1] is essentially the only process. Although reaction [3] is energetically possible at 2537 Å, he assigned an upper limit of 0.1 to its occurrence. He concluded that reaction [1] was still the major primary process at 3650 Å, although reaction [2] occurred to the extent of 0.3. These findings have been questioned by Steacie (2) in view of later work on the interfering effect of iodine in aldehyde photolyses.

Using the Paneth technique, Volman *et al.* (3) showed, by the removal of tellurium mirrors, that H atoms or HCO radicals must be formed in the photolysis at 2750 Å.

Calvert and Steacie (4) examined the photolysis at 3130 Å in some detail and found the mechanism to be consistent with the occurrence of reaction [1]. The extent to which reaction [2] occurred could not be determined from their results, however.

Klein and Schoen (5) photolysed mixtures of H_2CO and D_2CO at wavelengths from 3130 Å to 3750 Å. They found that at 3650 Å reaction [1] occurred, but to a smaller

extent than reported by Gorin (1), and they concluded that reaction [2] was the major process. The occurrence of reaction [1] at this wavelength requires that D(H—CHO) be less than 78 kcal/mole, and consequently that D(H—CO) in formyl must be greater than 27 kcal/mole. This conclusion has been questioned by Calvert (6) on the grounds that the observed rate of reaction [1] at 3650 Å could result from absorption by vibrationally excited formaldehyde molecules. The interpretation of these results and their bearing on the bond dissociation energy in HCHO and HCO is still controversial (7, 8). For the present purpose, however, a significant finding of Klein and Schoen was that reactions [1] and [2] both occurred at 3130 Å, the latter with a greater probability. Concerning the occurrence of reaction [2] at 2537 Å, on the other hand, there seems to be no unambiguous evidence either for or against.

It was thought that a measurement of the relative probabilities of reactions [1] and [2] in the mercury-photosensitized reaction at 2537 Å would be of interest for comparison with the direct photolytic experiments at longer wavelengths. A similar investigation of the mercury-photosensitized decomposition of acetaldehyde (9) showed that the corresponding intramolecular reaction to form CH_4 and CO did not occur to any appreciable extent, although there is evidence in the literature for its participation in the direct photolytic decomposition.

EXPERIMENTAL

The mercury-photosensitized reaction was carried out at 55° C in a fast-flow reaction system coupled to a mass spectrometer (10). A portion of the stream of reaction products from the illuminated zone was allowed to flow directly into the ionization chamber. A modification to the original apparatus has been described recently (11), together with some considerations regarding the experimental conditions in the reactor. The partial pressure of formaldehyde was in the region of 1–6 microns, carried in a stream of helium at 8–10 mm. Addition of formaldehyde to the helium stream was controlled by means of metal needle valves leading to samples of liquid formaldehyde maintained at −78° C.

The sample of D_2CO, prepared for us through the kindness of Dr. L. C. Leitch, had an isotopic purity of about 99%.

RESULTS AND DISCUSSION

In preliminary experiments formaldehyde was found to have a relatively large cross section for reaction with Hg^3P_1 atoms. In a contact time of 0.001 second formaldehyde at a partial pressure of 6.0 microns was decomposed to the extent of 24.4%. At the same pressure and contact time acetone was decomposed to the extent of 21.9%. The yield of CO was found to be essentially quantitative (97%); consequently the polymerization of formaldehyde vapor was negligible. Using electrons of low energy, no increase in the mass 29 peak attributable to the HCO radical could be observed. Earlier experiments have indicated, however, that the sensitivity for detection of HCO radical in this instrument is quite low (9), presumably as a result of the dissociation of HCO on surfaces in the ionization chamber. No formation of the dimer, glyoxal, was observed.

The participation of reaction [2] was demonstrated using H_2CO–D_2CO mixtures in a manner similar to that previously employed for acetaldehyde (9). The results are given in Table I. In experiments using H_2CO alone, the yield of H_2 per H_2CO decomposed was 0.96 to 0.98, and independent of the partial pressure of H_2CO over the range 1.84–5.63 microns. When D_2CO was added to the reaction stream containing H_2CO, the yield of H_2 per H_2CO decomposed decreased progressively as the mole fraction of D_2CO was

TABLE I

Decomposition of H_2CO–D_2CO mixtures

Partial pressures (μ)				Decomposed				H_2 produced (μ)	$H_2/\Delta H_2CO$	Mole fraction, H_2CO $\dfrac{H_2CO}{H_2CO+D_2CO}$
Lamp off		Lamp on		μ		%				
H_2CO	D_2CO	H_2CO	D_2CO	H_2CO	D_2CO	H_2CO	D_2CO			
1.84_2	—	1.20_5	—	0.63_7	—	34.5_8	—	0.61	0.96	1.00
3.22_2	—	2.20_5	—	1.02_7	—	31.8_2	—	1.00	0.97	1.00
5.62_8	—	3.97_6	—	1.65_2	—	29.3_5	—	1.62	0.98	1.00
5.38_2	1.70_2	3.91_5	1.24_7	1.46_5	0.45_5	27.2_1	26.7_3	1.23	0.84	0.76_0
5.62_8	2.77_0	4.12_9	2.05_1	1.49_9	0.71_9	26.6_2	25.9_6	1.17	0.78	0.67_0
2.75_0	2.78_2	2.01_6	2.05_1	0.73_4	0.73_1	26.6_9	26.2_8	0.52_7	0.72	0.49_7
2.93_0	5.06_1	2.14_5	3.77_0	0.78_5	1.29_1	26.7_9	25.5_0	0.46_4	0.59	0.36_7
1.71_7	5.23_1	1.26_1	3.86_7	0.45_6	1.36_4	26.5_5	26.0_7	0.25_3	0.55	0.24_7
1.03_7	5.59_7	0.76_4	4.13_5	0.27_3	1.46_2	26.3_2	26.1_2	0.13_3	0.49	0.15_6
4.60_4	4.55_4	3.54_5	3.50_9	1.05_9	1.04_5	22.9_3	22.9_6	0.72_9	0.69	0.50_3

increased. In these mixtures HD and D_2 were formed. It is evident that, as the ratio D_2CO/H_2CO is made very large, any H atoms produced in the primary dissociation step must result in the formation of HD rather than H_2. In this respect it makes no difference whether the H atoms are removed by any or all of the three possible reactions:

$$H + D\,(+\,M) \rightarrow HD\,(+\,M), \qquad [4]$$

$$H + DCO \rightarrow HD + CO, \qquad [5]$$

$$H + D_2CO \rightarrow HD + DCO. \qquad [6]$$

Any H_2 produced in mixtures containing a very large excess of D_2CO must therefore have been formed by the intramolecular process [2]. The yield of H_2 as a function of the mole fraction of H_2CO in the mixture, shown graphically in Fig. 1, was an approximately straight line. An extrapolation of the line to infinite dilution of H_2CO by D_2CO indicates that about 40% of the H_2CO must decompose to give H_2 in one step. One can therefore assign the relative probability of 0.40 ± 0.05 to reaction [2], leaving 0.6 ± 0.05 to be divided between reactions [1] and [3].

The relative probability of reaction [2] can also be calculated independently from HD production in mixtures of H_2CO and D_2CO. With the approximately equimolar mixture given in the last line of Table I, the partial pressure of HD formed was 0.660 micron. Neglecting possible interference from a very small amount of HDCO (see below), we may assume that all the HD was formed by reactions [4] and [5] and the isotopic equivalent of [5]:

$$D + HCO \rightarrow HD + CO. \qquad [7]$$

The amount of HD formed by reaction [6] is extremely small. That this reaction is negligibly slow under the reaction conditions employed is shown by the fact that the percentage of formaldehyde decomposed showed no increase with increasing partial pressure. With the further assumption that the fraction of formaldehyde dissociating by reaction [2] is the same for both isotopic species, and that consequently in this experiment $[H] \simeq [D]$ and $[HCO] \simeq [DCO]$, the amounts of H_2, HD, and D_2 formed by reactions [4], [5], and [6] and their isotopic equivalents would be in the ratio 1:2:1. The total amount of isotopic hydrogens formed as a consequence of the primary reactions [1] and [3] will then be twice the amount of HD observed, i.e. 1.32 microns. Since the total amount of formaldehyde decomposed was $1.059+1.045 = 2.104$ microns, reactions

[1] and [3] must account for 1.32/2.104 or 0.63 of the total reaction. The remainder, 0.37, is the relative probability of reaction [2]. This result agrees closely with the extrapolation in Fig. 1.
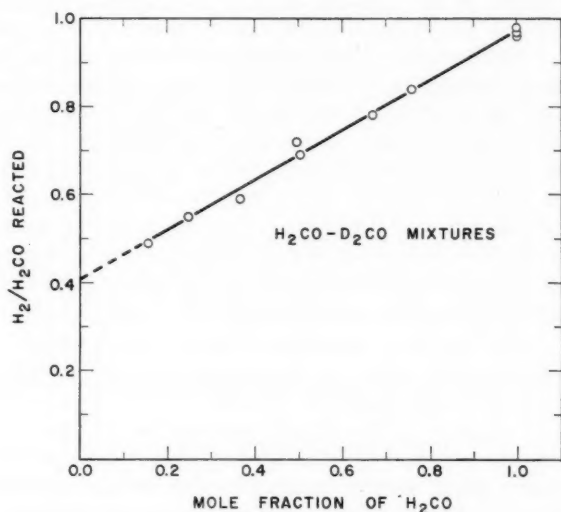
Although the data given above provide good evidence that about 40% of the total reaction goes by way of reaction [2], there remains the question as to whether the remainder of the reaction is better described by reaction [1] or reaction [3]. The energy available from $^3P_1$ mercury atoms, 112 kcal/mole, is more than sufficient to bring about reaction [3], for which the energy requirement is 105 kcal/mole. It is evident therefore that HCO radicals formed in reaction [1] would have sufficient excitation to dissociate spontaneously. Unless some effective means of deactivation is available, reactions [1] and [3] would consequently be indistinguishable. In the present experiments conditions would appear to be quite unfavorable for rapid deactivation, since helium at 8 mm pressure would be quite ineffective in this respect, and the partial pressure of formaldehyde was only a few microns. Nevertheless, some evidence for the presence of an appreciable concentration of formyl radicals in the reactor was obtained. It was observed that when mixtures of H_2CO and D_2CO were decomposed, a significant amount of the mixed aldehyde HDCO was formed. Possible modes of formation of HDCO are the following:

$$HCO + DCO \rightarrow HDCO + CO, \qquad [8]$$

$$H + DCO \rightarrow HDCO, \qquad [9]$$

$$H + D_2CO \rightarrow HDCO + D. \qquad [10]$$

In a separate experiment in which the photosensitized decomposition of a mixture of H_2 and D_2CO in the reactor was carried out, no HDCO was formed. The formation of HD in this reaction showed, however, that H atoms were present either as a result of quenching of Hg^3P_1 atoms by H_2, or by exchange of D atoms with H_2. Since no HDCO

was formed, even though an appreciable quantity of H atoms was present, it may be concluded that reactions [9] and [10] are negligibly slow under the present reaction conditions. It would appear, then, that in mixtures of H_2CO and D_2CO, reaction [8] is the most probable source of the observed HDCO. In one such experiment, in which the amounts of H_2CO and D_2CO decomposed were 1.20 and 1.29 microns respectively, the partial pressure of HDCO formed was estimated to be 0.06 micron. (For this calculation the mass spectral sensitivity for HDCO at mass 31 was assumed to be the mean of the parent ion sensitivities for H_2CO and D_2CO.) If, as seems probable, the concentrations of HCO and DCO were not greatly different, the amounts of isotopic formaldehydes formed by disproportionation would be in the ratio 1:2:1. The total formaldehydes resulting from reaction [8] would then be 0.12 micron, and the total of formyl radicals involved equal to 0.24 micron. This amount corresponds to a lower limit of about 0.1 for reaction [1]. The fraction of primary reaction yielding such "stable" formyls is undoubtedly much greater than this, since formyls will be destroyed by other reactions. By analogy with the reaction of CH_3 with HCO (9), the abstraction reaction

$$H + HCO \rightarrow H_2 + CO \qquad\qquad [11]$$

is probably quite rapid. Some formyls may also be decomposed by reaction with a second excited mercury atom:

$$HCO + Hg^3P_1 \rightarrow H + CO + Hg^1S_0. \qquad\qquad [12]$$
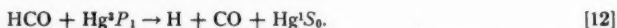
From the present experiments, therefore, a lower limit for the occurrence of reaction [3] cannot be set. It might be expected that at higher pressures, where the possibility for deactivation of HCO radicals formed in [1] is increased, reaction [1] would be favored over reaction [3]. In the present reactor the effect of pressure could not be examined over a range wide enough to be significant.

In view of the large excess of energy available at 2537 Å, it is surprising that such a large part of the primary reaction proceeds by the almost thermoneutral formation of H_2 and CO rather than by rupture of a C—H bond. The substitution of CH_3 for H, as in acetaldehyde, is sufficient to reduce the similar intramolecular processes

$$CH_3CHO + Hg^3P_1 \rightarrow CH_4 + CO + Hg^1S_0 \qquad\qquad [13]$$

$$\rightarrow H_2 + CH_2 = CO \qquad\qquad [14]$$
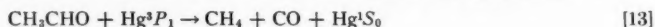
to negligible proportions (9).

REFERENCES

1. E. Gorin. J. Chem. Phys. **7**, 256 (1939).
2. E. W. R. Steacie. Atomic and free radical reactions. 2nd. ed. Reinhold Publishing Corp., New York. 1954.
3. D. H. Volman, P. A. Leighton, F. E. Blacet, and R. K. Brinton. J. Chem. Phys. **18**, 203 (1950).
4. J. G. Calvert and E. W. R. Steacie. J. Chem. Phys. **19**, 176 (1951).
5. R. Klein and L. G. Schoen. J. Chem. Phys. **24**, 1094 (1956).
6. J. G. Calvert. J. Phys. Chem. **61**, 1206 (1957).
7. R. Klein and L. J. Schoen. J. Chem. Phys **29**, 953 (1958).
8. J. G. Calvert. J. Chem. Phys. **29**, 954 (1958).
9. F. P. Lossing. Can. J. Chem. **35**, 305 (1957).
10. F. P. Lossing, D. G. H. Marsden, and J. B. Farmer. Can. J. Chem. **34**, 701 (1956).
11. P. Kebarle and F. P. Lossing. Can. J. Chem. **37**, 389 (1956).

LONG-RANGE COUPLING CONSTANTS IN THE
N.M.R. SPECTRA OF OLEFINES[1]

ROBERT R. FRASER

ABSTRACT

The spectra of tiglic and angelic acids and their methyl esters have been determined and analyzed by first-order perturbation theory. The magnitudes of the long-range coupling constants were found to be greater in each instance for *trans* oriented hydrogens than for *cis* hydrogens. All long-range coupling constants already reported have been examined and found to be consistent with the proposal that *trans* coupling constants are larger than *cis* coupling constants for hydrogens separated by more than three bonds.

Thus far, N.M.R. spectroscopy has been utilized in two ways to assign configuration to a pair of isomeric olefines. The magnitude of the coupling constant between the hydrogens attached to opposite ends of the double bond of a disubstituted olefine has been observed consistently to be larger for *trans* hydrogens than for *cis* hydrogens (1). These observations are in agreement with the theoretical calculation of coupling constants for olefines which were recently reported by Karplus (2). In symmetrically substituted olefines where coupling is not observable due to identical chemical shifts for the two protons on the double bond, the constant has been determined by examination of the peaks produced by interaction of the ethylenic hydrogens with the C^{13} nuclei present in natural abundance (3). The second method, proposed by Jackman and Wiley (4), assigns configuration to olefines on the basis of observations that a substituent β to a methoxycarbonyl group (each attached to one end of a double bond) will appear at a lower field strength when oriented *cis* to the ester group. A third method may be applicable by determination of the relative magnitude of long-range coupling constants between hydrogens *cis* or *trans* to each other.
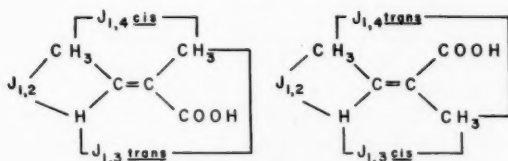

FIG. 1. Coupling constant nomenclature for tiglic (left) and angelic (right) acids.

Although the magnitude of spin–spin coupling decreases rapidly with increasing distance between the nuclei, the decrease is not so large when one of the intervening bonds possesses unsaturation. In olefines the size of the coupling constant between hydrogens separated by four bonds, hereafter called $J_{1,3}$, generally varies from 0.4 to 2.0 cycles per second (see Fig. 1 for nomenclature). Surprisingly we have observed equally large coupling constants between hydrogens separated by five bonds ($J_{1,4}$) as well. An examination of the literature revealed only relatively few cases where the spectra of a pair of *cis* and *trans* olefines are reported, including the $J_{1,3}$ values. We have measured the spectra of tiglic and angelic acids, and their methyl esters, to determine whether or not a simple relationship exists between the relative magnitude of 1,3 coupling constants and the geometrical relationship of the interacting nuclei. Should such a relationship obtain,

assignment of configuration to trisubstituted olefines on this basis would be possible. Furthermore, as Muller and Pritchard have pointed out (5) such distant interaction indicates appreciable contribution of hitherto neglected structures to the ground-state wave function of the molecule. Thus the data obtained should be of use in estimating such contributions as was the case for ethylene (2).

TABLE I

Literature values for 1,3 coupling constants in cycles/sec

Compound	$J_{1,3}$ trans	$J_{1,3}$ cis	Reference
Butene-1	1.3	1.9	(6)
α-Methyl styrene	0.7	1.4	(7)
cis-Propenylbenzene	1.4	—	(7)
trans-Propenylbenzene	—	1.9	(8)
cis–cis-Dimethylmuconate	1.3	—	(9)
trans–trans-Dimethylmuconate	—	0.7	(9)
trans*-1,2,3-Trichloropropene-1	0.8	—	(10)
cis-1,2,3-Trichloropropene-1	—	0.4	(10)
cis†-1,3-Dichloropropene-1	0.9	—	(10)
	1.2	—	(11)
trans-1,3-Dichloropropene-1		0.5	(10)
		1.2	(11)

*cis and trans refer to the orientation of the two chlorine atoms on the double bond.
†cis and trans refer to the orientation of the two chlorine-containing groups.

The values of 1,3 coupling constants reported in the literature are given in Table I. At first glance no clear-cut relationship is obvious. Each set of values, however, must be critically appraised. The constants reported by Alexander (6) were obtained after a complete analysis of the spin wave functions for a system of five nuclei. The purpose of his analysis was to determine the relative signs of $J_{1,2}$ and $J_{1,3}$ and he found by testing various values for nine adjustable parameters that the best fit with the observed spectrum was obtained with the indicated values. An inversion of the magnitudes of $J_{1,3}$ cis and $J_{1,3}$ trans was not tested for comparison with the observed spectrum and could well be as acceptable. The relative magnitude of the coupling constants listed for α-methylstyrene depends on the assignment of peaks to the two ethylenic hydrogens. Pople, Bernstein, and Schneider (7) have only tentatively assigned the peak at high field to the hydrogen cis to the methyl group. The opposite assignment, perhaps even more acceptable,* would reverse the values for $J_{1,3}$ trans and $J_{1,3}$ cis. The results for the isomeric propenyl benzenes are more difficult to assess as details of the analysis of the cis isomer have not been reported. Should the values listed for the first three systems prove erroneous then the general rule $J_{trans} > J_{cis}$ would be obeyed.

Similar uncertainties exist in the remaining reported values in Table I with the exception of the trichloropropenes, which gave a simple spectrum. The most reliable values can only be obtained from spectra which can be analyzed by first-order perturbation theory. Such spectra have been obtained for tiglic and angelic acids and their methyl esters. The

*The effect of the benzene ring on its cis hydrogen can be either diamagnetic or paramagnetic depending on its orientation with respect to the rest of the molecule (12). The ultraviolet spectrum of α-methylstyrene shows a K-band maximum at lower wavelength with diminished intensity compared with that of styrene (13). Such a shift is most likely attributed to deviation of the aromatic ring from coplanarity with the ethylene system, the amount of which determines the strength of the paramagnetic effect.

spectra for tiglic acid and methyl tiglate were first measured in carbon tetrachloride and showed complications in structure due to lack of a difference in chemical shift between the two methyl groups. When the spectra were measured on 10% solutions in benzene, solute–solvent interactions caused a preferential shift of the β-methyl group by 20 cycles/sec to high field thus allowing first-order analysis to be applied. Figure 2 shows the
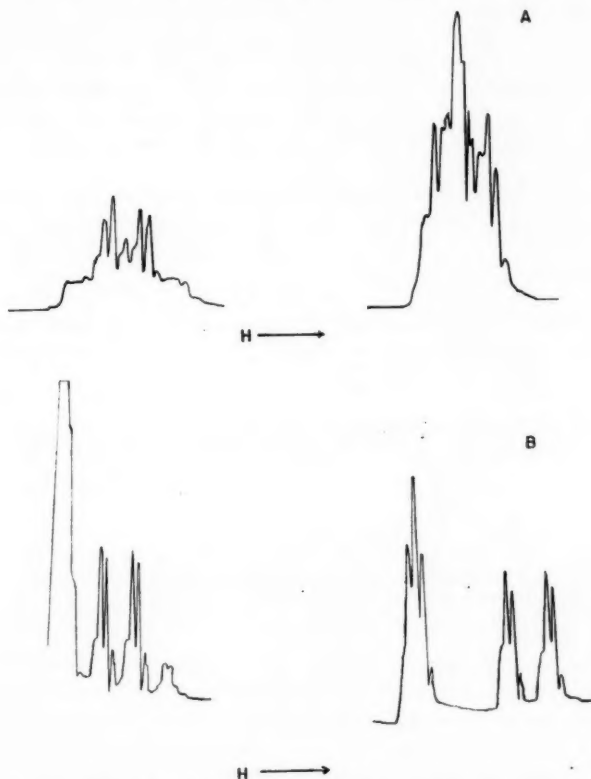

FIG. 2. Spectra due to ethylenic hydrogen (low-field peak) and methyl groups of tiglic acid. (A) 10% solution in carbon tetrachloride; (B) 10% solution in 93% deuterated benzene. (The 7% of benzene protons obscures the first quartet of the ethylenic absorption.)

absorption peaks for the ethylenic hydrogen and the two methyl groups of tiglic acid in carbon tetrachloride and deuterobenzene solutions. Assignment of the two quartets at highest field to the β-methyl group is made on the basis of the assumption that the larger CH_3—C—H coupling will occur between hydrogens on adjacent carbon atoms. Exceptions to this assumption are known but are not likely here. The reverse assignment for the two methyl groups would require $J_{1,3}$ to be 7.11 cycles/sec and $J_{1,2}$ to be 1.43 cycles/sec, a highly improbable situation. Any doubt as to the structures of tiglic and angelic acids has recently been removed by the irrefutable evidence of X-ray analysis (14).

The measured values for the chemical shifts and coupling constants are given in Table II. The results obtained show $J_{1,3}$ trans > $J_{1,3}$ cis in both pairs of isomers. In addition $J_{1,4}$ trans > $J_{1,4}$ cis. The only other pair of geometrical isomers whose $J_{1,4}$ values have been

CANADIAN JOURNAL OF CHEMISTRY. VOL. 38, 1960

TABLE II

Chemical shifts* and coupling constants† for tiglic and angelic acids and their methyl esters

Compound	Formula	$J_{1,3}$	$J_{1,4}$	$J_{1,2}$
Tiglic acid	(8.13) CH₃ — (8.13) CH₃ / C=C / (3.03) H — (−2.62) COOH	1.43 ($\sigma = 0.03$)	1.17 ($\sigma = 0.06$) σ = standard deviation	7.11 ($\sigma = 0.05$)
Angelic acid	(7.94) CH₃ — (−2.75) COOH / C=C / (3.82) H — (8.10) CH₃	1.28 ($\sigma = 0.05$)	1.46 ($\sigma = 0.06$)	7.16 ($\sigma = 0.11$)
Methyl tiglate	(8.25) CH₃ — (8.20) CH₃ / C=C / (3.28) H — (6.35) COOCH₃	1.37 ($\sigma = 0.04$)	1.20 ($\sigma = 0.04$)	7.18 ($\sigma = 0.14$)
Methyl angelate	(8.05) CH₃ — (6.35) COOCH₃ / C=C / (4.03) H — (8.13) CH₃	1.22 ($\sigma = 0.03$)	1.51 ($\sigma = 0.05$)	6.96 ($\sigma = 0.14$)

*Determined from 10% solutions in carbon tetrachloride containing 1% of tetramethylsilane and reported in parentheses as τ values (parts per million with tetramethylsilane assigned a value 10.00).
†In units of cycles per second.

determined are the butene-2 isomers. There, too, $J_{1,4}$ *trans* was found to be greater than $J_{1,4}$ *cis* (15). Demonstration that such a general relationship is true for long-range coupling constants in all olefines must await the accumulation of sufficient empirical and theoretical evidence. Work is continuing in this direction. Finally, it is interesting to note that our chemical shift data agree with the findings of Jackman and Wiley (4).

EXPERIMENTAL

The spectra were measured with a Varian V-4302 high resolution N.M.R. spectrometer. Peak separations in each multiplet were measured by the side band technique (16) employing a Hewlett–Packard wide-range oscillator. The accuracy of the oscillator was checked with a Hewlett–Packard standardized frequency counter and the error was found to be less than 0.5% in the range employed for coupling constant determinations and less than 0.75% when used for determination of chemical shifts. Each coupling constant is reported as the average of at least four determinations and the standard deviation is reported with each value. The spectrum of angelic acid was measured on a 10% solution in carbon tetrachloride. Those for tiglic acid and its methyl ester were obtained from 10% solutions in deuterobenzene and benzene respectively. Methyl angelate was run as the pure liquid. All chemical shifts were measured from 10% solutions in carbon tetra-chloride containing 1% of tetramethylsilane as internal standard (17).

Tiglic Acid

This compound was prepared by the oxidation of tiglaldehyde by a modification of the method of Goldberg and Lindstead (18). A mixture of 52 g (0.6 mole) of tiglaldehyde, b.p. 114–115°, and 260 g (1.6 mole) of silver nitrate in 840 ml of 28% ethanol in a 3-l. flask was stirred for 4 hours. After standing for 12 hours the mixture was filtered. The filtrate was acidified and treated with 34 g (0.3 mole) of calcium chloride in 75 ml of water. The precipitated calcium salt was filtered off, and converted to the sodium salt by boiling with an excess of 10% sodium carbonate. The solution of the sodium salt was acidified, extracted with ether, and the dried extracts upon evaporation gave 32.5 g (53%) of tiglic acid, m.p. 64–65° (literature m.p. 64° (19)).

Methyl Tiglate

The methyl ester was obtained by esterification according to the method of Buckles and Mock (20). Methyl tiglate, b.p. 133–135°, n_D^{24} 1.4360 was obtained in 91% yield (literature b.p. 137.5–139°, n_D^{20} 1.4371 (20)).

Angelic Acid

Tiglic acid was converted to angelic acid by the procedure of Buckles and Mock (20). The over-all yield of angelic acid, m.p. 42–44°, was 39% (literature m.p 44–45.2° (21)).

Methyl Angelate

Angelic acid was esterified by the procedure of Buckles and Mock (20). From 2.5 g of acid was obtained 1.5 g (52%) of methyl angelate, b.p. 125–126°, n_D^{24} 1.4307 (literature b.p. 127.2–128°, n_D^{20} 1.4330 (20)).

ACKNOWLEDGMENTS

REFERENCES

1. J. A. POPLE, W. G. SCHNEIDER, and H. J. BERNSTEIN. High resolution nuclear magnetic resonance. McGraw-Hill Book Co., Inc., New York. 1959. p. 194.
2. M. KARPLUS. J. Chem. Phys. **30**, 11 (1959).
3. A. D. COHEN, N. SHEPPARD, and J. J. TURNER. Proc. Chem. Soc. 118 (1958).
4. L. M. JACKMAN and R. H. WILEY. Proc. Chem. Soc. 196 (1958).
5. N. MULLER and D. E. PRITCHARD. J. Chem. Phys. **31**, 771 (1959).
6. S. ALEXANDER. J. Chem. Phys. **28**, 358 (1958).
7. M. KARPLUS. J. Chem. Phys. **30**, 238 (1959).
8. R. W. FESSENDEN and J. S. WAUGH. J. Chem. Phys. **30**, 944 (1959).
9. J. A. ELVIDGE and L. M. JACKMAN. Proc. Chem. Soc. 89 (1959).
10. F. S. MORTIMER. J. Mol. Spectroscopy, **3**, 340 (1959).
11. C. N. BANWELL, A. D. COHEN, N. SHEPPARD, and J. J. TURNER. Proc. Chem. Soc. 266 (1959).
12. REFERENCE 1, p. 180. J. Chem. Phys. **30**, 174 (1959).
13. R. T. ARNOLD and S. SEARLES. J. Am. Chem. Soc. **71**, 2022 (1949).
14. A. L. PORTE and J. M. ROBERTSON. J. Chem. Soc. 817 (1959).
15. F. A. L. ANET. Private communication.
16. REFERENCE 1, p. 74.
17. G. V. D. TIERS. J. Phys. Chem. **62**, 1151 (1958).
18. A. A. GOLDBERG and R. P. LINSTEAD. J. Chem. Soc. 2355 (1928).
19. I. HEILBRON and H. M. BUNBURY. Dictionary of organic compounds. Eyre & Spottiswoode Ltd., London. 1953. p. 510.
20. R. E. BUCKLES and G. V. MOCK. J. Org. Chem. **15**, 680 (1950).
21. S. W. PELLETIER and W. L. McLEISH. J. Am. Chem. Soc. **74**, 6292 (1952).

TRYPTAMINES, CARBOLINES, AND RELATED COMPOUNDS

## PART V. 3-(α-ALKYL-β-AMINOETHYL)INDOLES[1,2]

R. A. ABRAMOVITCH AND J. M. MUCHOWSKI

ABSTRACT

The scope of the tryptamine synthesis via 1-oxo-1,2,3,4-tetrahydro-β-carbolines has been extended to tryptamines bearing a side-chain α-alkyl group. The preparation of 3-(2-amino-1-methylethyl)indole by this procedure is described.

In a previous paper (1) an attempt was made to extend the method of synthesis of tryptamines via 1-oxo-1,2,3,4-tetrahydro-β-carbolines (2, 3) to the elaboration of the physostigmine ring system. The intermediate 4-methyl-2,3-dioxopiperidine 3-phenylhydrazone did not, however, undergo Fischer cyclization but instead rearranged to the geometrically isomeric phenylhydrazone. In order to examine the scope of this method of tryptamine synthesis the cyclization of 5-alkyl-substituted 2,3-dioxopiperidine 3-phenylhydrazones was examined, in particular that of 5-methyl-2,3-dioxopiperidine 3-phenylhydrazone (III). This reaction sequence should eventually lead to 3-(2-amino-1-methylethyl)indole (VI). This type of compound may be of physiological interest since Velluz (4) has shown that when a methyl substituent is introduced into the corresponding position in reserpine a more physiologically active compound is obtained.

The synthesis of the required indole was uneventful and followed the path described in the previous examples (2, 3):
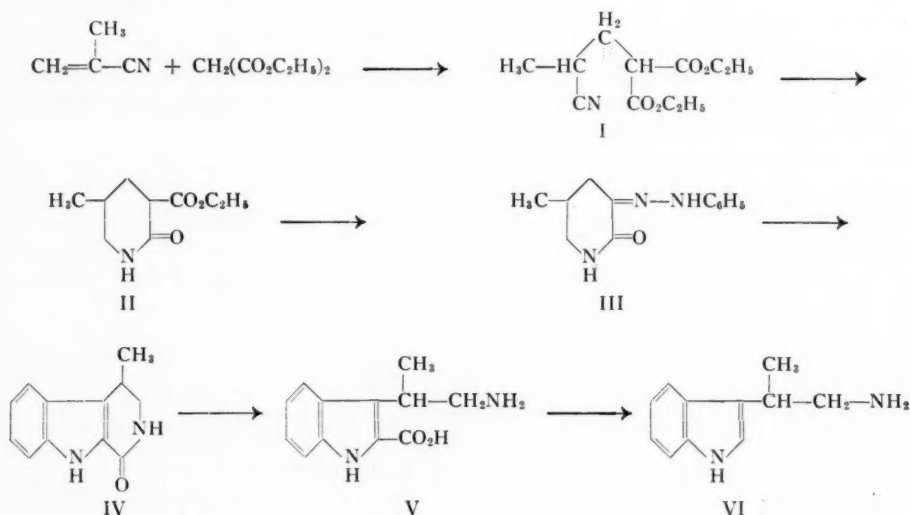
Ethyl malonate was condensed with methacrylonitrile in the presence of sodium ethoxide giving diethyl 2-cyanopropylmalonate (I), which was hydrogenated to 3-ethoxycarbonyl-5-methyl-2-oxopiperidine (II). This underwent a Japp–Klingemann

reaction with benzenediazonium chloride at pH 5 to give 5-methyl-2,3-dioxopiperidine 3-phenylhydrazone (III) which, unlike the corresponding 4-methyl-derivative, was cyclized quite smoothly to 4-methyl-1-oxo-1,2,3,4-tetrahydro-β-carboline (IV). Hydrolysis gave the amino acid (V). Decarboxylation of this acid takes place less readily than in the case of the unsubstituted tryptamine-2-carboxylic acid itself. Thus, whereas the latter yielded tryptamine in 75% yield after it was boiled for 1 hour with 10% hydrochloric acid, the methyl substituted acid only gave a 49% yield of 3-(2-amino-1-methylethyl)indole (VI) after it was boiled with 10% hydrochloric acid for 2 hours. In the latter case, an appreciable amount (44%) of unchanged acid is recovered. The methyltryptamine so obtained was identical with the product described by Noland and Lange (5) which these authors prepared from indole and 1-nitro-1-propene.

The method described above should be amenable to extension to the introduction of other alkyl groups, besides methyl, into the α-position of the tryptamine side chain, as well as to the preparation of such tryptamines bearing substituents in the benzene ring or on the nitrogen atoms (3).

EXPERIMENTAL

Melting points and boiling points are uncorrected. Infrared spectra were measured on a Perkin–Elmer Model 21 double-beam instrument using sodium chloride optics.

Diethyl 2-Cyanopropylmalonate (I)

To a cold solution of sodium (0.1 g) in absolute ethanol (10 ml) was added freshly distilled ethyl malonate (9.3 g). Methacrylonitrile (1.8 g) was added dropwise to the solution at such a rate that the temperature did not exceed 35°. The mixture was then stirred for 5 hours at room temperature, treated with acetic acid (0.3 g), diluted with water (15 ml), and extracted with ether (3×15 ml). The dried (MgSO$_4$) ether extract was evaporated and the residue distilled, ethyl malonate and any other low boiling products being collected below 130°. Vacuum distillation of the residual oil gave diethyl 2-cyanopropylmalonate (5.0 g, 84%) as a colorless liquid, b.p. 101–105°/0.23 mm. Calc. for C$_{10}$H$_{15}$O$_4$N: C, 58.16; H, 7.55. Found: C, 58.14; H, 7.79. Infrared spectrum (liquid film) (main bands only): 2240 (w), 1743 (s), 1728 cm^{-1} (s).

3-Ethoxycarbonyl-5-methyl-2-oxopiperidine (II)

Diethyl 2-cyanopropylmalonate (5.5 g) in absolute alcohol (100 ml) was hydrogenated over Raney nickel (0.2 g) at 80° and 1200 p.s.i. for 6 hours. The cooled solution was then filtered, evaporated on a steam bath, and the residue poured into 100 ml of light petroleum (b.p. 60–80°). The product crystallized immediately as a colorless solid (2.7 g, 60.2%). Recrystallization from light petroleum (b.p. 60–80°) containing a small amount of benzene gave colorless needles, m.p. 100–101°. Calc. for C$_9$H$_{15}$O$_3$N: C, 58.36; H, 8.16. Found: C, 58.47; H, 8.06. Infrared spectrum (Nujol mull) (main peaks only): 3196 (w), 1728 (s), 1674 (s), 1658 cm^{-1} (s).

5-Methyl-2,3-dioxopiperidine 3-Phenylhydrazone (III)

3-Ethoxycarbonyl-5-methyl-2-oxopiperidine (2.1 g) in water (25 ml) containing potassium hydroxide (0.7 g) was kept at room temperature overnight. The solution was cooled in an ice bath, stirred, and treated with a solution of benzenediazonium chloride (30 ml) (prepared from aniline (1.2 g), sodium nitrite (1.0 g), and concentrated hydrochloric acid (3 ml)). The mixture was immediately adjusted to pH 5 by the addition of cold 45% aqueous sodium acetate (25 ml). Stirring was continued at 0–10° for 4 hours, after which time the orange solid was filtered and dried, to give the phenylhydrazone

(2.0 g, 81.2%). Recrystallization from dilute alcohol gave light yellow needles, m.p. 238–239°. Calc. for $C_{12}H_{15}ON_3$: C, 66.34; H, 6.96. Found: C, 66.35; H, 7.05. Infrared spectrum (Nujol mull) (main peaks only): 3174 (m) (br), 1660 (s), 1603 (m), 1564 (s), 753 (m), 693 cm^{-1} (m).

4-Methyl-1-oxo-1,2,3,4-tetrahydro-β-carboline (IV)

The phenylhydrazone (2.2 g) was boiled under reflux with 90% formic acid (10 ml) for 1 hour, the hot solution diluted with water, and the brown oil which separated just brought into solution with hot absolute alcohol. The hot solution, on cooling, gave the oxocarboline (1.6 g, 80%) which, on recrystallization from absolute alcohol, gave white plates, m.p. 204–206°. Calc. for $C_{12}H_{12}ON_2$: C, 71.98; H, 6.04. Found: C, 71.58; H, 6.17. Infrared spectrum (Nujol mull)(main peaks only): 3195 (m) (br), 1649 (s), 1620 (m), 747 cm^{-1} (s). The picrate separated from alcohol as deep red rectangular rods, m.p. 185–187°.

3-(2-Amino-1-methylethyl)indole-2-carboxylic Acid (V)

4-Methyl-1-oxo-1,2,3,4-tetrahydro-β-carboline (0.45 g) in 50% aqueous ethanol (10 ml) containing potassium hydroxide (1.1 g) was boiled under reflux for 6 hours. The solvent was evaporated down to 5 ml, water (5 ml) was added, and the cooled solution filtered and acidified with acetic acid giving the amino acid (0.48 g, 96.8%). Recrystallization from dilute ethanol gave lustrous white plates, m.p. 242–243° (decomp.). Calc. for $C_{12}H_{14}O_2N_2$: C, 66.03; H, 6.47. Found: C, 65.65; H, 6.86. Infrared spectrum (Nujol mull) (main peaks only): 3420 (w), 2121 (w), 1642 (w) (br), 1624 (m), 1563 (m), 1544 (m) (br), 755 cm^{-1} (s).

3-(2-Amino-1-methylethyl)indole (VI)

3-(2-Amino-1-methylethyl)indole-2-carboxylic acid (0.30 g) was boiled under reflux with 10% hydrochloric acid (10 ml) for 2 hours. The cooled solution was made alkaline with dilute sodium hydroxide, extracted with ether, the ether layer dried ($MgSO_4$), and evaporated leaving the tryptamine (0.117 g, 48.8%) as a light brown oil. Neutralization of the aqueous layer with dilute hydrochloric acid resulted in the recovery of unreacted amino acid (0.133 g). The indole was converted to the picrate (from ether). Recrystallization from water gave the picrate as deep orange plates, m.p. 224–226° (decomp.). Noland and Lange (5) report m.p. 224–226° for this picrate. Calc. for $C_{11}H_{14}N_2$, $C_6H_3O_7N_3$: C, 50.62; H, 4.25. Found: C, 50.18; H, 3.90.

REFERENCES

1. R. A. Abramovitch. Can. J. Chem. **36**, 354 (1958).
2. R. A. Abramovitch and D. Shapiro. J. Chem. Soc. 4589 (1956).
3. R. A. Abramovitch. J. Chem. Soc. 4593 (1956).
4. X. Velluz. *Quoted by* R. Robinson. Chem. and Ind. 964 (1959).
5. W. E. Noland and R. F. Lange. J. Am. Chem. Soc. **81**, 1203 (1959).

TRYPTAMINES, CARBOLINES, AND RELATED COMPOUNDS
PART VI. STEREOCHEMISTRY OF THE MICHAEL ADDITION OF ETHYL MALONATE TO 1-CYCLOHEXENE CYANIDE[1,2]

R. A. ABRAMOVITCH AND J. M. MUCHOWSKI

ABSTRACT

The Michael addition of diethyl malonate to 1-cyclohexene cyanide has been shown to give a mixture of the *cis*- and *trans*-diethyl 2-cyanocyclohexylmalonates in 72% and 28% yields respectively. The stereochemistry of the products was established by their unambiguous conversion to the respective *cis*- and *trans*-decahydroisoquinolines. Hydrogenation of a cyclohexane cyanide to the corresponding aminomethyl derivative takes place with retention of configuration. A number of substituted decahydroisoquinolines of known stereochemistry have been prepared. Decahydro-3,4-dioxoisoquinoline-4-phenylhydrazone underwent Fischer cyclization to a product assumed to be 2-oxo-octahydroindolo[2,3-d]isoquinoline indicating that the observation that 4-methyl-2,3-dioxopiperidine-3-phenylhydrazone did not undergo cyclization is not general for such 4-substituted piperidones.

It was shown in Part IV (1) that 4-methyl-2,3-dioxopiperidine-3-phenylhydrazone (I:R = CH₃) did not undergo Fischer cyclization to the indolenine but instead was rearranged to a geometrically isomeric phenylhydrazone. On the other hand, 5-methyl-2,3-dioxopiperidine-3-phenylhydrazone underwent smooth cyclization to the oxocarboline (2). It was, therefore, of interest to establish whether this limitation in what appears to be a widely applicable method of preparation of tryptamines was general for 2,3-dioxopiperidine-3-phenylhydrazones (I) having alkyl substituents at the 4-position. To this end it was decided to study the cyclization of decahydro-3,4-dioxoisoquinoline-4-phenylhydrazone (IV). The choice of that particular compound was of twofold interest:
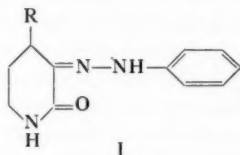
(*i*) the generality of the limitation mentioned above could be tested, and (*ii*) little is definitely known concerning the steric route of nucleophilic additions of the Michael type to cyclohexene derivatives, and the preparation of the required phenylhydrazone would involve a study of the addition of ethyl malonate to 1-cyclohexene cyanide, as shown in the following scheme:
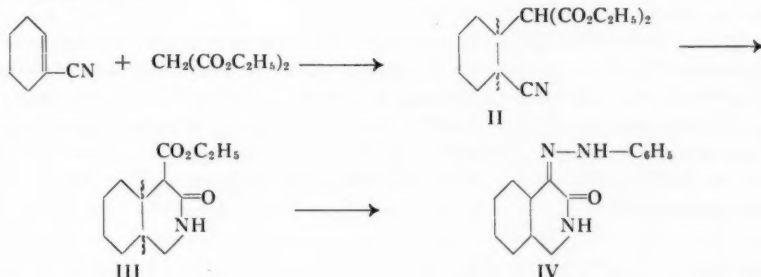
The work described in this paper involves mainly a study of the stereochemistry of the above Michael addition and eventually of the cyclization of the phenylhydrazone (IV).

Previous work in this field may be summarized briefly. Kon and Qudrat-I-Khuda (3) could only isolate cis-decahydro-4-carbethoxy-1,3-dioxonaphthalene from the condensation of 1-cyclohexenylmethyl ketone with ethyl malonate, whereas Ruzicka, Koolhaas, and Wind (4) and also Chuang and Tien (5) reported getting a mixture of the cis- and trans-isomers in this reaction. Boorman and Linstead (6) reported that 1-carbethoxy-cyclohexene yielded a triester of unspecified orientation on condensation with ethyl malonate. This ester, on hydrolysis with concentrated hydrochloric acid, yielded solely trans-hexahydrohomophthalic acid. Wohl and Losanitsch (7) carried out a similar reaction between ethyl malonate and 3-cyano-1,2,5,6-tetrahydropyridine and obtained a mixture of the cis- and trans-diethyl (3-cyano-4-piperidyl)malonates. Mixtures of stereoisomers were also obtained in the condensation of the sodio-derivative of 6-methoxy-1-tetralone with 1-acetylcyclopentene (8) and in the self-condensation of 1-acetylcyclohexene in the presence of sodamide (9, 10). On the other hand, Ginsburg and Pappo (11) condensed diethyl malonate with 2-phenyl-2-cyclohexenone; the orientation of the resulting malonate was not established, but after hydrolysis and decarboxylation to the acetic acid followed by Clemmensen reduction, trans-2-phenylcyclohexylacetic acid was obtained exclusively. As the authors rightly point out, isomerization to the more stable form may take place (particularly in the keto-malonate) so that the more stable form would be isolated after the sequence of reactions described. No conclusion can, therefore, be drawn concerning the steric mechanism of the addition reaction. The same comments would apply to the reactions studied by Bergmann and Szmuszkovicz (12). The above results do not provide conclusive evidence for the stereochemical course of addition. If, as seems likely, trans-addition predominates then the cis-isomer should be the one preferentially formed.

Addition of diethyl malonate to 1-cyanocyclohexene gave a mixture of the cis- and trans-diethyl 2-cyanocyclohexylmalonates (II). These could not be separated by fractional distillation so that a number of methods were explored to try and determine the relative proportions of the isomers. The mixture of cyano-esters was hydrolyzed to the corresponding mixture of hexahydrohomophthalic acids with boiling hydrochloric acid; it was hoped to separate these by fractional crystallization. This method of quantitative analysis of the cyano-esters was abandoned, however, when it was realized that the cis-acid may be converted to the more stable trans-form under the conditions used for the hydrolysis (13, 14). It is, therefore, not possible to assign any specific configuration to the triester obtained by Boorman and Linstead (6) which these authors hydrolyzed to trans-hexahydrohomophthalic acid using the above procedure.

The mixture of the stereoisomeric esters was hydrogenated to cis- and trans-decahydro-4-ethoxycarbonyl-3-oxoisoquinolines (V) which could be separated by chromatography on alumina into the two individual isomers: cis-68%, trans-32%. The configuration of each one of the isomers was established by converting it into the corresponding decahydro-isoquinoline (VIII) of known geometry (15) by a series of reactions which could not effect inversion of configuration at the ring junctions. The method used is illustrated by the following equations:
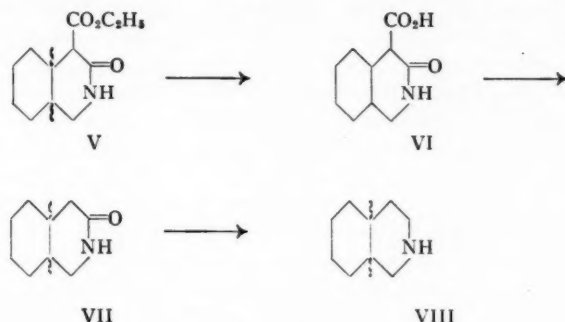
CO$_2$C$_2$H$_5$ CO$_2$H

V   VI

VII   VIII

CHART I.

The pure amido-ester was saponified at room temperature to the decahydro-3-oxo-isoquinoline-4-carboxylic acid (VI) which, on being heated to its melting point, underwent decarboxylation to the decahydro-3-oxoisoquinoline (VII). This was reduced with lithium aluminum hydride to the known *cis-* or *trans*-decahydroisoquinoline thus establishing the conformation of the amido-ester. The same series of reactions was carried out on the mixture of *cis-* and *trans-* (V) before chromatography, final separation of the isomers being effected by fractional crystallization of the picrates of the secondary amines (VIII). This method gave the values *cis*-66%, *trans*-34%, which, though undoubtedly less reliable than the estimation by chromatographic separation, is in close agreement with it.

It should be emphasized at this stage that the stereospecificity of the reduction of a nitrile such as (II) to a cyclic amide via the primary amine seems to have had, up to this time, no experimental backing in the literature, and could therefore not be assumed. Unless such a reduction was stereospecific the quantitative data for the ratio of *cis*-to-*trans* amido-esters (V) could not be assumed to hold for the cyano-esters (II). It is theoretically possible that on hydrogenation the cyano-esters could pass through an intermediate such as (IX), and if one assumes, as is likely, that the larger malonate group is equatorial (16) in both cases, this intermediate will be the same for both geometrical isomers. Such being the case one would expect to get either the *same* geometrical isomer starting from the *cis-* or the *trans*-cyanide or the same mixture of geometrical isomers from each on hydrogenation of the cyano group. The absence of such an effect could be taken as evidence that an intermediate of the type IX was not involved and that reduction was indeed stereospecific.

At that stage two rather fortunate observations were made. A number of unsuccessful attempts had been made to resolve the mixture of cyano-esters by vapor phase chromatography using a variety of columns such as silicone on firebrick and polyesters on celite. It was now found that the geometrical isomers could be easily separated and estimated quantitatively using an Apiezon "M" column operated at 160°. The ratio of the two isomers was 72% to 28% as determined by this method. There was, however, no way of knowing which was which until it was observed that a sample of the mixed cyano-esters which had been standing for a few months deposited crystals of one of the isomers. These were filtered off and, after further recrystallization, shown to consist of a single isomer by vapor phase chromatography. The residual oil, on repeated distillation, gave a pure sample of the other geometrical isomer. Each one of these isomers was now catalytically
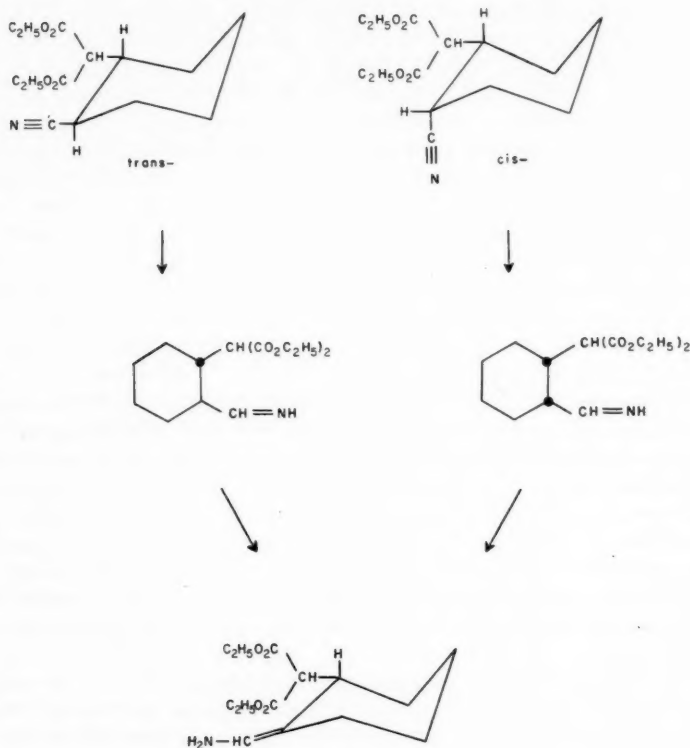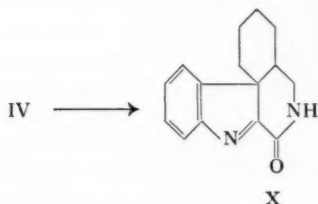
(IX)

CHART II.

reduced individually and each one gave a single geometrical isomer of the corresponding amido-esters: the *trans*-form from the crystalline cyano-ester, and the *cis*-form from the liquid one. From the considerations outlined above it may be concluded that the catalytic reduction of the nitriles did not involve a change in the configuration so that the ratio of isomers obtained from the Michael addition is *cis*-72%, *trans*-28%. These figures are in close agreement with those obtained from the chromatography of the amido-esters on alumina, and it is felt that the difference between them falls within the experimental error expected for this type of estimation.

The results indicate that, as anticipated, the addition of diethyl malonate to 1-cyano-cyclohexene gives predominently the *cis*-isomer, but that the *trans*-isomer is also formed in appreciable quantity. It should be emphasized that these results give the postequilibrium ratio of isomers. Work is at present under way to determine whether they apply also to pre-equilibrium conditions. If so, the mechanistic conclusion could be drawn that the Michael reaction proceeded, in this case, predominently by *trans*-addition. The equilibration of each of the cyano-esters is also being examined. The hydrogenation results indicate, however, that probably no equilibration of the cyano-esters takes place under vigorous treatment in the presence of base (the secondary amine is formed as a

by-product) so that predominent *trans*-addition might be tentatively assumed. As a by-product of the reactions a number of substituted decahydroisoquinolines (V, VI, VII) of known geometry have been obtained.

The mixture of amido-esters (V) was saponified and treated with benzenediazonium chloride to give a low yield of a single decahydro-3,4-dioxoisoquinoline-4-phenylhydrazone (IV). Since equilibration is possible at this stage one would expect the more stable of the two isomers, probably the *trans*-, to be formed. The geometry of the product was not determined though it is proposed to do so later. A red, tarry substance, assumed to be the phenylazo-derivative on the basis of its infrared spectrum, was also isolated but was not investigated further at this stage. When the phenylhydrazone was boiled with 90% formic acid a base was obtained which is tentatively assigned the structure 2-oxo-2,3,4,4*a*, 5,6,7,8-octahydroindolo[2,3-d]isoquinoline (X).* The evidence in support of this assign-

ment is based on the ultraviolet (see Fig. 1) and infrared spectra and on microanalytical data. The latter were not too good since, though the expected values were obtained in one instance, a somewhat lower value for carbon was obtained on a repeat analysis of a different sample. The nitrogen analysis also gave low values but indicated quite definitely that one nitrogen atom had been lost during the cyclization. There was not sufficient material on hand to repeat the purification of this compound, but this will be done as soon as possible. An interesting feature of the infrared spectrum of the cyclized product was the presence of *two* peaks in the 800–680 cm^{-1} region (765 and 685 cm^{-1}). This is unexpected, and might be due to some contamination which could perhaps be giving rise to the 685 cm^{-1} band, though the intensity of the latter seems to render this rather doubtful. The compound also exhibits two melting points, melting at 150°, resolidifying above that temperature, and melting again at 186–187°. After heating above 150°, the solid product only exhibited a *single* infrared peak in the aromatic C—H out-of-plane deformation region, at 758 cm^{-1}. Attempted hydrolysis of the amide (X) to an amino acid with ethanolic alkali gave rise instead to an isomeric product, m.p. 240–242°. The analysis of this substance agrees with the formula $C_{15}H_{16}ON_2$ but its infrared spectrum and particularly its ultraviolet absorption spectrum differ from those of X. The structure of this compound is presently under investigation.
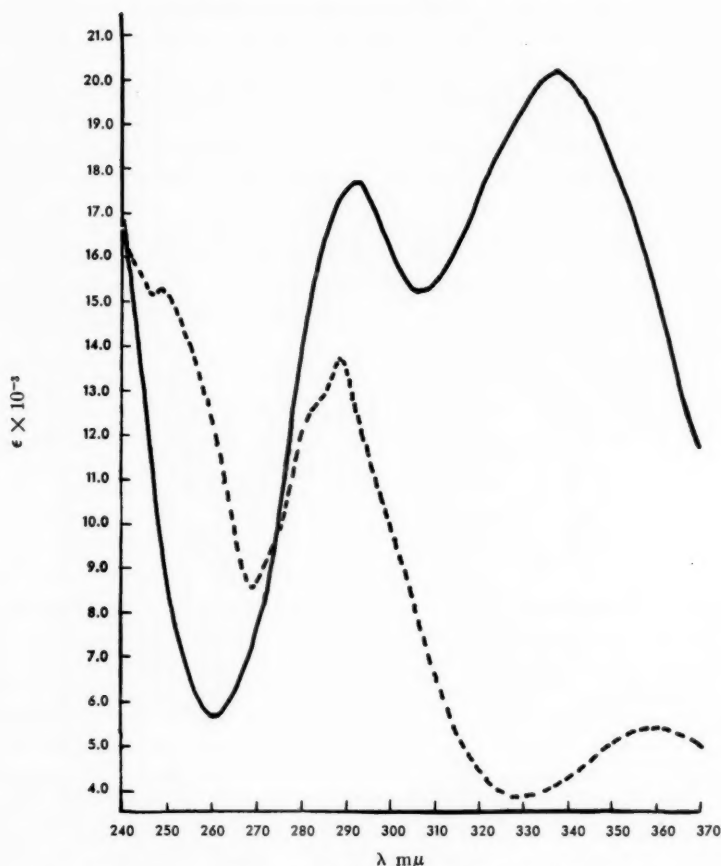
Proposed numbering for this ring system:
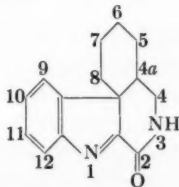
FIG. 1. ——— Decahydro-3,4-dioxoisoquinoline-4-phenylhydrazone.
– – – 2-Oxo-2,3,4,4a,5,6,7,8-octahydroindolo[2,3-b]isoquinoline.

The results of the acid treatment of the phenylhydrazone (IV) indicate at least that the limitation reported (1) in the attempted cyclization of (I: R = CH₃) is not a general one for 4-substituted 2,3-dioxopiperidine-3-phenylhydrazones, since cyclization of some sort has occurred in the present case. Clearly, further work is necessary to clarify the identity of the cyclized product and of the isomeric amide it gives on prolonged alkali treatment. This will be reported on at a later date.

EXPERIMENTAL

Melting points and boiling points are uncorrected. Infrared spectra were measured with a Perkin–Elmer Model 21 spectrometer using sodium chloride optics. Ultraviolet absorption spectra were recorded on a Beckman DK2 spectrophotomer.

Diethyl 2-cyanocyclohexylmalonate

To a stirred solution of sodium ethoxide (from 16.9 g of sodium in 300 ml of absolute alcohol) was added freshly distilled diethyl malonate (170.5 g). To this solution was

added 1-cyclohexene cyanide (29.8 g), prepared by the procedure of McElvain and Starn (17) and the solution boiled under reflux for 24 hours when the initially colorless solution turned yellow. The solution was cooled, treated with glacial acetic acid (46.0 g), extracted with water (3×100 ml), and the aqueous solution extracted with ether (3×50 ml). The ether extract and the organic layer were combined, dried (MgSO₄), and the solvent removed. The residue was distilled up to 130° (bath temp.)/15 mm to remove excess diethyl malonate and any other low-boiling material and the residue distilled in vacuo, the fraction boiling at 125–135°/0.34 mm (53.0 g, 71% yield) being collected as the mixture of geometrically isomeric cyano-esters. This on redistillation had b.p. 119–125°/0.28 mm. Calc. for $C_{14}H_{21}O_4N$: C, 62.90; H, 7.92. Found: C, 62.35; H, 7.61.

Separation and Quantitative Analysis of the cis- and trans-Diethyl 2-Cyanocyclohexyl-malonates by Vapor Phase Chromatography

A Beckman vapor phase chromatograph (Model GC-2) was used with a 4-ft Apiezon "M" on firebrick column operated at 160° and a helium inlet pressure of 20 p.s.i. The mixture (0.005 ml) was chromatographed and the areas under the curves for each isomer measured. The pure trans-isomer (0.005 ml) was then chromatographed and the area under the curve also measured.

% trans-diethyl 2-cyanocyclohexylmalonate: 27.6,
% cis-diethyl 2-cyanocyclohexylmalonate: 72.4 (by difference).

trans-Diethyl 2-Cyanocyclohexylmalonate

After standing for some months, trans-diethyl 2-cyanocyclohexylmalonate crystallized from the mixture as colorless needles. It was filtered and recrystallized from light petroleum (b.p. 60–80°) to give large, colorless, rectangular rods, m.p. 50–52°. Calc. for $C_{14}H_{21}O_4N$: C, 62.90: H, 7.92. Found: C, 63.26; H, 7.86. Infrared spectrum (liquid film) (main peaks only): 2242 (w), 1747 (s), 1732 cm⁻¹ (s).

cis-Diethyl 2-Cyanocyclohexylmalonate

After removal of the trans-isomer by filtration from the above mixture the filtrate consisted almost entirely of cis-diethyl 2-cyanocyclohexylmalonate (as shown by vapor phase chromatography). Distillation under reduced pressure gave the pure cis-isomer, entirely free of the trans-form as far as could be detected by vapor phase chromatography, as a colorless mobile liquid, b.p. 118–120°/0.28 mm. Found: C, 62.56; H, 7.83. Infrared spectrum (liquid film) (main peaks only): 2242 (w), 1746(s), 1731 cm⁻¹ (s).

cis- and trans-Hexahydrohomophthalic acid

The mixed diethyl 2-cyanocyclohexylmalonates (1.0 g) were boiled under reflux with 10% hydrochloric acid (30 ml) for 4 hours. The solvent was evaporated giving a brown oil (0.65 g, 93.2%) which solidified on cooling. Recrystallization of the product from water gave white rosettes of the mixture of the two isomeric acids, m.p. 90–130°. Infrared spectrum (Nujol mull) (main peaks only): 2645 (m)(br), 1705 (s), 1689 cm⁻¹ (s). Windaus, Hückel, and Reverey (13) report m.p. 146° for cis- and m.p. 157° for trans-hexahydro-homophthalic acid respectively.

cis- and trans-Decahydro-4-ethoxycarbonyl-3-oxoisoquinoline

The mixture of stereoisomeric diethyl 2-cyanocyclohexylmalonates (5.5 g) in commercial absolute alcohol (50 ml) was hydrogenated over Raney nickel (0.2 g) at 110–120° and 1200 p.s.i. for 9 hours. The solution was filtered, the ethanol removed on a steam bath, and the residue distilled under reduced pressure to give the mixture of amido-esters as a very viscous liquid (3.1 g, 66.8%), b.p. 160–185°/0.4 mm. Calc. for $C_{12}H_{14}O_3N$: C, 63.97;

H, 8.50. Found: C, 63.74; H, 8.55. The mixture of esters (1.269 g) was chromatographed on a column of neutral alumina (3/4 in.$\times$12 in.). Elution with ether–ethanol (200 ml) (20:1 v/v) gave the *trans*-isomer (0.406 g, 32.5%) identical with the product obtained as described below. Elution with hot alcohol (500 ml) gave the *cis*-isomer (0.843 g, 67.5%) identical with the product described below.

trans-Decahydro-4-ethoxycarbonyl-3-oxoisoquinoline

trans-Diethyl 2-cyanocyclohexylmalonate (3.0 g) was hydrogenated as described for the mixture of cyanides to give the pure *trans*-β-amido-ester (1.6 g, 63.3%) as a colorless, viscous liquid, b.p. 160–170°/0.04 mm, which slowly solidified. Crystallization from light petroleum (b.p. 60–80°) gave colorless needles, m.p. 114–115°. Calc. for $C_{12}H_{14}O_3N$: C, 63.97; H, 8.50. Found: C, 64.58; H, 7.95. Infrared spectrum (Nujol mull) (main peaks only): 3208 (w)(br), 1729 (s), 1673 cm^{-1} (s).

cis-Decahydro-4-ethoxycarbonyl-3-oxoisoquinoline

cis-Diethyl 2-cyanocyclohexylmalonate (4.8 g) treated in a manner analogous to the *trans*-compound yielded the *cis*-amido-ester (2.4 g, 59.4%) as a colorless viscous liquid, b.p. 136–140°/0.022 mm. Found: C, 64.25; H, 8.51. Infrared spectrum (liquid film) (main peaks only): 3187 (m)(br), 1724 (s), 1656 cm^{-1} (s).

trans-Decahydro-3-oxoisoquinoline-4-carboxylic Acid

trans-Decahydro-4-ethoxycarbonyl-3-oxoisoquinoline (0.62 g) in water (10 ml) containing potassium hydroxide (0.3 g) was shaken mechanically at room temperature for 12 hours, the solution filtered, acidified with concentrated hydrochloric acid, and set aside. After 2 hours the β-amido-acid had separated out (0.54 g, 100%) as short, colorless needles which on recrystallization from water had m.p. 113–115° (decomp.). Calc. for $C_{10}H_{15}O_3N$: C, 60.89; H, 7.67. Found: C, 60.37; H, 7.31. Infrared spectrum (Nujol mull) (main peaks only): 3297 (w)(sh), 3194 (m), 2590 (m)(br), 1735 (s), 1645 cm^{-1} (s).

trans-Decahydro-3-oxoisoquinoline

trans-Decahydro-3-oxoisoquinoline-4-carboxylic acid (0.180 g) was heated in an oil bath at 110–120° until effervescence ceased. The viscous oil remaining was sublimed at 110–120°/20 mm giving the colorless amide (0.060 g, 42.8%) which was recrystallized from light petroleum (b.p. 60–80°) containing a small amount of benzene and had m.p. 165–167°. Calc. for $C_9H_{15}ON$: C, 70.55; H, 9.87. Found: C, 70.61; H, 9.75. Infrared spectrum (Nujol mull) (main peaks only): 3216 (m), 3042 (m)(sh), 1654 cm^{-1} (s).

trans-Decahydroisoquinoline

trans-Decahydro-3-oxoisoquinoline (0.200 g) in dry dioxan (5 ml) was added to a suspension of lithium aluminum hydride (0.200 g) in dry ether (25 ml) at such a rate as to keep the ether boiling. When the addition was complete the mixture was boiled under reflux in an atmosphere of nitrogen for 5 hours. The suspension was cooled, the excess metal hydride decomposed by the careful addition of water, and the product extracted with ether (3$\times$25 ml) and dried (MgSO$_4$). The solvent was evaporated, eventually under vacuum, to give the base (0.130 g, 71.4%) as a colorless oil. The amine was converted to its picrate (from ethanol); this, on recrystallization from methanol, gave *trans*-deca-hydroisoquinoline picrate, m.p. 172–174°. Gray and Heitmeier (18) report m.p. 173–174° for this picrate.

cis-Decahydro-3-oxoisoquinoline

cis-Decahydro-4-ethoxycarbonyl-3-oxoisoquinoline (2.83 g) in water (25 ml) containing potassium hydroxide (1.0 g) was mechanically shaken at room temperature for 12 hours.

The solution was filtered, acidified with concentrated hydrochloric acid, and kept in the refrigerator. After 24 hours a few crystals of the acid had separated as fine colorless needles. No attempt was made to purify this acid. The acidic solution was evaporated to dryness, the solid residue extracted with absolute alcohol (3×10 ml), the alcohol solution filtered and evaporated, and the residue heated in an oil bath at 100–$110°$. When effervescence had ceased the viscous oil obtained was sublimed at 100–$110°/20$ mm to give the cis-amide (1.05 g, 59.4%); this, on recrystallization from light petroleum (b.p. 60–$80°$), gave colorless flakes, m.p. 149–$151°$. Calc. for $C_9H_{15}ON$: C, 70.55; H, 9.87. Found: C, 70.60; H, 9.85. Infrared spectrum (Nujol mull) (main peaks only): 3214 (w), 3044 (w)(sh), 1654 cm^{-1} (s).

cis-Decahydroisoquinoline

The above amide (0.30 g) was treated with lithium aluminum hydride as described for the trans-amide to give the cis-base (0.20 g, 73.3%). The picrate, on recrystallization from methanol, gave pale yellow plates, m.p. 150–$152°$. Witkop (15) reported m.p. $150°$ for cis-decahydroisoquinoline picrate.

cis- and trans-Decahydro-3-oxoisoquinoline

The mixed decahydro-4-ethoxycarbonyl-3-oxoisoquinolines (0.219 g) were hydrolyzed and decarboxylated as described in the preparation of pure cis-decahydro-3-oxoisoquinoline. The mixture of amides (0.105 g, 70.5%), after sublimation at 100–$110°/20$ mm, had m.p. 65–$95°$.

cis- and trans-Decahydroisoquinoline

The mixture of cis- and trans-decahydro-3-oxoisoquinolines (0.585 g) in dry dioxan (10 ml) was reduced with lithium aluminum hydride (0.750 g) in dry ether (50 ml) as described for the preparation of trans-decahydroisoquinoline to give the mixture of bases (0.449 g, 84.5%) as a colorless oil. The picrates were prepared and fractionally crystallized as follows: The dried picrates (0.400 g) were washed five times with 1-ml portions of cold methanol. This removed mainly the trans-decahydroisoquinoline picrate. Recrystallization of the residue from methanol gave the cis-picrate (0.260 g, 66.2%), m.p. 150–$152°$. The combined cooled methanol extracts were slowly evaporated to give the trans-picrate as large, yellow, rectangular prisms which could easily be separated mechanically from some cis-picrate. After two recrystallizations from methanol the trans-picrate (0.133 g, 33.8%) had m.p. 172–$174°$.

Decahydro-3,4-dioxoisoquinoline-4-phenylhydrazone

Decahydro-4-ethoxycarbonyl-3-oxoisoquinoline (10.1 g, cis and trans) in water (50 ml) containing potassium hydroxide (2.6 g) was shaken mechanically at room temperature for 12 hours. The solution was cooled to $0°$ and adjusted to pH 5 with glacial acetic acid. To the stirred solution was added a solution of benzenediazonium chloride (70 ml) (prepared from 4.3 g of aniline, 3.4 g of sodium nitrite, and concentrated hydrochloric acid (7.0 ml)). The mixture was immediately adjusted to pH 5 by the addition of cold, 45% aqueous sodium acetate. Stirring was continued at 0–$10°$ for 10 hours after which the suspension was kept in a refrigerator for 12 hours. The yellow brown solid (6.5 g) was filtered, dried, and extracted with benzene leaving behind the phenylhydrazone as a pale yellow solid (2.6 g, 22.6%). Recrystallization from dilute ethanol gave pale yellow needles, m.p. 214.5–$215.5°$. Calc. for $C_{15}H_{19}ON_3$: C, 70.00; H, 7.44. Found: C, 69.69; H, 7.68. Infrared spectrum (Nujol mull) (main peaks only): 3163 (w)(br), 1660 (s), 1602 (m), 1564 (m), 750 (m), 694 cm^{-1} (m). Ultraviolet absorption spectrum (in absolute ethanol), $\lambda_{max} 293, 338$ mμ. $\epsilon \times 10^{-3}$ 17.67, 20.16.

Evaporation of the benzene washings above gave a red, tarry substance, assumed to be the phenylazo-derivative, which was not investigated further at this stage. Infrared spectrum (liquid film) (main peaks only): 3140 (s)(br), 1714 (m)(sh), 1639 (s), 1604 (s), 1547 (s), 752 (s), 692 cm^{-1} (s).

2-Oxo-2,3,4,4a,5,6,7,8-octahydroindolo[2,3-d]isoquinoline

The phenylhydrazone (0.993 g) was boiled under reflux with 90% formic acid (8 ml) for 1/2 hour, the solution cooled and filtered. The filtrate was made slightly alkaline (pH 8) with dilute sodium hydroxide, and the solid which separated (0.424 g, 45.7%) filtered and recrystallized from benzene, to give colorless needles, melting completely and sharply at 150°, resolidifying above that temperature, and melting again at 186–187°. Calc. for $C_{15}H_{16}ON_2$: C, 74.70; H, 6.72. Found: C, 74.97; H, 6.72. Infrared spectrum (Nujol mull) (main peaks only): 3192 (w)(br), 1672 (s), 1640 (m)(sh), 1599 (m), 765 (s), 685 cm^{-1} (m). Ultraviolet absorption spectrum (in absolute ethanol): λ_{max} 248 (infl.), 289, 360 mμ. $\epsilon \times 10^{-3}$ 15.27, 13.69, 5.4. After being heated to 150° and cooled again the compound exhibited the following peaks in the infrared: 3330 (w)(br), 1680 (s), 1602 (m), 758 cm^{-1} (m).

Alkali Isomerization of 2-Oxo-2,3,4,4a,5,6,7,8-octahydroindolo[2,3-d]isoquinoline

The indolenine (0.070 g) in 50% aqueous ethanol (5 ml) containing potassium hydroxide (0.5 g) was boiled under reflux for $6\frac{1}{2}$ hours. The hot solution was filtered and gave, on cooling, a white crystalline solid (0.035 g). Acidification of the mother liquors with acetic acid did not give any of the expected amino acid. The solid obtained above was recrystallized from benzene to give colorless needles, m.p. 240–242° (decomp.). Calc. for $C_{15}H_{16}ON_2$: C, 74.97; H, 6.72. Found: C, 74.61; H, 7.21. Infrared spectrum (Nujol mull) (main peaks only): 3365 (m), 3182 (w)(br), 1667 (s), 1608 (m), 740 cm^{-1} (s). Ultraviolet absorption spectrum (in absolute ethanol): λ_{max} 235, 236 (infl.), 243, 248, 254, 260 mμ. $\epsilon \times 10^{-3}$ 13.66, 13.45, 12.79, 11.97, 11.20, 9.47.

ACKNOWLEDGMENTS

REFERENCES

1. R. A. ABRAMOVITCH. Can. J. Chem. 36, 354 (1958).
2. R. A. ABRAMOVITCH and J. M. MUCHOWSKI. Can. J. Chem. This issue.
3. G. A. R. KON and M. QUDRAT-I-KHUDA. J. Chem. Soc. 3071 (1926).
4. L. RUZICKA, D. R. KOOLHAAS, and A. H. WIND. Helv. Chim. Acta, 14, 1151 (1931).
5. CH. K. CHUANG and Y. L. TIEN. Ber. 69, 25 (1936).
6. E. J. BOORMAN and R. P. LINSTEAD. J. Chem. Soc. 258 (1935).
7. A. WOHL and M. S. LOSANITSCH. Ber. 40, 4698 (1907).
8. D. A. PEAK and R. ROBINSON. J. Chem. Soc. 1581 (1937).
9. W. S. RAPSON and R. ROBINSON. J. Chem. Soc. 1285 (1935).
10. E. R. H. JONES and H. P. KOCH. J. Chem. Soc. 393 (1942).
11. D. GINSBURG and R. PAPPO. J. Chem. Soc. 938 (1951).
12. E. D. BERGMANN and J. SZMUSZKOVICZ. J. Am. Chem. Soc. 75, 3226 (1953).
13. A. WINDAUS, W. HÜCKEL, and G. REVEREY. Ber. 56, 91 (1923).
14. S. S G. SIRCAR. J. Chem. Soc. 1252 (1927).
15. B. WITKOP. J. Am. Chem. Soc. 70, 2617 (1948).
16. E. J. COREY. J. Am. Chem. Soc. 77, 1044 (1955).
17. S. M. MCELVAIN and R. E. STARN, JR. J. Am. Chem. Soc. 77, 4571 (1955).
18. A. P. GRAY and D. E. HEITMEIER. J. Am. Chem. Soc. 80, 6274 (1958).

THE KINETICS OF THE FORMATION OF THE MONO–FLUORO COMPLEX OF IRON (III) IN AQUEOUS SOLUTION[1]

D. Pouli[2] and W. MacF. Smith[3]

ABSTRACT

The kinetics of the reactions involved in the formation of the mono–fluoro complex of iron (III) in aqueous solutions have been examined spectrophotometrically at ionic strength 0.5 and over the temperature interval 0.1 to 12.1° C. The results are interpretable on the assumption that the following two reactions contribute significantly to the rate $Fe^{+++} + F^- = FeF^{++}$ and $Fe^{+++} + HF = FeF^{++} + H^+$, the former having a heat of activation of 22.8 ± 2.5 kcal mole^{-1} and an entropy of activation of 35 ± 9 cal deg^{-1} mole^{-1}, the latter having a heat of activation of 8.7 ± 0.7 kcal mole^{-1} and an entropy of activation of -24.5 ± 3 cal deg^{-1} mole^{-1}.

INTRODUCTION

Reactions involving association of cations and anions may be considered displacement reactions in which the ligand displaced from the cation is a solvent molecule, e.g. $M(H_2O)_n{}^+ + X^- \rightarrow M(H_2O)_{n-1}X + H_2O$. Kinetic aspects of such reactions will reflect the nature of the path by which reaction occurs. The transition state associated with the prevailing path may involve loss of solvent molecules from the inner solvation spheres of the interacting ions (1) as well as reorganization of more distant solvent. It is also possible that protolytic changes in the co-ordinated solvent may be involved in some of the alternative mechanisms by which the net reactions may occur (2, 3, 4).

Although these so-called association reactions are among the simplest of those occurring in solution, experimental data relating to their kinetics are restricted. Eigen (5) is contributing valuable data about very fast reactions through his technique of relaxation spectrometry. The slow associations of chromic and thiocyanate have been studied by Postmus and King (2), of chromic and oxalate by Hamm and Davis (3). Below, Connick, and Coppel have recently published work on the ferric–thiocyanate association (4). Smith found that ferric and fluoride associates at a rate measurable with stop watch timing (6).

This paper deals with an extension of Smith's work to a wider range of acidities (and of necessity to a higher ionic strength) and to a range of temperatures. A spectrophotometric rather than the redox method used in the preliminary work has been used to follow the reaction, but the conditions studied have been restricted to those yielding rates measurable with stop watch timing.

EXPERIMENTAL

The course of the reaction was followed spectrophotometrically at 260 mμ using Beckman quartz cells of 1 cm path length as reaction vessels. At this wavelength there is a substantial increase in transmission accompanying the association reaction, ranging from about 25 to 300% under the range of conditions studied. The segment of a Beckman DU spectrophotometer normally housing the cell holder was replaced by an extended segment which housed a specially constructed holder for two quartz cells. This holder was machined from a brass block so that it had channels to carry thermostating water and demisting tubes which directed thermostated dry gas against the windows of the cells.

During a kinetic run 2 ml of a solution containing ferric perchlorate, perchloric acid, and sodium perchlorate, previously brought close to reaction temperature in a thermostat bath, was pipetted into the reaction cell and also into a reference cell in the cell holder. The solution containing fluoride was added to the solution in the reaction vessel from a fine polythene tube connected to a 5-ml glass syringe. Prior to addition, the small volume (about 0.03 ml) of solution containing hydrogen fluoride, sodium perchlorate, and perchloric acid was in a length of the polythene tubing within the quartz cell. Pushing the plunger of the syringe introduced the solution of fluoride followed by a stream of gas which ensured mixing. The volume of solution introduced was reproducible to $\pm 2\%$. A small length of gas in the tubing between the fluoride solution and the exit of the tubing prevented loss of fluoride to the ferric solution prior to the pressing of the syringe.

Adequacy of mixing involved in this procedure was examined by adding acidified ferric perchlorate solution to dilute perchloric acid in the reaction vessel, using the same volumes as those involved during addition of fluoride, and noting the time required for attainment of a steady value for the transmission. It was found that a steady reading was attained within the time required to deliver the gas from a regular 5- or 10-ml syringe which was about three seconds. It should be noted that the values of the rate constant determined as indicated below are not dependent on knowledge of the exact time of mixing or the exact amount of reaction occurring during the mixing period and that some variability in the amount of reaction during the mixing procedure would not introduce an error in the rate constant. Trial kinetic runs carried out using various slit widths and wavelength settings of 240 mμ and 250 mμ as well as 260 mμ indicated no significant dependence between apparent reaction rate and slit width or wave length. The removal of fluoride by reaction with the wall of the reaction vessel was examined by gently agitating the equilibrium mixture containing ferric and fluoride for about thirty minutes (a period much in excess of that of a kinetic run) and noting the dependence of transmission on time. Four quartz vessels were examined and one only yielded a change of transmission with time. This vessel also gave irreproducible kinetic results. It was not used in further kinetic measurements and the data obtained during its use are not included in the results given below.

Initial and final transmittance readings were made on both reaction and reference cells but no attempt was made to correct the transmittance readings obtained with the reaction cell during the main course of the association which occupied periods ranging from about 150 down to 60 seconds after addition of fluoride.

All solutions were prepared from triply distilled water, the second distillation being from alkaline permanganate solution. Sodium perchlorate (anhydrous), perchlorate acid (70%), and ferric perchlorate were reagent grade chemicals obtained from G. Frederick Smith Chemical Company. The 50% hydrofluoric acid was Fisher reagent. The stock solutions of hydrofluoric acid were stored and manipulated in polythene ware and the concentrations of the diluted solutions which served as stocks were estimated by adding slight excess of sodium hydroxide and back titrating with hydrochloric acid using phenolphthalein as indicator. The stock solutions of sodium perchlorate were prepared from sodium perchlorate which had been heated for about two hours at 140° C prior to weighing. The stock solution of ferric perchlorate was prepared by dissolving the reagent in approximately 1 molar perchloric acid. Iron content of this solution was determined by redox titration (7) and gravimetry (8). Total acid plus iron (precipitated as $Fe(OH)_3$) was determined by titration with sodium hydroxide to phenolphthalein end point.

TREATMENT OF THE DATA

The data involving transmission were interpreted using the relation

[1]
$$\frac{x}{c_e} = \frac{\log T_t - \log T_0}{\log T_\infty - \log T_0}$$

where x is the concentration of FeF^{++} at time t, c_e is that at equilibrium, and T_0, T_t, and T_∞ represent transmittance readings before association, at time t, and at equilibrium. In the lower range of acidities used in this work hydrolysis of ferric ion is appreciable and $FeOH^{++}$ as well as Fe^{+++} and FeF^{++} will contribute to the effective extinction coefficient. However, as the hydrogen ion concentration remained substantially constant during a single run, so will the ratio $[Fe^{+++}]/[FeOH^{++}]$ and consequently a single effective extinction coefficient may be associated with all Fe (III) in the forms Fe^{+++} and $FeOH^{++}$ at a given acidity and temperature, and the change in optical density will be proportional to concentration of FeF^{++} as long as the production of FeF_2^+ is negligible.

To estimate the value of x from the primary experimental data it was necessary to know the value of c_e for a given set of conditions. This may be calculated using the relationship

[2]
$$\frac{c_e}{rs(m - c_e)(n - c_e)} = K_e$$

where

$m = [Fe^{+++}] + [FeOH^{++}] + [FeF^{++}]$ = total iron (III) concentration,

$n = [F^-] + [HF] + [FeF^{++}]$ = total fluoride concentration,

$r = \dfrac{[Fe^{+++}]}{[Fe^{+++}] + [FeOH^{++}]} = \dfrac{[H^+]}{K_h + [H^+]}$,

$s = \dfrac{[F^-]}{[F^-] + [HF]} = \dfrac{K_a}{K_a + [H^+]}$.

K_e is the association quotient for the reaction $Fe^{+++} + F^- \rightleftharpoons FeF^{++}$, e.g., K_e is the equilibrium value of $[FeF^{++}]/[Fe^{+++}][F^-]$ where [ ] signifies concentration in moles/per liter,

K_h is the hydrolysis quotient for the reaction $Fe^{+++} + H_2O \rightleftharpoons FeOH^{++} + H^+$;

K_a is the ionization quotient for the reaction $HF \rightleftharpoons H^+ + F^-$.

Our measurements were made at ionic strength 0.50 with sodium perchlorate the main contributor and consequently the equilibrium quotient for any one of these three reactions should have a unique value at one temperature.

The values of the various equilibrium quotients used in reducing our data are given in Table I. They were obtained by extrapolation of $\log K$–$(1/T)$ plots of the values for

TABLE I

Equilibrium quotients used in reduction of kinetic data

| Temperature (°C)	Ionic strength	$K_a \times 10^3$ (mole liter^{-1})	$K_h \times 10^4$	$K_e \times 10^{-5}$ (mole^{-1} liter)
0.11	0.50	1.96	5.02	1.07
7.16	0.50	1.67	7.47	1.19
12.10	0.50	1.52	10.1	1.28

K_a, K_e, and K_h for ionic strength 0.5 and temperatures 15°, 25°, and 35° C given by Connick and co-workers (9).

Substitution of the value of c_e appropriate to a given set of conditions along with values of transmittance readings obtained during a kinetic run in equation 1 allowed values of x at various times during approach to equilibrium to be estimated. These were interpreted to yield rate constants by the method described below.

It was initially assumed that the sole reaction involved in the formation of FeF^{++} was a second-order association opposed by a first-order dissociation as summarized by

$$Fe^{+++} + F^- \underset{k_{-I}}{\overset{k_I}{\rightleftharpoons}} FeF^{++}. \tag{I}$$
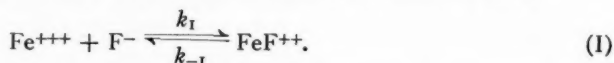
To interpret the data obtained over a range of acid concentrations, it was necessary to assume that the second-order reactions

$$Fe^{+++} + HF \underset{k_{-II}}{\overset{k_{II}}{\rightleftharpoons}} FeF^{++} + H^+ \tag{II}$$
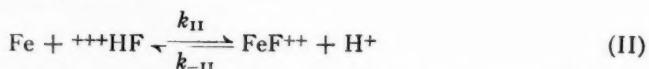
are also contributing substantially at higher acidities. Since [HF] is proportional to $[H^+][F^-]$, kinetic data will not distinguish between II and a hydrogen ion catalyzed association.

If I is the sole set of reactions involved, then

[3]
$$\frac{d}{dt}[FeF^{++}] = k_I[Fe^{+++}][F^-] - \frac{k_I}{K_e}[FeF^{++}]$$

or

$$\frac{dx}{dt} = k_I\left\{rs(m-x)(n-x) - \frac{1}{K_e}x\right\}$$

if the rates of ionization of hydrogen fluoride and of hydrolysis of ferric ion are relatively fast.

If reactions II are also involved,

$$\frac{d[FeF^{++}]}{dt} = k_I[Fe^{+++}][F^-] + k_{II}[Fe^{+++}][HF] - \frac{k_I}{K_e}[FeF^{++}] - \frac{k_{II}}{K_e K_a}[FeF^{++}][H^+].$$

This may be rewritten as

[4]
$$\frac{dx}{dt} = \left(k_I + \frac{1-s}{s}k_{II}\right)\left\{rs(m-x)(n-x) - \frac{1}{K_e}x\right\}$$
$$= k'\left\{rs(m-x)(n-x) - \frac{1}{K_e}x\right\}.$$

The solution of [3] is

[5]
$$\frac{1}{rs}\frac{1}{\sqrt{q}}\log\frac{2ax+b-\sqrt{q}}{2ax+b+\sqrt{q}} = k_I t + \text{constant}$$

where
$$a = 1,$$
$$b = -m-n-\frac{1}{K_e rs},$$
$$c = mn,$$
$$q = b^2 - 4ac.$$

The solution of [4] is the same except that k_I of [5] is replaced by k' where $k' = k_I + \{(1/s) - 1\}k_{II}$.

If the above-mentioned assumptions are correct a plot of the values of the expression on the left of equation 5 against time should lie in a straight line. If reactions I are the sole contributors, the slope will be independent of $[H^+]$ and equal to k_I. If reactions II are also contributing then the slope will be dependent on $[H^+]$ and equal to k' $(= k_I + \{(1/s)-1\} k_{II})$. In the latter event a plot of k' against $1/s-1$ should yield a straight line with intercept at $1/s-1 = 0$ equal to k_I and slope equal to k_{II}.

EXPERIMENTAL RESULTS

Most of our measurements have been carried out at ionic strength 0.50, with acid concentrations ranging from 0.02 to 0.40 molar and the maximum Fe (III) concentration about 10^{-3} molar. The highest concentrations of Fe (III) which could be conveniently studied in the 1-cm cells were limited by the very high molecular extinction coefficient of ferric ion at 260 mμ (10) and also at lower acidities by complications which would be introduced due to the formation of condensed species such as $Fe_2(OH)_2^{4+}$ (10, 11). In all determinations the concentration of total fluoride was less than that of total ion, a condition particularly important at higher concentrations in maintaining a low value for the ratio $[FeF_2^+]/[FeF^{++}]$. We estimate, using values for the first and second association quotients derived from Connick's values (9), that the maximum equilibrium value for this ratio under any of our experimental conditions was less than 0.03.

The data obtained under each set of conditions which we examined were interpreted as indicated above and the quantity on the left of equation 5 when plotted against time yielded quite good straight lines regardless of the conditions. Figure 1 shows a plot of
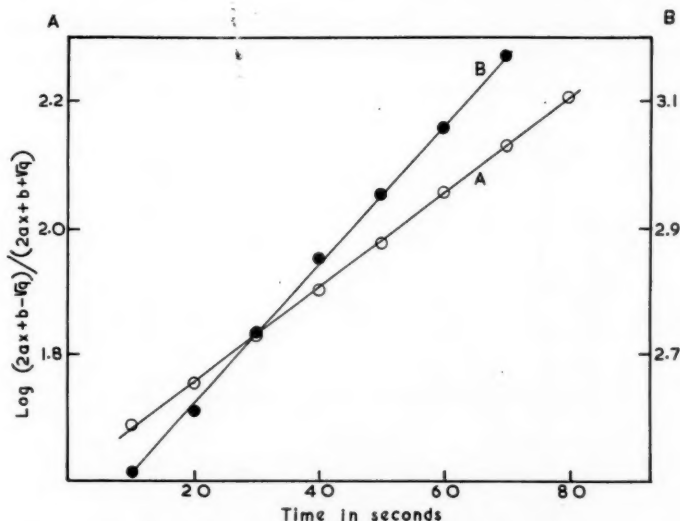

FIG. 1. Plot in accord with equation 5 using data from two runs at ionic strength 0.5 and temperature 0.11° C.

	[HClO$_4$]	[Total iron (III)]	[Total fluoride]
A	0.20 M	7.69×10^{-4}	1.50×10^{-4}
B	0.40	8.87×10^{-4}	0.89×10^{-4}

$\log (2ax + b - \sqrt{q})/(2ax + b + \sqrt{q})$ against time derived from data for two runs at 0.11° C. The plotted points involving the greatest time for each run refer to the formation of FeF^{++} to the extents of 0.92 and 0.85 of the amounts at equilibrium.

The values of k' obtained by this method from the data obtained at 0.1° C for three acid concentrations are given in Table II. Although the values obtained at any one acidity

TABLE II

Values of k^1 at 0.11° C and three acid concentrations

Hydrogen ion concn. (moles liter⁻¹)	Total iron (III) concn.	Total fluoride concn.	k' (mole⁻¹ liter second⁻¹)	Hydrogen ion concn. (moles liter⁻¹)	Total iron (III) concn.	Total fluoride concn.	k' (mole⁻¹ liter second⁻¹)
0.020	9.03	3.01	228	0.10	7.69	0.75	344
0.020	9.03	3.01	240	0.10	4.73	1.50	267
0.020	9.03	1.50	235	0.10	4.73	0.75	335
0.020	9.03	0.75	216				
				0.40	10.06	3.01	798
0.10	10.06	3.01	326	0.40	10.06	1.50	725
0.10	10.06	3.01	304	0.40	10.06	0.75	816
0.10	10.06	1.50	275	0.40	8.87	3.01	726
0.10	10.06	0.75	305	0.40	8.87	1.50	778
0.10	8.87	3.01	295	0.40	8.87	0.75	797
0.10	8.87	1.50	284	0.40	7.69	3.01	792
0.10	7.69	3.01	297	0.40	7.69	1.50	759
0.10	7.69	1.50	335	0.40	7.69	0.75	685

have a moderate scatter there is no significant dependence on the total concentration of iron (III) or of fluoride. However, there is a positive and significant dependence on the hydrogen ion concentration (which we take as identical with the concentration of perchloric acid). A 20-fold increase in hydrogen ion concentration leads to a 3-fold increase in the apparent rate constant on 0.1° C.

The values of k' plotted against $1/s-1$ ($= \{[H^+]/K_a\}$) for each of the three temperatures investigated (0.11, 7.16, and 12.10° C) are shown in Fig. 2. There appears to be the
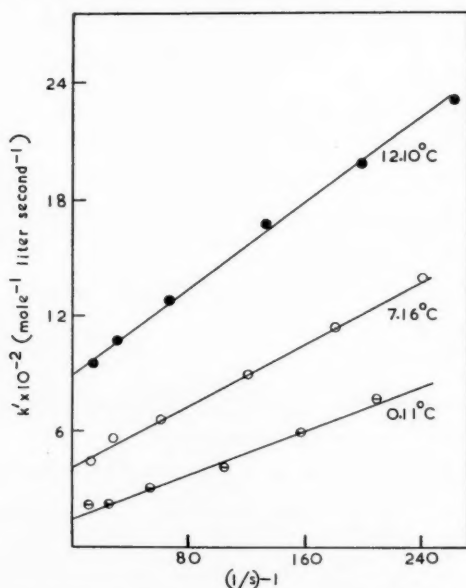

FIG. 2.   Variation of effective rate constant k' with $1/s-1 (= [H^+]/K_a)$.

linear relationship between k' and $\{(1/s)-1\}$ which would be expected if reactions I and II are involved. If a reaction involving $FeOH^{++}$ and fluoride ion were contributing appreciably to the rate, then the values of k' applying to the lower range of acidities should be greater than those indicated by the linear extrapolations of the points applying to the higher acidities. The data for 0.11° C may be consistent with a slight trend of this sort, but there is no evidence for such a trend at the higher temperatures.*

Values of k_I and k_{II} have been estimated from the intercepts and slopes of the lines of regression in Fig. 2 and are given in Table III. As can be seen from inspection of Fig. 2 the

TABLE III

The rate constants k_I and k_{II} in mole^{-1}
liter second^{-1}

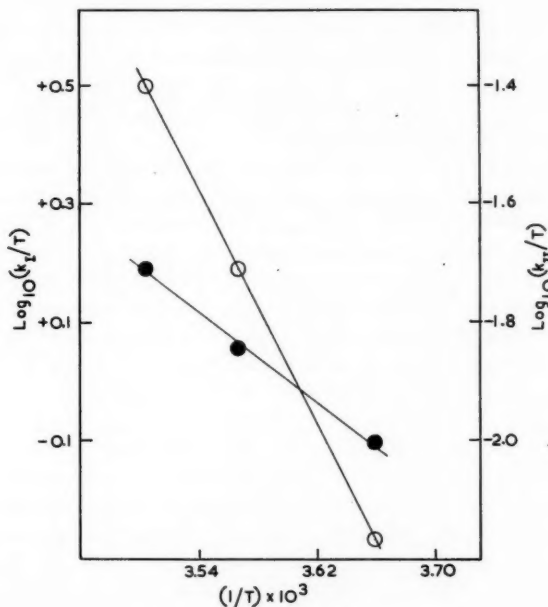| Temperature (° C)	k_I	k_{II}
0.11	147	2.71
7.16	433	4.01
12.10	900	5.57

FIG. 3.   Modified Arrhenius plots.

○ log (k_I/T) for reaction $Fe^{+++} + F^- \rightarrow FeF^{++}$,
● log (k_{II}/T) for reaction $Fe^{+++} + HF \rightarrow FeF^{++} + H^+$.

*We have made measurements at 0.1° C, at ionic strength 0.05, and perchloric acid concentrations down to 0.01 molar and find that the apparent rate constant at this acidity is not significantly different from that at acid concentration 0.045 molar. Smith's preliminary measurements suggested such a lack of dependence of rate on acidity over this range, but the values he found were about 30% lower than ours. The interpretation of the spectro-photometric measurements for lower acidities may be complicated by the formation of FeF_2^+ and $Fe_2(OH)_4^{4+}$ but this apparent lack of dependence of rate constant on acidity suggests that a significant contribution to the rate at acid concentration 0.01 by a reaction involving $FeOH^{++}$ cannot be definitely ruled out.

uncertainties associated with the values of k_I are considerable and the third figure recorded in Table III for each value is of doubtful significance.

Plots of log (k_I/T) against $(1/T)$ and of log (k_{II}/T) against $(1/T)$ are given in Fig. 3. Heats and entropies of activation for the two reactions estimated from these plots are as follows:

For the reaction $Fe^{+++} + F^- \rightarrow FeF^{++}$

$$\Delta H_I^{\ddagger} = 22.8 \pm 2.5 \text{ kcal mole}^{-1} \text{ and } \Delta S_I^{\ddagger} = 35 \pm 9 \text{ cal deg}^{-1} \text{ mole}^{-1}.$$

For the reaction $Fe^{+++} + HF \rightarrow FeF^{++} + H^+$

$$\Delta H_{II}^{\ddagger} = 8.7 \pm 0.7 \text{ kcal mole}^{-1} \text{ and } \Delta S_{II}^{\ddagger} = -24 \pm 3 \text{ cal deg}^{-1} \text{ mole}^{-1}.$$

DISCUSSION

Below, Connick, and Coppel carried out their investigations of the ferric–thiocyanate association (4) at ionic strength 0.4 and obtained for the purely ionic association $Fe^{+++} + SCN^- \rightarrow Fe(SCN)^{++}$ a heat of activation of 13.0 ± 1.4 kcal per mole and an entropy of activation of -5 ± 5 cal deg^{-1} mole^{-1}. They did not detect any reaction catalyzed by hydrogen ions or involving any species protonated beyond that of triply charged ferric ion or singly charged thiocyanate, but they did find an increase of rate with decrease in acidity which they attributed to the reaction involving $Fe(OH)(H_2O)_5^{++}$ and the anion. The effect on the heat of activation or the entropy of activation of changing the ionic strength from 0.4 to 0.5 is small (12) and our values and those of Below, Connick, and Coppel may be considered comparable.

The values of $\Delta H^{\ddagger}$ and $\Delta S^{\ddagger}$ which we estimate for the forward reaction I are decidedly larger than those found for the ferric–thiocyanate association. This is possibly due to fluoride ion being much more firmly solvated than thiocyanate. If the attainment of the transition state involves marked desolvation of the anion then the reaction involving fluoride may be more demanding energetically and have a higher heat of activation. Likewise as has been pointed out by Below et al. (4) the entropy increase accompanying liberation of water from the anions will be more marked for fluoride than for thiocyanate.

Connick and co-workers have estimated the entropies of reaction for these two associations at ionic strength 0.4 and at 25° C. For the thiocyanate association $\Delta S°$ was given as 4.6 cal deg^{-1} mole^{-1} (4), and for the fluoride association as 30 cal deg^{-1} mole^{-1} (9). A moderate parallelism between the entropy of activation and the entropy of reaction for each of these reactions is apparent. The entropies of activation and reaction for the fluoride association are close in magnitude and positive. This supports the view that the organization of solvent in the transition state approaches that of the final state, even though the states are quite different energetically, and that the fluoride is actively involved in the transition state (i.e. the mechanism is S_N2). The entropies of activation and reaction for the thiocyanate association are both small and it appears that the entropy of activation is significantly more negative. However, in view of the weak solvation of thiocyanate ion and the lack of marked dependence of entropy change on the involvement or non-involvement of thiocyanate it is difficult to interpret these data as supporting either an S_N2 or an S_N1 mechanism.

The increase in apparent rate constant with acidity which we find could be attributed to either a hydrogen ion catalyzed reaction or to one involving HF. We favor the latter because it is difficult to envisage a likely mechanism for hydrogen ion catalysis, but possible to envisage a process where the reaction involving HF has a lower heat activation

than the mechanism involving fluoride. We consider that, relative to the conditions obtaining in the mechanism involving fluoride ion, the weaker solvation of HF may contribute more to the reduction of the heat of activation than does the reduced electrostatic interaction between ferric ion and hydrogen fluoride (relative to that between ferric and fluoride ions) contribute to its increase.

The values discussed above for the heats and entropies of activation for the reactions involving fluoride with ferric ions and thiocyanate with ferric ions were obtained from measurements made in solutions where the ionic strength was adjusted to 0.5 or 0.4 with sodium perchlorate and these values should be comparable. However, in view of the possibility of some association between ferric and perchlorate ions complicating the interpretation of the measurements at high ionic strength, it seems worth while to examine the kinetics of both the ferric–fluoride and ferric–thiocyanate associations over a wider range of ionic strengths and temperatures in an effort to obtain data applicable to limitingly low ionic strength and concentrations of competing ions.

ACKNOWLEDGMENTS

REFERENCES

1. R. G. PEARSON. J. Phys. Chem. 63, 321 (1959).
2. C. POSTMUS and E. L. KING. J. Phys. Chem. 59, 1216 (1955).
3. R. E. HAMM and R. E. DAVIS. J. Am. Chem. Soc. 75, 3085 (1953).
4. J. F. BELOW, JR., R. E. CONNICK, and C. P. COPPEL. J. Am. Chem. Soc. 80, 2961 (1958).
5. M. EIGEN. Discussions Faraday Soc. 17, 194 (1954).
6. W. MacF. SMITH. Proc. Chem. Soc. 207 (1957).
7. M. G. MELLON. Quantitative analysis. Thomas Y. Crowell Co., New York. 1955. p. 429.
8. A. I. VOGEL. Quantitative inorganic chemistry. 2nd ed. Longmans Green & Co., Ltd., London. 1958. p. 408.
9. R. E. CONNICK, L. G. HEPLER, Z. Z. HUGUS, JR., J. W. KURY, W. M. LATIMER, and MAAK-SANG TSAO. J. Am. Chem. Soc. 78, 1827 (1956).
10. L. N. MULAY and P. W. SELWOOD. J. Am. Chem. Soc. 77, 2693 (1955).
11. R. M. MILBURN and W. C. VOSBURGH. J. Am. Chem. Soc. 77, 1352 (1955).
12. S. GLASSTONE, K. J. LAIDLER, and H. EYRING. The theory of rate processes. McGraw-Hill Book Co., Inc., New York. 1941. Chap. 8.

THEORY OF THE POLARIZATION CURVE TECHNIQUE FOR STUDYING CORROSION AND ELECTROCHEMICAL PROTECTION[1]

W. A. MUELLER

ABSTRACT

This study of the analysis of polarization curves is based on the identification of the partial currents of the single electrochemical reactions involved. The relationship between the gradient of polarization curves and the corrosion rate in uninhibited corrosion processes is investigated. The analysis of polarization curves is explained and two methods of using polarization curves in corrosion studies are compared. The conditions for stability of the active and the passive states are specified for application in anodic and cathodic protection.

I. INTRODUCTION

In the course of studies of the corrosion of steel in the presence of hot alkaline solutions (as in the kraft process of pulping of wood), some basic features of the electrochemical theory of corrosion were defined, and two methods for recording polarization curves were developed (1). The theory and experimental methods are expected to apply generally to the electrochemical reactions of any metal with any electrolyte. In this paper the practical corrosion problem, as studied previously, is considered only as an example of the general application of the theory and methods.

The practical problem concerned carbon-steel digesters attacked by alkaline pulping liquors in kraft mills. The cooking liquors contain 40 to 75% mill white liquor, the remainder being black liquor. The constituents of white liquor are about 100 g/liter sodium hydroxide and 35 g/liter sodium sulphide and minor quantities of sodium thiosulphate and polysulphides. Black liquor is the product of the reaction between the liquor mixture and wood (2).

The initial laboratory studies measured corrosion rates as a function of the liquor composition. Ruus and Stockman (3) found by laboratory experiments that sodium hydroxide, sodium sulphide, and sodium thiosulphate are main factors determining the corrosion rate in cooking liquor. This finding was corroborated by a Canadian field study (4). The role of polysulphide, thiosulphate, and dimethyldisulphide as depolarizers has also been described (5, 6, 7). However, two independent studies (3, 8) reported that the corrosion rates were not always reproducible even under presumably identical conditions. For instance, in an extreme case negligibly small corrosion rates of 10 or 20 M.P.Y. (milli-inches per year) were found alternating with rates of 650 and 750 M.P.Y. It appeared that the conditions were close to the border line between the stable active and passive states. Several series of potential–time curves revealed that steel immersed in white liquor at room temperature assumes either the active state at a potential of about -1.05 volt or the passive state at about -0.7 to -0.8 volt in reference to a saturated calomel cell (1) depending only on minor differences in the pretreatment of the steel. Another problem was provided by the observation that, during the heating period of the cook, the corrosion rate is high and falls unexpectedly during the later phase of the cook (3).

These observations, together with the problems connected with applying anodic or cathodic protection to steel in contact with these solutions, indicated a need for a basic study of the processes. The search for a theory and for experimental methods capable of

clarifying these problems was directed towards electrochemical methods for analyzing localized attack as well as general uniform corrosion. Electrochemical corrosion in the narrow meaning of the term requires that areas of anodic and cathodic reaction can be distinguished. The mechanism of extremely localized corrosion, characterized by complete separation of areas in which anodic or cathodic reactions occur, has been previously explained (9, 10) on this basis; but this principle does not apply in the case of general, uniform corrosion. However, a solution was found by assuming electrochemical reactions in the broad meaning of the term (11, 12, 13, 14, 15, 16) which implies the exchange of positive or negative electrical charges between metal and electrolyte, whereby anodic and cathodic reactions may occur on the same metal surfaces simultaneously. On this basis the general laws which govern the increase of corrosion resistance by means of alloying were examined by Tomashov (17).

Pourbaix (14) derived electrochemical equilibrium diagrams, which describe the effect of pH on electrochemical reactions at varied potentials. During recent years the "measurement of the corrosion rate of iron by the polarization curve techniques" has been studied by several workers (18, 19, 20) applying different principles. They showed empirically that the slope of the polarization curve of iron in certain solutions is related to the corrosion rate. This relationship was theoretically derived by Stern (21). It receives an improved and more detailed formulation in this paper on the basis of a different derivation.

However, the analysis of "current density – potential curves",* to determine their components, was considered to be an appropriate approach to the initially stated problem. This principle, introduced by Wagner and Traud (22) was applied by Bonhoeffer (23) to the analysis of the polarization curve of iron immersed in sulphuric acid. A very detailed account of the analysis was published by Schwarz (16). The analysis of polarization curves was recently discussed by Stern (15) and applied to criticize the "current–potential break" criterion as used in cathodic protection. The principle of the analysis has been extended, in an independent study (1), to cover both the active and passive states and particularly the potential range around the boundary between them. In this connection the studies of Edeleanu (24) are of particular interest.

This paper intends to clarify some basic problems of the polarization curve theory and its application in the study of corrosion problems. It shows how the polarization curve is combined from the waves of the single reactions (25) involved. Some new aspects are revealed of the relation between the corrosion rate, the slope of the polarization curve, and the diffusion conditions in the corrosive environment of the metal. Finally, the conditions of the stability of the active and passive states are explained.

II. ELECTROCHEMICAL ANALYSIS OF POLARIZATION CURVES

When the polarizing and the depolarizing reactions occur at separate electrodes, a cell is formed, causing corrosion of the anodic specimen (9) if it is in the active state. The corrosion rate is proportional to the strength of the current in agreement with Faraday's law. However, the total current is decreased when the partial reactions occur at the same electrode. When both reactions occur at equal rates all over the metal, there is no current flow, for as the partial currents are opposed, their sum is zero. The partial currents are governed by the same quantitative relationships, independently of the current distribution. An applied current causes a shift of the potential difference between metal and

*This term, which is normally used in continental Europe, implies that the potential is considered primarily as the independent variable, to be plotted on the abscissa, and the current or current density as the dependent variable, to be plotted on the ordinate. In this paper the expression polarization curve is used without discrimination and the potential is recorded on the abscissa as the independent variable.

electrolyte and this in turn causes an alteration of the partial currents. The potential shifts until the external current equals the sum of the partial currents (some of which may be negative). This quantitative relationship was experimentally proved by Bonhoeffer (23) for iron dissolving in sulphuric acid.

Identification of the single reactions is often possible when the current density is considered as the sum of partial currents, each of which is caused by one single reaction and represents an independent function of the potential difference between metal and electrolyte. The combination of single reactions with their respective reverse reaction has been discussed in another paper (25). This paper is concerned with polarization curves as combined from the single reactions which include their reverse reactions.

III. THE RELATIONSHIP BETWEEN THE POLARIZATION CURVE AND THE CORROSION RATE

In the introduction an empirical rule was mentioned which relates the corrosion rate to the slope of the polarization curve (20) and which can be formulated as:

$$[1] \qquad \frac{dE}{dI} = \frac{K}{-\left(\dfrac{dW}{dt}\right)^s}$$

where K = constant, $-dW/dt$ = corrosion rate, W = weight per unit area, S = exponent, $S > 1$. To avoid misunderstanding it may be pointed out that "the slope of the polarization curve" given by Skold and Larson (20) and by Stern (21) is defined as the reciprocal of the value used in this paper. The following derivation is based on the assumption that the partial currents are independent of one another. This implies that the corrosion rate is primarily related to the anodic dissolution current, but not to the polarization curve, which refers to the depolarization current in addition.

A method for determining corrosion rates from linear polarization data has been developed by Stern (21). In the following, a new derivation is given of this relation, and the deviations from Stern's equations are discussed. If the possible reverse reaction is included, the anodic dissolution current I_a on a metal surface free of a protective film can be formulated as a modified Tafel relation (25, 26)

$$[2] \qquad I_a = I_1 \exp \frac{a_a n_a F}{RT} (E - E_1)$$

where n_a = valency of ions formed in the dissolution process,

I_1 and E_1 are a couple of interconnected values of current density and potential,

a_a = apparent symmetry factor as defined and derived in a study of the transition from equilibrium conditions to single electrochemical reactions (25).

If I_a contains only the current caused by the forward reaction, a_a becomes identical with the symmetry factor α_a and eq. 2 becomes a conventional Tafel relation. If a reverse reaction is superposed on the forward reaction, the following relation is valid

$$[3] \qquad \alpha_a \leqq a_a \leqq 1$$

where $a_a = 1$ at equilibrium. Only in a limited potential range can "a" values be considered as constants. If "a_a" changes, I_1 and E_1 do so also.

If I_a equals the absolute value of the depolarizing current of an oxidizing reagent I_{ox}, $I_a = -I_{ox} = I_{corr}$ and the slope of I_a becomes

[4]
$$\left(\frac{dI_a}{dE}\right)_{I_a=I_{corr}} = I_{corr} \frac{a_a n_a F}{RT}$$

where I_{corr} = corrosion current.

The current–potential relation referring to the depolarizing reaction represents a typical redox wave, caused by the reaction of an oxidizing reagent, which might be counteracted by the produced reducing reagent (25). This relation can be formulated

[5]
$$\ln \frac{I_d - I_{ox}}{I_{ox}} = a_{ox} \frac{n_{ox} F}{RT} (E - E_{\frac{1}{2}})$$

where I_{ox} = current density of the depolarizing reaction of the oxidizing reagent,

I_d = current density of the diffusion current (I_d and I_{ox} are negative),

n_{ox} = valency involved in the depolarizing reaction,

$E_{\frac{1}{2}}$ = half wave potential of the depolarizing reaction,

a_{ox} = apparent symmetry factor of the depolarizing reaction of the oxidizing reagent. For an oxidizing reaction without reverse reaction $a_{ox} = \alpha_{ox}$ which is the symmetry factor of the oxidizing reaction. At equilibrium $a_{ox} = 1$.

This eq. 5 is basically different from Stern's corresponding eq. 2

[6]
$$E_{conc} = 2.3 \frac{RT}{nF} \log\left(1 - \frac{I}{I_L}\right)$$

where E_{conc} = change of potential caused by concentration polarization,

I_L = I_d of this paper.

Equation 6 is valid with respect to a metal in equilibrium with its ions in solution (27) as it has been derived from

[7]
$$E_{conc} = 2.3 \frac{RT}{nF} \log \frac{c}{c_b}$$

where c = concentration of the metal ions at the interface,

c_b = bulk concentration.

This is the overpotential of a metal in contact with a solution of its ions close to equilibrium; it is not the overpotential caused by a depolarizing reaction.

Differentiation of eq. 5 with respect to E results in

[8]
$$-\frac{dI_{ox}}{dE} \frac{1}{I_d - I_{ox}} - \frac{dI_{ox}}{dE} \frac{1}{I_{ox}} = \frac{a_{ox} n F}{RT}.$$

Accordingly the slope of the partial current density of the depolarizing reaction under steady-state conditions ($I_a = -I_{ox} = I_{corr}$) is

[9]
$$\left(\frac{dI_{ox}}{dE}\right)_{(I_a=I_{corr})} = I_{corr} \frac{a_{ox} n_{ox} F}{RT} \frac{-I_d - I_{corr}}{-I_d}.$$

Hence the relation between the slope of the polarization curve $dI/dE = (dI_a/dE) + (dI_{ox}/dE)$ and the corrosion rate can be expressed

[10]
$$\left(\frac{dI}{dE}\right)_{(I_a=-I_{ox}=I_{corr})} = I_{corr} \frac{F}{RT} \left(a_a n_a + a_{ox} n_{ox} \frac{-I_d - I_{corr}}{-I_d}\right).$$

To show the meaning of eq. 10, the anodic dissolution current (ADC) and three polarigraphic waves (W1, W2, and W3) of oxidizing reagents are plotted in Fig. 1 as a schematic
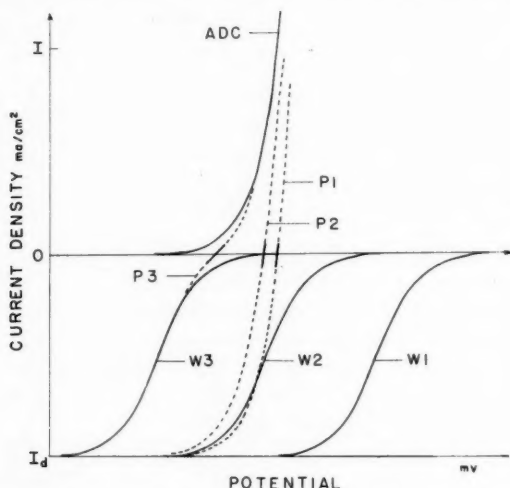

FIG. 1. Polarization curves and their slope combined from partial currents and the respective slopes.

demonstration. Three polarization curves (P1, P2, and P3) are derived from the combination of the anodic dissolution current with the waves. The slope of the diffusion controlled curve P1 is equal to the slope of the anodic dissolution current; the slopes of the curves Pa and P3 are combined from two partial slopes each.

When replacing I_{corr} by

$$\left(-\frac{dW}{dt}\right)\frac{Fn_a}{A \cdot 24 \cdot 3600}$$

eq. 10 results in

$$[11] \qquad \frac{dI}{dE} = \left(-\frac{dW}{dt}\right)\frac{F^2 n_a}{RTA \cdot 24 \cdot 3600}\left(a_a n_a + a_{ox}n_{ox}\frac{-I_d - I_{corr}}{-I_d}\right)$$

where A = atomic weight, W = weight per unit area, $(-dW/dt) = mg(dm)^{-2}(day)^{-1}$ (corrosion rate).

In double logarithmic plotting the values of the corrosion current are located on or between two limiting lines (L1 and L2) which result from eqs. 10 and 11 when $(-I_d)_{ox} = I_{corr}$ (L1) and when $(-I_d)_{ox} \gg I_{corr}$ (L2).

These conditions may be illustrated by a comparison of the relation calculated on the arbitrary assumption $a_a = 1/4$, $n_a = 2$, $a_{ox} = 1/2$, and $n_{ox} = 4$ with the experimental values of Skold and Larson (20). Figure 2 shows that the measured values are close to, or between, the calculated lines. The position of the measured points indicates that the corrosion was controlled by diffusion mainly at high values of the gradients of the polarization curve as expected. The derivation suggests that the empirical relation (Le) is valid only between the calculated lines. For the exact calculation of the limiting lines the coefficients $a_a n_a$ and $a_{ox}n_{ox}$ have to be known.

A final comparison with Stern's equation (21) shows an agreement only of Stern's eq. 8
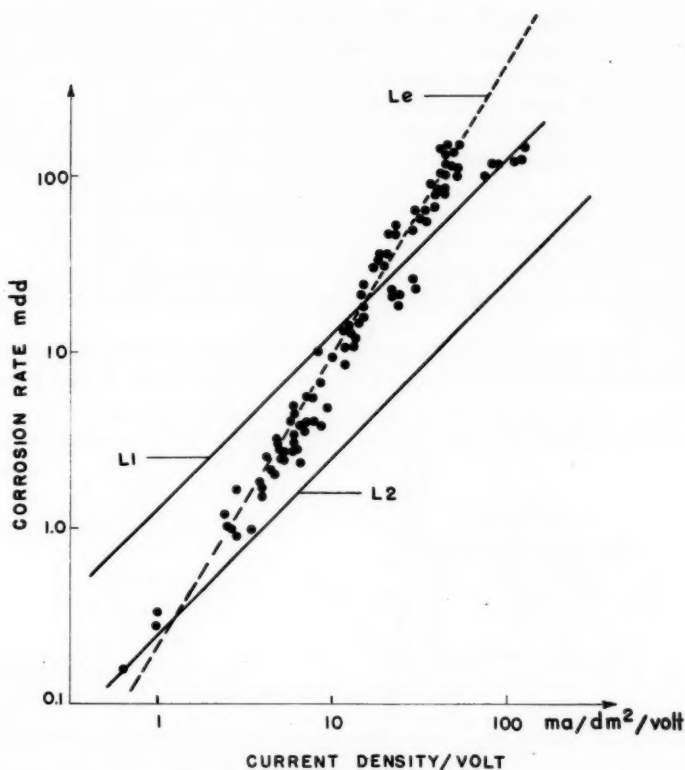
FIG. 2. Skold and Larson's (20) empirical relation between corrosion rate and the slope of the polarization curve (dotted line) in comparison with the calculated limiting condition (extended lines).

with eq. 10 of this paper if the redox reaction is completely controlled by concentration polarization and if Stern's $\beta = RT/a_a n_a F$. This is the well-known case derived from a Tafel reaction according to eq. 4. However, eqs. 10 and 11 are valid at any degree of concentration polarization. In addition to Stern's formulation eqs. 10 and 11 give an explicit relation to the valencies involved in the reaction and the relation to the diffusion current. Equations 10 and 11 reveal to which degree the corrosion under study is diffusion controlled when the "$a.n$" values are known, and they allow a close estimation of corrosion rates from the slope of the polarization curves even if only the metal and the depolarizer are known. The effect of possible reverse reactions such as electrodeposition of the dissolved metal and reducing redox reactions have also been included in these derivations.

The exact validity of the derived equations is limited to polarization curves composed of the partial currents of anodic dissolution of the metal (eq. 2) and of the depolarizing current (eq. 5). If other partial currents, such as listed in the following chapter, contribute to the polarization curve the above equations become inaccurate. Adsorption of anions can also change the basic equations of redox reactions (28).

IV. THE POLARIZATION CURVE COMBINED FROM PARTIAL CURRENTS

The polarization curve of a metal immersed in an electrolyte represents the dependence of the sum of well-defined partial currents on the potential, as follows:

1. In the active state the anodic dissolution current of the metal which can be characterized by the constants a_a, a_n, I_1, and E_1 (eq. 2). When passivation begins, a characteristic rapid decline of the current density occurs (24, 1, 29).

2. Anodic dissolution current of hydrogen contained in the metal.

3. The partial currents due to redox reactions the products of which are soluble in the oxidized and reduced state. These currents are characterized by n, a_{ox} or a_r, I_d, $E_{\frac{1}{2}}$, and E° (eq. 5)

where a_r = apparent symmetry factor of the reaction of the reducing reagent (25),

   E° = standard redox potential.

4. The partial current of deposition of metals also characterized by a, n, I_d, $E_{\frac{1}{2}}$, and E°.

5. The partial current due to slow dissolution and rebuilding of the passive film (30), in the passive state.

The various partial currents combined result in the polarization curve. As an example, Fig. 3 shows the schematic construction of the polarization curve of iron in laboratory
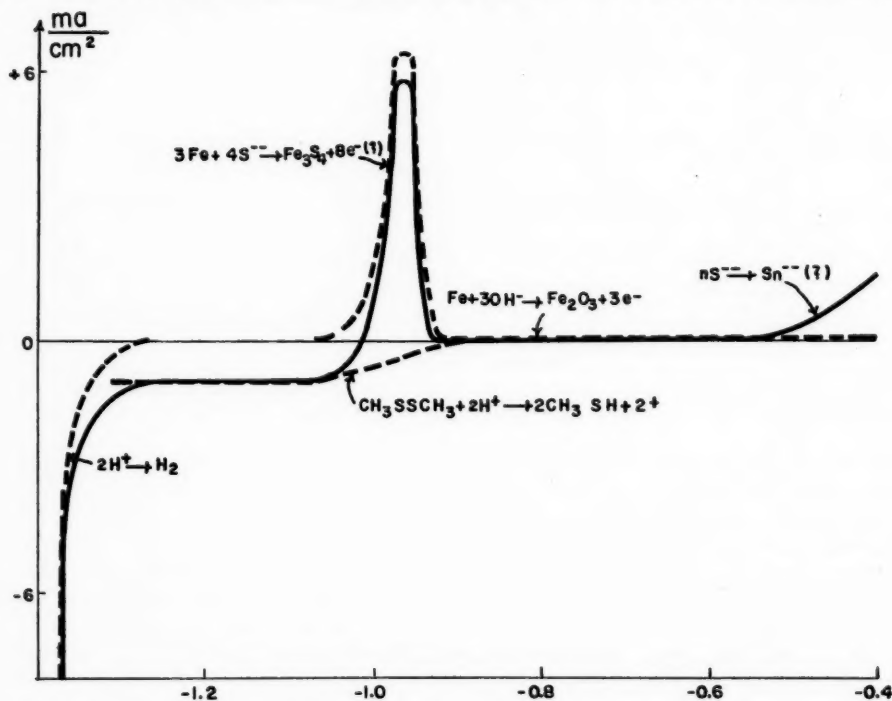

FIG. 3. Construction of the polarization curves of iron in alkaline pulping liquor from the partial currents involved.

white liquor containing 1 g/liter dimethyldisulphide. The partial currents are caused by the development of hydrogen, the redox reaction of dimethyldisulphide, the anodic dissolution current, the slow dissolution and rebuilding process of the passive film, and finally an anodic current probably due to formation of polysulphides from sulphides. The corrosion rate at a certain potential is proportional to the partial current of the anodic dissolution of the metal when in the active state or of the dissolution of the passive film when it is passive.

When specimens of two different metals, in metallic contact, are immersed in the same electrolyte the respective anodic dissolution currents are different and so are the depolarization currents due to different overpotentials. The same is true with respect to identical specimens in metallic contact when immersed in electrolytes of different composition. The potentials approach one another more closely with improved conductivity of the circuit. The final values of the potentials are located between the potential values of disconnected specimens and they depend on the gradients of the polarization curves and the extent of the exposed areas, as explained before (9, 10).

These conditions can be calculated when currents, rather than current densities, are compared. The potentials E_A and E_C shift to values where

(a) the net anodic current of the specimen A equals the net cathodic current of the specimen C;

(b) the potential difference $E_A - E_C$ equals the product of the current and the resistance in the cell circuit.

For comparison these conditions are expressed by the diagram of Evans and Hoar (10) in Fig. 4(a), and according to Schwarz (16) in Fig. 4(b), with reference to two connected
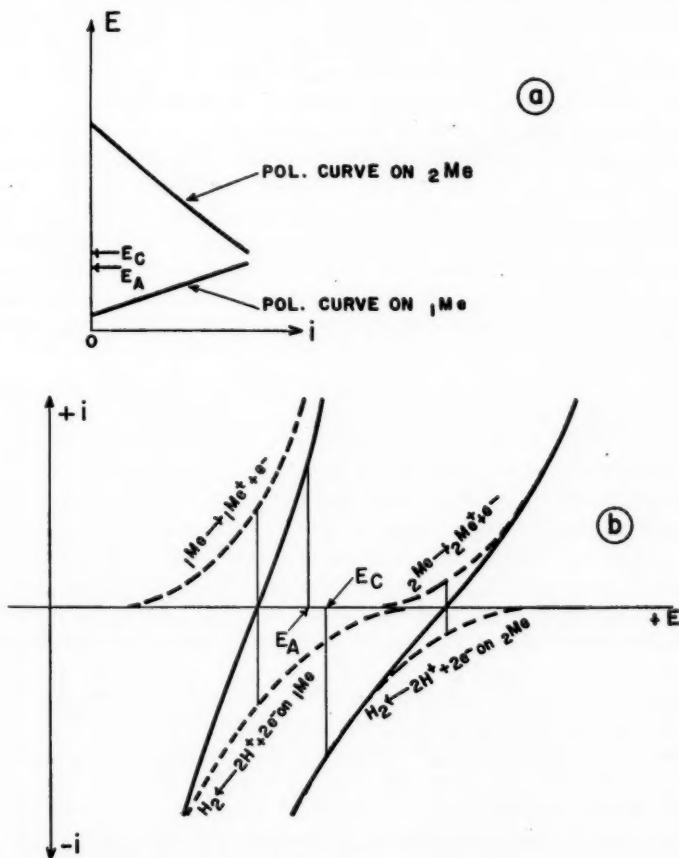

FIG. 4. The electrochemical behavior of a bimetallic system: (a) as plotted by Evans, (b) as plotted by Schwarz.

metals immersed in an acidic solution. Anodic and cathodic currents in Fig. 4(a) are plotted on the abscissa and the potentials on the ordinate. The corrosion rate is proportional to the current. The figure below (Fig. 4(b)) shows the same conditions plotted similarly to the other polarization curves in this paper. The clear distinction between anodic and cathodic currents and the clarification of the sources of these currents are assumed to be advantages of the way of plotting used in Fig. 4(b). This advantage becomes evident as soon as at least one of the compared currents results from more than one partial current. Only the method of Fig. 4(b) indicates the rate of anodic dissolution, i.e., the corrosion rate, reliably.

V. STABILITY OF THE ACTIVE AND THE PASSIVE STATES AND APPLICABILITY OF ANODIC PROTECTION

The stability of the passive state is of basic importance when it forms the basis of corrosion protection. Two types of stability have to be distinguished with respect to passivity. This paper is not concerned with instability phenomena (31), which cause rhythmic behavior or propagation of activating and passivating waves, nor with the irreversible behavior exhibited by a potential jump which is connected with the change from active to passive states (32). In this paper stability for instance of the passive state means that the passivity is maintained without supply of anodic current. The instability or low degree of stability of the active and passive states of steel in contact with alkaline cooking liquors points to the necessity for clarifying these conditions.

These conditions of stability have been discussed before by Vetter (33) and Edeleanu (24) on the basis of single electrochemical reactions and, in complete agreement with these derivations, by Mueller (1) on the basis of combined polarization curves. The experience gathered during the application of anodic protection of alkaline pulping digesters (34) may justify another discussion, which is mainly concerned with the practical application. Single reactions explain the mechanism of the electrochemical reactions involved. But combined polarization curves are usually measured and they give the information that is practically required, even if none of the single reactions is known; hence they have been chosen for this discussion.

The conditions of electrochemical equilibrium can be expressed by analogy to the definition of a mechanical equilibrium as follows: An equilibrium potential is reached if the potential is constant at zero current density. The equilibrium is stable if the potential, after receiving a small displacement, tends to return to its original values. The criterion of a stable equilibrium (S, Fig. 5) is a positive value of the gradient of the current density versus potential at a zero current density. Stability means that a current which restores the original potential is produced when the potential is changed. The criterion of unstable equilibrium (UE) is a negative gradient of the polarization curve when passing through zero current density. The presence of two stable potentials (Fig. 5(b)) requires a positive maximum of the polarization curve in the active state and a negative minimum in the passive state.

If there is no negative minimum of the current density in the passive state (Fig. 5(a)) the positive current, which leaves the metal, removes positive charges from the metal thus causing a shift of the potentials to the more negative values in the active state, i.e., the passive state is unstable; and so is the active state (Fig. 5(c)) if there is no positive maximum of the current density in the active range. The degree of the stability of the active state is proportional to the value of the positive maximum of current density; and the degree of the stability of the passive state is proportional to the value of the negative
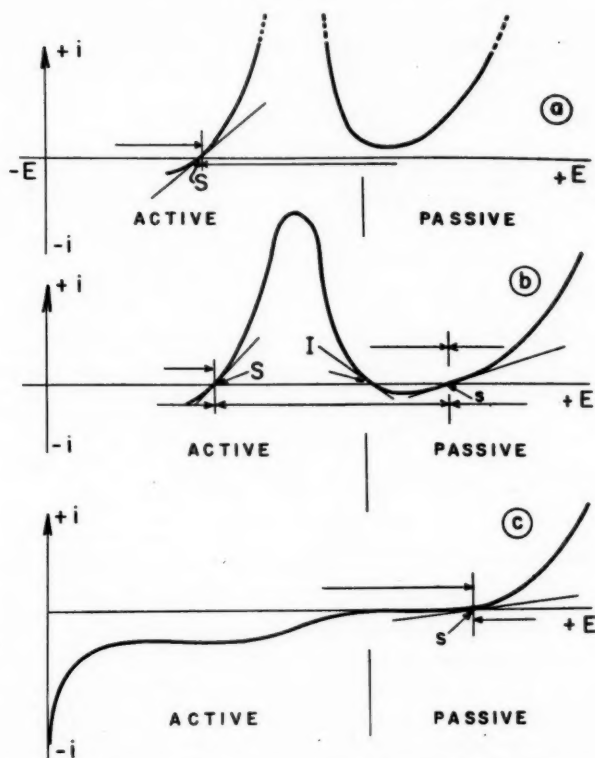
FIG. 5. Stability and instability of the electrochemical equilibrium in the active and passive states: (a) only active state stable, (b) active and passive states stable, (c) only passive state stable.

minimum of the current density. For establishing a stable passivity it is important to know how the partial currents depend on the composition of the electrolyte and on the diffusion conditions.

The three cases of electrochemical stability are demonstrated by potential time curves recorded at alkaline pulping digesters during application of anodic protection (34). The shift of the potential to the active range, when no current is supplied at the beginning of each cook (Fig. 6), shows that only the active state is then stable. Without application of anodic protection the digester remains in the active state for about two hours. However, when applying anodic protection for about one hour the digester apparently has then reached a stable passive state because the potential does not shift back when the current supply is shut off. At the end of the cook only the passive state is stable as the potential shifts to the passive range even without current supply. Thus the three mentioned cases of electrochemical stability are passed in succession during a cook in an alkaline pulping digester. Polarization curves recorded under these conditions corroborated this conclusion.

As another example, this principle gives a new explanation to the result of the study of Brauns and Pier (35) on the intercrystalline corrosion of stainless steel in boiling 5% sulphuric acid. In the case of a properly heat-treated specimen, which is free of inter-crystalline corrosion and displays a stable passivity, the minimum of the current density
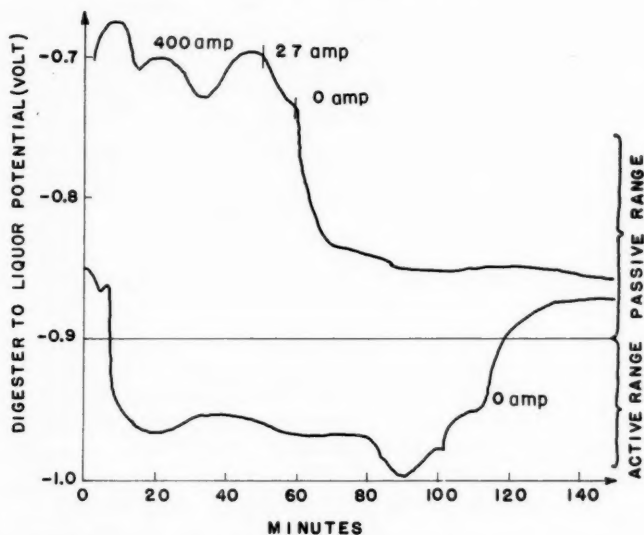
FIG. 6.   Potential time curves recorded by varying the current during directly steamed cooks of alkaline pulping digesters.

in the passive state is negative. However, with increasing instability to intercrystalline attack, the minimum shifts to increasingly positive values of the current density.

The known effect of depolarizers, such as oxygen or other oxidizing substances, of stabilizing the passive state consists in the formation of a cathodic partial current which must be sufficiently high to make the minimum current density of the polarization curve in the passive range cathodic. This effect was observed with different concentrations of dimethyl disulphide, which is one of the main depolarizers in oxidized black liquor.

For the passivation of a metal which is in the active state, a high initial current is required to shift the potential past the maximum in the polarization curve in the active state. This current can be reduced by passivating different areas in succession. After reaching stable passivity (stable equilibrium in the passive state) the current can be switched off without causing re-activation. However, if there is no stable equilibrium in the passive state, a current has to be maintained at a level higher than the minimum current indicated by the polarization curve in the passive range. Insufficient supply of current or of depolarizers does not passivate or protect the electrode; on the contrary, it increases the corrosion rate.

The danger of corrosion caused by reaching the transpassive state has also to be taken into consideration for the application of anodic protection. Evidently a shift to extreme anodic potentials may be caused by some changes during long time operation, for instance, when scale is formed on an increasing ratio of the surface. A potential shift to the transpassive range is easily prevented if the polarization curve shows high current densities in the passive range, before reaching transpassivity. If this is not the case potentiostatic control of the applied current is required to prevent a shift of the potential to the transpassive potential range. Figure 3 demonstrates a system in which corrosion by shifting to the transpassive state is not very likely because in the extreme anodic range the anodic

current density reaches high values when corrosion is still literally zero. Thus the field experiment with the application of anodic protection to alkaline pulping digesters (34) is the first practical application of these theories.

REFERENCES

1. W. A. MUELLER. Can. J. Technol. **34**, 162 (1956).
2. J. N. STEPHENSON. Pulp and paper manufacture. Vol. 1. McGraw-Hill Book Co., New York. 1950.
3. L. RUUS and L. STOCKMAN. Svensk Papperstidn. **56**, 857 (1953); Paper Ind. **35**, 1242 (1954).
4. C. B. CHRISTIANSEN and J. B. LATHROP. Pulp & Paper Mag. Can. **55**, 113 (1954).
5. B. HAEGLUND and B. ROALD. Norsk Skogind. **9**, 351 (1955).
6. W. A. MUELLER. Tappi, **40**, 129 (1957).
7. R. B. KESLER and J. F. BAKKEN. Tappi, **41**, 97–102 (1958).
8. T. W. HASSLER. Tappi, **38**, 265 (1955).
9. U. R. EVANS. Metallic corrosion, passivity and protection. 2nd ed. Edward Arnold & Co., London. (1946).
10. U. R. EVANS. J. Electrochem. Soc. 103, 73 (1956); T. P. HOAR. Proc. Roy. Soc. A, **137**, 359 (1932).
11. H. GRUBITSCH. Chem. Ing. Techn. **27**, 287 (1955); **28**, 9 (1956).
12. E. LANGE and K. NAGEL. Z. Elektrochem. **53**, 21 (1949).
13. G. MASING. Werkstoffe u. Korrosion, **1**, 433 (1950).
14. M. POURBAIX. J. Electrochem. Soc. **101**, 217 C (1954).
15. M. STERN. J. Electrochem. Soc. **102**, 609 (1955); **104**, 56 (1957).
16. W. SCHWARZ. Metall. **10**, 513 (1956); **10**, 921 (1956).
17. N. D. TOMASHOV. Corrosion, **14**, 229 T (1958).
18. W. J. SCHWERDTFEGER and O. N. McDORMAN. J. Electrochem. Soc. **99**, 407 (1952).
19. E. J. SIMMONS. Corrosion, **11**, 255 (1955).
20. R. V. SKOLD and T. E. LARSON. Corrosion, **13**, 139 (1957).
21. M. STERN. Corrosion, **14**, 440 T (1958).
22. C. WAGNER and W. TRAUD. Z. Electrochem. **44**, 391 (1938).
23. K. F. BONHOEFFER. Z. Elektrochem. **55**, 151 (1951).
24. C. EDELEANU. Nature, **173**, 739 (1954); Metallurgia, **50**, 113 (1954); J. Iron Steel Inst. **185**, 482 (1957); **188**, 122 (1958).
25. W. A. MUELLER. In preparation.
26. J. TAFEL. Z. physik. Chem. **50**, 641 (1905).
27. C. W. TOBIAS, M. EISENBERG, and C. R. WILKE. J. Electrochem. Soc. **99**, 359 C (1952).
28. Y. M. KOLOTYRKIN. Trans. Faraday Soc. **55**, 455 (1959).
29. W. A. MUELLER. J. Electrochem. Soc. In preparation.
30. H. GÖHR and F. LANGE. Z. Elektrochem. **61**, 1291 (1957).
31. U. F. FRANK. Z. Elektrochem. **62**, 649 (1958).
32. H. J. ROCHA. In Handbuch der Sonderstahlkunde. Vol. I. E. HOUDREMONT. Springer-Verlag. 1956.
33. K. J. VETTER. In Passivierende Filme und Deckschichten. H. FISCHER, K. HAUFFE, and WIEDERHOLT. Springer-Verlag. 1956.
34. W. A. MUELLER. Pulp and Paper Mag. Can. **10**, 3 (1959); Tappi, **42**, 179 (1959).
35. E. BRAUNS and G. PIER. Stahl und Eisen, **75**, 579 (1955).

RATES OF ADSORPTION OF HYDROGEN ON PALLADIUM AND ON RHODIUM[1]

MANFRED J. D. LOW

ABSTRACT

A study of the effects of temperature and initial gas pressure on the kinetics of chemisorption of hydrogen on alumina-supported palladium and rhodium catalysts revealed, for both gas–solid systems, that the adsorption proceeded via three distinct and consecutive kinetic stages. Each stage could be described by the Elovich equation. The temporal range of existence of each kinetic stage was temperature- and pressure-sensitive, low initial pressures and high temperatures favoring early appearance of each stage. On increasing the temperatures from 0° to 400° C, the amounts of hydrogen adsorbed on both solids decrease. Over that temperature range the rates of adsorption on Pd decrease, while those on Rh increase, with increasing temperature. The general effect of increasing the initial gas pressure over the range 10–60 mm Hg is to increase both rates and extents of adsorption.

INTRODUCTION

The rates of chemisorption in many gas–solid systems have been shown (1) to obey the Elovich equation,

$$\frac{dq}{dt} = ae^{-\alpha q},$$

where q is the amount of gas taken up at time t, and a and α are constants. The q–t relation can be expressed by an integrated form of the Elovich equation as

$$q = \frac{2.3}{\alpha} \log_{10}(t+k) + \text{constant},$$

where k is a constant, so that a plot of q versus $\log_{10}(t+k)$ is linear. In certain systems isothermal discontinuities (1), or breaks, have been reported, in that abrupt changes in slope occurred in the $q - \log_{10}(t+k)$ plots, and such behavior was ascribed to adsorption on different sites (1). The change in slope corresponded to relatively increased or to decreased rates of adsorption, changes in both directions sometimes occurring within the same gas–solid system (2). Preliminary experiments had shown that such breaks occurred in the system H_2–Pd and H_2–Rh, and suggested more extensive work.

EXPERIMENTAL DETAILS

The uptake of gas by the solids was followed by measuring decreases in pressure with time in systems of constant volume, using previously described techniques (2–6). The adsorbents were: 20.46-g sample of 0.5% Pd supported on the exterior of 3×5 mm γ-Al_2O_3 pellets; 15.85-g sample of 0.5% Pd on exterior of 1×3 mm γ-Al_2O_3 extrudates. The unreduced commercial catalysts were black in color. On heating of the catalysts to 500° C *in vacuo* a copious evolution of gas occurred. A part of the gas was condensible and probably water. After pumping overnight at 500° C a pressure $\leqslant 10^{-6}$ mm Hg was attained, the original black coloration being retained. On exposure to H_2 the catalysts turned gray. A test was made for efficiency of reduction by (a) reducing the catalysts at 500° for a specific time with H_2 at 20 l. N.T.P./hour, (b) degassing at 500° overnight, (c) measuring H_2 uptake on the degassed surface. No significant change in adsorption

occurred on increasing the reduction period from 10 minutes to 48 hours. Identical results were obtained by three alternate steps of exposures to H_2 (at 1 atm for 1 hour at 500°) and degassing at 500° for 30 minutes.

EXPERIMENTS, RESULTS, AND DISCUSSION

The General Nature of the Adsorption

For both gas–solid systems, most plots of q versus log t show the previously described breaks. For all plots k was indistinguishable from zero. Five general types of plots were obtained, shown schematically in Fig. 1. A few linear plots, such as plot 4, were obtained.
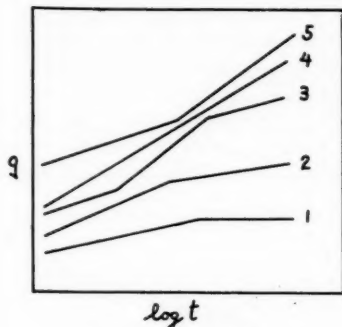
FIG. 1. Types of plots.

For most runs the $q - \log t$ plots were discontinuous, and the rate of adsorption, proportional to the slope of the $q - \log t$ line and hence to the constant $1/\alpha$, became relatively faster (as in plot 5) or relatively slower (as in plot 2).

Inspection of the plots of all data revealed certain consistent features in the occurrence of the various types of plots of Fig. 1. In comparing rate curves of experiments performed at different initial gas pressures and at different temperatures it became apparent that comparisons of kinetic stages, i.e. linear portions of $q - \log t$ plots, on the basis of their temporal order of appearance resulted in misleading correlation and interpretation. If stages were compared on the basis of the relative magnitude of the constant α of the following kinetic stage, using the scheme depicted in Fig. 2, then correlation of the rate
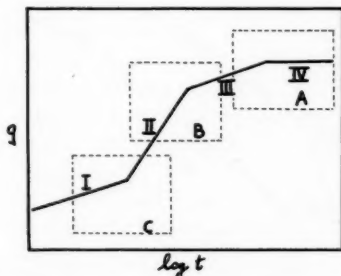

FIG. 2. Composite of multiple kinetic stages.

parameters of individual stages with temperature and pressure became possible. In Fig. 2 the different kinetic stages are arbitrarily termed I, II, III, and IV, the last representing completion of adsorption.

It is probable that all stages are present in any one run but, because of limitations imposed by the technique and by the experimental variables of temperature and pressure, not all stages necessarily are detected during the course of a single experiment.

Effects of Temperature and Pressure on Kinetic Stages

The plots 1 to 5 of Fig. 1 represent in general fashion the order of appearance of the various types of plots with increasing initial pressure, P_s. For the adsorption of H_2 on Pd and on Rh at pressures of about 10 to 20 cm DBP (dibutylphthalate) several runs were obtained which had the appearance of the schematic plot 1 of Fig. 1. For such runs the $q - \log t$ plots are equivalent to the region A enclosed by dotted lines of Fig. 2. According to the scheme of that figure the segments of the $q - \log t$ plots showing positive slope correspond to stage III, while the portions parallel to the abscissa correspond to stage IV. For such cases the preceding stages I and II are assumed to have appeared before the time of the first measurement.
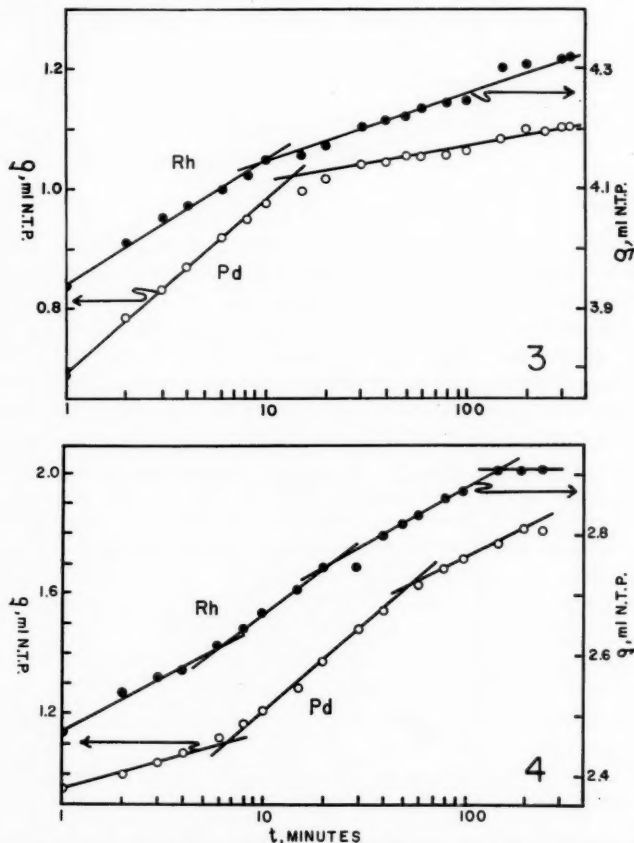

FIG. 3. Typical runs. Rh: run D65, 56° C, 50.5 cm DBP; Pd: run E57, 200° C, 44.2 cm DBP.
FIG. 4. Typical runs. Rh: run D66, 257° C, 51.7 cm DBP; Pd: run E74, 56° C, 50.88 cm DBP.

At intermediate pressures of about 20 to 50 cm DBP, stages II and III generally appear. The experimental plots have the appearance of the schematic plot 2 of Fig. 1, and correspond to the region B of Fig. 2. Examples of such data are shown by the plots of Fig. 3. For such cases the preceding stage I is assumed to have appeared before the time of the first measurement. Stage IV, the termination of the adsorption, must appear at higher t values.

At intermediate pressures some plots showed the presence of stages I, II, and III, having an appearance like the schematic plot 3 of Fig. 1. This corresponds to a combination of the regions B and C of Fig. 2. Such data is illustrated by the plots of Fig. 4. Such three-stage plots were found frequently with the H_2–Pd system.

Also, at intermediate pressures, several plots were obtained which were linear throughout, like the schematic curve 4 of Fig. 1. Such plots were assigned stage II connotation because the value of the corresponding α corresponds very closely to stage II α values to be expected from a knowledge of α values of stage II of other runs.

At P_s from about 40 to 70 cm DBP, the $q - \log t$ plots had the appearance of the schematic curve 5 of Fig. 1. This implies the appearance of stages I and II. Such plots correspond to the region C of Fig. 2. Examples of such data are shown by the plots of Fig. 5. For these
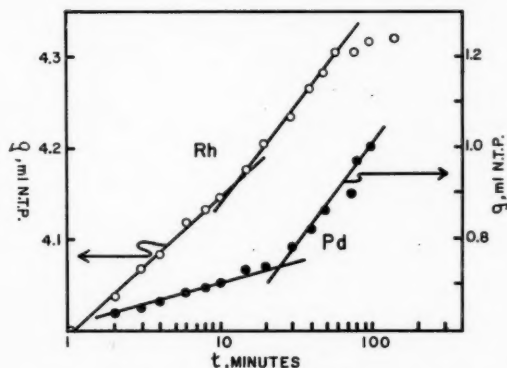

FIG. 5. Typical runs. Rh: run D40, 100° C, 51.3 cm DBP; Pd: run E36, 100° C, 51.7 cm DBP.

cases, stages III and IV would appear if the adsorption could be followed for a sufficiently long period of time. In practice this is frequently not possible because the rate of adsorption at long times becomes so slow that the precision of measurements is poor and hence continuation of the experiment is useless.

The kinetic multiplicity is further complicated by effects of P_s and temperature on the α and a values of individual kinetic stages. Changes in the slopes of the $q - \log t$ plots with changing temperature or pressure are reflected as changes in the co-ordinates of the intersections of two kinetic stages. Such effects are illustrated by the plots of Figs. 6, 7, and 8. In Fig. 6 the q-co-ordinate of the intersection of stages I and II, q_{bI}, is seen to decrease with increasing temperatures. Increase in P_s causes increase in q_{bI} and in q_{bII}, the latter being the co-ordinate of intersection of stages II and III. The corresponding t-co-ordinates, t_{bI} and t_{bII}, decline with increasing P_s, as illustrated by Fig. 8. The t_b-temperature relations are not clear.

The appearance of three consecutive stages in some plots, such as those of Fig. 4, as well as the consistent changes in α values of corresponding stages with changing
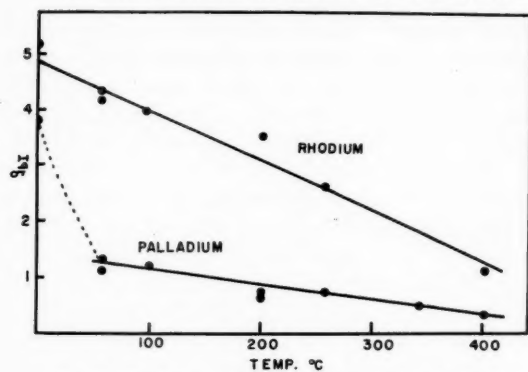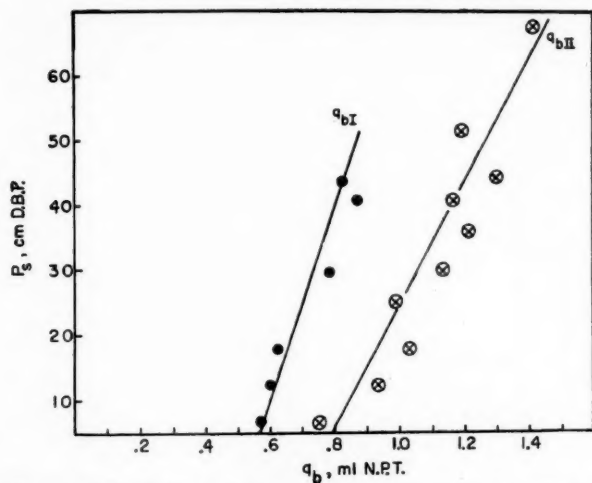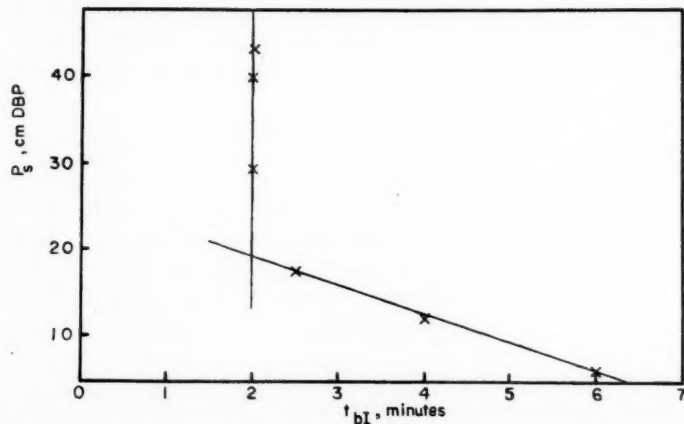
FIG. 6. The influence of temperature on the break.

FIG. 7. The influence of P_s on the break. q_{bI} and q_{bII} refer to the q-co-ordinates of the intersection of stages I and II, and stages II and III, respectively. H_2–Pd, 100° C.

FIG. 8. The influence of P_s on the break. t_{bI} is the t-co-ordinate of the intersection of stages I and II. H_2–Pd, 100° C.

temperature or pressure, suggest that the composite structure of Fig. 2 is consistent with the data. Similar changes to both relatively faster and slower rates, apparently occurring haphazardly, have been found previously in the system H_2–$ZnO.Cr_2O_3$ (2, 7), and in the system H_2–Ir–Al_2O_3 (4), while in the system H_2–ZnO (8) breaks towards a relatively faster rate were consistently obtained. It appears probable that in those systems a similar succession of kinetic stages exists.

The Effects of P_s and Temperature

At 100°, 200°, and 257° C a series of runs were made at random at different P_s, permitting some observations to be made on the effects of P_s and temperature on the constants a and α. If the scheme of Fig. 2 is adopted then a consistent correlation between values of the parameter a or α for any one stage and P_s and temperature is possible. In this fashion values of α for stage II lines (α_2), for example, are compared with other α_2 values, and the temporal order of appearance of the lines on q – log t plots is disregarded.

The effects found are less clearcut than those of previous studies because (a) different kinetic stages appeared under different conditions of temperature and P_s, in a manner discussed above, so that over some P_s regions not enough data are available for correlation, and (b) scatter of parameter values with changing P_s was encountered, this being particularly noticeable in the highly sensitive a values. The correlations between parameters and P_s and temperature were similar to those obtained previously (2–6), roughly linear changes being obtained, so that the following statements, illustrated by the plots of Figs. 9 and 10, suffice to describe the data. (a) Multiple kinetic stages exist, as described above. (b) For both adsorption systems, an increase in temperature decreases the amounts of gas adsorbed over the range 56°–400° C. This is shown by the plots of Fig. 9, which are
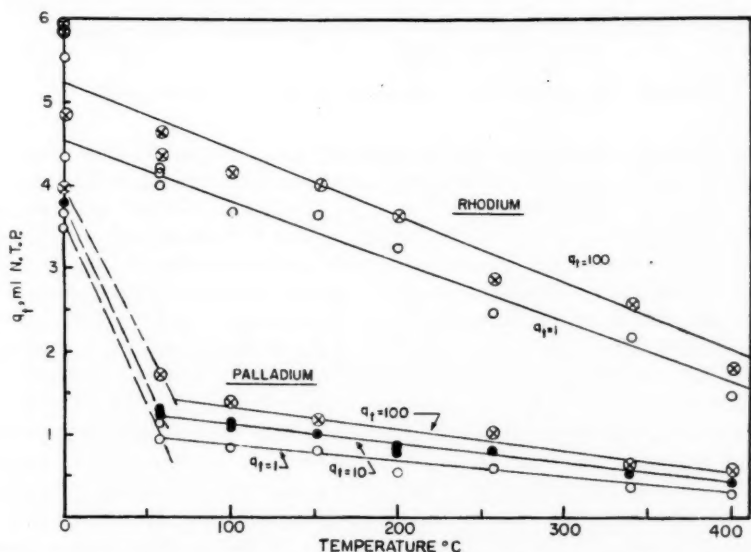

FIG. 9. The effect of temperature on adsorption. q_t is the amount adsorbed after t minutes.

essentially isobars at $P_s = 51$ cm DBP. (c) For the H_2–Rh system, momentary rates of adsorption ($\propto 1/\alpha$) are increased, but values of a are decreased with increasing temperature. (d) For the H_2–Pd system, momentary rates of adsorption are decreased with increasing temperatures, and initial rates similarly decrease slightly or remain constant.

(e) For both adsorption systems the general effect of increasing initial gas pressure is to increase adsorption rates, but in discontinuous fashion. At pressures below about 30 cm DBP the effects of increasing P_s on parameter values are larger than those above that pressure. Such discontinuity is illustrated by the α–P_s plots of Fig. 10.
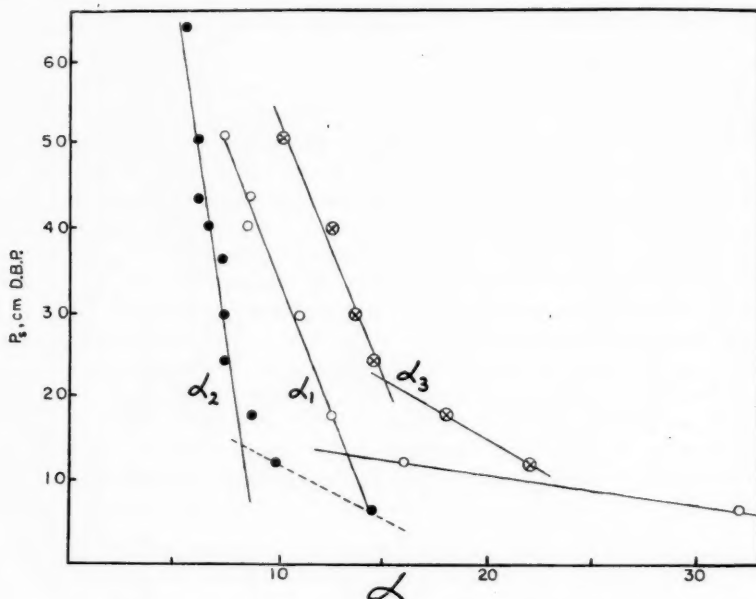

FIG. 10. The effect of P_s on α values. H_2 adsorption on Pd at 100° C.

A complete, physical explanation for the observed multiple stages has not been devised. It is possible that they may result from surface contamination, a suggestion supported by such observations as: originally (3) linear q – log t plots were found with the system H_2–Ru, while in a later study (5) breaks occurred; with CO adsorption on clean Ru (5) the rate declined monotonically whereas it was discontinuous when H_2 was preadsorbed on the solid; for the H_2–Ni–SiO_2 system (9) on rigorous reduction a fast adsorption was increased in magnitude at the expense of a slow adsorption; under conditions of pre-adsorption of CO on Ru, two kinetic processes of H_2 adsorption exist (5), the region of discontinuity of rates being approximately linearly dependent on the amount of pre-adsorbed CO. However, the rigorous reduction conditions, the apparent stability of the adsorbent surfaces, and the dependence of kinetic stages on temperature and pressure suggest that a simple poisoning phenomenon is unlikely to account for the present observations. Rather, some model of a surface is required which changes its character drastically by the very act of adsorption. The present results are reminiscent of the observations of Becker (10) on the change of sticking coefficient with coverage of several molecules on W ribbons, which led to the suggestion that the adsorption properties of a metal surface change rather abruptly when adsorbed species make the first set of valence bonds with every surface metal atom and again when they make second valence bonds. The observed temperature and pressure dependencies of the kinetic stages, however,

require a different model, such as that suggested by Taylor and Thon (1), according to which the discontinuities would represent change-over of the adsorption process from one kind of site to another before coverage is complete. With homotatic surfaces such as those presented by the probably polycrystalline Ru and Pd adsorbents, such a mechanism is not implausible.

REFERENCES

1. H. A. TAYLOR and N. THON.   J. Am. Chem. Soc. **74**, 4169 (1952).
2. M. J. D. LOW and H. A. TAYLOR.   J. Electrochem. Soc. **106**, 524 (1959).
3. M. J. D. LOW and H. A. TAYLOR.   Can. J. Chem. **37**, 544 (1959).
4. M. J. D. LOW and H. A. TAYLOR.   Can. J. Chem. **37**, 915 (1959).
5. M. J. D. LOW and H. A. TAYLOR.   J. Electrochem. Soc. **106**, 138 (1959).
6. L. LEIBOWITZ, M. J. D. LOW, and H. A. TAYLOR.   J. Phys. Chem. **62**, 471 (1958).
7. J. DECRUE.   Ph.D. Thesis, Princeton University, Princeton, New Jersey. 1951.
8. M. J. D. LOW.   Can. J. Chem. **37**, 1916 (1959).
9. G. C. A. SCHUIT and N. H. DE BOER.   Rec. trav. chim. **70**, 1067 (1957).
10. J. A. BECKER.   Solid state physics. Vol. VII. *Edited by* F. Seitz and D. Turnbull. Academic Press Inc., New York. 1958. p. 379.

DECOMPOSITION OF ZINC OXIDE[1]

E. A. SECCO

ABSTRACT

Experimental results on the loss in weight of zinc oxide in a closed vessel under varying conditions of temperature, initial zinc pressure, oxygen pressure, and vacuum are reported. The data show more consistency interpreted in terms of dissociation rather than sublimation of the oxide. Plots of $\log_{10} K_p$ versus $1/T$ and $\log_{10} P_{ZnO}$ versus $1/T$ yield slopes corresponding to 24.0 ± 2.0 kcal and 43.0 ± 5.0 kcal, respectively. These results cannot be explained on the basis of available thermodynamic data. Interpretations of these results in terms of an unstable suboxide and non-equilibrium are discussed.

INTRODUCTION

It was observed in 1954 during a study (1) on the exchange between zinc vapor and single crystals of zinc oxide that there occurred appreciable losses from a bucket carrying the oxide in a closed quartz vessel at 1025° C. The oxide losses from the bucket were much greater at low zinc pressures. It was further confirmed that considerable oxide was lost from the bucket in a vacuum, i.e., 5×10^{-4} mm Hg. These observations could not be explained by a decomposition reaction on the basis of the standard free energy for the reaction

$$\text{ZnO}_{(e)} = \text{Zn}_{(g)} + \tfrac{1}{2}\text{O}_{2(g)}$$
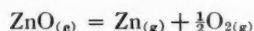
that is, $\Delta G° = -114{,}640 + 51.65\ T$ cal/mole (2). The equilibrium pressures of zinc and oxygen from the above reaction as estimated from the equilibrium constant $K_p = P_{Zn}P_{O_2}^{\frac{1}{2}}$ are many orders of magnitude below the experimental pressures.

A recent study (3) involving zinc oxide at low pressures and lower temperatures has shown a recurrence of appreciable losses of the oxide. This report contains experimental data pertaining to loss in weight of zinc oxide under varying conditions of temperature, initial zinc pressure, oxygen pressure, and vacuum.

EXPERIMENTAL

The polycrystalline ZnO used in this work was the Fisher Certified Reagent Grade with a certified purity of 99.98%. The zinc oxide was stated to be a product of the Dry Process. The oxide powder was dried in an oven at 150° C for at least 10 hours before using. The surface area of the oxide powder was found to be 3.39 m²/g as determined by krypton adsorption measurements. The particle size is calculated to be ca. 3×10^{-5} cm.

These experiments were carried out in a static system with the use of quartz vessels which has already been described (1). All weighings were done on a single pan, constant load, Gram-atic Balance (E. Mettler, Zürich, Switzerland) and the weights were obtained to 0.05 mg. The weighed bucket bearing the zinc oxide was suspended at the center in the quartz vessel. The vessel was connected to a vacuum system, evacuated for 1 hour at 200° C, sealed, and placed in the furnace. The furnace with its temperature regulation and the timing of the anneal was already described (3). After the anneal the vessel was withdrawn, allowed to cool to room temperature, and opened. The bucket was withdrawn and reweighed. The difference in weighings represented the loss in weight of the oxide.

RESULTS

In Table I are given the losses in weight of zinc oxide at different temperatures while maintaining a constant initial zinc pressure, calculated from the ideal gas equation, i.e.,

TABLE I

Constant initial $P_{Zn} = 0.25$ atm and $s = 0.45$

Run	T °K	Observed loss in weight (mg)	Time (min)	P_{ZnO} (atm)	P_{O_2} (atm)	K_p $(P_{Zn}P_{O_2}^{\frac{1}{2}})$
1	1073	0.7	70.0	3.2×10^{-3}	1.6×10^{-3}	1.0×10^{-2}
2	1093	1.1	70.1	5.1×10^{-3}	2.5×10^{-3}	1.3×10^{-2}
3	1113	1.3	71.4	6.1×10^{-3}	3.1×10^{-3}	1.4×10^{-2}
4	1133	2.3	70.2	1.1×10^{-2}	5.5×10^{-3}	1.9×10^{-2}
5	1153	3.0	70.2	1.5×10^{-2}	7.5×10^{-3}	2.3×10^{-2}
6	1173	4.5	70.1	2.2×10^{-2}	1.1×10^{-2}	2.8×10^{-2}
7	1193	4.6	75.1	2.3×10^{-2}	1.2×10^{-2}	2.9×10^{-2}
8	1193	2.3	77.2	1.2×10^{-2}	6.0×10^{-3}	2.0×10^{-2}
9	1213	9.0	77.3	4.6×10^{-2}	2.3×10^{-2}	4.5×10^{-2}
10	1233	4.7	76.3	2.4×10^{-2}	1.2×10^{-2}	3.0×10^{-2}
11	1233	4.5	79.1	2.4×10^{-2}	1.2×10^{-2}	3.0×10^{-2}
12	1253	5.7	75.4	3.0×10^{-2}	1.5×10^{-2}	3.4×10^{-2}
13	1253	6.0	77.7	3.2×10^{-2}	1.6×10^{-2}	3.6×10^{-2}
14	1273	13.0	85.0	7.0×10^{-2}	3.5×10^{-2}	6.0×10^{-2}

$PV = nRT$, and constant mole fraction of zinc in the solid oxide, s. The volume of the vessel, V, was 0.24 liter. Included in this table are the observed losses in terms of the pressure of zinc oxide vapor, P_{ZnO}, if the loss was due to evaporation of the oxide and the oxygen pressure, P_{O_2}, if dissociation occurred. The terminal column contains the values of the equilibrium constant, $K_p = P_{Zn}P_{O_2}^{\frac{1}{2}}$, for the dissociation reaction.

Table II contains the loss in weight as a function of initial zinc pressure at constant temperature and constant s. The weight losses are given in terms of P_{ZnO}, P_{O_2}, and K_p as in Table I. The average values of P_{ZnO} and K_p are shown on the bottom of their respective columns. On withdrawal of the vessel from the furnace after the anneal it was invariably observed for experiments involving an initial zinc pressure that the zinc oxide was dark gray or black. The color of the oxide transformed to pale cream within 1 minute after withdrawal, indicating that the adsorbed zinc on the oxide condensed on the cooler walls of the vessel. In experiments 27 and 29 of Table II metallic zinc deposits were observed

TABLE II

Constant $T = 1193°$ K and $s = 0.45$

Run	Observed loss in weight (mg)	Initial P_{Zn} (atm)	Time (min)	P_{ZnO} (atm)	P_{O_2} (atm)	K_p $(P_{Zn}P_{O_2}^{\frac{1}{2}})$
15	4.0	0.11	81.0	2.0×10^{-2}	1.0×10^{-2}	1.3×10^{-2}
16	3.4	0.16	80.3	1.7×10^{-2}	8.5×10^{-3}	1.6×10^{-2}
17	2.2	0.21	80.5	1.1×10^{-2}	5.5×10^{-3}	1.6×10^{-2}
18	2.9	0.30	80.3	1.5×10^{-2}	7.5×10^{-3}	2.7×10^{-2}
19	2.2	0.41	81.6	1.1×10^{-2}	5.5×10^{-3}	3.1×10^{-2}
20	2.0	0.45	80.5	1.0×10^{-2}	5.0×10^{-3}	3.3×10^{-2}
21	1.6	0.50	80.3	8.1×10^{-3}	4.0×10^{-3}	3.1×10^{-2}
22	2.0	0.57	80.4	1.0×10^{-2}	5.0×10^{-3}	4.1×10^{-2}
23	2.3	0.68	84.1	1.2×10^{-2}	6.0×10^{-3}	5.4×10^{-2}
24	0.9	0.79	80.3	4.5×10^{-3}	2.3×10^{-3}	3.8×10^{-2}
25	1.5	0.82	80.3	7.5×10^{-3}	3.8×10^{-3}	5.1×10^{-2}
26	1.5	0.96	85.5	7.5×10^{-3}	3.8×10^{-3}	5.9×10^{-2}
27	18.6	0	80.2	9.3×10^{-2}	4.7×10^{-2}	2.0×10^{-2}*
28	8.6	0	123.5	4.3×10^{-2}	2.2×10^{-2}	6.4×10^{-3}*
29	53.3	0	82.4	0.27	0.14	1.0×10^{-1}*
Mean values				3.6×10^{-2}		3.6×10^{-2}

*Exchanged radioactive ZnO was used in these experiments.

on the vessel walls along with a slight yellow zinc oxide deposit which became white on cooling. The zinc deposit in experiment 29 was especially noticeable and was estimated to be ca. 30 mg.
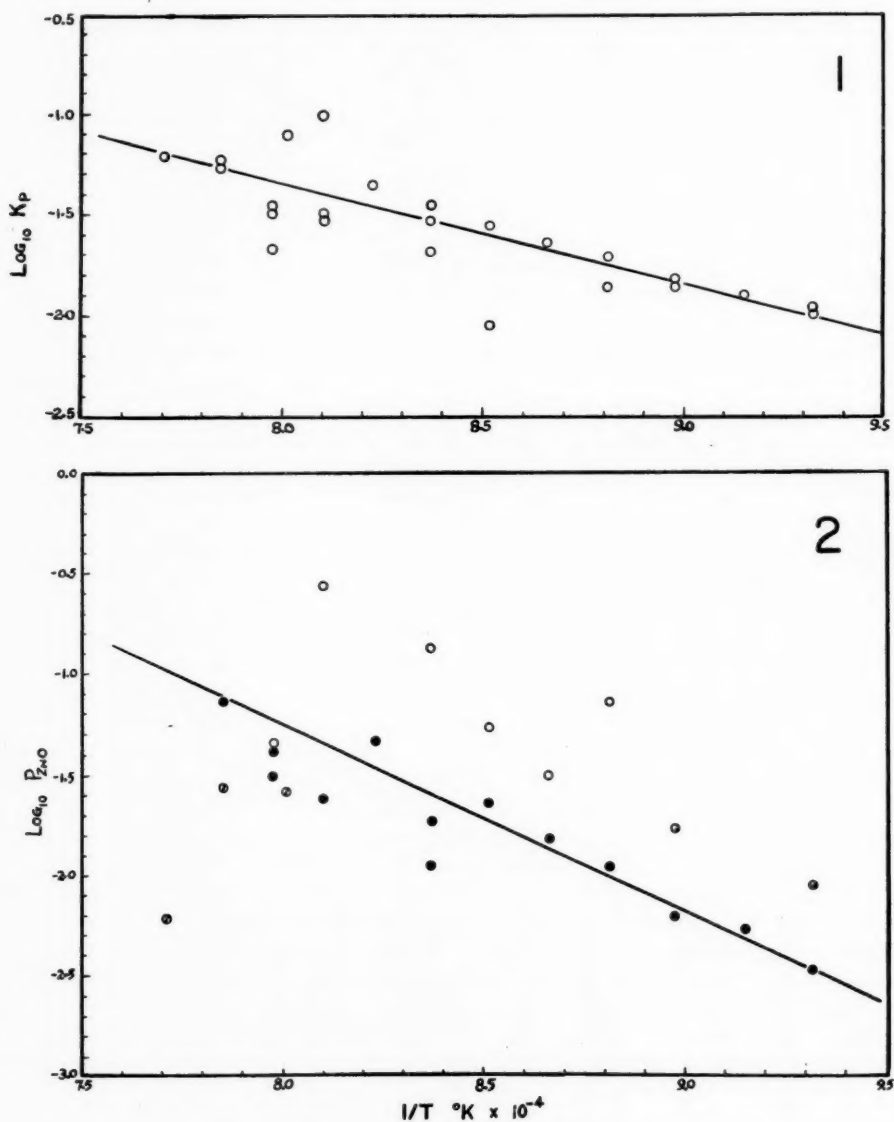

FIG. 1.   Plot of $\log_{10} K_p$ against the reciprocal of absolute temperature.
FIG. 2.   Plot of $\log_{10} P_{ZnO}$ against the reciprocal of absolute temperature.

● Initial $P_{Zn} = 0.25$ atm.   ⊘ Single crystals ZnO.
◑ Initial $P_{Zn} = 0.14$ atm.   ○ Vacuum, i.e., 5×10^{-4} mm Hg.

Figure 1 shows a plot of the logarithm of the dissociation constant K_p against the reciprocal of the absolute temperature with the slope of the best straight line yielding an energy term of 24.0 ± 2.0 kcal/mole. In Fig. 2 is given a plot of the logarithm of zinc

TABLE III

Constant $T = 1153°$ K and in vacuum, i.e., 5×10^{-4} mm Hg

Run	Observed loss in weight (mg)	Time (min)	P_{ZnO} (atm)	P_{O_2} (atm)	K_p $(P_{Zn}P_{O_2}^{\frac{1}{2}})$
30	4.3	30.3	2.1×10^{-2}	1.0×10^{-2}	$2.1 \times 10^{-3*}$
31	10.1	100.3	4.9×10^{-2}	2.5×10^{-2}	$7.7 \times 10^{-3*}$
32	2.8	55.3	1.4×10^{-2}	7.0×10^{-3}	$1.1 \times 10^{-3*}$
33	9.3	76.0	4.5×10^{-2}	2.3×10^{-2}	$7.5 \times 10^{-3*}$
34	6.2	135.8	3.0×10^{-2}	1.5×10^{-2}	$3.7 \times 10^{-3*}$
35	4.8	90.3	2.4×10^{-2}	1.2×10^{-2}	$2.6 \times 10^{-3*}$
Mean values			3.1×10^{-2}		4.5×10^{-3}

*Exchanged radioactive ZnO was used in these experiments.

TABLE IV

Constant $T = 1253°$ K

Run	Observed loss in weight (mg)	Initial P_{Zn} (atm)	Time (min)	P_{ZnO} (atm)	P_{O_2} (atm)	K_p $(P_{Zn}P_{O_2}^{\frac{1}{2}})$
36	8.1	0	45.1	4.6×10^{-2}	2.3×10^{-2}	7.0×10^{-3}
37	7.9	0	77.3	4.2×10^{-2}	2.1×10^{-2}	6.1×10^{-3}
38	11.8	0.075	62.1	6.3×10^{-2}	3.2×10^{-2}	2.5×10^{-2}
39	7.5	0.075	32.1	4.0×10^{-2}	2.0×10^{-2}	1.6×10^{-2}
40	9.2	0.075	116.2	4.9×10^{-2}	2.5×10^{-2}	2.0×10^{-2}
41	7.6	0.075	73.3	4.0×10^{-2}	2.0×10^{-2}	1.6×10^{-2}
42	12.9	0.075	135.5	6.9×10^{-2}	3.5×10^{-2}	2.7×10^{-2}
43	3.6	0.075	69.4	1.9×10^{-2}	1.0×10^{-2}	9.4×10^{-3}
44	17.2	0.075	327.4	9.1×10^{-2}	4.6×10^{-2}	3.6×10^{-2}
Mean values				5.3×10^{-2}		2.1×10^{-2}

TABLE V

Run	T °K	Observed loss in weight (mg)	Initial P_{Zn} (atm)	Time (min)	P_{ZnO} (atm)	P_{O_2} (atm)	K_p $P_{Zn}P_{O_2}^{\frac{1}{2}})$
45	1133	14.9	0	70.2	7.1×10^{-2}	3.6×10^{-2}	1.4×10^{-2}
46	1173	10.7	0	70.2	5.3×10^{-2}	2.7×10^{-2}	8.7×10^{-3}
47	1233	52.2	0	61.0	0.27	0.14	1.0×10^{-1}
48	1193	0.0	air (1 atm)	600.0	—	—	—*
49	1073	1.9	0.14	60.0	8.6×10^{-3}	4.3×10^{-3}	1.0×10^{-2}
50	1113	3.5	0.14	60.0	1.7×10^{-2}	8.5×10^{-3}	1.5×10^{-2}
51	1248	0.5	1.12	60.0	2.6×10^{-3}	1.3×10^{-3}	1.3×10^{-2}
52	1298	1.1	1.12	45.0	6.0×10^{-3}	3.0×10^{-3}	6.1×10^{-2}
53	1273	0.0	1.96	60.0	—	—	—
54	1273	2.0	0.20	60.0	—	—	—†
55	1273	10.8	0	150.0	5.8×10^{-2}	2.9×10^{-2}	$1.0 \times 10^{-2*}$
56	1273	1.2	1.12	60.0	6.4×10^{-3}	3.2×10^{-3}	6.4×10^{-2}
57	1273	27.8	0.22	120.0	1.5×10^{-1}	7.5×10^{-2}	1.0×10^{-1}
Mean values					7.2×10^{-2}		5.8×10^{-2}

*Exchanged radioactive ZnO was used in these experiments.
†Pressure of argon in reaction vessel ca. 1 atm.

oxide pressure, P_{ZnO}, against the reciprocal of the absolute temperature with the slope of
the best straight line corresponding to an energy of 43.0 ± 5 kcal/mole. The values of
P_{ZnO} and K_p plotted in Figs. 1 and 2 include all values from all tables; where two or more
experiments were carried out at constant temperature, the average values of P_{ZnO} and K_p
were plotted. The average values plotted are given on the bottom of their respective
columns in each table. It is noteworthy that the K_p values corresponding to the weight
losses observed for single crystals, experiments 51, 52, 55–57, are in agreement with the
values obtained in this work.

DISCUSSION

The results reported herein defy explanation by simple conventional equilibria, i.e.,

[1] $$ZnO_{(s)} = Zn_{(g)} + \tfrac{1}{2}O_{2(g)}$$

and

[2] $$ZnO_{(s)} = ZnO_{(g)}$$

where the heat of sublimation of [2] is 10.1 kcal/mole (4). Since it has been established (5)
that ZnO sublimes only by dissociation into $Zn_{(g)}$ and $O_{2(g)}$, reaction [2] is disregarded in
favor of reaction [1] in this discussion. There has been passing reference (6, 7) to the fact
that there is an apparent oxygen dissociation pressure of zinc oxide, which is many orders
of magnitude greater than that deduced theoretically from the thermodynamic data.
More recently Moore and Williams (8) reported some data on dissociation of zinc oxide
by zinc vapor. According to their data the rate of evaporation of ZnO in zinc vapor is
ca. 10^9 times the equilibrium value as calculated from the standard free energy data.
Moore and Williams' data are concordant with our results which indicate that our
equilibrium dissociation constant is greater than that calculated from the standard free
energy data by a factor of ca. 10^8.

How can ZnO decompose under conditions deemed thermodynamically unfeasible?
One *ad hoc* possibility is the existence of an unstable superficial suboxide such as Zn_2O or
Zn_4O_3. If the surface of the ZnO becomes covered with an impervious layer of the sub-
oxide so as to isolate the oxide, the dissociation reaction is essentially that of the solid
suboxide. This possibility is supported by the observation that the oxide is completely
covered with zinc during the anneal. Further evidence for a zinc-rich film on the oxide
surface was obtained during sintering studies at 500° C and at oxygen pressure at 10 mm
when the oxide became gray and exhibited a positive temperature coefficient of resistance
and very high conductivity (7). The formation of the zinc-rich surface on zinc oxide in the
latter case has been explained in terms of Schottky disorder where zinc leaves its normal
lattice site and takes up normal positions on the surface of the oxide.

Appreciable dissociation of ZnO may be the result of a highly defective surface zone (9)
which is without the limits of thermodynamics. Although it is not certain what is defined
by this defective surface zone it must be recognized that some surface variable exists
which could play an important role in the dissociation reaction. It is of significance that
heat treatment and adsorbed gases can affect the activity and hence the defect constitu-
tion of the surface. In this regard, experiment 54 shows negligible loss with ca. 1-atm
argon as contrasted to experiment 57 without argon. Furthermore, widely divergent weight
losses were observed in experiments 27–29 following an identical procedure. In experiment
48, when zinc oxide was exposed to the atmosphere in an open vessel no loss was observed.
It is quite reasonable therefore to believe that a non-equilibrium condition exists where

the decomposition is determined by rate processes, such as diffusion of defects to surfaces and interface reactions. This problem of oxide decomposition at temperatures much lower than those predicted from thermodynamic data is not restricted to ZnO. The decomposition of NiO and alumina have already been reported (10, 11). Very little is known about the detailed mechanisms of such a reaction as decomposition of an oxide at the crystal–gas interface, but the present observations, if extended, may show that such reactions proceed through more complex mechanisms than have been hitherto suspected.

ACKNOWLEDGMENTS

REFERENCES

1. E. A. SECCO and W. J. MOORE. J. Chem. Phys. **26**, 942 (1957). W. J. MOORE and E. A. SECCO. Diffusion and exchange of zinc in crystalline zinc oxide. U.S. Atomic Energy Comm. Rept., Bloomington, Indiana. August, 1955.
2. J. A. KITCHENER and S. IGNATOWICZ. Trans. Faraday Soc. **47**, 1278 (1951).
3. E. A. SECCO. Discussions Faraday Soc. In press. 1959.
4. G. HÜTTIG. Z. anorg. Chem. **207**, 273 (1932).
5. M. POURBAIX. Bull. soc. chim. Belges, **53**, 159 (1944).
6. T. J. GRAY. Discussion during Symposium on Sintering, University of Bristol, England. 1952.
7. T. J. GRAY. J. Am. Ceram. Soc. **37**, 534 (1954).
8. W. J. MOORE and E. L. WILLIAMS. J. Phys. Chem. **63**, 1516 (1959).
9. T. J. GRAY. The defect solid state. Interscience Publishers, Inc., New York. 1957. p. 114.
10. S. J. TEICHNER and J. A. MORRISON. Trans. Faraday Soc. **51**, 961 (1955).
11. S. J. TEICHNER. Discussions Faraday Soc. In press. 1959.

THE ACIDITY FUNCTIONS H_0 AND $J_0(H_R)$ FOR THE SYSTEM FORMIC ACID – WATER[1]

Ross Stewart and Trevor Mathews

ABSTRACT

The acidity functions H_0 and $J_0(H_R)$ have been measured for the whole range of the formic acid – water system. The large negative J_0 values for the more concentrated solutions fail to correlate with the functions derived by Gold on the basis of certain assumptions regarding the activity coefficients of the species involved. The cause of this deviation is discussed. The term $\log [R^+]/[ROH]$ for the ionization of triphenylcarbinols in formic acid has been found to vary linearly with $1/T$.

The Hammett acidity function, H_0, which measures the tendency of a solvent to transfer a proton to a neutral base has found wide application in two important fields, viz. the determination of the strengths of very weak bases and the study of acid-catalyzed reaction mechanisms in strongly acid media. It describes the simple ionization

$$B + H^+ \rightleftharpoons BH^+ \tag{1}$$

and H_0 values, defined by the equation

$$[2] \qquad H_0 \equiv pK_{BH^+} - \log [BH^+]/[B],$$

have been determined for solutions of several strong acids in water and other solvents (1, 2). The values of pK_{BH^+} for the various indicators used to establish the H_0 scale must be obtained by a stepwise operation starting from a dilute aqueous solution of the acid where the activities of the various species involved in the equilibrium are assumed to be the same as in pure water.

A different acidity function governs the ionization of secondary bases, i.e. those compounds which ionize as follows:

$$ROH + H^+ \rightleftharpoons R^+ + H_2O. \tag{3}$$

Lowen, Murray, and Williams examined such a system and used the term H_R to describe the acidity function governing the ionization (3). Gold and Hawes (4) soon after used the symbol J_0 for this function which is defined as follows:

$$[4] \qquad J_0 \equiv pK_{R^+} - \log [R^+]/[ROH].$$

K_{R^+} is the ionization constant which governs reaction 3 and is defined as

$$[5] \qquad K_{R^+} = \frac{a_{ROH} \cdot a_{H^+}}{a_{R^+} \cdot a_{H_2O}}.$$

(Throughout this paper "a" stands for activity, "f" for activity coefficient, [ ] for molar concentration, and [ ]$_N$ for concentration in units of mole fraction). Here again a stepwise operation is required to find the values of pK_{R^+} for the indicators used to establish the J_0 scale for concentrated acid solutions.

It can be shown that

$$[6] \qquad H_0 = -\log (a_{H^+} \cdot f_B/f_{BH^+})$$

$$[7] \qquad J_0 = -\log \left(a_{H^+} \cdot f_{ROH}/f_{R^+} \cdot \frac{1}{a_{H_2O}} \right)$$

and Gold and Hawes (4) suggested that $J_0 = H_0 + \log a_{H_2O}$ (equation 7) which is based

on the assumption—a reasonable one in view of earlier work—that $f_B/f_{ROH} = f_{BH^+}/f_{R^+}$ (equation 8) where ROH is a secondary base, such as triphenylcarbinol, and where B is a base of the ammonia type used to establish the H_0 scale. Cryoscopic measurements show clearly that triphenylcarbinol is ionized by sulphuric acid as follows (5, 6):

$$(C_6H_5)_3COH + 2H_2SO_4 \rightleftharpoons (C_6H_5)_3C^+ + H_3O^+ + 2HSO_4^-. \qquad [8]$$
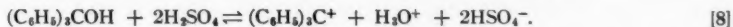
Gold and Hawes used vapor pressure data to obtain the acitivity of water in sulphuric acid solutions and thus calculated J_0 values for sulphuric acid solutions of from 5% to 95% composition by means of equation 7. Since at that time values of pK_{R^+} had not been established for any secondary bases, the only test of equation 7 and the principles used in its derivation was to plot values of log [R+]/[ROH] for a secondary base dissolved in sulphuric acid against values of J_0 calculated using equation 7. Equation 4 shows that a straight line of unit slope should result. When data for 4,4',4''-trinitrotriphenylcarbinol was plotted in this way, a straight line of slope 1.16 was obtained in fairly close agreement with theory.

In 1955 Deno, Jaruzelski, and Schriesheim (7), starting with dilute aqueous solution, used the stepwise technique to determine values of pK_{R^+} for a series of substituted triphenylcarbinols and also values of the acidity function for secondary bases in sulphuric acid from 0–98% concentration. They observed that the acidity function departed very seriously from the values of J_0 obtained from equation 7 and suggested the symbol C_0 for the function defined by equation 4. They showed that this function correlated the change in rate with change in sulphuric acid concentration of several chemical reactions which were believed to proceed via the ionization reactions shown in equation 3.

At about the same time, Gold (8) derived two additional equations similar in form to equation 7 based on certain assumptions regarding the behavior of the various activity coefficients. These functions were designated J_0'' and J_0''' and the function defined by equation 7 as J_0'. Thus the true acidity function for secondary bases defined by equation 4 is referred to by Gold as J_0, and by Deno et al. first as C_0 (7) and subsequently as H_R (9). The function defined by equation 7 is now referred to by Gold as J_0' and by Deno et al. as J_0. Paul and Long in their review article (1) use J_0 as the symbol for the experimentally determined acidity function for secondary bases. However, since then Deno et al. (9) have abandoned C_0 in favor of Williams original symbol, H_R, and it would seem that both J_0 and H_R will continue to appear in the literature for some time. We have accordingly used both symbols throughout this paper to refer to the experimental acidity function and primed J_0 symbols for the derived functions.

Previous work by Stewart (10) and by Evans et al. (11) has shown that formic acid reduces the triphenylcarbinol to triphenylmethane probably via hydride transfer from formate ion to the carbonium ion. Formic acid is a medium which facilitates reduction of tertiary carbinols by this mechanism. It is sufficiently acidic to ionize triphenylcarbinols and some olefins to carbonium ions; it has a high dielectric constant (58.5 at 16°) and a high degree of autoprotolysis producing a reasonable concentration of formate ion, the reductant; and its oxidation product, carbon dioxide, is of low energy.

The purpose of this work, then, was to determine the values of the acidity functions, H_0 and $J_0(H_R)$, for formic acid solutions primarily for future use in kinetic studies, but in addition as a test of the validity of Gold's derived functions, J_0', J_0'', and J_0''', as approximations to the experimentally determined function J_0 in a solvent other than sulphuric acid. Bascombe and Bell have recently reported a careful investigation of acidity functions of some aqueous acids but did not list H_0 values for formic acid because of apparent discrepancies between values obtained with different indicators (12).

EXPERIMENTAL

Indicators

Triphenylcarbinol and *o*- and *p*-nitroaniline were reagent grade chemicals which were crystallized repeatedly to constant melting point. *p*-Nitrodiphenylamine was prepared from *p*-nitroaniline and bromobenzene by the method of Goldberg and Sissoeff (13). 4-Methoxytriphenylcarbinol was prepared by the Grignard synthesis using phenyl-magnesium bromide and ethyl anisate after the method of Brand (14). 4,4′,4″-Trim-ethoxytriphenylcarbinol was also prepared by this method using 4,4′-dimethoxybenzo-phenone and *p*-bromoanisole.

Formic Acid

Reagent grade 88–90% formic acid, Baker and Adamson (4 l.), was distilled at reduced pressure and middle cuts of 1600 and 1200 ml were used as stock solutions. Titrations with standard base showed the formic acid content to be 94.5% and 87.4% respectively.

Anhydrous formic acid was prepared by zone freezing, as previously described (10), one liter of formic acid taken from the middle cut of two liters of Baker and Adamson 98–100% formic acid which had been distilled *in vacuo*. After three zone freezings the melting point of the residue (about 400 ml) was found to be 8.4° (15). Titration with standard base gave the formic acid content as 99.9%.

Measurement of H_0

H_0 values were calculated using equation 4 and the revised pK_{BH^+} values of Paul and Long (1). Measurements of the $[BH^+]/[B]$ ratio were made by adding 0.1 ml of a solution of the particular indicator dissolved in acetone to a 1-cm absorption cell fitted with a ground-glass neck and stopper. The acetone was evaporated, 3 ml of formic acid of known composition was added, and the optical density of the resulting solution which was generally of the order of 10^{-4} M in indicator was determined at λ_{max} using a Beckman DU spectrophotometer. Then 0.1 ml of the same indicator solution was dissolved in a known volume of water and the light absorption measured as before. The temperature was controlled to 25°±0.5° by means of thermospacers. Each of the indicators was colorless in the ionized form but absorbed strongly in the visible or near ultraviolet in the unionized form. It was observed that a slow reaction occurred between the nitroanilines and the formic acid since the spectrum of the solution changed on long standing to resemble that of the corresponding formanilide (16). Extrapolations to zero time were made wherever the reaction was appreciable. Beer's law was checked for each indicator under conditions where $[BH^+]$ is negligible and each indicator was checked to ensure that no shift in λ_{max} occurred in going from water to formic acid solutions. It was observed, however, that values of $[BH^+]/[B]$ were not independent of the concentration of the base. Plots of the ratio against concentration of the base produced approximately straight lines which were extrapolated to zero concentration to determine the ratio used in the calculation.

Measurement of $J_0(H_R)$

$J_0(H_R)$ values were calculated using equation 4 and the pK_{R^+} values of Deno, Jaruzelski, and Schriesheim (7). The method of determining $[R^+]/[ROH]$ was similar to that used in determining $[BH^+]/[B]$ except that ROH was determined by addition of 0.1 ml of the carbinol solution to a known volume of formic acid of such concentration as to completely ionize the carbinol. For these compounds, of course, the colored species is the ion. The solutions were of the order of 10^{-4} to 10^{-5} M. The assumption that no change in extinction coefficient occurs with changing formic acid concentration was tested by measuring the optical density of the methoxy-substituted carbinols at λ_{max} for a range of 25% formic

acid above that at which the alcohol was effectively completely ionized to the carbonium ion. In these cases no change in extinction coefficient was observed.

As in the H_0 measurements the values of [R+]/[ROH] were found to be not independent of the concentration of the carbinol. Deno et al. (7) observed this phenomenon in sulphuric acid but found that at extremely low concentrations of carbinol using long path cells the ratio did become independent of concentration. In this work a linear extrapolation was used to find the limiting value of the ratio. This value may be very slightly in error in the light of the work of Deno et al., but, if so, the error is small.

Since reduction of the carbinol can occur (10) in formic acid a plot of optical density against time was made for each carbinol solution in which appreciable fading of the carbonium ion occurred. This plot was extrapolated back to zero time in order to obtain [R+].

RESULTS AND DISCUSSION

Table I and Fig. 1 show the values of H_0 as a function of formic acid concentration.

TABLE I

H_0 values

o-Nitroaniline

pK = −0.29; λ_{max} = 412 mμ

% formic acid	[BH+]/[B]	H_0
100	79.5	−2.19
99.6	60.0	−2.07
98.8	22.4	−1.65
97.8	13.2	−1.41
96.0	8.90	−1.24
94.4	6.3	−1.08
92.6	4.1	−0.90
89.4	2.9	−0.75
86.5	1.70	−0.52
83.5	1.32	−0.41
80.7	1.08	−0.25
77.5	0.675	−0.12
71.4	.33	+0.19
67.5	.275	+0.27
62.7	.174	+0.47
57.7	.145	+0.55

p-Nitroaniline

pK = +0.99; λ_{max} = 380 mμ

% formic acid	[BH+]/[B]	H_0
86.5	31.0	−0.50
83.5	24.5	−0.40
77.5	13.1	−0.13
71.4	6.3	+0.19
66.5	5.4	+0.26
62.7	3.7	+0.44
57.7	2.7	+0.56
46.5	1.4	+0.85
41.5	1.2	+0.93
35.9	0.93	+1.03
29.5	.676	+1.16
23.9	.540	+1.26
19.2	.431	+1.35
14.7	.355	+1.44
11.2	.324	+1.48
6.1	.268	+1.58
4.4	.230	+1.63
2.0	.173	+1.75
.92	.098	+2.00

TABLE I *(Concluded)*

H_0 values

p-Nitrodiphenylamine

$pK = -2.48;$ $\lambda_{max} = 404\,m\mu$

% formic acid	[BH+]/[B]	H_0
100	0.55	−2.24
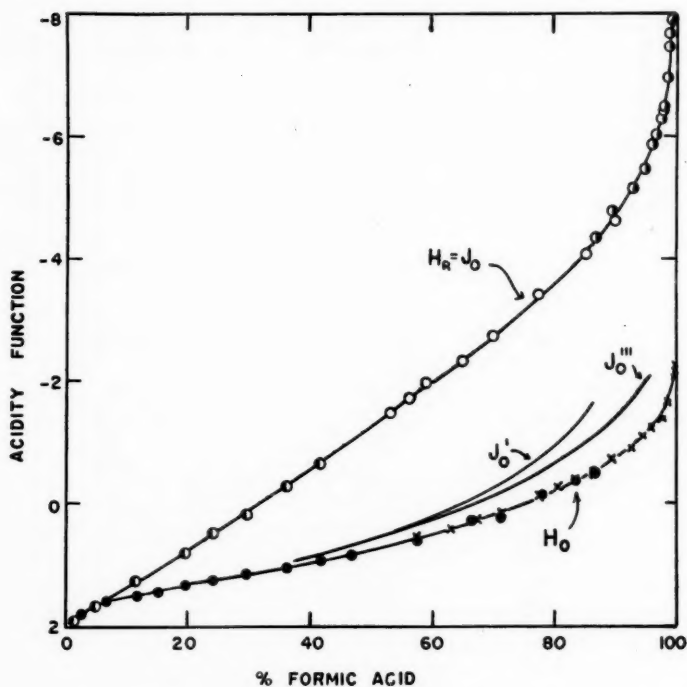
FIG. 1. Variation of acidity functions with formic acid concentration.
◑ Triphenylcarbinol. ○ 4-Methoxytriphenylcarbinol.
◐ 4,4′,4″-Trimethoxytriphenylcarbinol.
× *o*-Nitroaniline. ● *p*-Nitroaniline.

There appears to be satisfactory overlap in H_0 values for the indicators used, indicating that H_0 is independent of the base used for the determination. It should be pointed out, however, that less satisfactory agreement is obtained with our data using the indicator pK values of Bascombe and Bell (12) and that there is a variation in indicator ratio with indicator concentration, as described in the experimental section. This may account for our not observing the discrepancies noted by them. We can only report that for the indicators used in the present work a fair correlation was obtained indicating that H_0 is an approximately valid function in formic acid. In dilute solution the values of H_0 approach pH as required. The pH of 0.22 M formic acid in water should be 2.18; H_0 for this solution is 2.00.
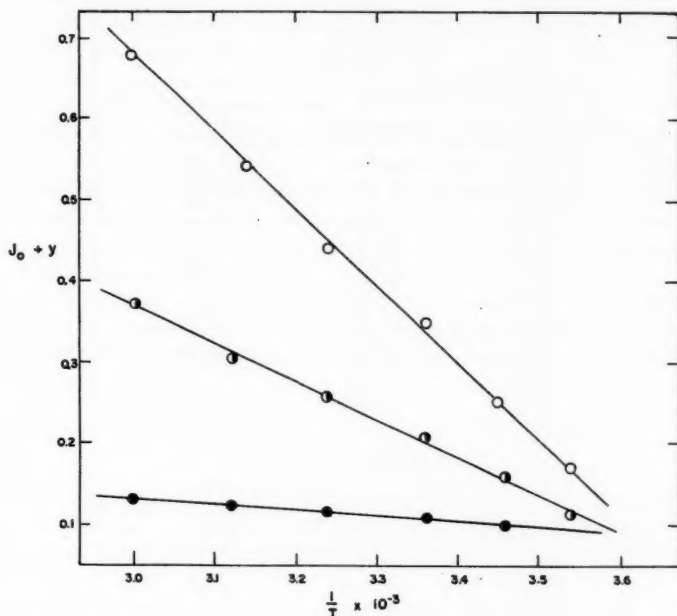
FIG. 2. Variation of apparent $J_0(H_R)$ with absolute temperature.
○ Triphenylcarbinol, $Y = 5.9$.   ◑ 4-Methoxytriphenylcarbinol, $Y = 3.8$.
● 4,4',4''-Trimethoxytriphenylcarbinol, $Y = 1.5$.

Table II and Fig. 1 show $J_0(H_R)$ as a function of formic acid concentration. There is reasonable overlap between triphenylcarbinol and 4-methoxytriphenylcarbinol. Although there is no overlap between 4-methoxytriphenylcarbinol and 4,4',4''-trimethoxytriphenyl-carbinol $dJ_0/d\%$ formic acid is the same for the lower region of the former curve and the upper region of the latter, a sufficient substitute for overlap. The $J_0(H_R)$ function therefore appears to be a valid acidity function in formic acid. As required, the values of $J_0(H_R)$ approach H_0 and pH in dilute formic acid.

Turning to Gold's derived quantities J_0', J_0'', and J_0''' we find them deviating rather widely from the experimental function $J_0(H_R)$. J_0' is defined by equation 9

[9] $$J_0' = H_0 + \log a_{H_2O}.$$

Values for the activity of water in formic acid solutions were calculated using the vapor pressure data of Takagi (17) and the equation $a_{H_2O} = p_{H_2O}/p_{H_2O}^0$ where $p_{H_2O}^0$ is the vapor pressure of pure water at the same temperature. A slight extrapolation was required to obtain the partial pressures of water at 25° in these solutions but any errors involved in the calculations are small compared with the difference between $J_0(H_R)$ and J_0' as shown in Fig. 1.

J_0'' is defined by equation 10,

[10] $$J_0'' = 2H_0 + \log [H_3O^+]_N + 1.74.$$

TABLE II

J_0 values

Triphenylcarbinol

$pK_{R^+} = -6.63;$ $\lambda_{max} = 431$ mμ (ion)

% formic acid	[R$^+$]/[ROH]	$J_0(H_R)$
99.5	19.0[a]	−7.91[a]
99.1	11.5[a]	−7.69[a]
98.7	6.7[a]	−7.46[a]
98.3	2.14	−6.96
98.0	0.73	−6.49
97.9	0.667	−6.45
97.5	0.47	−6.30
96.6	0.242	−6.01
96.0	0.184	−5.89
94.5	0.069	−5.47
94.3	0.064	−5.43
92.7	0.036	−5.19
89.4	0.020	−4.81
86.5	0.005	−4.33

4-Methoxytriphenyl carbinol

$pK_{R^+} = -3.40;$ $\lambda_{max} = 472$ mμ (ion)

% formic acid	[R$^+$]/[ROH]	$J_0(H_R)$
90.1	16.5	−4.62
85.0	4.5	−4.05
77.7	1.0	−3.40
70.1	0.23	−2.76
64.9	0.084	−2.32
58.8	0.037	−1.97
55.9	0.023	−1.76
53.0	0.0125	−1.50

4,4′,4″-Trimethoxytriphenyl carbinol

$pK_{R^+} = 0.82;$ $\lambda_{max} = 483$ mμ (ion)

% formic acid	[R$^+$]/[ROH]	$J_0(H_R)$
41.5	32.0	−0.69
35.9	12.9	−0.29
29.5	4.16	+0.20
23.9	2.08	+0.50
19.2	1.02	+0.81
11.2	0.36	+1.27
4.4	0.14	+1.67

[a] These values must be regarded as approximations only since [R$^+$] is calculated using the extinction coefficient of the carbonium ion in sulphuric acid.

Information does not appear to be available in the literature for the hydronium ion concentration but it can be shown that, at least for concentrated formic acid solution, rather unlikely values of the hydronium ion concentration would be required to make $J_0(H_R)$ and J_0'' coincide. Thus in 90% to 95% formic acid an hydronium ion concentration of the order of 10^{-4} molar must be assumed decreasing for 99% formic acid to a value closer to 10^{-5} molar. This compares with a known hydronium ion concentration of the order of 10^{-2} molar in 0.1 M formic acid and at the other end of the scale a known con-

centration of $HCO_2H_2^+$ of about 10^{-3} molar in 100% formic acid (6). The H_3O^+ concentration in the 90–99% range must therefore be considerably greater than this.

J_0''' is defined by the equation

[11] $$J_0''' = H_0 + \log [H_2O]_N.$$

Gold found that for sulphuric acid solutions this was the least satisfactory of the three functions as approximations to $J_0(H_R)$. In agreement with this we find that J_0''' lies between J_0' and H_0 for formic acid solutions. If the data of Gold (8) and Deno et al. (7) for sulphuric acid are combined it can be shown that the derived functions all fall between the experimental ones H_0 and $J_0(H_R)$ with J_0'' being the only one of the three which is closer to $J_0(H_R)$ than to H_0.

Thus both in sulphuric acid and in formic acid, secondary bases such as triphenylcarbinol ionize to a much greater extent than would be expected from a consideration of equations 9–11. Consider equation 12, which is obtained by the combination of equations 5 and 6; all activity coefficients refer to dilute aqueous solution as the standard state.

[12] $$J_0(H_R) = H_0 + \log a_{H_2O} + \log \frac{f_B \cdot f_{R^+}}{f_{BH^+} \cdot f_{ROH}}.$$

It can be seen from Fig. 1 that the final term in the above equation must make a considerable contribution to $-J_0(H_R)$ and it is worth while speculating on the reason for this since for two bases of the ammonia type, B_1 and B_2, the value of $\log f_{B_1} f_{B_2H^+} / f_{B_1H^+} f_{B_2}$ is effectively zero (1).

Since solvation effects are usually more important for ions than for neutral molecules, we might assume that the principal change in activity due to solvation in going from water to sulphuric or formic acid solution is for the species BH^+ and R^+. In this connection Briegleb (18) has calculated the heat of hydration of typical amines to be 10–12 kcal mole^{-1} while that of the ammonium ions is 83–85 kcal mole^{-1}. Cations are solvated best by basic molecules, i.e. those with available pairs of electrons and one would expect water to perform this function better than either sulphuric or formic acid. Thus in going to the latter solutions from water the activity of the cations should increase.

The greatly increased solubility of some weak bases in sulphuric acid of strength below that required to cause appreciable ionization of the base shows that the term f_B can decrease markedly in going from water to sulphuric acid (19, 20). Thus a considerable change in the activity coefficients of the neutral species B and ROH may also occur but it is not obvious why this effect should be greatly different for B than for ROH. A principal difference between the ions BH^+, typified by the nitroanilinium ion (used to determine the H_0 scale), and the carbonium ions (used to determine the $J_0(H_R)$ scale) is the fact that in the former the charge is localized on the nitrogen atom as in I whereas in the carbonium ion (II) the charge is spread by resonance to a very considerable extent into the three rings.

I

II
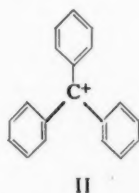
Thus solvation is less important to the carbonium ion and when it is transferred to a sulphuric or formic acid solution, the increase in its activity due to the decreased solvation should be less than that for the anilinium ion. This argument is, at least, in qualitative agreement with the experimental fact that the ratio $f_B f_{R^+}/f_{BH^+} f_{ROH}$ does decrease greatly in going from water to sulphuric and formic acid. Deno and Perrizolo (20) have recently determined the ratios of the activity coefficients of several ions in sulphuric acid – water mixtures. Comparing a small unshielded ion like K^+ with a large shielded ion like $(C_4H_9)_4N^+$ they found, in fact, that $d(f_{K^+}/f_{(C_4H_9)_4N^+})/d\%$ H_2SO_4 underwent a 25-fold increase on going from 0% to 70% sulphuric acid. Deno et al. found, however, that the concentration of the ion, NO^+, formed by the ionization of HNO_2, follows the acidity function $H_R(J_0)$ in sulphuric acid (9). Since this is a small ion in which extensive charge delocalization is not possible they have suggested that the group of cations which follows this acidity function (carbonium ions and the NO^+ ion) do so because of the presence of an empty available orbital (open sextet) in the ions. They propose that the weak bonding resulting from overlap of the cation's empty orbital and the solvent oxygen's orbitals is a different function of acidity from the usual cation–solvent interaction. It is difficult to reconcile this similarity in behavior of NO^+ and arylcarbonium ions with the charge delocalization concept which we have advanced herein to explain the difference between the experimental acidity function, $J_0(H_R)$, and the calculated values of Gold. Both factors referred to above may be important. It is worth pointing out here that the position of equilibrium between a charge localized ion and its tautomeric delocalized form has been shown in at least two cases (protonated Michler's ketone and Michler's hydrol) to be strongly affected by the nature of the solvent (21).

Variation of $J_0(H_R)$ with Temperature

The effect of a temperature change on $J_0(H_R)$ was determined for three different concentrations of formic acid. Although H_0 is altered only slightly by temperature change, it was found that the ionization of the carbinols studied increased with increasing temperature, the increase being small in dilute formic acid but much larger in concentrated solution. Plots of apparent $J_0(H_R)$, calculated by assuming pK_{R^+} to be constant, against $1/T$ gave straight lines as can be seen in Fig. 2. The significance of this result must await a determination of the effect of temperature on pK_{R^+}. (7).

ACKNOWLEDGMENT

REFERENCES

1. M. A. PAUL and F. A. LONG.   Chem. Rev. **57**, 1 (1957).
2. F. A. LONG and M. A. PAUL.   Chem. Rev. **57**, 935 (1957).
3. A. M. LOWEN, M. A. MURRAY, and G. WILLIAMS.   J. Chem. Soc. 3321 (1950).
4. V. GOLD and B. W. V. HAWES.   J. Chem. Soc. 2102 (1951).
5. A. HANTZSCH.   Z. physik. Chem. **61**, 257 (1908).
6. L. P. HAMMETT and A. J. DEYRUP.   J. Am. Chem. Soc. **55**, 1900 (1933).
7. N. C. DENO, J. J. JARUZELSKI, and A. SCHRIESHEIM.   J. Org. Chem. **19**, 155 (1954).
8. V. GOLD.   J. Chem. Soc. 1263 (1955).
9. N. C. DENO, H. E. BERKHEIMER, W. L. EVANS, and H. J. PETERSON.   J. Am. Chem. Soc. **81**, 2344 (1959).
10. R. STEWART.   Can. J. Chem. **35**, 766 (1957).
11. A. G. EVANS.   Personal communication.
12. K. N. BASCOMBE and R. P. BELL.   J. Chem. Soc. 1096 (1959).
13. I. GOLDBERG and C. SISSOEFF.   Ber. **40**, 4546 (1907).

14. K. Brand. J. prakt. Chem. **109**, 14 (1925).
15. J. A. Pinfold and F. Sebba. J. Am. Chem. Soc. **78**, 5193 (1956).
16. P. Grammaticakis. Bull. soc. chim. France, 158 (1950).
17. S. Takagi. Bull. Chem. Soc. Japan, **14**, 508 (1939).
18. G. Briegleb. Z. Electrochem. **53**, 350 (1949).
19. L. P. Hammett. Physical organic chemistry. McGraw Hill Book Co., Inc., New York. 1940. p. 273.
20. N. C. Deno and C. Perizzolo. J. Am. Chem. Soc. **79**, 1345 (1957).
21. R. Stewart and M. Mocek. Unpublished results.

SOLVENT EXTRACTION OF MINERAL ACIDS

PART III. SOLUTE–SOLVENT INTERACTION IN THE SYSTEM HYDROBROMIC ACID – WATER – TRI-n-BUTYL PHOSPHATE[1]

A. S. KERTES AND V. KERTES

ABSTRACT

Evidence, based on physical–chemical measurements of the organic layers, has been presented to show that tributyl phosphate extracts hydrobromic acid as its disolvate in medium acid concentrations, and probably as monosolvate in high concentrations. The determination of water in the tributyl phosphate phases indicates that at low and medium acid concentrations the acid is extracted as its tetrahydrate, and at high concentrations as an unhydrated species. From these results, the formation of $[(TBP)_2.HBr.(H_2O)_6]$ and $[TBP.HBr.(H_2O)_3]$ could be deduced.

Compared with the extensive literature on the extraction of inorganic nitrates from aqueous nitric acid solutions by tributyl phosphate, relatively few investigations have dealt with tributyl phosphate extraction of inorganic halides from aqueous solutions of the corresponding hydrohalic acid. The reactions between metal salts or ions and tributyl phosphate can only be correctly understood if the very pronounced tendency of this basic extractant to react with the acid present in such systems is taken into account. It was therefore considered necessary to investigate more thoroughly the solute–solvent interactions involved in the heterogeneous equilibria existing in systems of hydrohalic acid – water – tributyl phosphate. Our earlier research determined the species formed as a result of solute–solvent interaction in the system HCl–H$_2$O–TBP (1). The second paper in this series dealt with the hydration phenomena of tributyl phosphate – hydrochloric acid complexes existing in the organic layer (2). In the continuation of this research we made a similar investigation of the system HBr–H$_2$O–TBP.

On the experimental side, the present research is an extension of that carried out recently by Baldwin, Higgins, and Soldano (3), in which the distribution coefficient of hydrobromic acid, and its hydration number, were investigated. These authors found that HBr is more effectively extracted than HCl into TBP, and that at low acid concentrations the halogen acids carried water along into the TBP, at the rate of approximately 4H$_2$O per HX. At high acid concentrations it seemed to these authors that water was again forced from the tributyl phosphate. It was also indicated (4) that hydrobromic acid entered the organic phase along with the four water molecules at low acid concentrations. No other studies have been published in the open literature dealing with tributyl phosphate extraction of HBr.

The results reported here reveal the certain existence of a well-defined compound among hydrobromic acid, tributyl phosphate, and water, and indicate the existence of another. The mechanism of extraction of the compounds is suggested.

EXPERIMENTAL

Reagents

B. D. H. Analar grade colorless hydrobromic acid was standardized against standard carbonate-free sodium hydroxide solution. Calculated amounts were taken for 13 stock

solutions of various concentrations as listed in Table I. Tri-n-butyl phosphate was treated as reported previously.

Procedure

The procedure for the distribution experiments consisted of equilibrating 5 ml of pure undiluted TBP with 5 ml of initial aqueous acid solution of various concentrations. The changes in volume, the density, viscosity, and conductivity of the organic layers were measured as described in the previous paper (1). The acid and water determinations followed the methods outlined in Part I. All the measurements were performed at room temperature of $20° \pm 1°$ C and where necessary in a thermostatic water bath at $20° \pm 0.1°$ C.

RESULTS AND DISCUSSION

Partition and Ionization of the Acid

Column 2 of Table I shows the molarity of hydrobromic acid in the initial aqueous solutions, and columns 3 and 4 the molarity in the equilibrium aqueous and organic phases respectively. The concentration and mass distribution coefficients, as previously

TABLE I

| No. of soln. | Molarity of HBr in: | | | Volume increase of the organic phase, ml | α | μ | HBr in the organic phase, mmoles | HBr/ TBP ratio, mmoles | H$_2$O in the organic phase, mmoles | H$_2$O/TBP ratio, mmoles |
	Initial aq. soln.	Equilib. aq. phase	Equilib. org. phase							
(1)	(2)	(3)	(4)	(5)	(6)	(7)	(8)	(9)	(10)	(11)
1	0.089	0.090	0.005	0.30	0.052	0.058	0.03		18.9	1.0
2	0.178	0.176	0.011	0.30	0.063	0.071	0.06		19.4	1.1
3	0.446	0.433	0.036	0.30	0.083	0.094	0.19		21.2	1.2
4	0.891	0.811	0.123	0.30	0.151	0.171	0.65	0.04	25.0	1.4
5	1.782	1.576	0.312	0.40	0.199	0.232	1.68	0.09	27.9	1.5
6	2.673	2.275	0.578	0.55	0.254	0.318	3.21	0.18	35.0	1.9
7	3.564	2.986	0.844	0.75	0.283	0.382	4.85	0.27	41.2	2.2
8	4.420	3.783	1.095	0.90	0.290	0.417	6.46	0.35	47.2	2.6
9	5.347	4.578	1.389	1.10	0.303	0.475	8.47	0.46	52.4	2.9
10	6.257	5.347	1.717	1.25	0.321	0.535	10.72	0.59	55.2	3.0
11	7.129	6.304	2.025	1.35	0.322	0.546	12.57	0.69	57.2	3.1
12	8.034	6.968	2.332	1.45	0.334	0.606	15.04	0.82	56.5	3.1
13	8.911	7.774	2.631	1.55	0.339	0.643	17.23	0.95	56.8	3.1

defined (1), are compiled in columns 6 and 7 respectively. Figure 1 represents the graph of the acid molarity in the equilibrium phases. The non-uniform shape of the curve indicates that the species of HBr extracted from aqueous solutions of hydrobromic acid of initial concentrations up to about 1 M differ from those extracted from more concentrated solutions. Furthermore, when the TBP phase is equilibrated with aqueous solutions of initial concentrations as above, the decrease in the values of the equivalent conductance (column 5 of Table II, and Fig. 5) suggests that from these dilute aqueous acid solutions the acid passes into the organic phase to a large extent in ionized form. Increase in the acid concentration of the initial aqueous solutions promotes ion-pair formation and causes an increase in the acid content of the organic layer. It should be noted that this interpretation does not agree with the values of the degree of ionization estimated by means of Walden's rule, $\lambda\eta/60$, shown in column 6 of Table II.
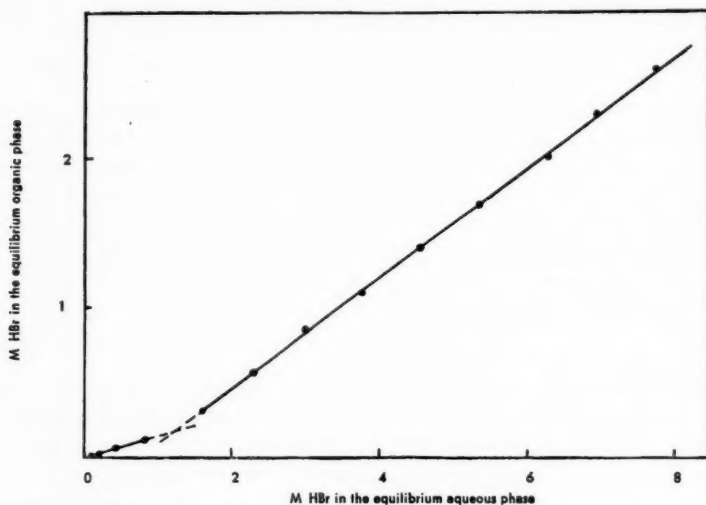
FIG. 1. The plot of HBr molarity in equilibrium organic phases versus its molarity in the equilibrium aqueous phases.

TABLE II

No. of soln.	Density at 20° C, g/cm³	Viscosity at 20° C, Centipoises	Specific conductance at 20° C, mhos 10³	Equivalent conductance at 20° C	Degree of ionization, %
(1)	(2)	(3)	(4)	(5)	(6)
1	0.977	5.964	0.005	1.086	0.11
2	0.977	5.920	0.011	0.982	0.10
3	0.981	6.172	0.034	0.945	0.10
4	0.986	6.770	0.093	0.760	0.09
5	0.998	8.774	0.515	1.650	0.24
6	1.015	10.97	1.210	2.091	0.38
7	1.029	12.95	1.915	2.269	0.43
8	1.045	15.93	2.583	2.360	0.63
9	1.061	18.16	3.594	2.515	0.77
10	1.079	20.45	4.306	2.508	0.85
11	1.095	21.46	4.483	2.214	0.79
12	1.107	23.59	4.675	2.005	0.79
13	1.123	24.71	4.917	1.870	0.61

Solvation of the Acid

The solvation number of hydrobromic acid in the extractant, i.e. the composition of the compound formed between the acid and the extractant as a result of their interaction, was determined by physical–chemical measurements of the organic layer.

On equilibrating 5 ml of pure TBP (18.35 mmoles) with an equal volume of aqueous acid solution, the volume of the organic phase increases. In Fig. 2 the changes in volume of the organic layer, shown in column 5 of Table I, are plotted against the acid content of this layer. It is clear that there are three different interactions, occurring in low, medium, and high acid concentrations respectively. For acid concentrations up to 1 M, the increase in volume of the organic phase is equal to the increase caused by pure water. For concentrations between 1 M and ～5.5 M there is a greater increase in volume, and
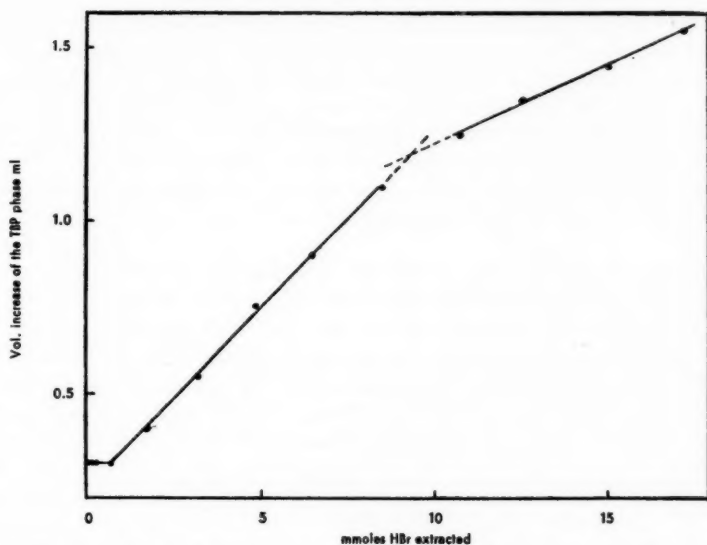
FIG. 2. The plot of the volume increase of the TBP layers after equilibration versus mmoles of HBr extracted.

a break occurs in the curve when the ratio TBP:HBr reaches two. The third type of interaction occurs when the acid concentration exceeds ~ 5.5 M.

When the densities and viscosities (Table II) are plotted against the acid content of the equilibrium organic layers, the curves shown in Figs. 3 and 4 are obtained. When the
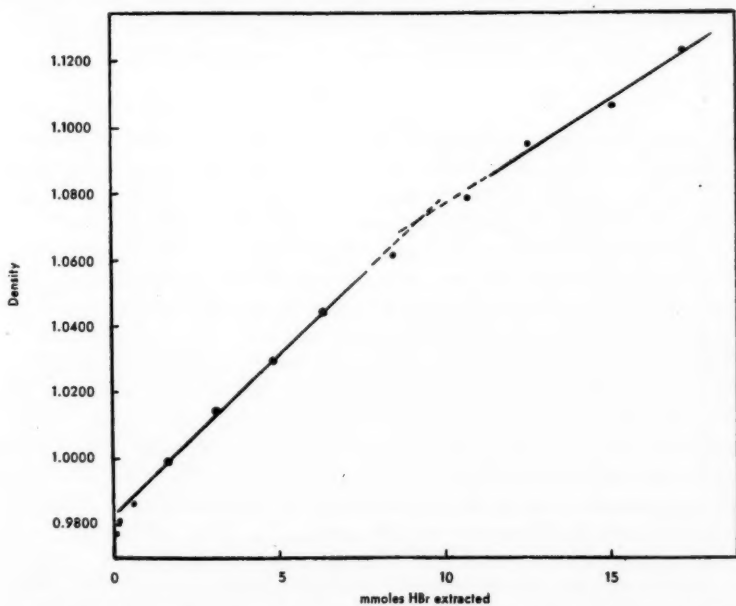
FIG. 3. The plot of density of the equilibrium organic layers versus mmoles of HBr extracted.
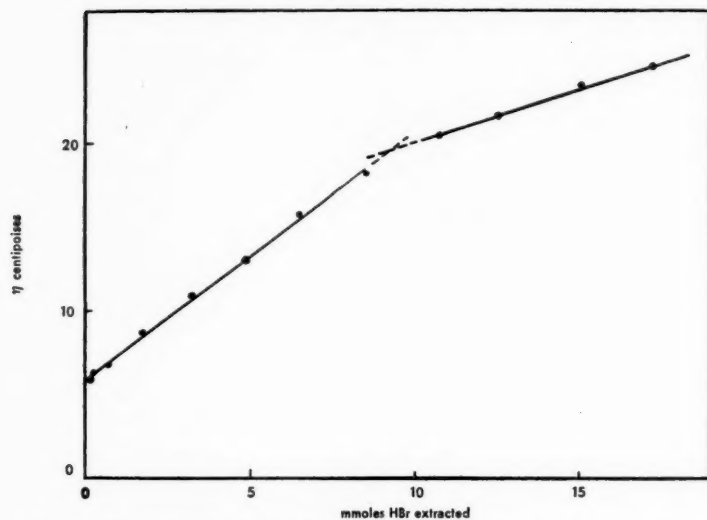
Fig. 4. The plot of viscosity of the equilibrium organic phases versus mmoles of HBr extracted.

TBP phase is equilibrated with aqueous solutions of concentrations up to ~1 M HBr, only very slow changes, if any, are observed in these physical data. The interaction in medium acid concentrations is demonstrated by a break in both curves, at a point when the organic layer contains 9.2 mmoles of hydrobromic acid and 18.35 mmoles of tributyl phosphate, i.e. a TBP:HBr ratio of two.

The results of conductivity measurements of the organic phase are given in columns 4 and 5 of Table II. Figure 5 shows the equivalent conductance values, plotted against the
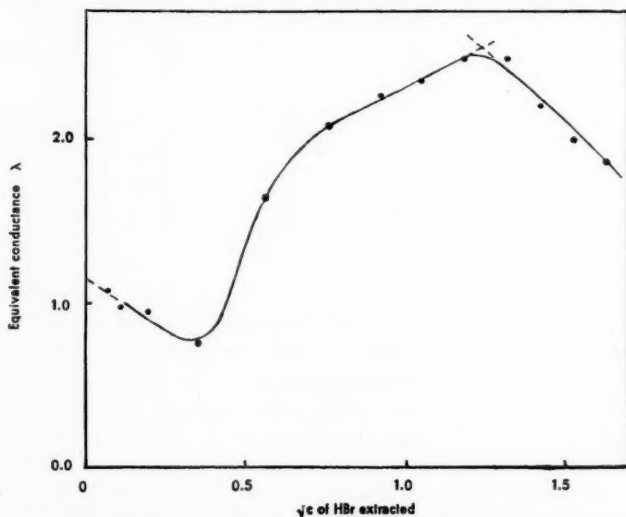
Fig. 5. The plot of equivalent conductance of the equilibrium organic phases versus the square root of the HBr concentration in the organic phase.

square root of the acid concentration, $\sqrt{c}$. It has already been noted that the appearance of a conductance minimum is very probably associated with the end of an ionization region (maximum concentration of the acid in the organic layers of this region being 0.1 M), and it is characteristic of polar compounds dissolved in media of low dielectric constant. Higher values can be explained by the increased extraction of HBr into the TBP due to ion-pair formation (5, 6). The curve, in addition, shows an interception, on extension over a flat maximum, between the medium and high acid concentration regions. This break corresponds to a TBP:HBr ratio of two, evidence for the formation of $(TBP)_2 \cdot HBr$.

The solvation number of inorganic species in organic solvents under conditions of liquid–liquid extraction have so far been deduced from partition data, using undiluted (7) and diluted extractants (8). By the methods employed in this study, the physical–chemical behavior of the tributyl phosphate extractant (in equilibrium with aqueous hydrobromic acid of various concentrations) has revealed that the extracted hydrobromic acid species contains two tributyl phosphate molecules per acid molecule. It was further shown that the solvation number is to a large extent dependent on the acid concentration. In high concentrations the solvation of the extracted acid species is determined by an interaction leading to the formation of a compound which probably contains a TBP:HBr ratio of unity. Although the formulation of this compound cannot be considered as established, the great change in the nature of the organic layers, when using high acid concentrations, seems to indicate results comparable with those of the similar system containing hydrochloric instead of hydrobromic acid (1).

With the exception of our study (1), there seem to be no examples of mineral acids being extracted with two tributyl phosphate molecules. In fact, the solvation numbers of nitric and perchloric acids extracted into TBP appear to be one. This was also found to be true for hydrochloric, and very probably hydrobromic, acids, but only in high acid concentrations. It has now been shown that for medium acid concentrations the main solute–solvent interaction leads to the formation of hydrobromic acid disolvate, analogous to hydrochloric acid disolvate.

Hydration of the Acid

The water content of the organic layer in millimoles, and the corresponding water:extractant ratios, are compiled in the last two columns of Table I. Figure 6 shows the curve obtained by plotting the water content against the acid content of the tributyl phosphate layer. The curve shows the water content of the organic phase in two stages. The points corresponding to tributyl phosphate phases with very low acid content (up to $\sim$0.1 M, that is up to about 0.5 mmole) could not be integrated into these stages, and so at these low acid concentrations nothing could be stated about the hydration mechanism of the acid. For medium acid concentrations (initial acid concentration between $\sim$1 and $\sim$5.5 M), the graph shows a straight line, of slope four, indicating that each acid molecule passing from the aqueous into the organic layer is associated with four water molecules. This relationship holds until the acid content of the tributyl phosphate layer is 9.2 mmoles, when the TBP:HBr ratio is two. After this, the water content no longer changes with increase in the acid content of the organic phase. For these high acid concentrations the H_2O:TBP ratio remains practically constant, and equal to three approximately.

The above results of the acid hydration are completely analogous to those obtained in the system with hydrochloric acid, as is also the stability of hydration (2) of the extracted species.
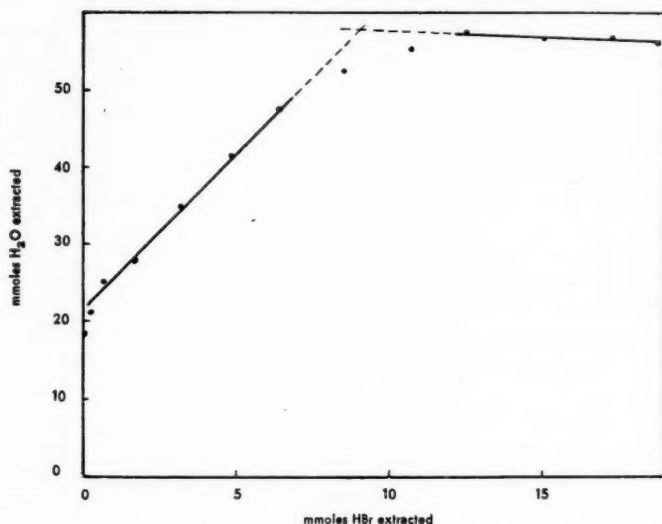
FIG. 6. The plot of mmoles of H_2O versus mmoles of HBr both in the equilibrium organic phases.

CONCLUSIONS

The acid passing into the tributyl phosphate phase from dilute aqueous hydrobromic acid is probably ionized. For these low acid concentrations, the main reaction involved is that between water and the extractant, resulting in the formation of the stable tributyl phosphate monohydrate. For medium acid concentrations, ion-pair formation becomes significant, and each acid molecule is extracted together with four water molecules. The acid–ester interaction leads to the formation of a compound with a TBP:HBr ratio of two, and H_2O:TBP ratio of three. These reactions could be formulated as follows:

$$TBP_{org} + H_2O_{aqu} \rightarrow [TBP.H_2O]_{org,} \tag{1}$$

$$2[TBP.H_2O]_{org} + H^+(H_2O)_{4\,aqu} + Br^-_{aqu} \rightarrow [(TBP)_2.HBr.(H_2O)_6]_{org}. \tag{2}$$
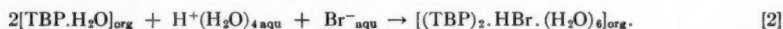
Both these reactions are analogous to those previously found in systems containing hydrochloric acid.

Under the experimental conditions of this investigation, it was found impossible to equilibrate the tributyl phosphate phase so that the acid content corresponded to a TBP:HBr ratio of unity. Therefore for high acid concentrations this system is not completely analogous to that containing HCl. Nevertheless, following the analogy between the two systems, it can be presumed that for high acid concentrations, when the extracted acid is unhydrated, the H_2O:TBP ratio is constant and practically equal to three, and as the TBP:HBr ratio decreases and approaches unity, a further reaction probably takes place. This reaction should be analogous to that in the HCl system at these high acid concentrations, and should be formulated as follows:

$$[(TBP)_2.HBr.(H_2O)_6]_{org} + H^+_{aqu} + Br^-_{aqu} \rightarrow 2[TBP.HBr.(H_2O)_3]_{org}. \tag{3}$$

REFERENCES

1. A. S. KERTES. J. Inorg. & Nuclear Chem. In press.
2. A. S. KERTES. J. Inorg. & Nuclear Chem. In press.
3. W. H. BALDWIN, C. E. HIGGINS, and B. A. SOLDANO. J. Phys. Chem. **63**, 118 (1959).
4. D. G. TUCK and R. M. DIAMOND. Proc. Chem. Soc. 236 (1958).
5. D. E. CAMPBELL, H. A. CLARK, and W. H. BAUER. J. Phys. Chem. **62**, 506 (1958).
6. H. A. C. MCKAY and A. R. MATHIESON. Trans. Faraday Soc. **47**, 428 (1951).
7. E. GLUECKAUF, H. A. C. MCKAY, and A. R. MATHIESON. Trans. Faraday Soc. **47**, 437 (1951).
8. K. ALCOCK, F. C. BEDFORD, W. H. HARDWICK, and H. A. C. MCKAY. J. Inorg. & Nuclear Chem. **4**, 100 (1957).

1,6-BIS(γ-CARBETHOXYPROPYL)-2,3,7,8-DIBENZOPYROCOLL. A BY-PRODUCT IN THE PREPARATION OF γ-(3-INDOLYL)BUTYRIC ACID

Richard H. Manske and Walter R. Boos

During the preparation of γ-(3-indolyl)butyric acid a by-product was obtained when the phenylhydrazone of the half ester of α-ketopimelic acid (I) was subjected to the Fischer indole synthesis and esterified to ethyl γ-(2-carbethoxy-3-indolyl)butyrate (II). The compound was identified as 1,6-bis(γ-carbethoxypropyl)-2,3,7,8-dibenzopyrocoll (III) by hydrolytic ring fission to γ-(2-carboxy-3-indolyl)butyric acid.
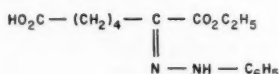
(I)
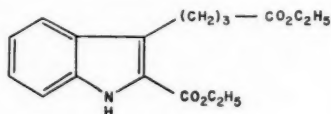
(II)
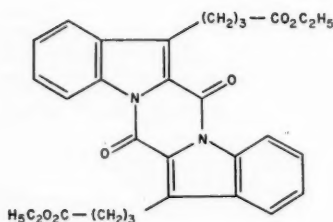
(III)

EXPERIMENTAL

1,6-Bis(γ-Carbethoxypropyl)-2,3,7,8-dibenzopyrocoll (III)

A 5-liter round-bottom flask equipped with a reflux condenser was charged with 1052 g of the half ethyl ester of the phenylhydrazone of α-ketopimelic acid (I), 3 liters of 99% ethanol, and 270 ml of sulphuric acid (density = 1.84). The mixture was boiled for 20 hours under reflux on a steam bath. Subsequently the ethanol was distilled off and the remaining liquid was taken up in 1 liter of benzene, washed well with water, then with 5% aqueous sodium bicarbonate solution, and again with water. The benzene was distilled from the extract and an attempt to distill the residue at a pressure of 0.1 mm failed due to partial decomposition. On cooling crystals were obtained, and these were taken

up in 1.5 liters of 99% ethanol. The yellow crystalline material which then separated was removed by filtration; yield was 180 g. (The filtrate was stripped of ethanol and distilled at 0.1 mm and 210° C and yielded 506 g of ethyl γ-(2-carbethoxy-3-indolyl)butyrate (II).) The precipitate was recrystallized twice from benzene and yielded pale yellow plates, m.p. 214.5–215° C. Calc. for $C_{30}H_{30}N_2O_6$: C, 70.02; H, 5.88; N, 5.44; mol. wt., 514. Found: C, 70.06; H, 5.81; N, 5.80; mol. wt., 548 (Rast).

Hydrolytic Degradation of III *to the Diacid of* II

Three grams of the pyrocoll (III) was hydrolyzed by refluxing for 1 hour in 70 ml of propanol together with 5 g of potassium hydroxide. On cooling a colorless precipitate was obtained which was filtered off, washed with propanol, and dissolved in 60 ml of distilled water. Addition of dilute hydrochloric acid yielded a colorless precipitate which was washed with distilled water and recrystallized from 20 ml of a 1:1 mixture of methanol and benzene: yield 2.3 g of colorless plates; m.p. 210° with loss of carbon dioxide. Calc. for $C_{13}H_{13}NO_4$: C, 63.15; H, 5.30. Found: C, 62.82; H, 5.26. Decarboxylation at 220 to 230° in a nitrogen atmosphere readily yielded γ-(3-indolyl)butyric acid melting at 124° either alone or in admixture with an authentic specimen (1).

1. R. W. JACKSON and R. H. MANSKE. J. Am. Chem. Soc. **52**, 5029 (1930).

MAGNETIC MOMENT OF Ni²⁺ ION IN (Ph₃P)₂NiBr₂(PhBr)₂

YOSHIO MATSUNAGA

Recently Gill, Nyholm, and Pauling (1) have suggested that a regular tetrahedral arrangement of four-covalent spin-free Ni²⁺ complexes is much less probable than a distorted one. If distortion from a regular tetrahedron is small, the magnetic moment of Ni²⁺ ion should be larger than the spin-only value of 2.8 B.M. They have observed the magnetic moment of the Ni²⁺ ion in $(Et_4N)_2(NiCl_4)$ and $(Et_4N)_2(NiBr_4)$ being in the range of 3.8 to 3.9 B.M. Similar high moments have been found in the following cases: the Ni²⁺ ion in the tetrahedral hole of glass, 3.6 B.M. (2), the Ni²⁺ ion in the tetrahedral site of spinel, about 3.6 B.M. (3), and the Ni²⁺ ion in $[(Ph_3PO)_4Ni](ClO_4)_2$, 3.51 B.M. (4). In all of the above-mentioned cases, Ni²⁺ ion is surrounded by four equivalent ions or atoms. Venanzi (5) has found that complexes of the type $(Ph_3P)_2NiX_2$ show the magnetic moments which are only a little higher than the spin-only value and are monomeric in benzene solution. It has been shown by X-ray studies that the Ni²⁺ ion is located at the center of a distorted tetrahedron (6). Here we wish to report the increase of the magnetic moment of the Ni²⁺ ion in $(Ph_3P)_2NiBr_2$ by addition of crystalline solvent.

A number of compounds of the types $(Ph_3P)_2NiX_2Y$ and $(Ph_3P)_2NiX_2Y_2$, where Y is alkyl or phenyl halide, have been described by Reppe and Schweckendiek (7) and by Yamamoto (8). Among them we examined the compounds $(Ph_3P)_2NiBr_2$, $(Ph_3P)_2NiBr_2$ *tert.* BuBr, and $(Ph_3P)_2NiBr_2(PhBr)_2$, which are intense green, green, and grayish blue, respectively. The following values of specific magnetic susceptibility at room temperature and effective magnetic moment of Ni²⁺ ion were obtained: $(Ph_3P)_2NiBr_2$,

5.64×10^{-6} c.g.s.-e.m.u., 3.2 B.M.; $(Ph_3P)_2NiBr_2$ *tert*. BuBr, 5.37×10^{-6}, 3.4 B.M.; and $(Ph_3P)_2NiBr_2(PhBr)_2$, 5.59×10^{-6}, 3.8 B.M. The high magnetic moment of the Ni^{2+} ion in the latter two suggests that distortion from a regular tetrahedral arrangement can be decreased by the presence of crystalline solvent. The distortion in the compounds $(Ph_3P)_2NiX_2$ (X = Cl, Br, I, and NO_3) seems to be partially due to the steric requirement by the size difference between triphenylphosphine and halide ion. To compensate for such a steric effect in $(Ph_3P)_2NiBr_2$ two molecules of bromobenzene may be more suitable than one molecule of tert. butyl bromide. The appearance of blue tint in many cases of compounds of the types $(Ph_3P)_2NiX_2Y$ and $(Ph_3P)_2NiX_2Y_2$ may have some correlation with rather small distortion from a regular tetrahedral arrangement.

1. N. S. GILL, R. S. NYHOLM, and P. PAULING. Nature, **182**, 168 (1958).
2. P. W. SELWOOD. Magnetochemistry. Interscience Publishers, Inc., New York. 1956. p. 186.
3. J. T. RICHARDSON and W. O. MILLIGAN. J. Phys. Chem. **60**, 1223 (1956).
4. F. A. COTTON, E. BANNISTER, R. BARNES, and R. H. HOLM. Proc. Chem. Soc. 158 (1959).
5. L. M. VENANZI. J. Chem. Soc. 719 (1958).
6. L. M. VENANZI and H. M. POWELL. *Cited in* reference 1.
7. W. REPPE and W. J. SCHWECKENDIEK. Ann. **560**, 104 (1948).
8. K. YAMAMOTO. Bull. Chem. Soc. Japan, **27**, 501 (1954).

CRYSTALLINE GLYOXYLIC ACID AND ITS SODIUM–CALCIUM SALT

A. A. EISENBRAUN* AND C. B. PURVES

Early researches on the preparation and properties of glyoxylic acid were extensively reviewed by Debus (1) and by Hendricks (2), who noted that the substance occasionally yielded ill-defined rhombic crystals of a monohydrate when stored over a drying agent. In 1925, Hatcher and Holden (3) used the electrochemical method to reduce oxalic acid, isolated barium glyoxylate, decomposed the latter with sulphuric acid, and prepared anhydrous glyoxylic acid for the first time as monoclinic crystals melting at 98°. This result was questioned by Hendricks (2) because oxalic acid monohydrate, a probable impurity, melted at 99° and occurred as monoclinic crystals, and also because his attempts to repeat the crystallization of glyoxylic acid failed. Later workers oxidized tartaric acid or its esters with a glycol-cleaving agent, periodic acid or a periodate (4, 5, 6), lead tetraacetate (7), or sodium perbismuthate (8, 9), but apparently restricted their interest to the preparation of various esters and metallic salts of glyoxylic acid.

In the present work, tartaric acid was oxidized with aqueous periodic acid, by-product iodic acid was removed as the insoluble lead salt, and, after neutralization with barium hydroxide, crystalline barium glyoxylate dihydrate was recovered in high yield. An ion-exchange resin eliminated the cations from an aqueous solution of this salt, and evaporation of the effluent left glyoxylic acid as a clear syrup which eventually crystallized. The melting point was 104–107°, with softening at 94°. The replacement of periodic acid by sodium metaperiodate in the above oxidation, followed by the removal of iodate ion, left

a solution which was mixed with an equimolar amount of aqueous calcium acetate. A white, crystalline, sodium–calcium salt, $CaNa_2(C_2HO_3)_4 \cdot 4H_2O$, promptly separated. This salt was thought to be new.

EXPERIMENTAL

Glyoxylic Acid

An aqueous solution, 300 ml, containing 15 g (0.1 mole) of L-tartaric acid and 25.1 g (0.11 mole) of paraperiodic acid (H_5IO_6) was kept at 23° in the dark for 10 hours, when a titration by the sodium arsenite – iodine method showed that all of the periodic acid had been reduced. The addition of 110 ml of 0.52 M lead acetate (0.114 equivalent) caused the nearly quantitative separation of lead iodate, which was removed by filtration. After residual lead ions were removed as lead sulphide, the clarified liquor was evaporated *in vacuo* to a syrup, by-product acetic and formic acids being incidentally eliminated. The acidity of the syrup was cautiously reduced to pH 8 by the addition of cold 0.3 N barium hydroxide, and partial evaporation of the liquor caused the crystallization of 27.8 g (86.8%) of barium glyoxylate dihydrate. Although the solubility of the salt in water was reported (3) as only 0.005% at 18° and 0.08% at 68°, the present sample could be readily recrystallized from hot water. This recrystallization did not significantly change the composition. Calc. for $Ba(C_2HO_3)_2 \cdot 2H_2O$: Ba, 43.0%. Found: Ba, 42.8, 43.0%. Samples, 0.2580 g and 0.2577 g, reduced 32.5, 32.5 ml, respectively, of 0.104 N potassium permanganate (3), the calculated amount being 30.9 ml.

An aqueous solution of 8.0 g of the above salt was freed of barium ions by passage through a column of Amberlite IR-120 cation-exchange resin, and the effluent was evaporated *in vacuo* to a thick syrup. This syrup was dried to nearly constant weight by storage over phosphorus pentoxide in an evacuated desiccator at room temperature. After several months the colorless product, 3.68 g or 99% yield, crystallized solidly. The melting point was 104–107°, with softening at 94°. No solvent suitable for recrystallizing the glyoxylic acid was found.

Sodium – Calcium Glyoxylate Tetrahydrate

Fifteen grams (0.1 mole) of L-tartaric acid dissolved in 300 ml of water was mixed with 200 ml of 0.515 M sodium metaperiodate (0.103 mole). The reduction of the latter was complete after the mixture had been kept in the dark and at room temperature for 36 hours. After iodate ion was removed as the lead salt, the filtrate was evaporated *in vacuo* to 50 ml, and was adjusted to pH 8 with 2 N sodium hydroxide. A concentrated aqueous solution of 17 g (0.1 mole) of calcium acetate monohydrate was then added, and 19.6 g (87.1%) of the sodium–calcium salt separated as white crystals. Calc. for $Na_2Ca(C_2HO_3)_4 \cdot 4H_2O$: Na, 10.2; Ca, 8.3%. Found: Na, 9.65, 9.58; Ca, 9.27, 9.21%. Samples, 0.1338 g, 0.2038 g, and 0.1024 g, reduced 24.6 ml, 37.7 ml, and 19.0 ml of 0.101 N potassium permanganate (3), the calculated volumes being 23.6 ml, 35.9 ml, and 18.1 ml, respectively.

Two recrystallizations from hot water reduced the over-all yield to about 75% but failed to alter the composition significantly. A 0.0365-g sample of the salt when treated with 2,4-dinitrophenylhydrazine yielded 0.0658 g (79%) of crystalline glyoxylic acid 2,4-dinitrophenylhydrazone with the correct (10) melting point of 191–191.5°.

1. H. Debus. J. Chem. Soc. **85**, 1382 (1904).
2. R. H. Hendricks. Ph.D. Dissertation, St. Louis University, Missouri, Ill. 1935. Univ. Microfilms (Ann Arbor, Mich.) Pub. No. 183; Chem. Abstr. **35**, 2475 (1941).
3. W. H. Hatcher and G. W. Holden. Trans. Roy. Soc. Canada, Section III (3), **19**, 11 (1925).

4. P. FLEURY and G. BON-BERNATETS. J. Pharm. Chim. **23**, 85 (1936).
5. A. WEISSBACH and D. B. SPRINSON. J. Biol. Chem. **203**, 1023 (1953).
6. D. E. METZLER, J. OLIVARD, and E. E. SNELL. J. Am. Chem. Soc. **76**, 644 (1954).
7. F. J. WOLFF and J. WEIJLARD. Org. Syntheses, **35**, 18 (1955).
8. W. RIGBY. J. Chem. Soc. 1907 (1950).
9. L. J. HEIDT, E. K. GLADDING, and C. B. PURVES. Paper Trade J. **121** (9), 81 (1945).
10. O. L. BRADY. J. Chem. Soc. 756 (1931).

DIFFERENTIATION BETWEEN SOME 2,3- AND 2,5-DISUBSTITUTED PYRIDINE DERIVATIVES BY INFRARED SPECTROSCOPY

R. A. ABRAMOVITCH, GIAM CHOO SENG, AND A. D. NOTATION

In connection with studies of the orientation in the nucleophilic addition of phenyl-lithium to 3-substituted pyridines (1, 2) it became necessary to find a simple method of determining whether the attacking phenyl group had entered into the 2- or the 6-position of the pyridine ring, i.e. of distinguishing between 2- and 6-phenyl-3-substituted pyridines. This could be done by examining the N.M.R. spectrum of the compounds (1, 3) but was limited in that these determinations could not be carried out in our own laboratories. We therefore turned to infrared spectroscopy for such a method.

In theory, it should be quite simple to differentiate between 2,3- and 2,5-disubstituted pyridines by an examination of the aromatic C—H out-of-plane deformation region between 830 and 700 cm^{-1}. Infrared spectra – structure correlations have been found for the alkylbenzenes in the 11–15 μ region which are characteristic of the substitution positions in the benzene ring (4, 5). If one then considers that the pyridine ring corresponds to a monosubstituted benzene as far as the aromatic C—H out-of-plane bendings are concerned then a 2,3-disubstituted pyridine derivative should be equivalent to a 1,2,3-trisubstituted benzene whereas a 2,5-disubstituted pyridine derivative should correspond to a 1,2,4-trisubstituted benzene. The 1,2,3-trisubstituted benzenes show absorption in the 810–750 cm^{-1} range with a second band of medium intensity in the 726–680 cm^{-1} region, whereas 1,2,4-trisubstituted benzenes give rise to a strong band in the range 860–800 cm^{-1} (6). A number of 2,3- and 2,5-disubstituted pyridine derivatives have recently been shown to fall in nicely with this pattern (7, 8, 9). In particular, Podall (7) has studied the problem systematically and shown that 2-methyl-5-alkylpyridines exhibited two bands at 828–813 cm^{-1} and 735–724 cm^{-1}, whereas 2-methyl-3-alkylpyridines (1,2,3-trisubstitution) showed two bands at 813–769 cm^{-1} and 752–725 cm^{-1}.

A number of minor discrepancies in the band pattern in this region were observed in the present work. 2-Phenylnicotine exhibited a band at 805 cm^{-1}, quinoline a band at 805 cm^{-1}, and 5,6,7,8-tetrahydroquinoline a band at 827 cm^{-1} (see also (8)). On the other hand, 2-phenyl-3-alkyl- and 2-phenyl-5-alkyl-pyridines exhibited the expected absorptions though the presence of the monosubstituted phenyl-group obscured the assignment of the higher wavelength band. All that could be said was that most 2-phenyl-5-substituted pyridines exhibited a band of medium intensity between 850 and 800 cm^{-1} whereas most 2-phenyl-3-substituted pyridines did not.

A new and quite useful empirical correlation has now been observed in the C=C and

C=N stretching vibration region, which seems to apply provided no substituents which absorb in this region ($—NH_2$, —CO—, $—NO_2$, etc. . . .) are present. Table I summarizes the results obtained; the compounds are divided into two groups according to whether they are classed as corresponding to 1,2,3-trisubstituted or to 1,2,4-trisubstituted benzenes. 1,2,3-Trisubstituted compounds exhibit a band in the range 1578–1588 cm^{-1} whereas 1,2,4-trisubstituted derivatives give a band in the 1599–1605 cm^{-1} range. A second band at a somewhat higher wavelength is also generally observed but does not seem to be too characteristic. The orientation of the two isomeric phenylnicotines obtained by the action of phenyllithium on nicotine (1) was first assigned on the basis of the infrared bands in this region and later confirmed both by chemical means and also through a comparison of the N.M.R. spectra of the two isomers. The isomeric ethylphenyl-pyridines were also so oriented and the structure then proved unambiguously by degradative experiments. It is important to emphasize that this new correlation is only useful in determining the orientation of disubstituted pyridines provided one is sure that only these are present. Some trisubstituted pyridines have no bands in this region above 1590 cm^{-1} (e.g. 3,4,5-collidine and 2,3,4-collidine (9)), whereas others have. It is, therefore, not applicable to the possible determination of the number of substitutents present in the pyridine ring as the correlation of the bands due to the aromatic C—H out-of-plane deformation frequencies potentially is.

EXPERIMENTAL

The infrared spectra were measured on a Perkin–Elmer Model 21 recording spectrometer using sodium chloride optics. All the spectra were measured on liquid films and the positions of the bands calibrated by comparison with a polystyrene-film spectrum. All the samples were freshly distilled before use. We wish to express our gratitude to Dr. Hardegger (Zürich) for samples of 3-butyl-4-methylpyridine picrate, 5-butyl-2-

TABLE I

Compound	ν, cm^{-1}	
1,2,4-Trisubstitution		
2,4-Dimethylpyridine	1605	1570
2,5-Dimethylpyridine	1603	1572
3-Butyl-4-methylpyridine	1600	1565
5-Butyl-2-methylpyridine	1603	1572
2-Butyl-5-methylpyridine (10)	1602	1568
5-Ethyl-2-methylpyridine	1605	1570
5-Methyl-2-phenylpyridine	1600	1569
5-Ethyl-2-phenylpyridine	1600	1567
6-Phenylnicotine	1600	1567
3,4-Dimethylpyridine	1600	1564
3-Ethyl-4-methylpyridine	1599	1563
1,2,3-Trisubstitution		
2,6-Dideuteropyridine (11)	1586	1568
2,3-Dimethylpyridine	1580	1540(w)
2,6-Dimethylpyridine	1580	—
3-Butyl-2-methylpyridine	1587	1575
2-Butyl-3-methylpyridine (10)	1588	1576
3-Methyl-2-phenylpyridine	1579	1573
3-Ethyl-2-phenylpyridine	1583	1577
2-Phenylnicotine	1578	1569
3-Hydroxy-2-phenylpyridine*	1578	—
3-Methoxy-2-phenylpyridine	1584	—
5,6,7,8-Tetrahydroquinoline	1588(sh)	1579
5,6,7,8,9-Pentahydrocyclohepta[b]pyridine	1585(sh)	1577

*Nujol mull.

methylpyridine picrate, and 3-butyl-2-methylpyridine picrate, and to Dr. E. Godar (Chicago) for samples of 5,6,7,8-tetrahydroquinoline and 5,6,7,8,9-pentahydrocyclo-hepta[b]pyridine. The preparation of the phenylpyridine derivatives will be described in forthcoming papers. The results are summarized in Table I. The hetero-nitrogen atom is considered here as corresponding to a substituted annular carbon atom in benzene.

ACKNOWLEDGMENTS

1. R. A. ABRAMOVITCH, A. D. NOTATION, and GIAM CHOO SENG. Tetrahedron Letters, **8**, 1 (1959).
2. R. A. ABRAMOVITCH and GIAM CHOO SENG. Unpublished work.
3. A. D. NOTATION. M.Sc. Thesis, University of Saskatchewan, Saskatoon, Saskatchewan. 1959.
4. N. B. COLTHRUP. J. Opt. Soc. Am. **40**, 397 (1950).
5. R. R. RANDLE and D. H. WHIFFEN. Rept. on Conf. of Molecular Spectroscopy. Paper No. 12. Institute of Petroleum. 1954. p. 111.
6. L. J. BELLAMY. Infrared spectra of complex molecules. Methuen & Co., Ltd., London. 1958. p. 78.
7. H. E. PODALL. Anal. Chem. **29**, 1423 (1957).
8. D. HEINERT and A. E. MARTELL. J. Am. Chem. Soc. **81**, 3933 (1959).
9. H. SHINDO and N. IKEKAWA. Pharm. Bull. (Tokyo), **4**, 192 (1596).
10. N. J. LEONARD and B. L. RYDER. J. Org. Chem. **18**, 598 (1953).
11. J. K. WILMSHURST and H. J. BERNSTEIN. Can. J. Chem. **35**, 1183 (1957).

AN N.M.R. STUDY OF ELECTRON RELEASE BY ALKYL AND ALKOXY GROUPS IN VARIOUS SOLVENTS

R. B. MOODIE*, T. M. CONNOR,† AND ROSS STEWART

Recently dipole moment studies (1) and measurements of substrate activity (2) have shown the importance of solvent effect on molecules in their ground state. We have used N.M.R. to measure the chemical shifts of aromatic protons in alkyl and alkoxy benzenes in various solvents. Table I gives the chemical shifts in cycles per second relative to benzene at the same concentration in the same solvent.

TABLE I

Chemical shifts from benzene for the aromatic protons, in cycles/sec

Compound	Solvent			
	C_6H_{12}	$(CH_3)_3N$	CH_3OH	CH_3NO_2
Toluene	5.9	6.2	6.4	6.8
Ethylbenzene	4.4	5.1	5.2	5.3
Isopropylbenzene	3.8	4.1	4.6	4.7
tert-Butylbenzene	1.1*	1.2*	0.9*	1.2*

*These measurements are not to a single peak (see discussion) and are therefore less accurate.
Probable error ±0.5 cycle/sec.

*National Research Council Postdoctorate Fellow 1958–60.
†Holder of a National Research Council Studentship 1957–59.

Shifts were measured on a 40-Mc Model 4300 Varian N.M.R. spectrometer by graphical interpolation between two side bands from the solvent resonances, set as near as possible on either side of the aromatic protons. The side bands were measured with a Hewlett–Packard frequency counter. Samples were 5% solutions sealed *in vacuo*. Six determinations of the cyclohexane–toluene shift by this technique gave a mean-square deviation of ±0.13 cycle/sec. An additional small error may be present in all these measurements
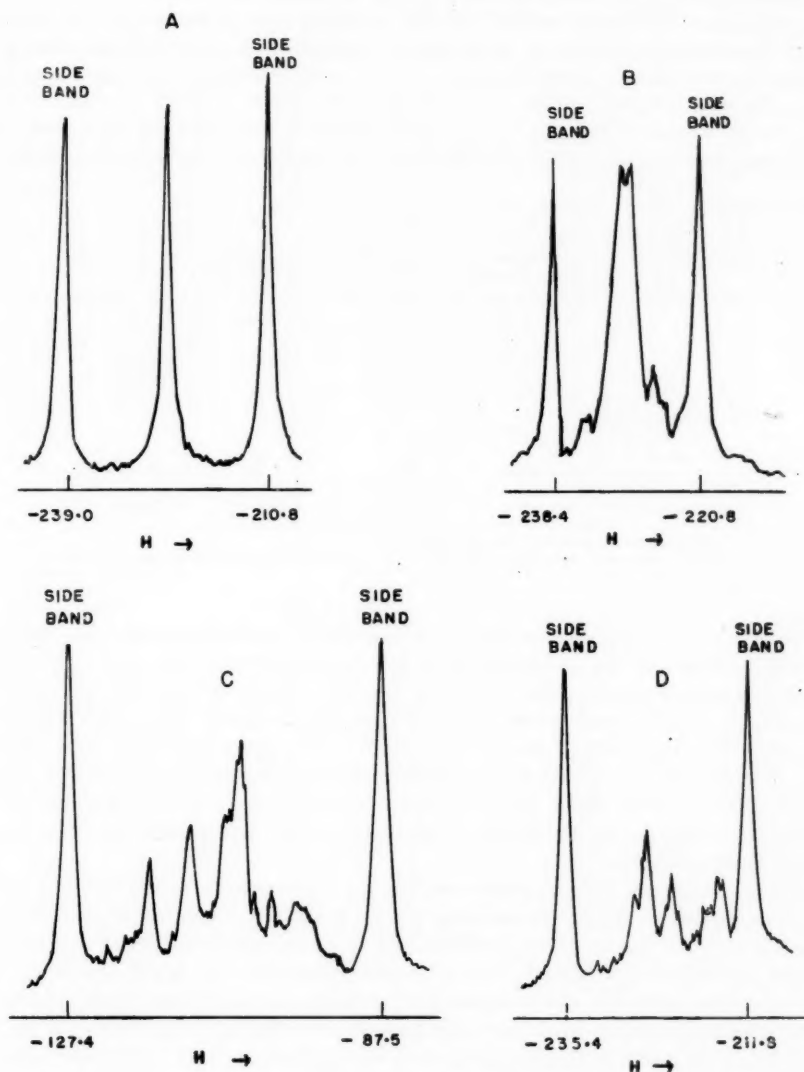
FIG. 1. Spectrum of aromatic protons with side band shifts in cycles per second from the solvent resonance: (A) toluene, (B) *tert*-butylbenzene in cyclohexane, (C) isopropyl phenyl ether in nitromethane, and (D) isopropyl phenyl ether in cyclohexane.

due to dilution effects, since these figures do not represent extrapolation to infinite dilution (3).

In so far as the shifts reflect the average electron density around the aromatic protons in the substituted compounds, the shifts of the alkylbenzenes indicate that the Baker–Nathan order prevails, even in cyclohexane, in contrast to the evidence of dipole moments (1). Since *tert*-butylbenzene shows a well-resolved fine structure but the other alkylbenzenes do not (Fig. 1), the conclusions for this compound are less valid. (Shifts are for the approximate "center of gravity" of the aromatic proton resonances for this compound.) In the comparison of *p*-bromo-*tert*-butylbenzene and *p*-bromotoluene this objection is removed since measurements on the quartet (which show further fine structure due to cross ring coupling) enable calculations of the chemical shifts of ortho and meta protons (4, 5). These values are given in Table II. (It is assumed that the protons ortho to the alkyl group are responsible for the high field doublet of the quartet.) These show

TABLE II

Ortho coupling constants and chemical shifts from benzene for the
aromatic protons in *p*-bromo-alkylbenzenes

	p-Bromotoluene in:		*p*-Bromo-*tert*-butylbenzene in:	
	Solvent C_6H_{12}	Solvent CH_3NO_2	Solvent C_6H_{12}	Solvent CH_3NO_2
Coupling constant in cycles/sec	8.7	8.8	8.6	—[b]
Chemical shift of ortho protons[a]	12.0	10.0	1.5	(-0.4)[b]
Chemical shift of meta protons[a]	−2.0	−0.9	−3.0	(-0.4)[b]

[a]The positions are relative to the alkyl group.
[b]Only a single peak was observed for the aromatic protons of *p*-bromo-*tert*-butylbenzene in nitromethane.

that the ortho and meta protons are more shielded in the methyl than the *tert*-butyl-substituted compound, in agreement with the evidence above. As might be expected, more polar solvents increase the degree of electron release of the alkyl groups in the alkylbenzenes. The benzene–toluene shift in a particular solvent may constitute a useful measure of solvent polarity, if the accuracy of the shift measurements can be improved (by, for example, using a 60-Mc spectrometer and taking the mean of a number of determinations). The solvent effect may be more marked in toluene, ethylbenzene, and isopropyl benzene than in *tert*-butylbenzene (6) but the effect is at present of the same order as the experimental error.

The alkoxy benzenes, anisole, phenetole, isopropyl phenyl ether, and *tert*-butyl phenyl ether, show a more complicated aromatic proton spectrum. Assignment of ortho, meta, and para proton resonances is not possible, and this precludes any precise determination of solvent and substituent effects. Two interesting observations may, however, be made. Firstly, in all four solvents, the aromatic proton resonances of *tert*-butyl phenyl ether are at lower field and show a much less well-defined fine structure than those of the other three ethers. This is due to steric hindrance to conjugation between the oxygen atom and the aromatic π electrons, an effect previously shown to exist from ultraviolet spectral data and from rates of bromination (7). Secondly, there is a sharp contrast between the spectra of anisole, phenetole, and isopropyl phenyl ether in cyclohexane and their spectra

in the other three solvents. Typical spectra of the two types are shown in Figs. 1C and 1D. This suggests that differential electron release to ortho, meta, and para positions varies with the solvent. A similar effect has been observed in the solvent dependence of the ortho/para ratio in the nitration of phenol (8).

By studying suitably substituted ethers it may be possible to eliminate the uncertainty due to spin–spin splitting of non-equivalent proton resonances.

ACKNOWLEDGMENTS

1. T. L. BROWN.   J. Am. Chem. Soc. **81**, 3232 (1959).
2. R. A. CLEMENT and M. R. RICE.   J. Am. Chem. Soc. **81**, 326 (1959).
3. J. A. POPLE, W. G. SCHNEIDER, and H. J. BERNSTEIN.   High resolution nuclear magnetic resonance. McGraw-Hill Book Co., New York. 1959. p. 424.
4. J. A. POPLE, W. G. SCHNEIDER, and H. J. BERNSTEIN.   High resolution nuclear magnetic resonance. McGraw-Hill Book Co., New York. 1959. p. 119.
5. R. B. MOODIE, T. M. CONNOR, and R. STEWART.   Can. J. Chem. **37**, 1402 (1959).
6. W. M. SCHUBERT, J. M. CRAVEN, G. MINTON, and R. B. MURPHY.   Tetrahedron, **5**, 194 (1959).
7. G. BADDELEY, N. H. P. SMITH, and M. A. VICKARS.   J. Chem. Soc. 2455 (1956).
8. J. PODKÓWKA and A. TARNAWSKI.   Monatsh. Chem. **90**, 178 (1959).

NOTES TO CONTRIBUTORS

Canadian Journal of Chemistry

MANUSCRIPTS

General.—Manuscripts, in English or French, should be typewritten, double spaced, on paper $8\frac{1}{2} \times 11$ in. **The original and one copy are to be submitted.** Tables and captions for the figures should be placed at the end of the manuscript. Every sheet of the manuscript should be numbered. Style, arrangement, spelling, and abbreviations should conform to the usage of recent numbers of this journal. Greek letters or unusual signs should be written plainly or explained by marginal notes. Characters to be set in bold face type should be indicated by a wavy line below the characters. Superscripts and subscripts must be legible and carefully placed. Manuscripts and illustrations should be carefully checked before they are submitted. Authors will be charged for unnecessary deviations from the usual format and for changes made in the proof that are considered excessive or unnecessary.

Abstract.—An abstract of not more than about 200 words, indicating the scope of the work and the principal findings, is required, except in Notes.

References.—These should be designated in the text by a key number and listed at the end of the paper, with the number, in the order in which they are cited. The form of the citations should be that used in this journal; in references to papers in periodicals, titles should not be given and only initial page numbers are required. The names of periodicals should be abbreviated in the form given in the most recent *List of Periodicals Abstracted by Chemical Abstracts*. All citations should be checked with the original articles and each one referred to in the text by the key number.

Tables.—Tables should be numbered in roman numerals and each table referred to in the text. Titles should always be given but should be brief; column headings should be brief and descriptive matter in the tables confined to a minimum. Vertical rules should not be used. Numerous small tables should be avoided.

ILLUSTRATIONS

General.—All figures (including each figure of the plates) should be numbered consecutively from 1 up, in arabic figures, and each figure referred to in the text. The author's name, title of the paper, and figure number should be written in the lower left corner of the sheets on which the illustrations appear. Captions should not be written on the illustrations.

Line drawings.—Drawings should be carefully made with India ink on white drawing paper, blue tracing paper, or co-ordinate paper ruled in blue only; any co-ordinate lines that are to appear in the reproduction should be ruled in black ink. Paper ruled in green, yellow, or red should not be used. All lines must be of sufficient thickness to reproduce well. Decimal points, periods, and stippled dots must be solid black circles large enough to be reduced if necessary. Letters and numerals should be neatly made, preferably with a stencil (do **NOT** use typewriting), and be of such size that the smallest lettering will not be less than 1 mm high when the figure is reduced to a suitable size. Many drawings are made too large; originals should not be more than 2 or 3 times the size of the desired reproduction. Wherever possible two or more drawings should be grouped to reduce the number of cuts required. In such groups of drawings, or in large drawings, full use of the space available should be made; the ratio of height to width should conform to that of a journal page ($5\frac{1}{4} \times 7\frac{1}{4}$ in.) but allowance must be made for the captions. **The original drawings and one set of clear copies (e.g. small photographs) are to be submitted.**

Photographs.—Prints should be made on glossy paper, with strong contrasts. They should be trimmed so that essential features only are shown and mounted carefully, with rubber cement, on white cardboard, with no space between those arranged in groups. In mounting, full use of the space available should be made. **Photographs are to be submitted in duplicate;** if they are to be reproduced in groups one set should be mounted, the duplicate set unmounted.

REPRINTS

A total of 100 reprints of each paper, without covers, are supplied free. Additional reprints, with or without covers, may be purchased at the time of publication.

Charges for reprints are based on the number of printed pages, which may be calculated approximately by multiplying by 0.5 the number of manuscript pages (double-space typewritten sheets, $8\frac{1}{2} \times 11$ in.) and including the space occupied by illustrations. Prices and instructions for ordering reprints are sent out with the galley proof.

Contents